

Analysis and Development of New Techniques and Possibilities of Using Geothermal Energy

(Análisis y desarrollo de nuevas técnicas y posibilidades de utilización de energía geotérmica)

Cristina Sáez Blázquez

Supervised by:

Dr. Diego González Aguilera

Dr. Arturo Farfán Martín

INTERNATIONAL DOCTORAL THESIS

UNIVERSITY OF SALAMANCA

Department of Cartographic and Land Engineering

2019

Copyright © 2019 by C. Sáez Blázquez

All rights reserved. No part of the material protected by this copyright may be reproduced or utilized in any form or by any means, electronic or mechanical, including photocopying, recording or by any information storage and retrieval system, without written consent from the author (u107596@usal.es).

Department of Cartographic and Land Engineering
Higher Polytechnic School of Avila
University of Salamanca

AUTHOR:

Cristina Sáez Blázquez

SUPERVISORS:

Dr. Diego González Aguilera

Dr. Arturo Farfán Martín

2019

Supervisors' report regarding the Doctoral Thesis

**"Analysis and Development of New Techniques and Possibilities
of Using Geothermal Energy"**

Presented at

the Department of Cartographic and Land Engineering

by

Cristina Sáez Blázquez

La Tesis Doctoral con mención internacional *"Analysis and Development of New Techniques and Possibilities of Using Geothermal Energy"*, presentada por Cristina Sáez Blázquez, se inserta en la línea de investigación de Energía correspondiente al Programa de Doctorado "Geotecnologías Aplicadas a la Construcción, Energía e Industria", más concretamente la energía renovable geotérmica mediante el desarrollo y mejora de sistemas geotérmicos de baja entalpía.

Se trata de una línea muy original y relevante en la comunidad científica internacional, con una clara propuesta metodológica de bajo coste que ha deparado exitosos resultados en el campo de las energías renovables y que ha deparado una altísima producción científica. Se trata asimismo de una línea de investigación promovida y desarrollada por el Grupo de Investigación TIDOP (<http://tidop.usal.es>) y de la Unidad de Geotermia derivada del propio grupo de investigación (<https://geoenergysize.usal.es/>), ambos pertenecientes a la Universidad de Salamanca.

Las energías renovables tienen un papel esencial en la mitigación continua del cambio climático. La sociedad actual requiere de la implementación de fuentes de energía verdes con el objetivo principal de reducir el uso de combustibles fósiles. Dentro del amplio espectro de energías renovables, la energía geotérmica constituye una base importante para un futuro desarrollo sostenible. Dependiendo de su caracterización térmica y geológica, el uso de esta energía está directamente relacionado con la generación de agua caliente doméstica o

el calentamiento/enfriamiento de un espacio determinado. La producción de electricidad también podría incluirse como aplicación geotérmica si las condiciones geológicas del recurso lo permitieran.

La Tesis Doctoral aborda un adecuado y amplio estado del arte de manera que permite identificar claramente la oportunidad estratégica de la aportación que se realiza como lo demuestra el hecho de que la Tesis se articula en torno a un gran número de artículos científicos publicados en revistas con impacto reconocido. Estos artículos han verificado los correspondientes procesos de evaluación crítica y revisión por parte de expertos internacionales de trayectoria reconocida. Estas contribuciones se centran en:

- Caracterización y estimación de la conductividad térmica del terreno en un sistema de bomba de calor.
- Establecimiento de los parámetros de configuración más eficientes en un sistema de muy baja entalpía.
- Implementación y comparativa de la geotermia de baja entalpía como sistema de calefacción.

La Tesis Doctoral concluye con el correspondiente apartado de Conclusiones en el que de forma precisa y concreta se especifican las principales aportaciones realizadas de tal manera que puedan ser objeto de crítica y de proyección hacia el desarrollo de futuros trabajos integrados en esta línea de investigación.

Ávila, 8 de mayo de 2019

Dr. Diego González Aguilera

Dr. Arturo Farfán Martín

International support concerning the Doctoral Thesis

**“Analysis and Development of New Techniques and Possibilities
of Using Geothermal Energy”**

Two assessment reports written by Doctors of a non-Spanish Institution are attached below. The mentioned reports come from the following Institutions:

- Energy Department, Polytechnic of Turin (Italy)
- Geoscience Department, University of Padua (Italy)

International support concerning the Doctoral Thesis



**POLITECNICO
DI TORINO**

Dipartimento Energia

Torino, 16/05/2019

EXTERNAL EVALUATION LETTER OF THE DOCTORAL THESIS WITH THE "INTERNATIONAL MENTION" FORM ORGANIZED AS A COMPENDIUM OF SCIENTIFIC PAPERS

With great pleasure I have been reading the PhD dissertation entitled "Analysis and Development of New Techniques and Possibilities of Using Geothermal Energy," written by Cristina Sáez Blázquez (Department of Cartographic and Land Engineering, University of Salamanca). Before presenting my evaluation, I will briefly summarize the content of this research.

The Doctoral Thesis opens with an introductory chapter in which the fundamentals and main principles of geothermal energy are thoroughly described. This chapter also includes the motivation and research objectives and a synthesis of the Doctoral Thesis structure.

The second chapter is focused on one of the purposes of the present Thesis, the characterization of the ground thermal conductivity in shallow geothermal systems. Different methodologies concerning the estimation of the thermal conductivity parameter are presented here. These methods belong to published scientific papers.

The third chapter is about the analysis of components usually found in very low geothermal installation. In particular, several grouting materials, different heat exchanger and heat pumps designs are evaluated through laboratory tests.

Chapter four considers the use of low geothermal energy in district heating systems. For that purpose, a technical study evaluates different district heating configurations including a geothermal one.

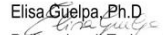
Finally, chapter five concludes the Doctoral Thesis discussing the principal results deduced from all the above.

Altogether the work described in this Thesis is very complete in the sense that the PhD candidate has been working on parameters with special relevance in the geothermal field. Results are based on both laboratory experiments and various types of fieldwork, executing the activities with considerable success, as described in the work. The research has led to convincing conclusions and recommendations for future works all with the aim of improving the utilization and performance of shallow geothermal systems. Additionally, the present Doctoral Thesis is very well written in the English language and is clearly structured. All this is also proven by the fact that the main chapters are supported by various scientific papers published in relevant peer-reviewed journals. Therefore, I strongly recommend Cristina Sáez Blázquez to obtain the degree of International Doctor at the University of Salamanca in Spain.

In the end, I would like to congratulate both the PhD candidate and her supervisors with this work.

Sincerely,

Elisa Guelpa, Ph.D.


Pólitecnico di Torino – Energy Department

Dipartimento Energia

Politecnico di Torino Corso Duca degli Abruzzi, 24 – 10129 Torino – Italia

tel: +39 011.090.4478 fax: +39 011.090.4499

elisa.guelpa@polito.it www.denerg.polito.it www.polito.it



DIPARTIMENTO
DI GEOSCENZE



UNIVERSITÀ
DEGLI STUDI
DI PADOVA

via Gradenigo, 6
35131 Padova
tel +39 049 8279110
fax +39 049 8279111
CF 80006480281
P.IVA 00742430283

Prof. ing. Paolo Scotton
Hydrogeology Laboratory
Department of Geosciences
Tel. -39 049 8289120
Cel. 320 6868047
e_mail: paolo.scotton@unipd.it

External examiner review for the International PHD thesis “Analysis and Development of New Techniques and Possibilities of Using Geothermal Energy” by Cristina Sáez Blázquez, Department of Cartographic and Land Engineering, University of Salamanca, Spain.

The PHD research work of Cristina Saez Blazquez develops in the field of renewable energies and, more in particular, it deals mainly with low enthalpy Geothermal Energy. This is a theme of paramount importance considering the need to overcome the economic dependence on fossil sources and, since the geothermal resource is characterized by low levels of greenhouse-gas emissions, its use is expected to increase in the next future. In the last 20-30 years a lot of technical applications have been done and fancied worldwide, followed by the need to understand scientifically the many involved physical and technical aspects.

This is a typical challenging environmental problem characterized by the need to face the three main research roads in order to progress in the knowledge in an aware and sustainable way: field activity, laboratory activity, physical and numerical approach.

Cristina Saez Blazquez dedicated her attention to all the cited research sectors. A lot of work has been done in order to define one of the most important field physical parameter, the thermal conductivity. It is an important part of Paper 1 where an original method for designing geothermal installation is proposed, starting from field temperature measurements and with the use of numerical software. It is the main object of Paper 2, that presents an experimental apparatus designed for its measurements, and of Paper 3, where thermal conductivity is related to the velocity of seismic waves P and S obtained from the application of MAWS and seismic refractions tests. In Paper 4 a thermal conductivity map of Avila region is proposed based on conductivity measurements (performed with two different methods) of the principal geological materials of the region, while in Paper 5 a comparison of different methods and measurements in the laboratory has been done, concluding that seismic measurements can provide values very similar to the values obtained by a Thermal Response Test. Another significant part of the work of Cristina Saez Blazquez is devoted to more technological subjects. The object of Paper 6 is the study, both from a thermal and mechanical point of view, of different grouting materials used to improve the energy exchange between the thermal sound and the surrounding ground. In Paper 7, various types of heat exchangers, among those traditionally adopted (single and double U-tubes) and more recent (helical pipe), are analysed in a small scale experimental apparatus, in terms of their efficiency. Paper 8 deals with another

DIPARTIMENTO DI GEOSCIENZE
DEPARTMENT OF GEOSCIENCES

fundamental technical component of low enthalpy geothermal systems: the heat pumps. Here the traditional EHP (electrical heat pump) and the more recent GEHP (gas engine heat pump) are compared and the compliance with the Energy Efficiency Directive about nZEB is analysed in three different study areas. Finally, in Paper 9, different district heating systems aided by geothermal systems are compared with traditional fossil installations both in terms of economic and environmental aspects, establishing the predominance of the geothermal district systems.

From the above it is clear the effort of the PHD candidate, and of her research group, to cover all the important aspects of the research theme, the final goal being the acquisition of technical awareness in the applications of geothermal systems. The matter is well proposed in high impact factor international journals. The methods are appropriate to the current state of knowledge. I particularly appreciated, depending probably on my cultural background, the experimental work devoted to the definition of the ground thermal conductivity, together with the application of seismic methods in the field, and on the efficiency analysis of different types of thermal sounds. An aspect that was not explicitly taken into consideration, probably due to the geology of the places under study, and that could be a future development, is the effect of the fluid motion in the aquifer on the energy exchange between the thermal sound and the surrounding environment.

In conclusion, I greatly appreciated the work done by the candidate both for the used methods and for the achieved results, and, as far as I am concerned, I strongly recommend the author to obtain the degree of International Doctor at the University of Salamanca in Spain.

Padova, 26 May 2019

Paolo Scotton, University of Padua, Italy



List of Publications

This Doctoral Thesis consists of a compendium of nine Scientific Papers published in high impact factor international journal that are specified below.

1. “Analysis of the process of design of a geothermal installation”

Cristina Sáez Blázquez¹, Arturo Farfán Martín¹, Pedro Carrasco García¹, Luis Santiago Sánchez Pérez¹, Sara Jiménez del Caso¹

¹Department of Cartographic and Land Engineering, University of Salamanca, Hornos Caleros, Ávila 05003, Spain

Renewable Energy, April 2016.

DOI: 10.1016/j.renene.2015.11.067

2. “Measuring of thermal conductivities of soils and rocks to be used in the calculation of a geothermal installation”

Cristina Sáez Blázquez¹, Arturo Farfán Martín¹, Ignacio Martín Nieto¹, Diego González-Aguilera¹

¹Department of Cartographic and Land Engineering, University of Salamanca, Hornos Caleros, Ávila 05003, Spain

Energies, June 2017.

DOI: 10.3390/en10060795

3. “Thermal conductivity map of the Avila region (Spain) based on thermal conductivity measurements of different rock and soil samples”

Cristina Sáez Blázquez¹, Arturo Farfán Martín¹, Ignacio Martín Nieto¹, Pedro Carrasco García¹, Luis Santiago Sánchez Pérez¹, Diego González-Aguilera¹

¹Department of Cartographic and Land Engineering, University of Salamanca, Hornos Caleros, Ávila 05003, Spain

Geothermics, January 2017.

DOI: 10.1016/j.geothermics.2016.09.001

4. “Thermal conductivity characterization of three geological formations by the implementation of geophysical methods”

Cristina Sáez Blázquez¹, Arturo Farfán Martín¹, Pedro Carrasco García¹, Diego González-Aguilera¹

¹Department of Cartographic and Land Engineering, University of Salamanca, Hornos Caleros, Ávila 05003, Spain

Geothermics, March 2018.

DOI: 10.1016/j.geothermics.2017.11.003

5. “Comparative analysis of different methodologies used to estimate the ground thermal conductivity in low enthalpy geothermal systems”

Cristina Sáez Blázquez¹, Ignacio Martín Nieto¹, Arturo Farfán Martín¹, Diego González-Aguilera¹ and Pedro Carrasco García¹

¹Department of Cartographic and Land Engineering, University of Salamanca, Hornos Caleros, Ávila 05003, Spain

Energies, Special Issue Volume II: Low Enthalpy Geothermal Energy, 2019.

DOI: 10.3390/en12091672

6. “Analysis and study of different grouting materials in vertical geothermal closed-loop systems”

Cristina Sáez Blázquez¹, Arturo Farfán Martín¹, Ignacio Martín Nieto¹, Pedro Carrasco García¹, Luis Santiago Sánchez Pérez¹, Diego González-Aguilera¹

¹Department of Cartographic and Land Engineering, University of Salamanca, Hornos Caleros, Ávila 05003, Spain

Renewable Energy, December 2017.

DOI: 10.1016/j.renene.2017.08.011

7. “Efficiency analysis of the main components of a vertical closed-loop system in a borehole heat exchanger”

Cristina Sáez Blázquez¹, Arturo Farfán Martín¹, Ignacio Martín Nieto¹, Pedro Carrasco García¹, Luis Santiago Sánchez Pérez¹, Diego González-Aguilera¹

¹Department of Cartographic and Land Engineering, University of Salamanca, Hornos Caleros, Ávila 05003, Spain

Energies, Special Issue “Low Enthalpy Geothermal Energy”, February 2017.

DOI: 10.3390/en10020201

8. “Technical optimization of the energy supply in geothermal heat pumps”

Cristina Sáez Blázquez¹, David Borge-Diez², Ignacio Martín Nieto¹, Arturo Farfán Martín¹, Diego González-Aguilera¹.

¹Department of Cartographic and Land Engineering, University of Salamanca, Hornos Caleros, Ávila 05003, Spain

²Department of Electric, System and Automatic Engineering, Universidad de León, León, Spain

Geothermics, 2019

DOI: 10.1016/j.geothermics.2019.04.008

9. “Economic and environmental analysis of different district heating systems aided by geothermal energy”

Cristina Sáez Blázquez¹, Arturo Farfán Martín¹, Ignacio Martín Nieto¹, Diego González-Aguilera¹

¹Department of Cartographic and Land Engineering, University of Salamanca, Hornos Caleros, Ávila 05003, Spain

Energies, Special Issue "Geothermal Energy: Utilization and Technology", May 2018.

DOI: 10.3390/en11051265

**To my parents, sisters and
partner**

**“The only impossible journey is the one you never
begin”.**

—Anthony Robbins

Abstract

Renewable energies have got an essential role in the continuous climate change mitigation. The present-day society requires the implementation of green energy sources with the principal aim of reducing the fossil's fuels use. Within the broad spectrum of renewable energies, geothermal energy constitutes an important part for a future sustainable development. Depending on its thermal and geological characterization, the use of this energy is directly related to the generation of domestic hot water and/or heating/cooling purposes. Electricity production could be also included as a geothermal application if the geological conditions of the resource allowed it. There is a large number of advantages that define this kind of renewable source (e.g. continuous use, reduced greenhouse gases emissions, minimum operational costs, geological independence for heating and cooling uses, etc.). However, the high initial investment commonly required for domestic installations and the lack of knowledge in the field, make the use of this energy limited in certain occasions.

The present Doctoral Thesis is framed within the analysis and evaluation of the principal parameters and components that, directly or indirectly, influence the development of low enthalpy geothermal systems. Specifically, the main goal of this research work is to define the most optimal schema of geothermal operation that helps to contribute in a more extensive use of this renewable technology. The research lines include extensive field work and laboratory tests, in addition to the computing processing and analysis of the experimental and simulation data.

The starting point of the research work was the identification of the weaknesses that characterize low enthalpy geothermal resources. After this first evaluation, efforts were focused on the realization of different tests on the parameters detected as essential in the previous stage. Experimental work was complemented with the use of specific software on the basis of the geothermal systems dimensioning, energy simulation and modelling apart from the corresponding numerical and theoretical studies. Conclusions obtained from the whole practical and theoretical work allowed establishing the most optimal geothermal methodology. In summary, the present Doctoral Thesis contains valuable information that has been compiled in numerous scientific works in which all the know-how and expertise arising during this research stage have been compiled.

Resumen

Las energías renovables juegan un papel imprescindible en la lucha constante contra el cambio climático. La sociedad de hoy en día requiere la implementación de fuentes de energías limpias con el objeto de reducir la utilización de combustibles fósiles. Dentro del amplio espectro de energías renovables, la energía geotérmica constituye un pilar importante en el futuro desarrollo sostenible. En función de su caracterización térmica y geológica, el uso de esta energía está directamente relacionado con la producción de agua caliente sanitaria o la climatización de un determinado espacio. La generación eléctrica puede también incluirse en las aplicaciones de la energía geotérmica si las condiciones geológicas del recurso lo permiten. Existen un gran número de ventajas que definen esta clase de recurso renovable (como por ejemplo; uso continuo, emisión de gases de efecto invernadero reducida, costes operativos mínimos, independencia geológica en aplicaciones de climatización, etc.). Sin embargo, la elevada inversión inicial que estas instalaciones requieren y la carencia de conocimiento en el ámbito, limitan el uso de esta energía en ciertas ocasiones.

La presente Tesis Doctoral se enmarca en el análisis y evaluación de los principales parámetros y componentes que directa o indirectamente influyen en el desarrollo de los sistemas geotérmicos de baja entalpía. En particular, el principal propósito de este trabajo es definir el esquema de funcionamiento geotérmico óptimo con el fin de contribuir a un uso más extensivo de esta tecnología renovable. Las líneas de investigación incluyen un extenso proceso de trabajo de campo y ensayos de laboratorio, así como el procesamiento y análisis de los datos experimentales y de simulación.

El punto de partida del trabajo de investigación dio comienzo con la identificación de los puntos débiles de los recursos geotérmicos de baja entalpía. Tras esta primera evaluación, los esfuerzos se centraron en la realización de diferentes ensayos sobre los parámetros detectados como esenciales en la etapa anterior. El trabajo experimental se complementó con el uso de software especializado en el dimensionamiento de sistemas geotérmicos, simulación y modelado energético además de la realización de los correspondientes estudios teóricos y numéricos. Las conclusiones extraídas de todo el desarrollo práctico y teórico han permitido establecer la metodología geotérmica más adecuada. En resumen, la presente Tesis

Doctoral está compuesta por información muy relevante para el campo geotérmico, que ha sido recogida en forma de artículos científicos donde se compila todo el conocimiento y experiencia adquiridos a lo largo de la etapa investigadora.

Acknowledgements

It is said that the best part of a journey is not the destination, but at the journey itself. Indeed, the best part of this work has been the journey: people I met, all the learning about the geothermal energy, field work activities, the PhD stays in Turin and Padua, research collaboration with other universities, without forgetting the stressful moments, deadlines, mistakes, nervousness before presentations... In the end, all these moments made my journey great. Thanks a lot!

However, this journey wouldn't have been possible without the support I received from numerous people.

Firstly, I would like to deeply acknowledge my daily supervisors Diego González-Aguilera and Arturo Farfán Martín. Thanks to Diego González-Aguilera for giving me the opportunity to conduct my PhD studies within his research group TIDOP at the Higher Polytechnic School of Ávila. Thank you for sharing all your knowledge, support, guidance and advices during all these years. I admire your dedication and commitment. And of course, thanks to Arturo Farfán Martín for your constant support since this adventure began. Beyond the scientific guidance, you have become someone essential in my life and I will be always eternally grateful to you. My greatest admiration for your dedication in everything you do. *This achievement is also yours!*

Thanks also to my lab colleagues of the TIDOP Research Group for their willingness to help me in every moment. Special thanks to Nacho for your support and all the great moments in the laboratory and field works.

I would also like to acknowledge to Vittorio Verda for hosting me as a visitor researcher at the Polytechnic of Turin and for all your accessibility and support. Thanks to Michele De Carli for also hosting me at the University of Padua and Paolo Scotton for being the main supervisor of my work in Padua and for sharing your wisdom and knowledge.

Thanks to Pedro Carrasco, Luis Santiago and Fernando for collaborating in the experimental phases of the research works. Thanks also to David Borge Diez for your availability and for sharing your great knowledge.

In the personal context, I deeply thank to my family, especially my parents, Isabel and Jesús for your unconditional love and support during my whole life and in the worst moments of this journey. You know better than anyone how hard this work has been. Thanks to my sisters, Esther and Marta for being my friends and helping me in every moment. Thanks to my niece Victoria for making me happy. And of course, thanks to my life partner, Miguel, for putting up with me and being my main support in all this period. Thank you for giving me strength when I needed. *This achievement is also yours! I love you!*

I want also thank to all my friends to follow my routine with the same passion as myself. Thanks to Leyre and Eva, for listening to me and for all the fun times. Special memory for my friend, Alberto, because you have sent me your strength and motivation from where you are. *I'll never forget you!*

Thanks to my running mates for making everything easier, special mention for trainer and friend Zipi. *Thanks for believing in me!*

And, finally, I could not imagine this journey without my dog Noah that has faithfully accompanied me in every moment. *Thanks princess!*

Thanks to everyone for making this achievement to happen!

Agradecimientos

Se dice que la mejor parte del camino no es el destino, sino el camino en sí. Ciertamente, la mejor parte de este trabajo ha sido el camino: la gente que he conocido, todo el aprendizaje en energía geotérmica, los trabajos de campo, las estancias en Turín y Padua, colaborar con otras universidades, sin olvidar los momentos de estrés, fechas límites, errores, nerviosismo antes de una presentación... Al final, todos estos momentos hicieron el camino magnífico. *¡Muchas gracias!*

Sin embargo, este camino no hubiera sido posible sin el apoyo recibido por muchas personas.

En primer lugar, me gustaría expresar mi agradecimiento a mis supervisores Diego González Aguilera y Arturo Farfán Martín. Gracias Diego por darme la oportunidad de dirigir mis estudios de doctorado dentro del grupo de investigación TIDOP en la Escuela Politécnica Superior de Ávila. Gracias por compartir tu conocimiento, apoyo, guía y consejos durante todos estos años. Admiro tu dedicación y compromiso. Y por supuesto, gracias Arturo por tu constante apoyo desde que esta aventura comenzó. Más allá del ámbito académico, te has convertido en alguien esencial en mi vida y siempre te estaré eternamente agradecida. Mi más sincera admiración por tu dedicación en todo lo que haces. *¡Esto también es tuyo!*

Gracias también a mis compañeros del Grupo de Investigación TIDOP por su disposición a ayudarme en todo momento. Gracias especialmente a Nacho, por tu apoyo y por todos los buenos momentos en el laboratorio y en los trabajos de campo.

También me gustaría agradecer a Vittorio Verda por acogerme como investigadora en la Universidad Politécnica de Turín y por tu apoyo y accesibilidad. Gracias a Michele de Carli por acogerme también en la Universidad de Padua y a Paolo Scotton por ser el principal supervisor de mi trabajo en Padua y por compartir conmigo tu gran conocimiento y dedicación.

Gracias a Pedro Carrasco, Luis Santiago y Fernando por vuestra colaboración en las fases experimentales del trabajo. Gracias también a David Borge Diez por tu disponibilidad y por compartir tu gran conocimiento.

En el ámbito personal, agradezco profundamente a mi familia, especialmente a mis padres, Isabel y Jesús, por vuestro amor y apoyo incondicional durante toda mi vida y en los peores momentos de esta aventura. Vosotros sabéis mejor que nadie lo duro que este trabajo ha sido. Gracias a mis hermanas, Esther y Marta por ser mis amigas y ayudarme en todo momento. Gracias también a mi sobrina Victoria, por hacerme feliz. Y, por supuesto, gracias a mi compañero de vida, Miguel, por aguantarme y por ser mi principal apoyo en todo este periodo. Gracias por darme fuerza cuando la necesitaba. *¡Esto también es vuestro! ¡Os quiero!*

También quiero agradecer a todos mis amigos por seguir mi rutina con la misma pasión que yo. Gracias a Leyre y Eva, por escucharme y por todos los momentos divertidos. Guardo especial recuerdo a mi amigo Alberto, me envías toda tu fuerza y motivación desde donde estés. *¡Nunca te olvidaré!*

Gracias a mis compañeros de carrera por hacer todo mucho más fácil, mi especial mención va para mi entrenador y amigo Zipi. *¡Gracias por creer en mí!*

Y, por último, no podría imaginarme este viaje sin mi perrita Noah que me ha acompañado fielmente en todo momento. *¡Gracias princesita!*

¡Gracias a todos por hacer que esto suceda!

Contents

Chapter I	31
I. Introduction	33
I.I Overall context	33
I.II. Theoretical background	33
I.II.I. Overview and fundamentals of geothermal energy	33
I.II.II. Geothermal resources	34
I.II.III. Historical use of geothermal energy	37
I.II.IV. Heat pump systems	40
I.III. Research background	43
I.IV. Motivation	44
I.V. Research objectives	45
I.VI. Structure of the Doctoral Thesis	45
Chapter II	49
II. Ground thermal characterization in GSHP systems	51
II.I. Fundamentals of the heat transfer process in a GSHP system	51
PAPER 1	55
PAPER 2	69
PAPER 3	89
PAPER 4	103
PAPER 5	117
Chapter III	133
III. Technical evaluation of the geothermal design	135
III.I. Configuration of the geothermal system	135
PAPER 6	139
PAPER 7	153

PAPER 8.....	171
Chapter IV	183
IV. District Heating Systems Aided by Geothermal Energy	185
IV.I. Renewable district heating review	185
PAPER 9	186
Chapter V	207
V. Conclusions and future work	209
V.I. Conclusions	209
V.I.I. In general terms	209
V.I.II. Ground thermal conductivity.....	210
V.I.III. Geothermal design.....	210
V.I.IV. Geothermal district heating	211
V.II. Future works.....	211
REFERENCES	213
APPENDIX A	225
Indexation and impact factor of journals	227
APPENDIX B	233
GES – Cal SOFTWARE.....	235
Curriculum Vitae.....	241

Chapter I

INTRODUCTION

I. Introduction

This introductory Chapter contains the overall context of the research topic treated in this dissertation. Next, the motivation and objectives of this Doctoral Thesis are stated and finally, the structure of the Thesis is presented at the end of the Chapter.

I.I Overall context

Geothermal energy, included in the group of renewable energies, has become essential in the current energy sector. It is the only renewable source independent of solar radiation and/or the gravitational attraction of the sun and moon (Younger, 2014). In this context, numerous scientific works focused on the evaluation and development of this energy can be found in the existing literature. Geothermal resources refer to the energy contained within the Earth that generates geological phenomena on a planetary scale (Dickson and Fanelli, 2003). Despite the large number of advantages this green energy has, certain technical and/or economic issues limit an extensive expansion of geothermal resources. The objective of this Doctoral Thesis is to cover the topics considered as essential in the development and common use of geothermal energy systems. Conclusions of this Thesis are expected to represent a significant contribution in the general geothermal field that, in turn, motivates an extensive use of the mentioned energy.

I.II. Theoretical background

I.II.I. Overview and fundamentals of geothermal energy

The origin of the Earth's thermal energy is linked to the internal structure of our planet and the physical processes occurring there. The presence of hot springs, volcanoes or other thermal phenomena led our ancestors to deduce that parts of Earth's interior were hot. Between the sixteenth and seventeenth century, the first mines were excavated to a few hundred meters under the ground level confirming that the Earth's temperature increased with depth. Thus, the existence of this heat is known because the rocks temperature increases with depth, proving that a geothermal gradient exists: this gradient averages 3°C/100m of depth. Assuming a conductive gradient and mean surface ambient temperature, the Earth temperature at the depth of 10 km would be over 300°C. However, in some areas of the Earth's

crust, gradients above the average can be found. This fact occurs when, a few kilometres from the surface there are magma bodies undergoing cooling, still in a fluid state or in the process of solidification, and releasing heat. On the contrary, in areas where there is not magmatic activity, the heat accumulation is derived from particular geological conditions of the crust. Armstead (1983) divided the Earth's crust into non-thermal and thermal areas, considering thermal areas those ones with temperature gradients greater than 40°C/km depth.

All the large quantity of heat accumulated needs to be transferred to accessible depths beneath the Earth's surface. Heat is generally moved from depth to sub-surface regions by conduction (firstly) and by convection (then) using geothermal fluids. In a natural way, these fluids are essentially constituted by rainwater that has penetrated into the Earth's crust and has been heated thanks to the contact with hot rocks and has been accumulated in aquifers (geothermal reservoirs).

Hot fluids are extracted from the reservoir by wells drilled in the surface. Depending on the temperature and pressure, these fluids can be used for the generation of electricity or for space heating/cooling and industrial processes (Enrico Barbier, 2002).

I.II.II. Geothermal resources

Geothermal resources are constituted by the thermal energy that could reasonably be extracted for a specific purpose. The diversity of both the nature of the geothermal resource and its exploitation usually generates a challenge in the context of its classification. Numerous possible criteria for such classification are available, but they are traditionally classified according to their reservoir temperatures. Temperature is the parameter used in the geothermal classification because it is the easiest to measure and understand. Average reservoir temperature is measured in exploration wells or estimated by geo-thermometers (Hochstein, 1990). According to White and Williams (1975) classification, geothermal resource types are classified as Table 1 shows.

Table 1. Geothermal resource classification.

Geothermal Resource Type		Temperature range (°C)
<i>Convective hydrothermal resources</i>	Vapour dominated	~240
	Hot-water dominated	20 - 350
<i>Other hydrothermal resources</i>	Sedimentary basin	20 - 150
	Geo-pressured	90 - 200
	Radiogenic	30 - 150
<i>Hot rock resources</i>	Solidified (hot dry rock)	90 - 650
	Part still molten (magma)	> 600

In general terms, resources with temperatures of above 150°C are used for electricity generation, although lower temperature resources have also been used for power production (Lund, 2006). Regarding geothermal resources below 150°C, they are commonly used for heating and cooling in direct-use projects. In the case of temperature ranges between 5 - 30°C, they can be also used by the implementation of geothermal heat pumps for both heating and cooling purposes (ground source/ground water heat pump systems).

A more extended and simple classification according to the uses and resource temperatures considers the following groups (IDAE, 2011):

- Very low enthalpy geothermal resources [$T < 30^{\circ}\text{C}$].
- Low enthalpy geothermal resources [$30^{\circ}\text{C} < T < 100^{\circ}\text{C}$].
- Medium enthalpy geothermal resources [$100^{\circ}\text{C} < T < 150^{\circ}\text{C}$].
- High enthalpy geothermal resources [$T > 150^{\circ}\text{C}$].

Very low enthalpy geothermal resources

Very low temperature geothermal resources can be practically found in the whole Earth's crust thanks to the constant ground temperature from depths of 8 - 10 meters. At any point of the crust, heat can be extracted for heating and cooling applications by the use of geothermal heat pumps. Seasonal temperature variations are

perceptible in the ground to a depth of around 10 m. From that depth, ground is able to store the heat even seasonally, so that ground temperature is practically constant throughout the year. From the depth of 15 m, the rocks temperature does not depend on the seasonal temperature variations or climate; it only depends on the geological and geothermal conditions.

Low enthalpy geothermal resources

These resources can be located in sedimentary basins in which the geothermal gradient is normal or slightly higher. The only geological condition required makes reference to the existence of permeable geological formations (at depths of around 1.500 – 2.000 m), capable of containing and allowing the circulation of fluids to extract the rocks heat.

There are numerous low enthalpy geothermal reservoirs in the planet: Amazon Basin and the River Plate in South America, Boise Region (Idaho) and the Mississippi Basin in North America, the Artesian Basin of Australia, the Peking Region and Central Asia, the Basins of Paris and Aquitaine in France, etc. (Trillo and Angulo, 2008)

Medium enthalpy geothermal resources

Geothermal resources with temperatures between 100 - 150°C are found in a large number of locations: sedimentary basins (depths of around 2.000 – 4.000 m), lithospheric thinning areas, deposits with elevated radioactive isotopes concentration, etc. These types of geothermal reservoirs are found in numerous localized areas, where, thanks to discontinuities and faults, water can easily raise the surface as thermal waters.

As in the case of high temperature reservoirs, these resources require a magmatic intrusion as heat source and a good recharge aquifer. However, in medium temperature geothermal resources, there is not an impermeable layer on the aquifer that maintains heat and pressure in the reservoir. Nearby examples in sedimentary basins are found in Germany and Austria (Trillo and Angulo, 2008).

The characteristic temperatures of these resources allow their use for power generation through binary cycles. However, they are being increasingly used in

combined processes of electricity production and centralized heat systems (district heating) improving the economic returns.

High enthalpy geothermal resources

These resources are located in geographical areas with an extraordinarily high geothermal gradient, up to 30°C/100 m. The existence of high temperature geothermal reservoirs is conditioned by the existence of an active heat source close to the Earth's surface, a permeable formation capable of containing and transmitting the geothermal fluid, and finally, a confining-waterproof layer that prevents the energy escape. Consisting of steam or a mixture of water-steam, they are usually used to produce electricity at depths of 1.500 – 3.000 meters.

The presence of these resources is commonly linked to the existence of notable geological phenomena, such as high seismic activity, recent volcanic activity and, mainly, volcanic regions placed on the edges of lithospheric plaques.

I.II.III. Historical use of geothermal energy

Since immemorial time, geothermal energy emerging at the Earth's surface as natural hot springs has been instinctively used by human beings for different purposes. In the ancient Roman Empire, the potential of several natural hot springs was analyzed in order to supply the hot water demands of public baths (Stober and Bucher, 2013).

The thermal energy of the Earth is immense, but only a fraction of it can be utilized by humankind. The use of this energy has been traditionally limited to areas in which the geological conditions allow to transfer the heat from deep hot zones to or near the surface. Geothermal sector has been exploited in many areas of life for different practical applications. At the beginning of the nineteenth century, geothermal fluids were already used for the energy content they had. In that period, Italy opened a chemical industry (known as Larderello) to extract boric acid from hot waters naturally emerging or from specific shallow boreholes. Natural steam began to be used for its mechanical energy, between 1910 and 1940 the low-pressure steam in the Tuscany region was brought into use to heat residential and industrial buildings and greenhouses. In this context, Iceland (also pioneer in the geothermal energy use) began to exploit geothermal fluids for heating purposes in 1928. All

these uses together with industrial heating applications are examples of direct use of geothermal resources (Dickson and Fannelli, 2005). Direct use of geothermal energy is one of the oldest and most common ways of utilizing this renewable energy. Regarding the mentioned non-electric applications of geothermal energy, the installed power and energy used worldwide were for the year 2000 of 15.145 MW_t and 190.699 TJ/yr respectively. The most common use is to heat pumps followed by bathing, space heating, greenhouses, aquaculture and industrial processes (Lund and Freeston, 2000). An evolution of the global thermal installed power from 1995 to 2015 is presented in Table 2.

Table 2. Evolution of the total direct use worldwide for the period 1995-2015 (Lund and Boyd, 2016).

Year	Total Installed Capacity (MW _t)
1995	8.664
2000	15.145
2005	28.269
2010	48.493
2015	70.885

The indirect use of geothermal energy is the power generation. The first efforts at producing electricity from geothermal steam were made at Larderello in 1904. Thank to this experiment, the industrial value of this energy was verified, beginning a new way of exploitation that meant an important commercial success. In this way, the installed geothermoelectric capacity was 127.650 kW_e by 1942. After the electricity generation success in Larderello, several countries followed the same procedure. Some examples are Japan, that drilled geothermal wells at Beppu in 1919 or United States, at The Geysers, California, in 1921. In New Zealand, a small geothermal power plant started to be operating in 1958, also in Mexico in 1959 and United States in 1960. Between 1975 and 1979, the geothermal electric capacity, installed in the developing countries, increased from 75 to 462 MW_e (Dickson and Fannelli, 1988). In 2000, geothermal power in these countries represented 47 per cent of the world total with 7,974 MW_e and 9,028 MW_e in 2003. This value continued increasing and, in 2017, there were 13.270 MW_e installed worldwide in

24 countries. The evolution of the worldwide geothermal installed capacity can be observed in Table 2.

Table 3. Evolution of the total worldwide installed capacity from 1995 to the end of 2015 and forecasting for year 2020 (Bertani, 2015).

Year	Total Installed Capacity (MW _e)
1995	6.832
2000	7.973
2005	8.903
2010	10.897
2015	12.635
Forecasting for 2020	21.443

Electricity generation

Geothermal power generation usually takes place in conventional steam turbines and binary plants. Fluids at temperatures of at least 150°C are required in the traditional steam turbines. Atmospheric exhaust turbines are easier and cheaper; steam passes through a turbine and is exhausted to the atmosphere. However, in these systems the steam consumption is double that of a condensing unit. Condensing units are commonly more complex and require bigger sizes of installations.

The production of electricity from geothermal fluids coming from low to medium temperature reservoirs has been improved thanks to the binary fluid technology. These systems use a secondary working fluid (organic fluid) that gains heat from the geothermal fluid through heat exchangers so this second fluid is heated and vaporized. This fluid is then cooled and condensed to begin a new cycle. Binary technology is especially reliable to convert into electricity, the energy available from water-dominated geothermal fields where temperatures are below 170°C. Kalina cycle, a new binary fluid cycle utilizes a water-ammonia mixture as working fluid. This cycle is considered to be up to 40 per cent more efficient than the existing binary power plants.

Direct heat applications

The use of geothermal energy for heat generation is one of the most versatile and oldest ways of utilization. Space and district heating technologies have progressed in the last years and these systems are widely distributed in European countries, United States, China, Japan, etc. The main costs of these installations are initial investment costs, for boreholes, pumps, heat exchangers and distribution networks. However, the subsequent operating costs are comparatively lower than in traditional systems and are attributed to the pumping power, and system control and maintenance. Regarding space cooling, it is also a possible geothermal use if heat pumps are adapted to that use. The technology is based on an absorption cycle that utilizes heat instead of electricity as the energy source.

Geothermal space conditioning (including both heating and cooling) has grown considerably since 1980 together with the development of geothermal heat pumps. These machines allow to economically extract the heat from low and very low temperature reservoirs such as the ground and shallow aquifers (Sanner, 2001). Most of the current heat pumps are reversible and are able to provide either heating or cooling in the space. These devices need energy to operate but, in suitable climatic conditions and with a proper design, the energy balance will be a positive one. Ground source and ground water heat pumps systems (GSHP and GWHP) are installed in a large number of countries. Grounds and aquifers with temperature in the range of 5 - 30°C are usually used in these systems.

I.II.IV. Heat pump systems

Geothermal heat pumps are capable of transferring heat, at a temperature suitable to maintain a comfortable environment within a space. In this sense, heat pumps can be coupled to the ground, making use of its thermal energy (Ground Source Heat Pumps – GSHP) or they can recover thermal energy stored naturally in groundwater or aquifers (Ground Water Heat Pumps – GWHP). Both systems are comprised of three main sections:

- Earth connection: allows the extraction of heat from the Earth thanks to the use of heat exchanger loops.
- Geothermal heat pump: moves the heat between the ground (or groundwater) and the building modifying the temperature of the heat carrier fluid.

- Heat distribution system: distributes the heat throughout the space.

Heat exchangers configuration

Ground loop heat exchangers or Earth connection consist of a collection of pipes that transfer heat between the heat pump and ground by the use of a heat carrier fluid (usually a mixture of glycol 25-30% and water 70-75% in GSHPs or groundwater in GWHPs). The basic configurations include closed loop or open loop systems.

Closed loop heat exchangers constitute the most common configuration. In these cases, the working fluid is enclosed in a circulating loop and the heat transfer with the ground occurs through the piping material (Cui et al, 2011). In this context, different types of closed loop heat exchange systems can be distinguished. The principal ones are the vertical and horizontal loops.

- Vertical heat exchangers are installed in boreholes of variable depths in the range of 75-150 meters. Pipes are fed into the hole and are connected at the bottom by a U-shaped connector. Typical piping configurations include single-U or double-U heat exchangers. The gap between the pipes and borehole is filled with a specific grouting material (Yang et al, 2009). Variant versions of these systems are the geothermal piles in which vertical heat exchangers are installed in the foundation piles of new buildings. Additionally, new vertical designs consider the use of helical pipes that require higher borehole diameter but reducing at the same time the total drilling depth.
- Horizontal closed loops are usually implemented when ample ground area is available. Heat exchangers are laid out horizontally slightly below the Earth's surface in backfilled trenches. The loops design can vary according to the heat transfer requirements and land availability. The most usual configurations are the basic horizontal loop, series loop and parallel design (Stuart et al, 2013). Given the shallow depths where these systems are placed, interaction between soil and ambient environment is high, affecting the global heat exchange. In this regard, spiral loop arrangements can be also found within the horizontal configurations. Piping is laid out in circular loops within the trench. These loops require less land space than the conventional horizontal loops but piping lengths are higher. In addition to all the above, closed pond loops which are spiral loop systems submerged in a water body, can be also chosen as geothermal heat exchanger.

The design of open loop systems is fairly simple. Groundwater is pumped from the ground through a production well. This fluid is then used in the heat pump and transmitted to the distribution system to be finally injected in the corresponding injection well into the same aquifer. Thus, water is extracted from a drilled production well and, after passing through the heat pump heat exchanger, is injected into the aquifer to a sufficient distance to avoid thermal interferences between wells (Omer, 2008). Groundwater temperature remains nearly constant contributing to increase the ground heat pump COP.

Heat pumps

Heat pumps allow extracting thermal energy from a heat source with a low temperature and making it available as useful thermal energy. In this way, geothermal fluids are an ideal heat source for heat pumps systems. Traditional heat pumps operate using electricity to provide the required work for the concentration and transport of thermal energy. Geothermal heat pumps move thermal energy between the ground and the space by controlling pressure and temperature by means of compression and expansion cycles (Wu, 2009; Bi et al, 2009). In the heating mode, the operating procedure of a geothermal heat pump would be as follows:

- The thermal energy is extracted from the ground and transported to the evaporator of the heat pump by the heat carrier fluid.
- Inside the heat pump, heat is transferred to the refrigerant of the heat pump (heat pump unit cold refrigerant) until it becomes a low pressure vapor.
- The vapor gets in the heat pump compressor, resulting in a high pressure and temperature vapor.
- High temperature and pressure vapor enters the condenser. The refrigerant has a higher temperature than the space so it transfers heat to the building. Then, the refrigerant cools and condenses, transforming into a high temperature and pressure liquid.
- Finally, high temperature liquid passes through an expansion valve that reduces its pressure and decreases its temperature. The refrigerant gets into the evaporator to begin a new heating cycle.

It is worth mentioning that most of the present-day heat pumps include a cooling mode thanks to a reversing valve that moves the fluid in the opposite direction in the above described cycle (Stuart et al, 2013).

Heat distribution system

The last section of a ground source heat pump system (or GWHP) refers to the distribution of the heat throughout the space. In this regard, two principal models of distribution systems can be found: water to air and water to water. In the first of them (water to air system), thermal energy is transferred from the ground to air, used as the medium to heat the space. Once heated, the air is moved throughout the building by the use of HVAC (*Heating Ventilation and Air Conditioning*) ducts and air vents (Bloomquist, 2003). In water to water systems another fluid is used as the heat transfer medium. That fluid is then pumped around the building and transfers the heat using in-floor radiant heaters, radiators or air coils.

It is also possible to find hybrid systems that combine both types of distribution systems, thus, a higher control and flexibility of the space temperature is achieved.

I.III. Research background

The research in the geothermal field is continuously growing up. Making special emphasis on shallow geothermal resources (the topic of this Thesis), there is a great scientific production within the context of optimizing the geothermal heat recovery. Throughout the present Doctoral Thesis, a review of the state of the art is provided in the subsequent Chapters for each of the topics addressed on them. Nevertheless, a brief mention to some of the most relevant studies in the geothermal context is presented below.

Different aspects of the geothermal operation as the potential of low enthalpy geothermal resources, the heat transfer and the heat production performance have been addressed in a large number of occasions (Hamza, 2003; Méndez et al, 2011; Colmenar-Santos et al, 2017; Aragón-Aguilar et al, 2017; Jalili et al, 2018; Song et al, 2018). As a result of these thermal evaluations, numerous maps have been produced to show the geothermal possibilities of the areas under study (Sipio et al, 2012; Galgaro et al, 2015; Casasso and Sethi, 2016; Stylianou et al, 2016; Casasso and Sethi, 2017; Siler et al, 2019).

Following in the context of the general study of the shallow geothermal performance, another common practice is the development of numerical and experimental analysis assessing the geothermal heat extraction (Ghoreishi-Madiseh

et al, 2015; Lyu et al, 2017; Yuksel and Ozturk, 2017; Wang et al; 2019; Kayaci et al, 2019; Qiao et al, 2019).

On top of the above, another major area of research interest is the development of alternative uses and applications of geothermal resources (Schüppler et al, 2019). In this regard, it is possible to find studies focused on the use of geothermal energy from abandoned mines or wells (Templeton et al, 2014; Wight and Bennett, 2015; Loredó et al, 2017; Røksland et al, 2017; Menéndez et al, 2019; Sui et al, 2019) or the integration of this energy with other heating plants or energy sources (Zafar and Dincer, 2014; Ghezelbash et al, 2015; Yildirim and Genc, 2015; Atkins et al, 2015; Jradi et al, 2017; Zayed et al, 2019; Yang and Zhai; 2019).

The previous literature review only represents a short example of the broad contribution existing in the shallow geothermal field. In addition to the already mentioned, the state of the art is analyzed for each of the topics approached in this Doctoral Thesis.

I.IV. Motivation

There is no doubt that geothermal energy has experienced a remarkable resurgence in most of European countries as an essential energy source for heating and cooling uses and for power generation in some of them. While it is true that geothermal energy is unique amongst renewables for its baseload and renewable heat provision capabilities, it still lags far behind those of solar and wind. This is mainly attributable to a lack of awareness in the global geothermal working configuration joined to the existence of uncertainties over resource availability in poorly-explored reservoirs and the concentration of full-lifetime costs into early-stage capital expenditure. Although it is true that the study of geothermal resources is quite ample nowadays, the exploration of this field is still below the research in other renewable sources. For these reasons, one of the main purposes of the present Doctoral Thesis is the analysis of the principal components that are part of the geothermal exchange. In this direction, very low enthalpy geothermal resources are the key issue of the global research process.

Since low and very low temperature geothermal systems are the most common way of exploiting this type of renewable energy, it raises the need for increasing the knowledge in this specific field. When a borehole heat exchanger is designed,

important factors are utilized in predicting the thermal response of the ground. Ground thermal properties, heat exchangers efficiency or optimization of the operational cycles are some of the intense research activities carried out within the scopes of this Doctoral work.

I.V. Research objectives

The general objective of the present Doctoral Thesis is to provide new and relevant information about the principal factors and parameters involved in the global thermal energy extraction in very low enthalpy geothermal systems. In order to achieve this general objective, the following specific objectives have been defined:

- i. Thermal conductivity characterization of the surrounding ground in GSHP systems to define the boundary conditions and optimize the ground thermal extraction capacity.
- ii. Evaluation and optimization of the main components of low temperature geothermal installations. Within this specific objective are:
 - a. Definition of the most efficient heat exchanger designs.
 - b. Development of alternative grouting materials and analysis and comparison with the most used geothermal grouts.
 - c. Selection of the most appropriate heat pump model according to the particular conditions of the geothermal system and location.
- iii. Development of a general sizing geothermal methodology to assess the influence of all the analyzed parameters on the determination of the borehole configuration, total drilling depth and number of boreholes.
- iv. Evaluation of possible green energy integrations to cover the energy demand of an extensive area or district.

I.VI. Structure of the Doctoral Thesis

This Doctoral Thesis is presented in the form of “a compendium of impact scientific articles” published in international journals in accordance with the Doctoral Regulations of the University of Salamanca. It is organized in five Chapters consisting of nine scientific articles published in international high impact journals.

An overall guide of the structure of Chapters and publications is presented in Figure 1.

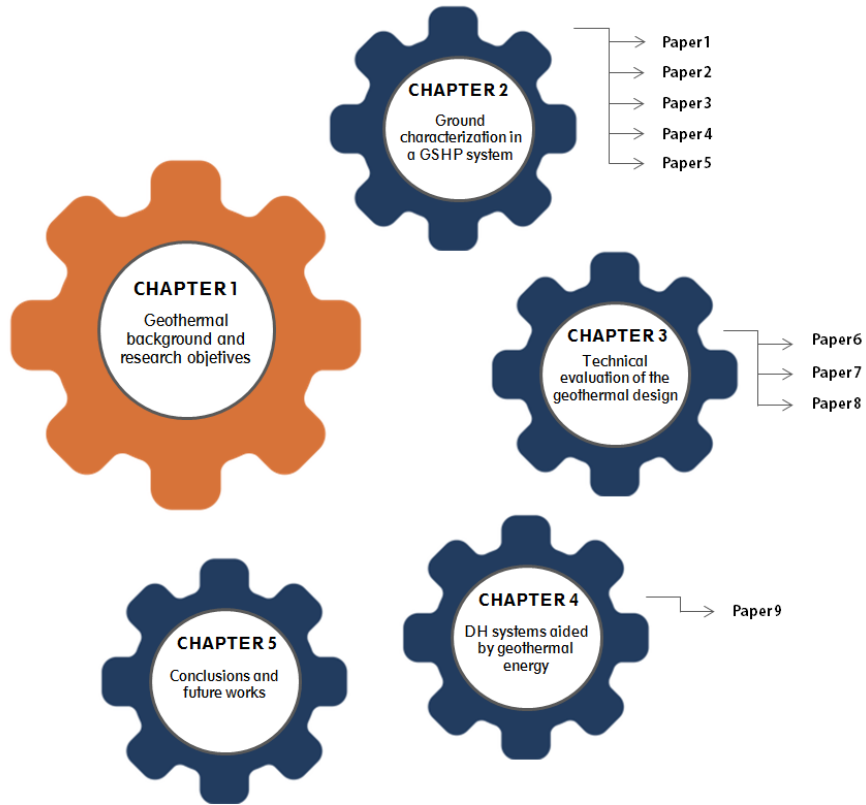


Figure 1. Structure of the present Doctoral Thesis.

- Chapter I: Introduction.
- Chapter II: Ground characterization in a GSHP system.
- Chapter III: Technical evaluation of the geothermal design.
- Chapter IV: DH systems aided by geothermal energy.
- Chapter V: Conclusions and future works.

Additionally, details of the content of each Chapter are presented below.

Chapter I: is an introduction to the overall context of the research topic. It also provides the overall objective and the specific objectives of the dissertation and its structure.

Chapter II: focuses on the first item considered in this dissertation, the estimation of the ground thermal conductivity in a ground source heat pump system. It provides a summary and discussion of a series of laboratory and theoretical solutions to provide the mentioned parameter. In this regard, Paper 1 contains a theoretical method to calculate the global thermal conductivity of the ensemble ground-heat pump. Paper 2 provides a general methodology to experimentally estimate the thermal conductivity of rocky samples. Paper 3 concludes with a thermal conductivity map derived from laboratory measurements. Paper 4 makes use of seismic parameters for the ground thermal characterization. Finally, Paper 5 compares the methodologies included in the previous research works with the results of a Thermal Response Test with the aim of evaluating the validity of the mentioned techniques.

Chapter III: establishes the most efficient configuration parameters in a very low enthalpy system. This Chapter includes Paper 6, which focuses on the analysis and evaluation of different grouting materials, Paper 7 that studies the common heat exchanger designs and their influence on the global operation of the geothermal installation and Paper 8 that addresses the analysis of the heat pump system.

Chapter IV: this Chapter considers the implementation of the very low enthalpy geothermal energy in a district heating system. It underlines the benefits offered by this energy in comparison with the traditional energy sources. Paper 9 is responsible for materializing this aim.

Chapter V: this final Chapter provides a technical discussion based on the results and conclusions deduced from the present Doctoral Thesis. Different open approaches towards the continuity of this research line are also set.

Chapter II
GROUND THERMAL
CHARACTERIZATION IN A
GSHP SYSTEM

II. Ground thermal characterization in GSHP systems

This Chapter describes the fundamentals of the heat transfer in GSHP systems focusing on the influence of the ground thermal conductivity. At the beginning, a review of existing methods for predicting the mentioned parameter is presented. The last part of the Chapter contains the Papers published in high impact journals.

II.1. Fundamentals of the heat transfer process in a GSHP system

In the frame of understanding the behavior of shallow geothermal reservoirs, a proper characterization of their thermal, hydrogeological and environmental properties is mandatory. In this context, thermal conduction is thought to be the dominant heat propagation mechanism involved in the geothermal phenomena. Thermal conductivity of the surrounding materials crucially determines the operation of a GSHP installation, being an essential parameter for the design of these systems. A geothermal system based on a misconception of the real thermal response of the underground may be considered a failure. Thus, ignoring the thermal conductivity of the ground could involve different problems as the soil thermal exhaustion or over sizing of the well loops that means unnecessary investments. With the aim of avoiding the above issues, the extraction rate of a geothermal system must be adapted to the ground thermal conditions so the thermal conductivity must be quantified.

In this context, despite the key role of the ground thermal conductivity in a GSHP system, its quantification is complex and depends on a large number of factors; mineralogical composition and internal structure, water content, temperature, etc. Research methods are mainly divided into two models. The first one is the numerical back analysis method that uses Fourier law to calculate the equivalent thermal conductivity based on the boundary conditions temperature distribution. The second method is the theoretical prediction model that establishes a prediction model of the thermal performance from test results and theory analysis (Pei et al, 2013).

In this area, numerous researches have been focused on the development of techniques that, based on one of the previous methods, allow the determination of the thermal conductivity. Thus, in the estimation of this property, several steady

state and transient techniques have been proposed over time (Lira-Cortés et al, 2008; Ramstad et al, 2009 Barry-Macaulay et al, 2013; Vijdea et al, 2014). Popular devices are the needle probe, the divided bar, the laser flash or the optical thermal conductivity scanner (Jorand et al, 2013), that are usually implemented in the laboratory through specific rock samples (on cores) or in situ.

Within the geothermal context, the most popular active method to evaluate the thermal conductivity of a whole borehole column is the Thermal Response Test (TRT) used for first time in the 1980s (Mogensen, 1983; Raymond, 2018). The traditional TRT method, where heat is injected underground and inlet and outlet temperatures are monitored, has evolved with alternative methodologies. Some variations of this test include the thermal recovery monitoring following heat injection, constant inlet temperature, temperature monitoring by heating cables or heat extraction tests (Raymond, 2018). However, given the high costs involved in the realization of a TRT, its use is not justified in small GSHP systems.

On the basis of the above, a significant proportion of this Thesis has been focused on the development of techniques and procedures regarding the evaluation of the ground thermal conductivity in shallow geothermal installations. All this information is contained in the following Papers.

The first study (Paper 1) considered in this Thesis describes an alternative estimation of the ground thermal conductivity from temperature measurements in a specific borehole, making special reference to the influence of this parameter in the geothermal design. Fourier's heat transfer equation is taken as the principal basis for the corresponding thermal conductivity calculation. Once deduced the thermal conductivity of the ground for several temperature variations and for each one of the hypothesis, geothermal designs were defined using "*Earth Energy Designer*" (EED) software. From the results of this software, the influence of the ground temperature in the thermal conductivity parameter and in the drilling length is analyzed. The study served on the one hand, to validate the constant temperature of the ground from a certain depth. On the other hand, this research offers a theoretical procedure to estimate the thermal conductivity of the ground when methods as the TRT are not available.

Paper 2 is focused on the development of a new procedure to measure the thermal conductivity of soils and rocks. With that aim, an experimental device was

constructed at laboratory scale. Once this device was completely prepared and checked, different tests were made on samples with different geological composition. After the experimental phase, an average thermal conductivity value was obtained for each study sample from the results of each test. Results were then validated according to the commonly accepted thermal conductivity values for each geological formation. Finally, the importance in the geothermal design of an accurate ground thermal conductivity value was highlighted by the use *Earth Energy Design* (EED) software.

The main purpose of Paper 3 is the creation of a thermal conductivity map of the Spanish region of Ávila. To that end, a specific methodology was implemented to analyze, from a thermal point of view, the principal geological formations of the mentioned region. From an initial identification, samples belonging to each geological group were collected and taken to the laboratory. The thermal conductivity of these samples was then measured by the use of KD2 Pro equipment supplied by Decagon Devices. Global test results were then organized to produce the thermal conductivity map of the region of Ávila. As shown in the Paper, a color scale was used to represent the different thermal conductivity ranges. As a result of this work, a valuable tool was created to identify the most appropriate areas for placing a shallow geothermal system. This work also served to highlight the great possibilities of Ávila regarding the use of low enthalpy geothermal energy.

In the context of Chapter II, Paper 4 addresses the prediction of the ground thermal behavior from the use of geophysical methods. *Multichannel analysis of surface waves* (MASW) and *seismic refraction* techniques were applied to determine the propagation velocities of *S* and *P* waves in three different geological formations. At the same time, thermal conductivities of samples with variable alteration ranges were measured through KD 2 Pro device and RK-1 sensor. The final product is the establishment of a correlation between *P* and *S* waves velocities and the thermal conductivity of the materials existing in each area. From these correlations, the Paper finally includes a 2D thermal conductivity section of the ground, that is to say, the evolution of the thermal conductivity parameter in depth for each geological formation considered in the study. Invisible underground phenomena, such as fracturing or heterogeneities thoroughly affect the thermal conductivity in those areas. Since seismic velocities qualitatively include information of the ground, the

mentioned areas are detected and taken into account for the prediction of the global thermal conductivity.

After the suggestion (in the previous research works) of alternative methods to estimate the ground thermal conductivity as a part of a proper shallow geothermal design, the final part of this Chapter is responsible for analyzing their validity. In this way, Paper 5 establishes a comparison between the thermal conductivity results obtained from the methodologies included in the studies described before and the results of a Thermal Response Test. The research work included in this Paper serves to evaluate the technical validity of the mentioned alternative solutions considered as useful tools in all situations in which the realization of a Thermal Response Test is not economically justified.

PAPER 1



Contents lists available at ScienceDirect

Renewable Energy

journal homepage: www.elsevier.com/locate/renene

Analysis of the process of design of a geothermal installation



Cristina Sáez Blázquez*, Arturo Farfán Martín, Pedro Carrasco García,
Luis Santiago Sánchez Pérez, Sara Jiménez del Caso

Department of Cartographic and Land Engineering, University of Salamanca, Higher Polytechnic School of Avila, Hornos Caleros 50, 05003, Avila, Spain

ARTICLE INFO

Article history:
Received in revised form
23 November 2015
Accepted 26 November 2015
Available online xxx

Keywords:
Geothermal
Perforation
Fourier law
Principles of thermodynamics
Earth energy designer

ABSTRACT

The present study shows a new way to calculate a geothermal installation. The process consists in measuring the temperatures inside a perforation. Once we have this parameter, we'll be able to determine the total depth of the perforations in a geothermal installation.

With this method, it'll be possible to dispense with other studies which are being used at the moment in this kind of installations. This fact will mean important economic savings and easier works.

Based on the "Principles of Thermodynamics and Fourier Law", and using the temperature values and other initial data, it was possible to determine the total perforation depth. During this process the software "Earth Energy Designer" was also used.

© 2015 Elsevier Ltd. All rights reserved.

1. Introduction

Geothermal comes from the Greek word "Geos", which means earth, and "Thermos", which signifies heat. Therefore, geothermal energy is the internal heat of the earth. This kind of energy plays an increasingly important role in the field of renewable energies. The main applications of geothermal energy are the production of electrical energy at geothermal plants, the production of SHW (Sanitary Hot Water) and to heat or cool a certain space. The present study has been focused on this last application [1,2,13,14,19].

A conventional geothermal installation used to warm a building up or to produce SHW consists of one or more drillings where a number of pipes are placed. A heat pump carries a fluid situated in these pipes from the inside of the drilling to the building, producing at the same time a transfer of heat from the earth to the building [7,15].

When it's necessary to measure this kind of installation, specific software is usually used to provide data of relevant importance, such as the heat pump power and the length of drilling required. During the process of calculation, this software requests some information from the area where the installation is going to be placed. This information includes the parameter of thermal conductivity of the ground, a coefficient that determines the capacity of

a material to conduct heat.

The determination of the real value of thermal conductivity can be achieved by two different methods: the first one lies in taking samples from different stratum of the hole in order to measure this parameter in the lab. This process could be quite arduous and expensive. The second one is called TRT (Thermal Response Test), which is a test used on the ground to determine the conductivity of the underground heat. This second method consists in applying an amount of heat to the subsoil for a period of 48–72 h. During this time, the temperature at the beginning and of the drilling and the power provided will be measured and stored in a computer to calculate the thermal conductivity. The data obtained by this test are qualitatively greater than the data obtained in the lab because its methodology does not modify the physical parameters of the earth [4].

The main disadvantage of a TRT is related to its price, because doing one of these tests involves a high cost. For this reason the present study has a huge importance because it suggests an alternative solution to calculate the thermal conductivity of the ground with a lower cost.

By measurements of temperatures made in the drilling, it has been possible to determine the thermal conductivity value and the length of drilling required as we will see in a more detailed way throughout this study.

Therefore, the novelty character of the presented method is the way used to determine the thermal conductivity and the following geothermal calculation. It just uses the value of temperature

* Corresponding author.
E-mail address: u107596@usal.es (C.S. Blázquez).

measured inside a hole in order to estimate the conductivity without complex equipment, only a temperature sounding line. The proposed method shows clear differences with respect to the TRT method. They both have the same objective, the calculation of the thermal conductivity; however, there are a lot of different points between them. The next Table 1 presents these differences:

Table 1
Differences between the suggested method and TRT essay.

TRT	Proposed method
Measurement "in situ" of the thermal conductivity parameter. The equipments utilized are complex and require the circulation of water through the pipes placed in a drilling. Data are downloaded into specific software. The duration of the essay fluctuates between 48 and 72 h. The execution of this study means a high cost around 4000–5000 Euros.	Measurement "in situ" of the internal temperature parameter. It uses a temperature sounding line easily placed inside a hole. Data are downloaded into specific software. The essay finishes when the register of temperatures is constant. The price is low given that the equipments used are also quite cheap.

2. Materials and methods

2.1. Method and initial data

The experimental methodology proposed tries to deduce the thermal conductivity parameter of a certain piece of ground. In order to achieve this objective, this study has been based on the "Fourier Law". This law allows us to quantify the heat flow carried in a zone when the temperature distribution in that area is known. It also establishes that the heat flow between two objects is directly proportional to the difference in temperature between them and this flow can travel in only one direction: the heat can only flow from the hottest object to the coldest one. The mechanical paths are conversely reversible: the opposite process can always be imagined. There is a diversity of phenomena that has not been produced by mechanic strengths, but they come from the heat present and accumulation. This part of the Natural Philosophy cannot be explained under dynamic theories; it has particular principles, using a similar method to the rest of sciencea [10,9,11,16].

The expression that materializes this law and has been used to estimate the thermal conductivity is the following one:
Constant Thermal Conductivity (Eq. (1)):

$$K_T = \frac{q_x x}{\Delta T} \quad (1)$$

This equation will be the basis of the calculation of the parameter followed throughout this work. However, in order to succeed in its determination, it is necessary to know the elements included in the mentioned equation. These elements are: Heat or flow transfer rate (q_x), Distance (x) and the Temperature Differential (ΔT).

A series of data common in every process of calculation of a geothermal installation are required to deduce the three parameters involved in the Equation (1) which will make the estimation of the thermal conductivity possible. Given that this study is general and not related to any specific installation, some values considered as usual in a geothermal installation will be initially used. Nevertheless, when this method is applied to a particular case, as it will be described in the Section 4 "Discussion", the real values will be used and the calculation will be carried out similarly to the ones explained along this work.

In this way, the initial data proposed are:

- The initial drilling depth supposed is 90 m.
- The diameter of the holes considered is 200 mm.
- Every hole has a double-U polyethylene pipe. According to the "Second Law of Thermodynamics" there is heat transfer from

the geothermal pipes to the ground, so finally they both reach the same temperature.

- The diameter of the supposed pipes is 32 mm.
- The distance between pipes in the same hole is 35 mm.

Once estimated those values, the next step to determine each of

the already mentioned parameters that are part of the equation (1).

> Heat or flow transfer rate (q_x)

In the first place, to establish the heat transfer rate (q_x) expressed in W/m^2 , it is necessary to specify what type of geothermal installation is going to be used, as it was said before, this work is an experimental test that is not related to any specific building, so, three different hypotheses recounted to three dwellings of $90 m^2$, $130 m^2$ y $360 m^2$ will be selected. The firm "Vaillant" has established the power of the heat pumps required to warm those buildings up. Every calculation included in this work will be made for each of these three hypotheses.

The next table (Table 2) shows the three heat pumps that supply the thermal needs of three dwellings of $90 m^2$, $130 m^2$ and $360 m^2$:

Table 2
Relation between dwelling m^2 and heat pump power [18].

Dwelling (m^2)	90	130	360
Total Power pump (W)	5900	8100	21100
Number of holes	1	1	3
Power pump per hole (W)	5900	8100	7033

According to this table, those values represent the heat transfer rate usually named with the letter "Q" whose units are watts (W). But, as the equation (1) shows, the parameter needed is the heat transfer rate per unit of area (q_x). Therefore, the area must be considered to obtain q_x from Q.

In this way, as it can be observed below, the equation (1), basis of the current study, can be also expressed including the parameters "Q" and "A" (Eq. (2)) instead of " q_x " (Eq. (1)).

$$K_T = \frac{q_x x}{\Delta T} \quad (1) \sim K_T = \frac{Q x}{A \Delta T} \quad (2)$$

Thus, equations (1) and (2) are identical, the only difference is that equation (1) is expressed using " q_x " and equation (2) "Q". However, in this case, it deals with a specific geometric configuration constituted by two parallel pipes, for this reason, to calculate " q_x "; another parameter must be had in mind to get to know the mentioned area "A". This parameter is known as form factor (S) and will be used to obtain " q_x ".

The form factor of two parallel pipes, (given that the ones supposed are double-U pipes) follows the next expression (Eq. (3)) [6].

$$S = \frac{2\pi L}{([\text{COSH}^{-1}]) \frac{(4Z^2 - D_1^2 - D_2^2)}{(2D_1 \cdot D_2)}} \quad (3)$$

Where: L is the pipe length; Z is the distance between pipes and D is the geothermal pipes diameter. Therefore, in this case, those parameters are: $L = 90$ m, $Z = 35$ mm and $D_1 = D_2 = 32$ mm.

Substituting values, the form factor (S) obtained is 658.01 m. For the three hypotheses studied, this form factor is the same because the pipes are identical and the power of the heat pumps is not used in its calculation.

By the calculation of this factor, only one of the two dimensions of the plane is being evaluated. Nevertheless, given that $L \gg D_1, D_2, z$, the remaining dimension that should be considered is so small in comparison with the first one that it can be regarded as void, being thus disregarded. In this way, the area used in the calculation of q_x has a value of 658.01 m².

Once known the power of the pumps and the area, it is possible to deduce the heat transfer per unit of area (q_x) for each one of the hypotheses. The next Table 3 shows these results:

	Heat pump power "Q" (W)	Heat transfer rate "qx" (W/m ²)
Dwelling 1	5900	8.96
Dwelling 2	8100	12.31
Dwelling 3	7033	10.68

> Distance (x):

This distance is the total drilling depth, as it was seen before; the initial distance considered is 90 m.

> Temperature Differential (ΔT):

The other parameter that takes part in the equation (1) is the temperature inside the hole. It is not a known value so a temperature sounding line is required to get that data in a concrete way. Depending on the area where the hole is placed, this value of

temperature will be different. Given that in the beginning the study is not focused on a certain drilling, it is necessary to take an interval of temperature that allows covering different possibilities of calculation, for that reason the interval comprises temperatures from 2 °C to 30 °C. At the end of this work, the method will be applied to a specific hole where the temperature will be measured inside. Once known the value of this parameter, it will be possible to determine simultaneously and thanks to this procedure the thermal conductivity of that ground.

Once these three parameters are known, the next step is to calculate the thermal conductivity using the equation (1) as it will be described in the section 3 "Results" where that parameter will be obtained for each heat pump and for each datum of temperature contained in the interval 2 °C and 30 °C.

In this way, this parameter will be got without a TRT study, with a temperature sounding line which will reduce significantly the price of the process managing the principal objective of the present work.

Once they are certain, the values of thermal conductivity for each datum of temperature and each heat pump, they are entered into the software "Earth Energy Designer". Using this programme, we are able to obtain the total drilling depth for each assumption, that is, for each value of thermal conductivity and heat pump.

In this way, this method proposes tables so that, knowing the value of temperature inside a hole, we can determine the parameter of thermal conductivity making the process of calculation of a geothermal installation faster and easier.

2.2. Materials

For practical purposes, the temperature record inside a hole is considered estimated by the periodic measurement of a temperature recorder suitable to work in presence of water and another one capable of working in a drilling without water. Fortunately, this

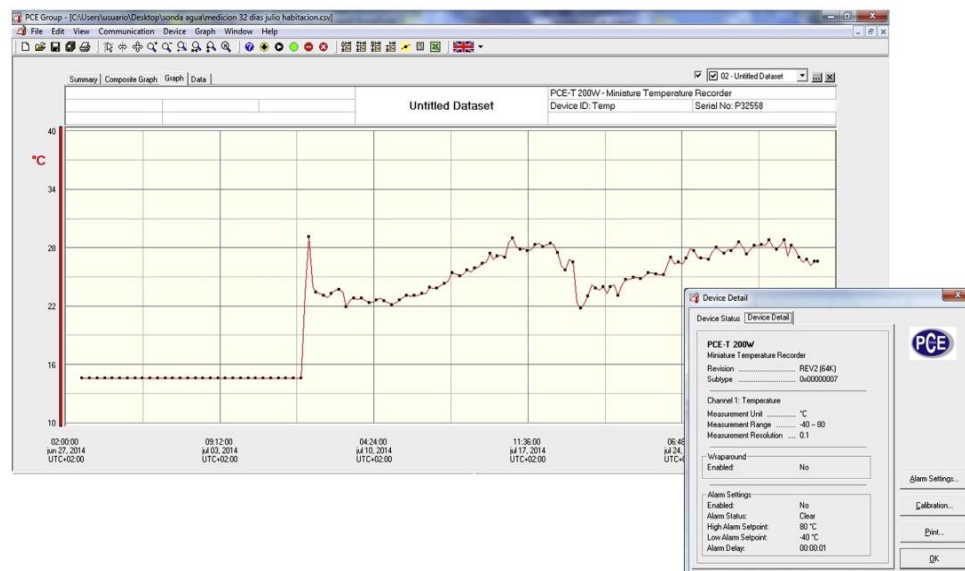


Fig. 1. Temperature graphic obtained by the register.

equipment is able to download the data to specific software (PCE Group 2.06), which makes these data available in a graphic way directly. This equipment will be used to measure the temperature in a certain hole with the goal of applying the suggested method (Fig. 1).

On the other hand, in order to complete this study, it has also been necessary to use design software of a geothermal installation, the programme mentioned above "Earth Energy Designer" (EED). This software allows us to establish the most important parameters of these kinds of installations: the number of holes and the drilling depth. This programme has been developed by "Blocon Software". The mathematical work of [8] and [12] concerning borehole field heat movement and storage is the basis for the calculations performed by the software, EED (Fig. 2).

drilling length [5].

Therefore, on the one hand, the input data required by the software are parameters from the ground in question like the thermal conductivity, annual medium temperatures of the area, as well as the energetic demand of the building or parameters of the installation such as the drilling diameter, the type of geothermal pump and pipes. On the other hand, the outputs of the software are the total drilling depth required in the geothermal installation, the number of holes and the depth of those drillings.

After concluding the description of the procedure purpose of this paper, the method will be applied in a certain hole as an example. The execution of the drilling took place on 11th March 2014.

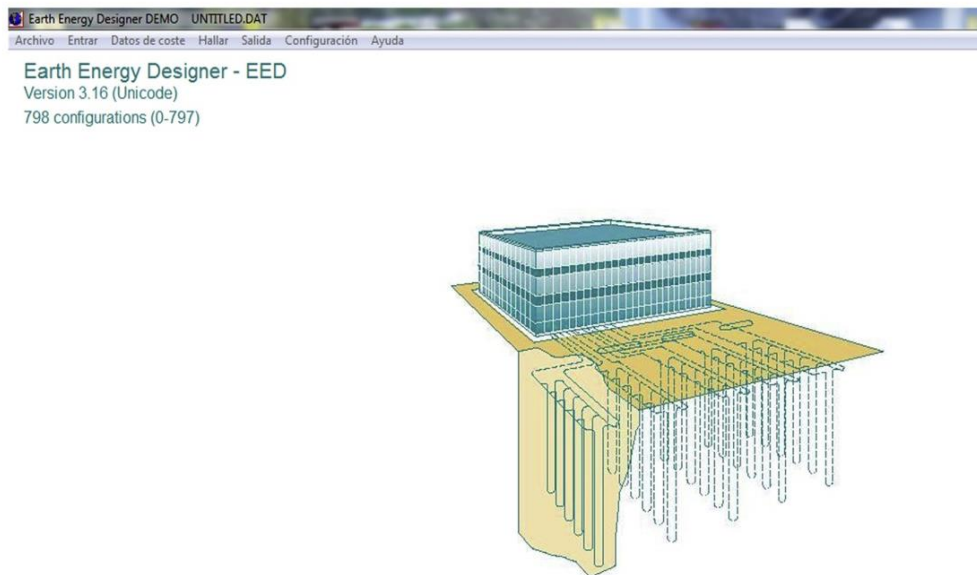


Fig. 2. Principal window "Earth Energy Designer" (Building Physics).

During the process of calculation of this software, a series of characteristic data of the ground, where the geothermal installation is going to be set up, must be introduced. One of these required data is the thermal conductivity that will be estimated with the present study.

Other parameters requested by the software are: the drilling diameter, type of geothermal pipe, type of working fluid and the energetic demand corresponding to the power of each heat pump.

Once these data are introduced, the programme proceeds to estimate the number of holes required in the geothermal installation as well as the drilling depth. Once the optimization process has finished, this software offers us different solutions, the first of them being the most suitable one, that is to say, the one with the least

The mentioned drilling has the next characteristics:

- Location: province of Avila (Spain)
- UTM coordinates:

$$X = 358.017 \quad Y = 4.501.350.$$

- Hole diameter: 220 mm
- Drilling length: 90 m
- Drilling method: Rotary percussive drilling with hammer.
- Exploitation of the resource: study of temperature on it.

The following images show the whole drilling process (Figs. 3–5):



Fig. 3. Stage 1. Drilling. (a) Positioning of the drilling machine. (b) First meters drilled. (c) Adding new drilling rods.



Fig. 4. Stage 2. Piped. (a) Piping the first meters. (b) Joining pipes with different tools.



Fig. 5. Stage 3. (a) Placing of the manhole. (b) Closing of the hole.

2.3. Test procedure

The proposed method allows us to analyze the variations of the drilling depth required in a geothermal installation according to the value of thermal conductivity of the ground in question.

The study has been carried out following the next procedure:

- Selection of three heat pumps “Vaillant” with different powers to carry out the present work.
- Estimation of a series of initial data, characterization of the drilling and the geothermal pipes.
- Selection of a range of temperatures given that the temperature inside the hole will not be the same everywhere, it will fluctuate in the supposed range.
- Calculation of the thermal conductivity for each value of temperature, applying the “Fourier Law”.
- Once this parameter has been estimated, the next step will be the calculation of the drilling depth using the software “Earth Energy Designer” for different values of thermal conductivity.
- Upon finishing this process of calculation, we will finally compare the variation of temperature of the subsoil with its thermal conductivity and the variation of the drilling depth with the thermal conductivity for each supposed case.

3. Results

The Tables (4–6) show the values of thermal conductivity in W/mk obtained for each value of temperature included in the interval of 2 °C to 30 °C for each of the three heat pumps considered. These values have been calculated using the equation 1 based on the Fourier Law. Once obtained the values of thermal conductivity, they have been evaluated by comparing them with the normal values of conductivity of a granitic ground because the study has been made on that kind of land. Since the thermal conductivity of a granitic ground fluctuates around 3 W/mK and the values of the tables change around 2–4 W/mK, the validity of the data is demonstrated.

Table 4
Thermal conductivities corresponding to the heat pump of 5.9 Kw.

Dwelling 1		
Area: 90 m ²	Pipe Diameter: 32 mm	
Pump Power: 5.9 kW	Form Factor (S) = 658.01	
Number of holes: 1	Distance between pipes in the hole (z) = 35 mm	
Distance (x): 90 m	Heat Transfer Speed (qx): 8.96 W/m ²	
Temperature increase (ΔT) °C	Temperature increase (ΔT) K	Thermal conductivity (k) W/mk
2	275.15	2.93
4	277.15	2.91
6	279.15	2.89
8	281.15	2.87
10	283.15	2.85
12	285.15	2.83
14	287.15	2.81
16	289.15	2.79
18	291.15	2.77
20	293.15	2.75
22	295.15	2.73
24	297.15	2.71
26	299.15	2.70
28	301.15	2.68
30	303.15	2.66

Table 5
Thermal conductivities corresponding to the heat pump of 8.1 Kw.

Dwelling 2		
Area: 130 m ²	Pipe Diameter: 32 mm	
Pump Power: 8.1 kW	Form Factor (S) = 658.01	
Number of holes: 1	Distance between pipes in the hole (z) = 35 mm	
Distance (x): 90 m	Heat Transfer Speed (qx): 12.31 W/m ²	
Temperature increase (ΔT) °C	Temperature increase (ΔT) K	Thermal conductivity (k) W/mk
2	275.15	4.03
4	277.15	4.00
6	279.15	3.97
8	281.15	3.94
10	283.15	3.91
12	285.15	3.89
14	287.15	3.86
16	289.15	3.83
18	291.15	3.81
20	293.15	3.78
22	295.15	3.75
24	297.15	3.73
26	299.15	3.70
28	301.15	3.68
30	303.15	3.65

Table 6
Thermal conductivities corresponding to the heat pump of 21.1 Kw.

Dwelling 3		
Area: 360 m ²	Pipe Diameter: 32 mm	
Pump Power: 21.1 kW	Form Factor (S) = 658.01	
Number of holes: 3	Distance between pipes in the hole (z) = 35 mm	
Distance (x): 90 m	Heat Transfer Speed (qx): 10.68 W/m ²	
Temperature increase (ΔT) °C	Temperature increase (ΔT) K	Thermal conductivity (k) W/mk
2	275.15	3.49
4	277.15	3.47
6	279.15	3.44
8	281.15	3.42
10	283.15	3.39
12	285.15	3.37
14	287.15	3.35
16	289.15	3.32
18	291.15	3.30
20	293.15	3.28
22	295.15	3.26
24	297.15	3.23
26	299.15	3.21
28	301.15	3.19
30	303.15	3.17

It should be clarified that the temperature values are reported in Celsius Degrees because the temperature sounding line measures in these unities and also in Kelvin given that, that is the unity used at the International System.

The next Tables (7–9) show for different values of thermal conductivity, the results of depth drilling obtained by the software “Earth Energy Designer” for each heat pump considered.

In the Figs. 6–8 we can see in a graphic way the relations between temperature-thermal conductivity and depth-thermal conductivity.

Finally, the next tables contain, for each heat pump, a summary of the aim pursued in the present work, that is, from a value of

Table 7 C.S. Blázquez et al. / Renewable Energy 89 (2016) 1–12
 Calculation with "Earth Energy Designer" for the heat pump of 5.9 Kw.

Pump 1					
Power Pump: 5.9 kW					
Number of Holes: 1					
Form factor (S)	Heat transfer speed (qx)W/m ²	Thermal conductivity (W/mK)	Depth (m)	Temperature (K)	Temperature (°C)
701.87	8.41	1.5	96	537.99	264.84
679.93	8.68	1.6	93	504.37	231.22
665.31	8.87	1.7	91	474.70	201.55
650.69	9.07	1.8	89	448.33	175.18
628.76	9.38	1.9	86	424.73	151.58
621.44	9.49	2	85	403.50	130.35
606.82	9.72	2.1	83	384.28	111.13
592.20	9.96	2.2	81	366.81	93.66
577.58	10.22	2.3	79	350.87	77.72
570.27	10.35	2.4	78	336.25	63.10
562.96	10.48	2.5	77	322.80	49.65
548.33	10.76	2.6	75	310.38	37.23
541.02	10.91	2.7	74	298.89	25.74
533.71	11.05	2.8	73	288.21	15.06
526.40	11.21	2.9	72	278.27	5.12
519.09	11.37	3	71	269.00	-4.15
511.78	11.53	3.1	70	260.32	-12.83
504.47	11.70	3.2	69	252.18	-20.97
497.16	11.87	3.3	68	244.54	-28.61
489.84	12.04	3.4	67	237.35	-35.80
482.53	12.23	3.5	66	230.57	-42.58
475.22	12.42	3.6	65	224.16	-48.99
475.22	12.42	3.7	65	218.11	-55.04
467.91	12.61	3.8	64	212.37	-60.78
460.60	12.81	3.9	63	206.92	-66.23
453.29	13.02	4	62	201.75	-71.40
453.29	13.02	4.1	62	196.83	-76.32
445.98	13.23	4.2	61	192.14	-81.01
445.98	13.23	4.3	61	187.67	-85.48
438.67	13.45	4.4	60	183.41	-89.74
438.67	13.45	4.5	60	179.33	-93.82

Table 8
 Calculation with "Earth Energy Designer" for the heat pump of 8.1 Kw.

Pump 2					
Power Pump: 8.1 kW					
Number of Holes: 1					
Form factor (S)	Heat transfer speed (qx)W/m ²	Thermal conductivity (W/mK)	Depth (m)	Temperature (K)	Temperature (°C)
943.13	8.59	1.5	129	738.60	465.45
921.20	8.79	1.6	126	692.44	419.29
899.27	9.01	1.7	123	651.71	378.56
877.33	9.23	1.8	120	615.50	342.35
862.71	9.39	1.9	118	583.11	309.96
840.78	9.63	2	115	553.95	280.80
826.16	9.80	2.1	113	527.57	254.42
811.53	9.98	2.2	111	503.59	230.44
796.91	10.16	2.3	109	481.70	208.55
782.29	10.35	2.4	107	461.63	188.48
767.67	10.55	2.5	105	443.16	170.01
760.36	10.65	2.6	104	426.12	152.97
745.73	10.86	2.7	102	410.33	137.18
731.11	11.08	2.8	100	395.68	122.53
723.80	11.19	2.9	99	382.04	108.89
716.49	11.31	3	98	369.30	96.15
701.87	11.54	3.1	96	357.39	84.24
694.56	11.66	3.2	95	346.22	73.07
687.24	11.79	3.3	94	335.73	62.58
679.93	11.91	3.4	93	325.85	52.70
672.62	12.04	3.5	92	316.54	43.39
665.31	12.17	3.6	91	307.75	34.60
658.00	12.31	3.7	90	299.43	26.28
650.69	12.45	3.8	89	291.55	18.40
643.38	12.59	3.9	88	284.08	10.93
636.07	12.73	4	87	276.98	3.83
628.76	12.88	4.1	86	270.22	-2.93
621.44	13.03	4.2	85	263.79	-9.36
614.13	13.19	4.3	84	257.65	-15.50
614.13	13.19	4.4	84	251.80	-21.35
606.82	13.35	4.5	83	246.20	-26.95

Table 9
Calculation with "Earth Energy Designer" for the heat pump of 21.1 Kw.

Pump 3					
Power Pump: 21.1 kW					
Number of Holes: 3					
Form factor (S)	Heat transfer speed (qx)W/m ²	Thermal conductivity (W/mK)	Depth (m)	Temperature (K)	Temperature (°C)
899.27	7.82	1.5	123	641.31	368.16
877.33	8.02	1.6	120	601.22	328.07
855.40	8.22	1.7	117	565.86	292.71
833.47	8.44	1.8	114	534.42	261.27
818.84	8.59	1.9	112	506.29	233.14
804.22	8.75	2	110	480.98	207.83
789.60	8.91	2.1	108	458.08	184.93
774.98	9.08	2.2	106	437.25	164.10
760.36	9.25	2.3	104	418.24	145.09
745.73	9.43	2.4	102	400.82	127.67
731.11	9.62	2.5	100	384.78	111.63
716.49	9.82	2.6	98	369.98	96.83
701.87	10.02	2.7	96	356.28	83.13
694.56	10.13	2.8	95	343.56	70.41
679.93	10.34	2.9	93	331.71	58.56
672.62	10.46	3	92	320.65	47.50
658.00	10.69	3.1	90	310.31	37.16
650.69	10.81	3.2	89	300.61	27.46
643.38	10.93	3.3	88	291.50	18.35
636.07	11.06	3.4	87	282.93	9.78
628.76	11.19	3.5	86	274.85	1.70
614.13	11.45	3.6	84	267.21	-5.94
606.82	11.59	3.7	83	259.99	-13.16
599.51	11.73	3.8	82	253.15	-20.00
592.20	11.88	3.9	81	246.66	-26.49
592.20	11.88	4	81	240.49	-32.66
584.89	12.02	4.1	80	234.62	-38.53
577.58	12.18	4.2	79	229.04	-44.11
570.27	12.33	4.3	78	223.71	-49.44
562.96	12.49	4.4	77	218.63	-54.52
555.64	12.66	4.5	76	213.77	-59.38

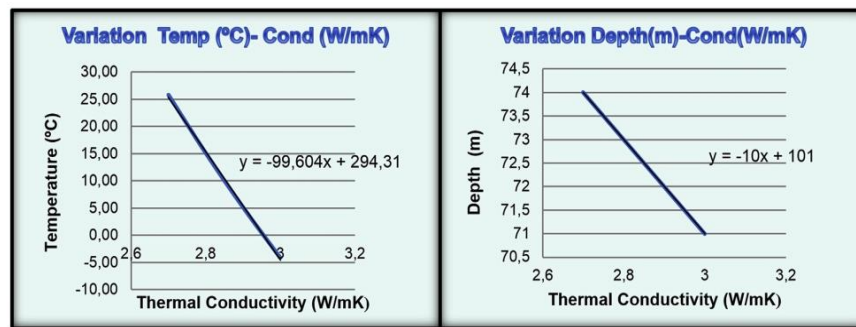


Fig. 6. Comparative temperature-thermal conductivity and depth-thermal conductivity (Pump 1).

temperature measured in the area in question, it has been possible to obtain directly the value of thermal conductivity of that piece of ground and the drilling depth required.

4. Discussion

As shown in the Tables (4–6), a different value of thermal conductivity has been obtained for each value of temperature, that is to say, the value of thermal conductivity in the ground depends

on the temperature registered in that ground. As we can see, when the temperature increases, the thermal conductivity decreases, that is, they are inversely proportional (as expected according to Fourier equations).

In the following Tables (7–9) there is a first estimation of the drilling depths obtained with the program "Earth Energy Designer". As we can see, the relation between the drilling depth and the thermal conductivity is inversely proportional too. As the thermal conductivity grows, the drilling depth required reduces. However,

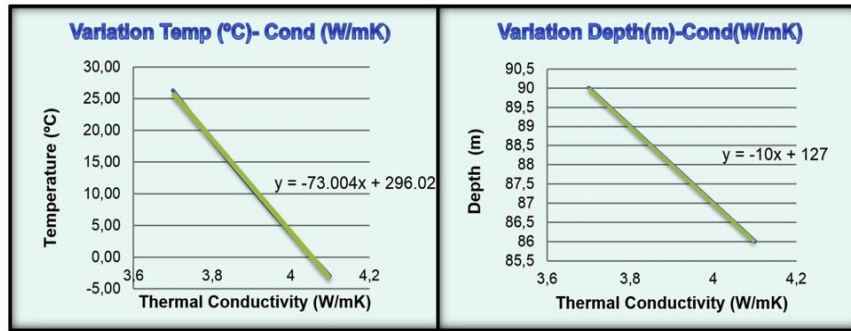


Fig. 7. Comparative temperature-thermal conductivity and depth-thermal conductivity (Pump II).

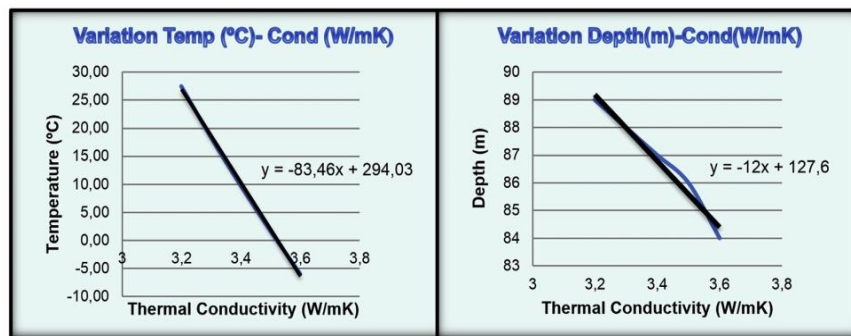


Fig. 8. Comparative temperature-thermal conductivity and depth-thermal conductivity (Pump III).

when the temperature of the ground decreases, the drilling depth also does so, thus, there is a directly proportional relationship between them.

Finally, the last Tables 10–12 provide for each heat pump the existing relations between the temperature registered inside the

hole, the thermal conductivity of that ground and the depth to be drilled. In this way, the process of calculation of a geothermal installation is solved without the need to turn to more expensive procedures.

Table 10
Relation temperature-conductivity-depth (Pump I).

Pump 1			
Temperature (K)	Temperature (°C)	Thermal conductivity (W/mK)	Depth (m)
297.15	24	2.71	73.94
295.15	22	2.73	73.74
293.15	20	2.75	73.54
291.15	18	2.77	73.34
289.15	16	2.79	73.14
287.15	14	2.81	72.94
285.15	12	2.83	72.74
283.15	10	2.85	72.54
281.15	8	2.87	72.34
279.15	6	2.89	72.14
277.15	4	2.91	71.94
275.15	2	2.93	71.74
273.15	0	2.95	71.54
271.15	-2	2.97	71.33
269.15	-4	2.99	71.13

Table 11
Relation temperature-conductivity-depth (Pump II).

Pump 2			
Temperature (K)	Temperature (°C)	Thermal conductivity (W/mK)	Depth (m)
297.15	24	3.73	89.85
295.15	22	3.75	89.58
293.15	20	3.78	89.30
291.15	18	3.81	89.03
289.15	16	3.84	88.76
287.15	14	3.86	88.48
285.15	12	3.89	88.21
283.15	10	3.92	87.94
281.15	8	3.95	87.66
279.15	6	3.97	87.39
277.15	4	4.00	87.11
275.15	2	4.03	86.84
273.15	0	4.05	86.57
271.15	-2	4.08	86.29
269.15	-4	4.11	86.02

Table 12
Relation temperature-conductivity-depth (Pump III).

Pump 3			
Temperature (K)	Temperature (°C)	Thermal conductivity (W/mK)	Depth (m)
297.15	24	3.24	88.89
295.15	22	3.26	88.61
293.15	20	3.28	88.32
291.15	18	3.31	88.03
289.15	16	3.33	87.74
287.15	14	3.36	87.46
285.15	12	3.38	87.17
283.15	10	3.40	86.88
281.15	8	3.43	86.59
279.15	6	3.45	86.31
277.15	4	3.48	86.02
275.15	2	3.50	85.73
273.15	0	3.52	85.44
271.15	-2	3.55	85.16
269.15	-4	3.57	84.87

4.1. Practical example

As a practical application of the whole process exposed throughout this study, the temperature inside a drilling has been registered in a specific area of the province of Ávila.

It is a 90 m deep drilling located in an eminently granitic area. A part of this hole is taken up by water.

The register of temperature has been made at a depth of 45 m by a recorder suitable to work in the presence of water. The next figure displays an image of it (Fig. 9).

The register of temperature in the mentioned depth of 45 m has been carried out three times a day, that is to say, every 8 h over a prolonged period in order to cover different months of the year, from the hottest months to the coldest ones.

The results obtained show a constant value of temperature of 14.6 °C (values of 14.5 °C and 14.7 °C have been obtained only eight times) in that depth regardless of external atmospheric conditions, that is, that value of temperature is not influenced by the different seasons in which we are.

By way of example, the following graphics show the results of the temperature recorder in a hot period like the month of June and in another colder period from October to December. In the rest of the months the results have been the same (Figs. 10 and 11).

Given that no physical quantity can be measured with perfect certainty, there are always errors in any measurement. This means that if we measure some quantity and, then, repeat the measurement, we will almost certainly measure a different value the second time.

When a measurement is repeated several times, the measured values are grouped around some central value. This grouping or distribution can be described with two numbers: the mean, which measures the central value, and the standard deviation which describes the spread or deviation of the measured values about the mean.

For a set of N measured values for some quantity x , the mean of x is represented by the symbol $\langle x \rangle$ and is calculated by the following formula (Eq. (4)):

$$\langle x \rangle = \frac{1}{N} \sum_{i=1}^N x_i = \frac{1}{N} (x_1 + x_2 + x_3 + \dots + x_{N-1} + x_N) \quad (4)$$

Where x_i is the i -th measured value of x . The mean is simply the sum of the measured values divided by the number of measured values.

The standard deviation of the measured values is represented by



Fig. 9. Recorder PCE-T 200 W.

the symbol σx and is given by the formula (Eq. (5)) [3,17].

$$\sigma x = \sqrt{\frac{1}{N-1} \sum_{i=1}^N (x_i - \langle x \rangle)^2} \quad (5)$$

In this case, the total number of measured values of temperature is 163, that is to say, $N = 163$, of those measurements, the value 14.5 °C was measured 6 times, the value 14.6 °C 155 times and finally the value 14.7 °C only 2 times. With these data, the above equations are solved following (Eq. (6)):

$$\langle T \rangle = \frac{1}{163} (2263 + 29.4 + 87) \sim 14.6 \text{ °C} \quad (6)$$

The standard deviation is given by (Eq. (7)):

$$\sigma_T = \sqrt{\frac{1}{163-1} \sum_{i=1}^{163} (T_i - 14.6)^2} = 0.022 \text{ °C} \quad (7)$$

Thus, the difference between the average and the considered value of the temperature in that extent of the subsoil differ for a quantity lower than the measure precision.

Once the temperature in the area of study is known, we can establish by the (Tables 10–12), the thermal conductivity of the ground and the drilling depth required in the installation for each hypothesis (the three geothermal heat pumps with different

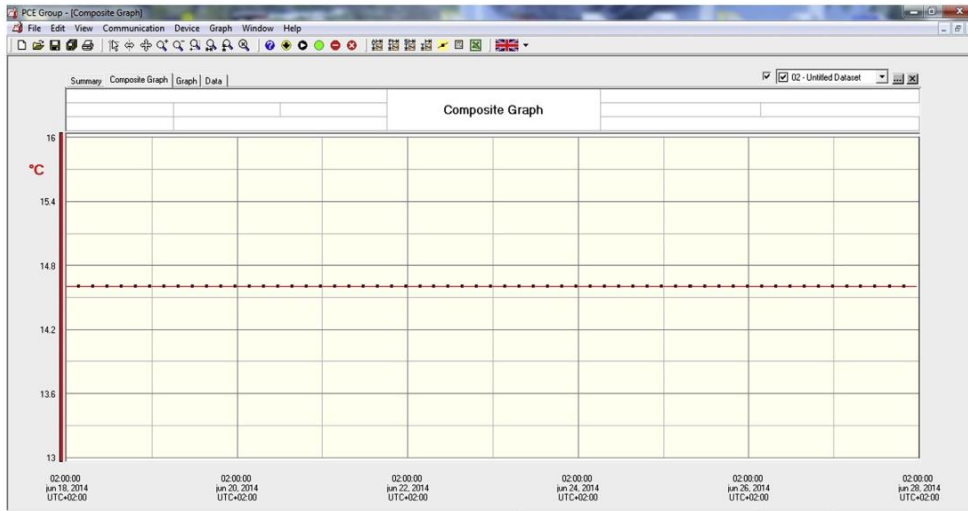


Fig. 10. Register of temperatures in the month of June.

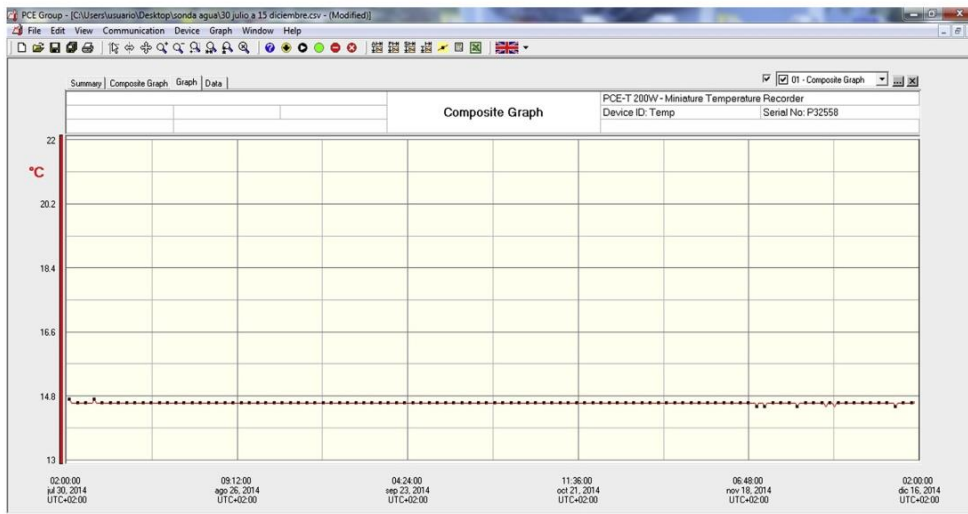


Fig. 11. Register of temperatures from October to December.

powers).

The Table 13 includes the results mentioned.

It is important to remember that in the case of pump 3, three drillings will be needed, so there will be three holes of 87.52 m

Table 13
Final results for the practical assumption.

	Temperature (K)	Temperature (°C)	Thermal conductivity (W/mK)	Drilling depth (m)
Pump 1	287.75	14.6	2.8	73
Pump 2	287.75	14.6	3.85	88.4
Pump 3	287.75	14.6	3.35	87.4

each one.

5. Conclusions

The present work has presented an experimental methodology to obtain the parameters required in the process of calculation of an installation that uses the geothermal energy.

The results have been achieved by three kinds of geothermal pumps currently on the market. However, this study is applicable to any other pump with different power.

The existing relations between the two most important parameters in this kind of installations, the temperature of the subsoil and its thermal conductivity or the capacity of the ground to carry the heat, have been verified throughout this study. Knowing these relations, we have been able to connect the thermal conductivity with the total drilling depth, in this way the installation is defined.

The explained methodology has proved to be suitable to calculate the real values (given that the initial data are the temperature values measured “in situ”) demanded for the calculation in installation which works with geothermal energy. In this sense, it is possible to apply the suggested method wherever we want and with geothermal pumps different to the ones used in this study.

In the future, the method will be applied to other areas with different types of grounds comparing the results with the ones obtained in the current manuscript.

Acknowledgments

Authors would like to thank the Department of Cartographic and Land Engineering of the Higher Polytechnic School of Avila, University of Salamanca, for allowing us to use their facilities and their collaboration during the experimental phase of this research.

References

- [1] Asim Balbay, Mehmet Esen, Experimental investigation of using ground source heat pump system for snow melting on pavements and bridge decks, *Sci. Res. Essays* 5 (24) (2010) 3955–3966.
- [2] Asim Balbay, Mehmet Esen, Temperature distributions in pavement and bridge slabs heated by using vertical ground-source heat pump systems, *Acta Scientiarum-Technology* 35 (4) (2013) 677–685.
- [3] R. Philip Bevington, Keith Robinson, *Data Reduction and Error Analysis for the Physical Sciences*, 2nd Edition, WCB/McGraw-Hill, 1992.
- [4] Pedro Casanova Pelaez, José Manuel Palomar Carnicero, Rafael López García, Fernando Cruz Peragon, Desarrollo de equipo para la realización de test de respuesta térmica del terreno (TRT) en instalaciones geotérmicas, *Dyna* 89 (2014) 316–324.
- [5] A. Casasso, R. Sethi, Technology and potentiality of geothermal heat pumps, *Geoing. Ambient. Mineraria* 138 (1) (2013) 13–22.
- [6] Yunus A. Cengel, Afshin J. Ghajar, *Heat and Mass Transfer, Fundamentals and Applications*, 2014.
- [7] Mehmet Esen, Tahsin Yuksel, Experimental evaluation of using various renewable energy sources for heating a greenhouse, *Energy Build.* 65 (2013) 340–351.
- [8] P. Eskilson, *Thermal analysis of Heat Extraction Boreholes*, PhD Thesis, Dept. of Mathematical Physics, University of Lund, 1987.
- [9] Jean-Baptiste Joseph Fourier, *Remarques Générales Sur Les Températures Du Globe Terrestre Et Des Espaces Planétaires*, *Ann. de Chimie de Physique* 27 (1824) 136–167.
- [10] Jean-Baptiste Joseph Fourier, *Théorie analytique de la chaleur*, 1822.
- [11] Jean-Baptiste Joseph Fourier, *Mémoire sur les températures du globe terrestre et des espaces planétaires*, *Mémoires l'Académie R. Sci.* 7 (1827) 569–604.
- [12] G. Hellstrom, *Ground Heat Storage: Thermal Analyses of Duct Storage Systems*, Dept. of Mathematical Physics, University of Lund, 1991.
- [13] M. Kabar, W. Nowak, R. Sobanski, *Principles of Exploitation Geothermal Energy Water at Targets of Heating Buildings Project KBN*, 1999.
- [14] K.C. Lee, Classification of geothermal resources by energy, *Geothermics* 30 (4) (2001) 431–442.
- [15] W. Nowak, R. Sobanski, M.M. Kabar, T. Kujawa, *Systems of Recruiting and Exploiting the Geothermal Energy*, Szczecin University of Technology, 2000.
- [16] S.-C. Pei, M.-H. Yeh, Improved discrete fractional Fourier transform, *Opt. Lett.* 22 (14) (1997) 1047–1049.
- [17] R. John Taylor, *An Introduction to Error Analysis: the Study of Uncertainties in Physical Measurements*, 2d Edition, University Science Books, 1997.
- [18] Vaillant Group, *Estimates for the Energy Needs of Each Home*, 2010.
- [19] B. Zheng, J. Xu, T. Ni, M. Li, Geothermal energy utilization trends from a technological paradigm perspective, *Renew. Energy* 77 (2015) 430–441.

PAPER 2

Article

Measuring of Thermal Conductivities of Soils and Rocks to Be Used in the Calculation of A Geothermal Installation

Cristina Sáez Blázquez *, Arturo Farfán Martín, Ignacio Martín Nieto and Diego González-Aguilera

Department of Cartographic and Land Engineering, University of Salamanca, Higher Polytechnic School of Avila, Hornos Caleros 50, 05003 Avila, Spain; afarfan@usal.es (A.F.M.); nachomartin@usal.es (I.M.N.); daguilera@usal.es (D.G.-A.)

* Correspondence: u107596@usal.es; Tel.: +34-67-553-6991

Academic Editor: Jacek Majorowicz

Received: 29 March 2017; Accepted: 6 June 2017; Published: 10 June 2017

Abstract: The thermal conductivity of soils and rocks constitutes an important property for the design of geothermal energy foundations and borehole heat exchange systems. Therefore, it is interesting to find new alternatives to define this parameter involved in the calculation of very low enthalpy geothermal installations. This work presents the development of an experimental set-up for measurements of thermal conductivity of soils and rocks. The device was designed based on the principle of the Guarded Hot Plate method using as heat source a laboratory heater. The thermal conductivity of thirteen rocky and soil samples was experimentally measured. Results are finally compared with the most common thermal conductivity values for each material. In summary, the aim of the present research is suggesting a procedure to determine the thermal conductivity parameter by a simple and economic way. Thus, increases of the final price of these systems that techniques such as the “*Thermal Response Test*” (TRT) involves, could be avoided. Calculations with software “*Earth Energy Designer*” (EED) highlighted the importance of knowing the thermal conductivity of the surrounding ground of these geothermal systems.

Keywords: thermal conductivity; very low enthalpy geothermal installation; Guarded Hot Plate method; Thermal Response Test (TRT); Earth Energy Designer (EED)

1. Introduction

With respect to the lithosphere, heat transfer is produced by thermal conduction; heat diffuses without transfer of matter. Conduction is the principal mechanism of thermal propagation that takes part in the process of thermal exchange in a very low temperature geothermal installation [1].

Thus, the parameter of thermal conductivity (W/mK) plays a fundamental role in these systems. When this value increases, the capacity of the ground to transmit the heat to the components of the installation is also bigger, increasing its efficiency. Therefore, thermal conductivity constitutes a reference to evaluate the speed of the energetic extraction through the geothermal pipes or the dissipation of heat through the ground. For these reasons, it is recommendable to define this parameter to carry out a suitable calculation of a low enthalpy geothermal installation [2–4].

There are many different ways to measure this thermal property. Generally, experimental methods can be grouped into two categories: (i) stable methods, which provide more precise results despite requiring long measurement periods; and (ii) non-stable methods, which stand out for their rapidity, although they offer a lower precision.

Regarding the geothermal field, in practice, tables providing reference values of thermal conductivity for a set of materials are commonly used. In such cases, only approximate values are

used, so the calculation of the installation may not be completely correct. This fact usually causes over-measurements that, in some cases, involve considerable increases of the final cost [5,6].

In large projects, another less frequent practice is the execution of a “Thermal Response Test” (TRT) that allows obtaining “in situ” the thermal conductivity parameter. The test allows studying the behavior of the ground when a constant thermal power is transmitted through the geothermal pipe. It constitutes a suitable solution in spite of the high cost that its realization implies, especially in small installations where a TRT could mean an important increase of the global budget.

Laboratory studies of the thermal conductivity of soils and rocks are usually carried out on samples collected from the ground.

The “Guarded Hot Plate” (GHP) method is the standard technique for measuring thermal conductivity of solid materials in the range from about 0.01 to 15 W/mK [7]. Two main versions of the GHP method can be differentiated: the double-sided (2S-GHP) which implies the use of two identical specimens, and the single-sided (1S-GHP) that only uses one specimen. Different techniques based on this method are used in the laboratory to measure the thermal conductivity of rocky and soil samples [8].

Ramstad et al. [9] designed equipment to measure the thermal diffusivity of rock samples. Thermal conductivity was calculated as a product of density, specific heat capacity and thermal diffusivity. Lira-Cortés et al. [10] implemented a system of thermal conductivity measurement for solid conductive materials. The system measured the thermal conductivity of an aluminum bar using a reference material.

Liou and Tien [11] estimated the thermal conductivity of granite using a combination of techniques, the “Transient Plane Source” (TPS) method [12], the thermal probe method and heat transfer test.

Krishnaiah et al. [13] designed a thermal probe to estimate different thermal properties such as thermal resistivity and diffusivity, and specific heat of rocks.

Kukkonen and Lindberg [14] measured the thermal conductivity of rocks making use of the steady-state divided bar method.

Jorand et al. [15] used the TCS method based on contact-free thermal conductivity scanning of a plane or cylindrical surface [16]. This instrument uses a focused, mobile and continuously operating heat source, together with two infrared temperature sensors at small distances behind and in front of the source, for measuring the thermal conductivity along scanning lines.

Table 1 presents a comparison among the works previously cited and the method proposed in the present study.

As examples of more recent studies, Xiao et al. [17] proposed an analytical model for effective thermal conductivity of nanofluids, while Cai et al. [18] provide a complete review about the recent investigations on the fractal models and fractal-based approaches applied for effective thermal conductivity.

Devices commercially produced to measure this property are numerous at present. As example, the equipment commercially known as KD2-PRO is commonly used to determine the thermal conductivity of different materials including rocks and soils [19,20]. However, most of the equipment is not cheap and the price of the whole geothermal system immediately grows.

The present research offers a description of a thermal conductivity measuring apparatus based on the 1S-GHP (a single-sided guarded hot plate) principle. The aim is to present a new alternative to estimate this parameter making use of usual equipment in a soil science laboratory: a laboratory heater. Throughout this work, we describe a new experimental application of the 1S-GHP method; we apply the method to a set of heterogeneous rocks and soil samples; and we compare these values with the theoretical ones.

The novelty of this study is the combination of both rocks and soils thermal conductivity measurements in the same device. The main strength of the method is the simplicity in the calculation of the thermal conductivity parameter by measuring temperatures in four horizons. The measurement range reaches the thermal conductivity of aluminum, used as reference sample in the current work.

Table 1. Contributions and limitations of past thermal conductivity works.

Authors	Contributions	Limitations
Terzic et al, 2016	The model offers an estimation of the both separate and total parasitic heat fluxes, improving the accuracy and uncertainty of final results.	The method is limited to solid materials with thermal conductivity values from 0.1 to 2 W/mK, in the temperature range 10–50 °C.
Ramstad et al, 2009	The measurement time is around 200 seconds. It allows thermal conductivity measurements up to 4.5 W/mK.	The improved version of this method requires a heat source with constant temperature of 300 °C.
Lira-Cortés et al, 2008	The system is suitable to measure the thermal conductivity of conductive materials with a design error of 2% order.	The method cannot be used in poor conductivity materials given the high design errors
Liou and Tien, 2016	The three techniques provide fairly similar values for the same granite sample. TPS method presents high accuracy and simplicity to sample preparation.	For the thermal probe test, it is difficult to ensure that the air in filled holes is completely removed.
Krishnaiah et al, 2004	The method considers the thermal conductivity variations with the samples porosity.	Trends variations of thermal conductivity with porosity were not established and validated in a standard way.
Kukkonen and Lindberg, 1995	Thermal conductivity is calculated from using the arithmetic, harmonic and geometric mean values and compared with the measured one.	The grain size and the textural variation of some samples affect the thermal conductivity measurements.
Jorand et al, 2013	It combines high-accuracy laboratory measurements and numerical petro physics. They use thermal conductivity scanning for obtaining 2-D thermal conductivity maps reflecting the structural heterogeneity in two samples. Measurements are made in two profiles along the core axis and perpendicular to it. Anisotropy of thermal conductivity is also estimated.	Heterogeneous proportions of lateral heat flow within the sample affect both heat transport in general and the determination of effective thermal conductivity. The method might not solve the entire upscaling problem.
Proposed method	The method allows both rocks and soils thermal conductivity measurements. It also allows thermal conductivity measurements up to the aluminum thermal conductivity. Thermal conductivity results agree with the common values officially accepted for each material.	Long term measurements. It requires a constant ambient temperature to avoid influencing the measurements. Anisotropy is not considered.

2. Materials and Methods

2.1. Description of the Suggested Method

In the laboratory of Rock Mechanics of the Higher Polytechnic School of Avila (Spain), a procedure to determine the thermal conductivity of different samples of rocks and soils was developed.

The method suggests, from two pattern samples (S_{K1} – S_{K2}) with well-known value of thermal conductivity, quantifying this property in any other sample (S) whose value of thermal conductivity wants to be known. A heat source (laboratory heater) that generates a constant heat flow Q_s , was used. This flow goes through the three samples (S_{K1} – S – S_{K2}) placed contiguous as shown in Figure 2. Temperatures are controlled in four horizons (T_1 , T_2 , T_3 , and T_4) by thermocouples (Figure 1). Once these temperatures are stabilized and known, they can be used in the corresponding calculation of the thermal conductivity parameter [21,22].

The cold source equally schematized in Figure 1 represents the temperature of the room where the measurement equipment was placed. It is important to highlight that this cold source was kept constant during the whole process of measurement, given that any variation could involve important changes in the results. Thus, the temperature of the cold source was controlled and set in the value of 296.65 K.

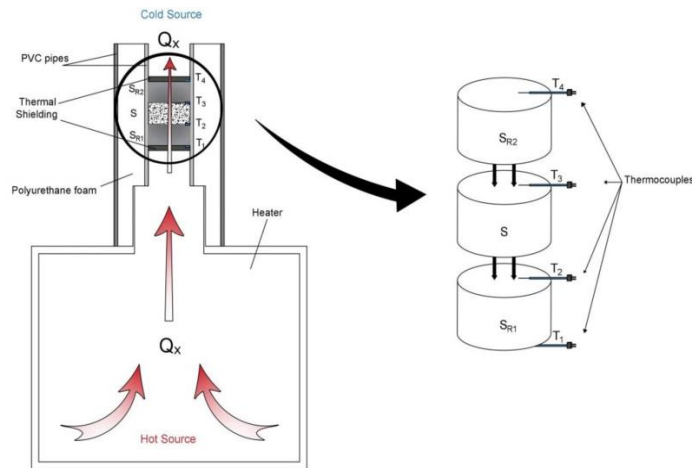


Figure 1. Schema of the suggested method.

2.2. Theoretical Basis

In the system described in Figure 1, the transfer of heat only occurs by conduction with one-dimensional flux and permanent state. The possible convection phenomena were prevented placing two aluminum sheets that behaved as insulations. The action of these sheets made the thermal transfer among the different samples purely conductive. Thermal conductivity is the physical property that controls the conduction of heat in a solid. It is materialized by Fourier's law (Equation (1)) which relates the specific heat flow and the gradient of temperature [23–25]:

$$\dot{Q}_x = -k A \frac{dT}{dx} \quad (1)$$

where \dot{Q}_x = Heat flux in the direction x ; k = Thermal conductivity; A = Area of the transverse section of the conductive object; and $\frac{dT}{dx}$ = Gradient of temperature in the direction x .

If we apply Equation (1) to each one of the samples that are part of the system, the resultant equations are:

$$\begin{aligned} \dot{Q}_1 &= -k_1 A_1 \frac{dT_1}{dx_1} \\ \dot{Q}_2 &= -k_2 A_2 \frac{dT_2}{dx_2} \\ \dot{Q}_3 &= -k_3 A_3 \frac{dT_3}{dx_3} \end{aligned} \quad (2)$$

Heat flux \dot{Q}_x was calculated using temperatures T_1 , T_2 , T_3 and T_4 (when they become steady) and Equation (1). This calculation was possible because of two main facts: the heat flux is constant and thus the same for each of the samples, and we use two reference samples with known thermal conductivity values (S_{R1} and S_{R2}).

From \dot{Q}_x value and considering the steady temperatures, the dimensions of sample S and Equation (1), thermal conductivity of the sample S can be easily calculated [26,27].

Therefore, by the implementation of the procedure detailed in the present paper, it is viable to obtain the value of thermal conductivity of a particular material S .

Equations (1) and (2) can be obtained based on Fourier's law. Heat transport in geo-materials is known of dual-phase-lagging type. It is important to mention that Fourier's law of heat conduction is valid only for some limiting cases, so the method will be limited to those situations.

2.3. Heat Flux Analysis

Until now, the heat flux has been considered as one-dimensional; it only flows in the longitudinal direction. However, after several tests and temperatures analysis, it was experimentally verified that, in spite of the insulation used, there was an additional heat flux in radial direction.

Analyzing temperatures T_1 , T_2 , T_3 and T_4 , it was observed that, through the first pattern sample S_{R1} , a substantial quantity of heat flux is lost as radial flux. As a result, sample S_{R1} was not used in the corresponding thermal conductivity calculations (it was only used as a stabilizing element of the system). The location of this sample minimizes the loss of heat as radial flux in the remaining samples (S and S_{R2}).

Nonetheless, axial heat flux in samples S and S_{R2} must also be considered, because, although smaller, it alters the final results too. To quantify this radial flux, the method was previously used on a sample with known thermal conductivity value. Once this flux was quantified, final thermal conductivity results were exempt from this kind of error.

The distribution of the heat flow is represented in Figure 2.

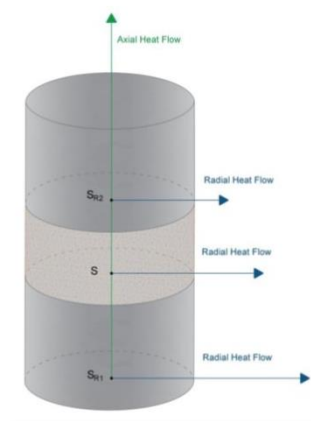


Figure 2. Heat flux distribution.

2.4. Equipment Description

The device designed to measure the thermal conductivity parameter consists of the following components:

- Sterilization and drying heater “Dry-Big” (Figure 3):
Heater with air force circulation mechanism, regulated by a microprocessor and with temperature and time digital reading. It constitutes the heat source used for the calculation of the thermal conductivity parameter.
A set of working temperatures was tested to analyze the evolution of the thermal conductivity with the temperature. Thus, heat source was regulated according to the most suitable temperature.
- PVC pipes (Figure 1):
Two PVC hollow cylinders were used in the construction of the equipment.
 1. Hollow cylinder of diameter slightly higher to the air outlet placed on the top of the heater. This PVC pipe of diameter (0.10 m) coupled to the air outlet was adiabatically insulated in the whole contour by polyurethane foam.

2. Hollow cylinder 0.052 m of diameter, placed inside the previous pipe. It behaves as fastener of the samples. The space between both pipes was adiabatically insulated by polyurethane foam.
- Polyurethane foam (Figure 1):
Polyurethane foam was used to insulate the system from any external influence getting at the same time one-dimensional circulation of the heat flux through the samples.
It is a porous plastic material made up of a bubble aggregation. It consists of the chemical reaction of two polyol and isocyanate, although it accepts multiple additives. Its insulation capacity comes from the low thermal conductivity of the gas that its closed cells send.
 - Pattern samples (Figure 2):
Two reference samples with known thermal conductivity values were used. These samples are made of pure aluminum. Given the high thermal conductivity of this element, it facilitates the heat flux transmission through the system. The dimensions of both patterns are: 0.10 m of thickness and 0.05 m of diameter.
 - Thermocouples (Figure 1):
Four sounding lines (constituted by chrome and aluminum alloys) connected to a digital thermometer made possible the measurement of temperatures in four areas. Before its use, thermocouples were duly calibrated [28].

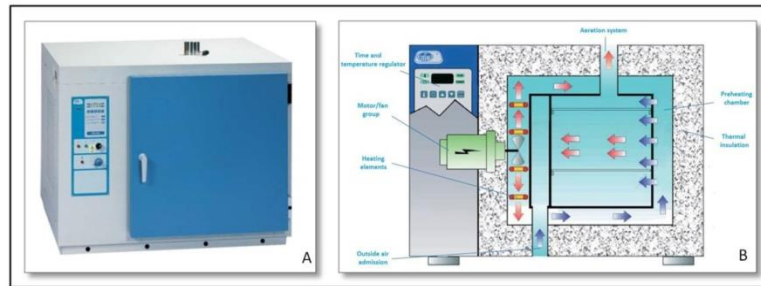


Figure 3. (A) Heater outside view; and (B) heater internal schema.

As explained in Section 2.2, calculations of the thermal conductivity parameter can only be carried out when the four temperatures recorded by the thermocouples keep a constant value over time. Figure 4 shows a graphical example of readings of these sounding lines. After a certain period of time, thermocouples record constant temperature values; these data are the ones used in the calculation of the thermal conductivity of sample S.

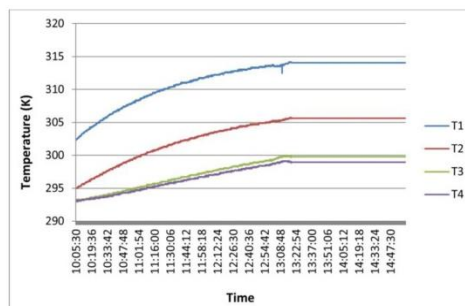


Figure 4. Measuring of temperatures with thermocouples.

First, the PVC pipe of 0.1 m was coupled to the heater air outlet. A central opening was left for the subsequent placement of the second PVC pipe. Space between the first pipe and the opening was filled with polyurethane foam. A pattern sample (S_{R1}) followed the sample whose conductivity wants to be measured (S) and the other pattern sample (S_{R2}) was introduced in the second pipe. After placing thermocouples in the corresponding horizons, the second pipe was placed in the central opening to begin the test.

3. Methodology of the Thermal Conductivity Test

The methodology of the proposed thermal conductivity test includes the next stages.

3.1. Materials Selection

A series of materials (rocks and soil) were selected to carry out the thermal conductivity measurements. These materials have different composition and nature so the study covers a varied geological range, defining with more precision the reliability of the methodology in question.

Table 2 shows the materials used in the study.

Table 2. Materials selected for the test.

Sample	Description
1	Constituted by quartz, feldspar and micas and very varied group of secondary minerals in percentages under 5% like: apatite, esfena, oxides, allanite, zircon, etc. <i>Common Granite</i>
2	Plutonic igneous rock, with more than 65% of silica and more than 20% of quartz. <i>Adamellite</i>
3	Plutonic rock of quartz, plagioclases, potassium feldspar, biotite and amphibole. <i>Granodiorite</i>
4	Igneous rock known as "Bleeding Granite" with a high silica con (more than 80%). <i>Red Granite</i>
5	Thin grain metamorphic rock with sericite, muscovite, chlorite and quartz. <i>Common Slate</i>
6	Hard metamorphic rock composed by quartz (more than 90%), it can also contain muscovite, orthoses or albite. Its structure presents soldered quartz crystals. <i>Quartzite</i>
7	Sedimentary rock with clasts about the size of the sand. The grains have quartz, feldspars or rock fragments. <i>Sandstone</i>
8	Mineral of hydrated calcium sulphate giving mono mineral sedimentary rocks. <i>Gypsum</i>
9	Vitreous volcanic igneous rock. It is grey with silica dioxide, aluminum oxide and other oxides. <i>Pumice</i>
10	Gneiss generated by dynamic metamorphism of eruptive rocks of silica. It is composed by quartz, feldspar and mica. <i>Orto gneiss</i>
11	Metamorphic compact rock with calcium carbonates (more than 90%). It is predominately white. <i>White marble</i>
12	Sandstones (<15% of matrix) whose content in rock fragments is superior to 25% and higher to the feldspar content. Its origin is basaltic, coming from a volcanic igneous rock characteristic for its dark color and mafic structure. <i>Basaltic sandstone</i>
13	Tertiary materials (clays, sands, sandstones and conglomerates) without compaction among the grains. <i>Tertiary Soils</i>

3.2. Samples Preparation

Samples used to test the thermal conductivity equipment, required a specific preparation whether they are rocks or soils.

3.2.1. Rocky Samples

Rocky samples are cylindrical blocks of 0.05 m in diameter and variable thickness. The preparation of these samples was carried out as follows:

Sample extraction (Figure 5): Using a rotating drilling machine equipped with diamond circular crown, it was possible to obtain cylinder blocks of each of the rocky materials. The diameter of these blocks was of 0.05 m and variable thickness depending on the size of the origin rock. During the process of extraction, the crown was cooled by water.

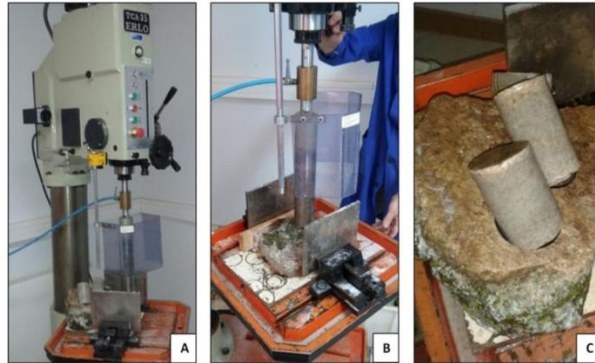


Figure 5. Sample extraction: (A) rock placing; (B) drilling; and (C) final samples.

Carving of samples (Figure 6): Cylinder samples were cut using a cutting-machine supplied with diamond disk to give the samples a certain thickness. Samples of different thickness were prepared, with the aim of analyzing the influence of this factor in the calculation of the thermal conductivity. Thickness of each one of the samples was measured by electronic caliper.

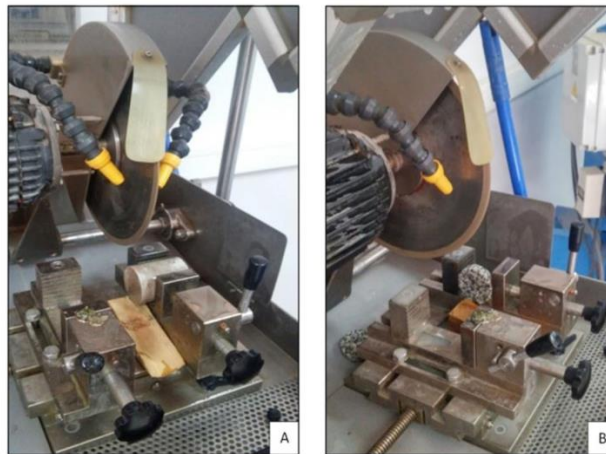


Figure 6. (A) Cutting of a quartzite sample; (B) Cutting of a granitic sample.

Samples cleaning: Samples surfaces were thoroughly cleaned to minimize any possibility of error at the heat transmission. It facilitates the contact with the temperature sounding lines or thermocouples. Figure 7 shows the final appearance of some of these samples.



Figure 7. Samples ready to be used in the suggested equipment.

3.2.2. Soil Samples

Soils materials followed a different procedure to equally get cylinder blocks of 0.05 m in diameter and variable thickness. The preparation of these samples was made according to the next steps.

Determination of humidity by drying in heater [29]: Thermal conductivity depends on the water content that a certain material has, thus, it is important to know the humidity conditions when measuring this parameter. Natural humidity of the soil at its origin was increased by adding a particular percentage of water. The addition of water facilitates the soil compaction in a mold to obtain cylinder samples that will be introduced into the measuring equipment.

Humidity was set to 11.55%.

Soil compaction: As already explained, the proposed system works with cylinder blocks of certain dimensions. Given that, in the case of soils, the material cannot be cut as rocks, it was compacted in a suitable mold. This compaction made easier the obtaining of cylinder samples ready for use in the thermal conductivity device

Soil compaction was made according to the *Proctor Test* conditions, in the point of the optimal humidity defined in the mentioned law [30].

3.3. Placing of Samples in the Measuring Equipment and Determination of Thermal Conductivities

Firstly, one of the aluminum reference samples S_{R1} was introduced in the carrier pipe, then sample S (whose thermal conductivity value wants to be measured) and finally the second aluminum reference sample S_{R2} . It is important to highlight that, before the first reference sample and after the second one, two thin aluminum sheets were placed. The function of these sheets is to get a shielding that avoids convection phenomena. In this way, all the heat transfer just happens by thermal conduction.

Once placed the respective samples and thermocouples in the thermal conductivity equipment, it starts working, sending a constant heat flux that goes through the samples. After letting enough time to make the stabilization of temperatures T_1 , T_2 , T_3 and T_4 , possible, the last step was making the correspondent calculations (as explained by the Section 2.2). Finally, thermal conductivities values of each of the samples were obtained.

Figure 8 shows the measuring equipment expounded over this work and schematized in Figure 1.



Figure 8. Equipment designed to measure thermal conductivities.

4. Analysis of the Measuring Process

Before the measuring of the thermal conductivity parameter in different materials, a series of tests were carried out on the same rocky sample (granite). They were used to analyze how the thermal conductivity changes with the heater temperature and the thickness of the sample in question (5).

These tests allowed the establishment of the appropriate working conditions (temperature of the heat source and sample thickness) to be used in the subsequent measuring of thermal conductivities of the samples presented in Table 2.

4.1. Evolution of the Thermal Conductivity with Temperature

In a crystalline solid, thermal conductivity depends on temperature; however, this dependence is not homogeneous. This dependence can be divided in four regions, so the variation of conductivity will be different based on the region where it is. In region I, of low temperature ($T \leq 20$ K), thermal conductivity quickly increases with temperature, being proportional to T^3 . In region II, it achieves a maximum value, usually at a temperature close to $T \approx \theta_D/20$ (where θ_D is the Debye's temperature). At higher temperatures, in region III, thermal conductivity decreases proportionally to T^{-1} . Finally, at very high temperatures ($T \geq \theta_D$) in region IV, it stops being dependent on temperature [31,32].

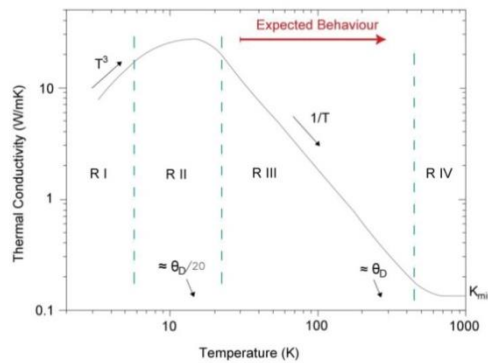
In this particular case, to analyze the behavior of the thermal conductivity with the temperature, the region where the present study is must be defined. To that end, in the first place, Debye's temperature was determined. Table 3 shows the values of Debye's temperatures for a series of substances.

The substance in Table 3 with the most similar composition to the studied material (granite) is silica. It has a Debye's temperature of 645 K, so that, if $T \approx 645 \text{ K}/20 = 32.25 \text{ K}$, in this value, thermal conductivity will get its maximum value and will decrease at higher temperatures until the point of $T \geq 645 \text{ K}$ where it starts being independent of temperature. Therefore, the assumption studied is in region III, which establishes an inversely proportional relation between temperature and thermal conductivity.

Table 3. Debye's temperatures for a series of substances.

Substance	Debye Temperature (K)
Aluminum	428
Cadmium	209
Chromium	630
Copper	343.5
Gold	165
Iron	470
Lead	105
Manganese	410
Nickel	450
Platinum	240
Silicon	645
Silver	225
Tantalum	240
Tin	200
Titanium	420
Wolfram	400
Zinc	327
Carbon	2230
Ice	192

Figure 9 presents the distribution of the regions and the behavior that the system should have in the area where it is, region III.

**Figure 9.** Dependence of thermal conductivity with temperature for a crystalline solid.

Graphically, taking from the graphic in Figure 9 two temperatures and the corresponding values of thermal conductivity according to the curve represented in region III, it is possible to establish the reduction of thermal conductivity with the temperature in that region. Thus, if we select the temperatures of 95 K and 100 K, we can verify the decrease of thermal conductivity with an increase of temperature of 5 K. In this way, and according to Debye's graphical, for the temperature of 95 K, the corresponding value of thermal conductivity is 2.01 W/mK, while for 100 K the value of thermal conductivity is 1.87 W/mK. It means that an increase of 5 K of temperature involves a reduction of thermal conductivity of 0.14 W/mK. That is to say, in a crystalline solid, per each grade of temperature increased, thermal conductivity decreases 0.028 W/mK.

Nevertheless, the granitic sample used to examine the variation of the thermal conductivity with the temperature, contains about 30% of silica. Thus, the reduction for this sample would not be of 0.028 W/mK (for a material constituted by 100% of silica), but 0.0084 W/mK per each grade of temperature increased in this material.

The above is the expected behavior of thermal conductivity based on theoretical knowledge. However, to know what really happens in the practice of this procedure, tests with this method were carried out at different working temperatures (313.15 K, 338.15 K and 358.15 K) and always with the same sample (granite whose content in silica is around 30%). It will allow determining the evolution of the thermal conductivity with these temperatures (Table 4).

4.2. Variation of the Thermal Conductivity with the Sample Thickness

Another of the tests consisted in analyzing the variation of the thermal conductivity parameter with different thicknesses of the sample *S*. In this way, the range of sample thickness for which the equipment properly worked was established, discarding those ones where the results obtained moved away from the reference values. Thus, through these tests, the limits of the system regarding the sample thickness were set.

As in the previous case, a series of measurements were made with the same granitic sample modifying in this case its thickness.

The results of these tests (modifying the working temperatures and the sample thickness) are described in Table 4.

Table 4. Thermal conductivity for different values of temperature and sample thickness.

Heat Source Temperature (K)	Sample Thickness (m)	Sample Medium Temperature (K)	Heat Flux "Q" (W)	Thermal Conductivity "k" (W/mK)
313.15	0.0061	295.95	8.13	2.11
	0.0090	295.92	5.42	2.16
	0.0131	295.80	5.42	2.13
	0.0162	299.55	8.13	5.59
338.15	0.0061	296.20	19.22	2.06
	0.0090	302.30	13.31	2.10
	0.0131	302.30	9.24	2.13
	0.0162	305.55	18.49	4.77
358.15	0.0061	305.90	23.58	1.98
	0.0090	309.90	22.43	2.09
	0.0131	308.15	17.83	2.12
	0.0162	306.10	21.28	4.75

Analyzing the results presented in Table 4 and focusing on the variation of the working temperature, thermal conductivity was measured for three values of working temperature and for each of these cases, four thickness of the same granitic sample. Tables 5 and 6 show the variation of the thermal conductivity for each thickness when the working temperature, increases from 313.15 K to 338.15 K and from 313.15 K to 338.15 K. Additionally, Tables 5 and 6 present the decrease of the thermal conductivity parameter for each grade that the sample temperature increases.

Table 5. Evolution of thermal conductivity when temperature increases from 313.15 K to 338.15 K.

Thickness (m)	Increase of Temperature from 313.15 K to 338.15 K		
	Increase of "T" among Samples (°)	Difference of "k" (W/mK)	Decrease by Grade (W/mK)
0.0061	0.25	0.05	0.2000
0.0090	6.38	0.06	0.0094
0.0131	6.50	0.00	0.0000
0.0162	6.00	0.82	0.1366

Table 6. Evolution of thermal conductivity when temperature increases from 338.15 K to 358.15 K.

Thickness (m)	Increase of Temperature from 338.15 K to 358.15 K		
	Increase of "T" among Samples (K)	Difference of "k" (W/mK)	Decrease by Grade (W/mK)
0.006	9.70	0.08	0.0082
0.009	7.60	0.01	0.0013
0.013	5.85	0.01	0.0017
0.016	0.55	0.02	0.0360

Some deductions can be drawn:

- Most of the thermal conductivity values are around 2 W/mK. Increasing the temperature, these values decrease as it was expected for a crystalline solid. However, the reduction of the thermal conductivity parameter is not constant in the different sample thicknesses, and is not the expected 0.0084 W/mK calculated in Section 4.1. Evolution of thermal conductivity with temperature.
Therefore, in a crystalline solid, thermal conductivity decreases when temperature grows. However, it was not possible to set a model of behavior of this reduction because it does not follow any constant pattern.
- Regarding the different sample thickness, Table 4 shows the measurements carried out at the laboratory equipment (four different thicknesses for each one of the three work temperatures). The optimal dimensions of the sample *S* could be established based on the results of these measurements.
Thus, analyzing Table 4, it can be observed that, for the three temperatures, the values of thermal conductivity for each of the thickness are around the same value (~2 W/mK). These data agree with the expected thermal conductivity value for a granitic material. However, for the case of the highest thickness, the result of thermal conductivity moves away from the rest of results for lower thickness. All this made it possible to set the sample thicknesses for which the present method works properly.
On the basis of these results, with sample thicknesses greater than 0.0131 m, the procedure described in this paper does not provide reliable values. In these cases, results are highly anomalous due to a high dissipation of the heat flux through the sample *S*.
- The following working conditions were established in the thermal conductivity apparatus:
 - Temperature of the heat source was set in 313.15 K. Although results were acceptable in the three temperatures (313.15 K, 338.15 K and 358.15 K), this value is closer to the ground temperature in a very low enthalpy geothermal installation.
 - Thickness of the sample *S* could not exceed in any case the mentioned 0.0131 m for the reasons previously justified.

5. Thermal Conductivity Results

The results of thermal conductivity measurements are presented in Table 7. Three measurements of this parameter were carried out on each of the samples considered.

Table 7. Thermal conductivities, standard deviation and derivate error for each material studied.

Sample	Thickness (m)	K ₁ (W/mK)	K ₂ (W/mK)	K ₃ (W/mK)	Medium K $\langle x \rangle$ (W/mK)	Standard Deviation σ_x	Derivate Error
1	0.0090	2.16	2.12	2.09	2.12	0.035	± 0.10
2	0.0102	3.58	3.42	3.51	3.50	0.080	± 0.10
3	0.0131	2.57	2.61	2.39	2.52	0.117	± 0.10
4	0.0103	2.15	2.11	2.13	2.13	0.020	± 0.10
5	0.0130	2.24	2.31	2.25	2.27	0.038	± 0.10
6	0.0124	3.11	3.10	3.18	3.13	0.043	± 0.10
7	0.0132	2.99	2.97	3.02	2.99	0.025	± 0.10
8	0.0085	0.53	0.53	0.51	0.52	0.012	± 0.10
9	0.0051	0.21	0.18	0.19	0.19	0.016	± 0.10
10	0.0082	3.15	3.24	3.17	3.19	0.047	± 0.10
11	0.0091	3.39	3.38	3.44	3.40	0.032	± 0.10
12	0.0063	2.63	2.59	2.61	2.61	0.020	± 0.10
13	0.0090	1.77	1.58	1.63	1.66	0.098	± 0.10

When a certain measurement is repeated several times, medium values group around a central value. This distribution can be described by statistical the mean $\langle x \rangle$ (Equation (3)) and the standard deviation σ_x (Equation (4)) [33,34]:

$$\langle x \rangle = \frac{1}{N} \sum_{i=1}^N x_i = \frac{1}{N} (x_1 + x_2 + x_3 + \dots + x_{N-1} + x_N) \quad (3)$$

$$\sigma x = \sqrt{\frac{1}{N-1} \sum_{i=1}^N (x_i - \langle x \rangle)^2} \quad (4)$$

Errors derived from the precision of the tools used to measure the different parameters (thickness and temperatures) must also be considered. For this reason, the total differential of our equation of calculation of conductivity was calculated (Equation (5)):

$$dk = \frac{\partial K}{\partial e} de + \frac{\partial K}{\partial T_{2-3}} dT_{2-3} + \frac{\partial K}{\partial T_{3-4}} dT_{3-4} \quad (5)$$

where $k = k(e, T_{2,3}, T_{3,4})$

where

k = Thermal conductivity (W/mK);

e = Sample thickness (m);

$T_{2,3}$ = Increase of temperature between thermocouples 2 and 3 (Figure 1); and

$T_{3,4}$ = Increase of temperature between thermocouples 3 and 4 (Figure 1).

Equation (5) was transformed into increases, and absolute values were taken to each partial derivate to estimate the derivate error (Equation (6)):

$$\Delta k = \left| \frac{\Delta k}{\Delta e} \right| \Delta e + \left| \frac{\Delta k}{\Delta T_{2-3}} \right| \Delta T_{2-3} + \left| \frac{\Delta k}{\Delta T_{3-4}} \right| \Delta T_{3-4} \quad (6)$$

Increases represent the absolute errors of the measuring dispositive and the growth of k symbolizes the derivate error.

From each one of the three thermal conductivities measurements of each material, derivate error was calculated. It was found that the reduction in precision did not exceed in any case one order of magnitude with respect to the precision of the least precise dispositive (thermocouples with ± 0.01 K). Derivate error was estimated as ± 0.10 for all samples.

6. Validity of the Method

The validity of the suggested thermal conductivity device was analyzed by comparing the results presented in Table 7 with the ones commonly accepted at the "Technical Code of Building" (CTE). From this comparison, the difference, with respect to the officially accepted value for that sample, was calculated.

CTE provides a certain thermal conductivity value for a wide variety of materials, including rocks and soils. Given the heterogeneity of samples 1, 2, 3 and 4 (granitic rocks) and the high presence of these rocks in numerous European geothermal installations, a different reference value was assigned to each of these samples starting from the CTE value. This assignment was made based on studies that relate the thermal conductivity of a rock with its quartz content [35,36].

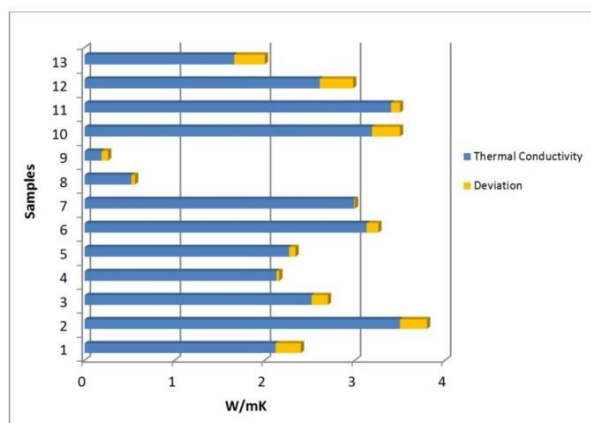
Thus, instead of the thermal conductivity value of 3 W/mK provided by the CTE for a granite rock, an interval of 2.0 W/mK–3.8 W/mK was taken for quartz contents between 3% and 50%.

Table 8 shows the reference thermal conductivity values set for each of the samples according to CTE. It also presents the thermal conductivity values measured with the equipment developed in this research and the difference between both values (common and measured values).

It is important to highlight that thermal conductivity parameter easily changes depending on different factors (temperature, anisotropy, humidity, etc.) and could be quite different in materials of similar geological origin. Despite these facts, the differences between the measured values and the reference ones are considerably low. The most unfavorable case was for sample 12 (0.37 W/mK of difference) and the most favorable one for sample 7 (0.01 W/mK of difference). Figure 10 shows a graphic of deviations presented in Table 8.

Table 8. Comparison between values of thermal conductivity measured and the reference ones.

Sample	K measured (W/mK)	K reference (W/mK)	Deviation-Reference Value (W/mK)
1	2.12	2.4 (15% of quartz)	0.28
2	3.50	3.2 (40% of quartz)	0.3
3	2.52	2.7 (25% of quartz)	0.18
4	2.13	2.1 (5% of quartz)	0.03
5	2.27	2.2	0.07
6	3.13	3	0.13
7	2.99	3	0.01
8	0.52	0.56	0.04
9	0.19	0.12	0.07
10	3.19	3.5	0.31
11	3.40	3.5	0.1
12	2.61	3	0.37
13	1.66	2	0.34

**Figure 10.** Deviations between the common and the measured thermal conductivity values.

7. Influence of the Thermal Conductivity Parameter in the Geothermal Measuring

“Earth Energy Designer” (EED) is software developed by “Blocon Software” that allows knowing the total drilling depth of a vertical closed-loop system. The calculation process of EED is based on a series of initial data (provided by the user) of the ground where the installation is going to be placed. One of these initial data is the thermal conductivity of the surrounding ground.

In order to understand the importance that the thermal conductivity parameter has in the dimensioning of a geothermal installation, some calculations were made with this software. The total drilling depth was calculated with the same conditions but changing the thermal conductivity of the ground for each of the samples of this study. Thus, for each sample, calculations were made with the measured thermal conductivity value and with interval of $\pm 15\%$ of that value (Table 9).

Depending on the material, with a variation of only $\pm 15\%$ in the thermal conductivity value, the total drilling length significantly changes. The most notable case is sample 9, where increasing the thermal conductivity from 0.19 W/mK to 0.22 W/mK, the drilling length decreases 27 meters, and reducing the thermal conductivity to 0.16 W/mK, the drilling length increases 34 meters.

As Table 9 shows, for the rest of samples, large variations are also experimented. Therefore, a proper knowledge of the thermal conductivity of the ground means important variations in the total drilling depth of a very low enthalpy geothermal installation.

Table 9. Measuring with EED software.

EED Measuring			
Sample 1			
k (W/mK)	2.12 *	1.80 **	2.44 ***
Drilling length (m)	185	194	174
Sample 2			
k (W/mK)	3.50 *	2.97 **	4.02 ***
Drilling length (m)	153	161	143
Sample 3			
k (W/mK)	2.52 *	2.14 **	2.90 ***
Drilling length (m)	174	182	163
Sample 4			
k (W/mK)	2.13 *	1.81 **	2.45 ***
Drilling length (m)	185	193	173
Sample 5			
k (W/mK)	2.27 *	1.93 **	2.61 ***
Drilling length (m)	181	192	172
Sample 6			
k (W/mK)	3.13 *	2.66 **	3.60 ***
Drilling length (m)	160	170	151
Sample 7			
k (W/mK)	2.99 *	2.54 **	3.44 ***
Drilling length (m)	163	174	154
Sample 8			
k (W/mK)	0.52 *	0.44 **	0.60 ***
Drilling length (m)	324	333	316
Sample 9			
k (W/mK)	0.19 *	0.16 **	0.22 ***
Drilling length (m)	449	483	422
Sample 10			
k (W/mK)	3.19 *	2.71 **	3.67 ***
Drilling length (m)	158	169	150
Sample 11			
k (W/mK)	3.40 *	2.89 **	3.91 ***
Drilling length (m)	155	166	147
Sample 12			
k (W/mK)	2.61 *	2.22 **	3.00 ***
Drilling length (m)	172	183	163
Sample 13			
k (W/mK)	1.66 *	1.41 **	1.91 ***
Drilling length (m)	206	216	196

* Measured thermal conductivity value; ** -15% of the measured thermal conductivity value;
*** +15% of the measured thermal conductivity value.

8. Conclusions

Thermal conductivity is a fundamental property in the process of measuring of a geothermal installation but, at the same time, it is a parameter of difficult quantification.

A series of difficulties of diverse nature appeared throughout this research:

- Temperature of the cold source (ambient temperature) was controlled at all times and set in a constant value to avoid external thermal influences on the thermal conductivity device.
- The insulation placed around the system minimized the radial heat flux but did not eliminate it. As a result, corrections of this heat flux were made for each of the temperatures set at the heater.
- A high precision was needed when measuring the sample thickness due to its excessive influence in the calculation of the thermal conductivity parameter.

- Thermocouples were carefully placed to ensure a complete contact with the faces of the samples.
- Long-term measurements to guarantee the stabilization of the heat flux.

Despite these facts, this method means an excellent solution when measuring the thermal conductivity parameter in an economical and simple way. It provides accurate results taking advantage of equipment present in most laboratories such as the heater. These results are applicable to the calculation of very low enthalpy geothermal installations, avoiding over measuring that raise the price of these renewable installations.

Finally, EED software allowed highlighting the importance of knowing the thermal conductivity of the surrounding ground in a geothermal system. This knowledge could mean important savings regarding the drilling length.

Acknowledgments: Authors would like to thank the Department of Cartographic and Land Engineering of the Higher Polytechnic School of Avila, University of Salamanca, for allowing us to use their facilities and their collaboration during the experimental phase of this research. Authors also want to thank the Ministry of Education, Culture and Sport for providing a *FPU Grant* (Training of University Teachers Grant) to the corresponding author of this paper what has made possible the realization of the present work.

Author Contributions: All authors conceived, designed and performed the experimental campaign. Cristina Sáez Blázquez, Arturo Farfán Martín and Ignacio Martín Nieto implemented the methodology and analyzed the results. Diego González-Aguilera provided technical and theoretical support. Cristina Sáez Blázquez wrote the manuscript and all authors read and approved the final version.

Conflicts of Interest: The authors declare no conflicts of interest.

References

1. Leach, A.G. The thermal conductivity of foams. I: Models for heat conduction. *J. Phys. D* **1993**, *26*, 733–739.
2. Balbay, A.; Esen, M. Experimental investigation of using ground source heat pump system for snow melting on pavements and bridge decks. *Sci. Res. Essays* **2010**, *5*, 3955–3966.
3. Balbay, A.; Esen, M. Temperature distributions in pavement and bridge slabs heated by using vertical ground-source heat pump systems. *Acta Sci. Technol.* **2013**, *35*, 677–685.
4. Kabar, M.; Nowak, W.; Sobanski, R. *Principles of Exploitation Geothermal Energy Water at Targets of Heating Buildings*; Project KBN; Energy Water at Targets of Heating Buildings: Szczecin, Poland, 1999.
5. Blázquez, C.S.; Martín, A.F.; García, P.C.; Sánchez Pérez, L.S.; del Caso, S.J. Analysis of the process of design of a geothermal installation. *Renew. Energy* **2016**, *89*, 188–199.
6. Peláez, P.C.; Carnicero, J.M.P.; García, R.L.; Peragon, F.C. Desarrollo de equipo para la realización de test de respuesta térmica del terreno (TRT) en instalaciones geotérmicas. *Dyna* **2014**, *89*, 316–324.
7. ASTM International. *ASTM Standard C 177-10, Standard Test Method for Steady-State Heat Flux Measurements and Thermal Transmission Properties by Means of the Guarded-Hot-Plate Apparatus*; ASTM International: West Conshohocken, PA, USA, 2010.
8. Terzic, M.; Milošević, N.; Stepanic, N.; Petricevic, S. Development of a single-sided guarded hot plate apparatus for thermal conductivity measurements. *Therm. Sci.* **2016**, *20*, S321–S329.
9. Ramstad, R.K.; de Beer, H.; Midtømme, K.; Koziel, J.; Wissing, B. *Thermal Diffusivity Measurement at NGU—Status and Method Development 2005–2008*; Geological Survey of Norway: Trondheim, Norway, 2009.
10. Lira-Cortés, L.; González Rodríguez, O.J.; Méndez-Lango, E. *Sistema de Medición de la Conductividad Térmica de Materiales Sólidos Conductores, Diseño y Construcción*; Simposio de Metrología Santiago de Querétaro: Querétaro, Mexico, 2008.
11. Liou, J.-C.; Tien, N.-C. Estimation of the thermal conductivity of granite using a combination of experiments and numerical simulation. *Int. J. Rock Mech. Min. Sci.* **2016**, *81*, 39–46.
12. Gustafsson, S.E. Transient plane source techniques for thermal conductivity and thermal diffusivity measurements of solid materials. *Rev. Sci. Instr.* **1991**, *62*, 797–804.
13. Krishnaiah, S.; Singh, D.N.; Jadhav, G.N. A methodology for determining thermal properties of rocks. *Min. Sci.* **2004**, *41*, 877–882.

14. Kukkonen, I.; Lindberg, A. *Thermal Conductivity of Rocks at the TVO Investigation Sites Olkiluoto, Romuvaara and Kivetty*. Report YJT-95-08, 29; Nuclear Waste Commission of Finnish Power Companies: Helsinki, Finland, 1995.
15. Jorand, R.; Vogt, C.; Marquart, G.; Clauser, C. Effective thermal conductivity of heterogeneous rocks from laboratory experiments and numerical modeling. *J. Geophys. Res.* **2013**, *118*, 5225–5235.
16. Popov, Y.A. Optical scanning technology for nondestructive contactless measurements of thermal conductivity and diffusivity of solid matters. In Proceedings of the 4th World Conference on Experimental Heat Transfer, Fluid Mechanics and Thermodynamics, Brussels, Belgium, 2–6 June 1997; pp. 109–116.
17. Xiao, B.; Yang, Y.; Chen, L. Developing a novel form of thermal conductivity of nanofluids with Brownian motion effect by means of fractal geometry. *Powder Technol.* **2013**, *239*, 409–414.
18. Cai, J.; Hu, X.; Xiao, B.; Zhou, Y.; Wei, W. Recent developments on fractal-based approaches to nanofluids and nanoparticle aggregation. *Int. J. Heat Mass Transf.* **2017**, *105*, 623–637.
19. Blázquez, C.S.; Martín, A.F.; Nieto, I.M.; García, P.C.; Pérez, L.S.S.; Aguilera, D.G. Thermal conductivity map of the Avila region (Spain) based on thermal conductivity measurements of different rock and soil samples. *Geothermics* **2017**, *65*, 60–71.
20. Barry-Macaulay, D.; Bouazza, A.; Singh, R.M.; Wang, B.; Ranjith, P.G. Thermal conductivity of soils and rocks from the Melbourne (Australia) region. *Eng. Geol.* **2013**, *164*, 131–138.
21. ASTM International. *ASTM D5334, Standard Test Method for Determination of Thermal Conductivity of Soil and Soft Rock by Thermal Needle Probe Procedure*; ASTM International: West Conshohocken, PA, USA, 2008.
22. ASTM International. *ASTM E1225-99, Standard Test Method for Thermal Conductivity of Solids by the Guarded Comparative Longitudinal Heat Flow Technique*; ASTM International: West Conshohocken, PA, USA, 1999.
23. Jean-Baptiste, J.F. Remarques generales sur les temperatures du globe terrestre et des espaces plan etaires. *Ann. Chim. Phys.* **1824**, *27*, 136–167.
24. Jean-Baptiste, J.F. *Theorie Analytique de la Chaleur*; Firmin Didot: Paris, France, 1822.
25. Jean-Baptiste, J.F. Memoire sur les temperatures du globe terrestre et des espaces planetaires. *Mem. l'Acad. R. Sci.* **1827**, *7*, 569–604.
26. Bevington, R.P.; Robinson, D.K. *Data Reduction and Error Analysis for the Physical Sciences*, 2nd ed.; WCB/McGraw-Hill: New York, NY, USA, 1992.
27. Pei, W.; Yu, W.; Li, S.; Zhou, J. A new method to model the thermal conductivity of soil–rock media in cold regions: An example from permafrost regions tunnel. *Cold Reg. Sci. Technol.* **2013**, *95*, 11–18.
28. ASTM International. *ASTM E220, Test Method for Calibration of Thermocouples by Comparison Techniques*; ASTM International: West Conshohocken, PA, USA, 2013.
29. AENOR. *UNE 103-300-93. Determinación de la Humedad de un Suelo Mediante Secado en Estufa*; AENOR: Marid, Spain, 1993.
30. AENOR. *UNE 103-500-94. Ensayo Proctor de Compactación*; AENOR: Marid, Spain, 1994.
31. Chung, P.W.; Tamma, K.K.; Namburu, R.R. Homogenization of temperature-dependent thermal conductivity in composite materials. *J. Thermophys. Heat Transf.* **2001**, *15*, 10–17.
32. Fernández, F.; Rondón, E.; Sánchez, F.; Salas, K.; García, V.; Briceño, J. Conductividad térmica en sólidos a altas temperaturas. *Rev. Fac. Ing. UCV* **2006**, *21*, 21–27.
33. Nakshabandi, G.A.I.; Kohnke, H. Thermal conductivity and diffusivity of soils as related to moisture tension and other physical properties. *Agric. Meteorol.* **1965**, *2*, 271–279.
34. Taylor, R.J. *An Introduction to Error Analysis: The Study of Uncertainties in Physical Measurements*, 2nd ed.; University Science Books: Herndon, VA, USA, 1997.
35. Kukkonen, I.; Lindberg, A. *Thermal Properties of Rocks at the Investigation Sites: Measured and Calculated thermal Conductivity, Specific Heat Capacity and Thermal Diffusivity*; Geological Survey of Finland: Espoo, Finland, 1998.
36. *Prontuario de Soluciones Constructivas; Código Técnico de la Edificación*. Instituto de Ciencias de la Construcción Eduardo Torroja e Instituto de Ciencias de la Construcción de Castilla y León: Castilla y León, Spain, 2007.

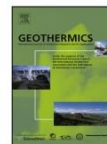


PAPER 3



Contents lists available at ScienceDirect

Geothermics

journal homepage: www.elsevier.com/locate/geothermics

Thermal conductivity map of the Avila region (Spain) based on thermal conductivity measurements of different rock and soil samples



Cristina Sáez Blázquez*, Arturo Farfán Martín, Ignacio Martín Nieto, Pedro Carrasco García, Luis Santiago Sánchez Pérez, Diego González Aguilera

Department of Cartographic and Land Engineering, University of Salamanca, Higher Polytechnic School of Avila, Hornos Caleros 50, 05003 Avila, Spain

ARTICLE INFO

Article history:

Received 18 May 2016

Received in revised form 3 August 2016

Accepted 2 September 2016

Keywords:

Thermal conductivity

Map

Geothermal heat pumps

Low-cost method

ABSTRACT

A thermal conductivity map constitutes an important basis with regards to the design and performance of geothermal heat pump installations. Although the execution of a Thermal Response Test means an ideal solution as it provides the average value of the thermal conductivity over the length of the borehole drilled for the BHE, in small projects it is not possible to carry out these tests because they involve a huge increase of the total budget of the user. This study describes a systematic methodology to produce a thermal conductivity map of an area geographically placed in the center of Spain, the province of Ávila. As a result, a map of thermal conductivity distribution of local rocks is proposed.

© 2016 Elsevier Ltd. All rights reserved.

1. Introduction

The use of geothermal energy is at a point of rapid growth and is expected to continue growing in the future. With respect to Spain, this energy is basically used to generate sanitary hot water (SHW) and/or heat/cool a certain space. The geothermal electric generation in this country is at a very early stage although at the moment, it is being developed in areas like Tenerife where, because of its thermal characteristics, the first Spanish geothermal electric central is going to be placed.

At user level, the very low temperature geothermal energy is used in the production of SHW or heating. For both uses, a careful design of the geothermal installation is required; one of the essential parameters that is decisive is the thermal conductivity of the ground where the installation will be placed. When measuring this parameter, a "Thermal Response Test" (TRT) is needed in order to get accurate values of the whole subsoil to the right design of the geothermal installation. However, in spite of providing this value directly, this test involves an important rise of the price of implementation of a geothermal installation, of little significance (from an economical point of view) at big projects but unviable at small installations. In case of not making this essay, the most usual is not to determine the thermal conductivity of the land and consider the most unfavorable case, that is to say, that value of thermal conduc-

tivity (for the type of soil-rock where the installation is located) that requires the highest heat pump power (in function of theoretical tables), rising equally the global budget (Blázquez et al., 2016; Peláez et al., 2014).

In the present paper, measurements of the thermal conductivity of different samples of the characteristic geological materials that occur in the province of Ávila were carried out in the laboratory. Data obtained in soils were compared with the ones obtained by the use of the program ThermoMap developed by a diverse combination of institutions (*GeoZentrum, BRGM, ISOR, MFCI, IGR, BGS, EGEC, RBINS-GBS, REHAU, GBI, PLUS, IGME*) (Thermo Map, 2013). Data acquired in the laboratory and in the case of soils also verified by ThermoMap have allowed generating thus, a thermal conductivity map of the mentioned province. This knowledge will make possible to improve the design of the geothermal heat pump installations (Vijdea et al., 2014; Galgaroa et al., 2015; Clauser and Huenges, 1995; Barry-Macaulay et al., 2013).

The purpose of this study is to obtain values of thermal conductivity by measurements in the laboratory and using the program ThermoMap (only in the case of soils), representative of the Ávila region, to be presented as a thermal conductivity detailed map. For that, a procedure of localization, collection and preparation of samples at the laboratory and analysis of the thermal conductivity parameter of each one of the samples was developed. Thermal conductivities of soils were also estimated by the calculator ThermoMap to carry out a comparison of both methods in these samples.

* Corresponding author.

E-mail address: u107596@usal.es (C. Sáez Blázquez).

This map of thermal conductivities can be used along with the corresponding geological data, as basic information at the design phase of a geothermal heat pump project (Jackson and Taylor, 1986).

2. Materials and methods

2.1. Study site

As it has already been mentioned, the determination of the thermal conductivity parameter has been carried out on the most representative geological materials that are part of the province of Ávila; therefore, the map obtained as a result of this study will reflect an analysis of the geothermal situation of the province (in terms of thermal conductivities of the materials) and the possibilities of making use of this energy in this place (Fig. 1).

The Geological and Mining Institute of Spain "IGME" puts at the disposal of the users geological information of all the regions of Spain, in this way, this country is divided into a series of grids to scale 1:50,000 that contain the geology of the area represented. By graphic design software the grids that divide the province of Ávila were digitized and overlapped with the aim of locating each one of the materials found in the study area and calculating the expanse taking up by each one of them. Fig. 2 shows the rock types of this province (Geological and Mining Institute of Spain (IGME), 1972–2003).

As shown in Fig. 2, the province of Ávila is geologically formed by two clearly defined blocks:

- On the one hand, materials belonging to the Hercynian Massif, constituted by igneous rocks from the Upper Carboniferous-Low Permian (mainly granitic rocks) and metamorphic rocks from the Pre-Cambrian-Low Cambrian.
- On the other hand, there is a block constituted by sedimentary materials from the Mesozoic, Tertiary and Quaternary, located in the oriental area of the Amble's valley (Ávila) (César et al., 2014).

Additionally, Table 1 contains the list of materials that constitute the province represented in Fig. 2, the area taken up by each one of them expressed in: area unities (m²) and as percentage (%) with respect to the total area of the province. It can be observed in this Table 1 that, more than half of materials placed in this province have granitic origin.

2.2. Sample collection

Due to the lack of information about the thermal conductivity properties of the materials of Ávila, a sampling selecting different sample collection points according to the rock type, lithology and geographical position was carried out. In this way, representative samples of the formations of this region were taken. Given the difficulty to measure the thermal conductivity property "in situ", samples were moved to the lab where, after opportune preparation, measurements were made. Basically two types of rocks have been collected and investigated: solid (rock) and unconsolidated (soil). With the aim of reproducing the conditions of the materials in nature, measurements of thermal conductivity were carried out for different states of water content, in those materials that allow changing its humidity (i.e. soils).

Fig. 3 shows the points where the samples representative of each material presented in Table 1 were taken. As it can be observed, for the same rock type, four different samples were collected with the object of getting a more precise determination of the mentioned thermal conductivity property and the correspondent geothermal map of the province. For three of the investigated rock types

(leucogneiss, gneiss and quartzite) the four samples collected for these rocks come from sites next to each other due to the short area taken up by these materials.

2.3. Thermal conductivity measurements

2.3.1. KD2 Pro equipment

Equipment used at the measuring of thermal conductivities was the thermal properties analyzer commercially known as KD2 Pro developed by Decagon Devices (Decagon Devices, 2016). It is constituted by a portable controller and a certain sensor (RK-1) usually used in geothermal practice and customarily termed "needle probe" that make possible the measuring of two thermal properties: the thermal resistivity and the focus parameter of this work; the thermal conductivity. Its operation is based on the infinite line heat source theory and calculates the thermal conductivity by monitoring the dissipation of heat from the needle probe. Heat is applied to the needle for a set heating time, t_h and temperature is measured in the monitoring needle during heating and for an additional time equal to t_h after heating. The temperature during heating is computed from Equation (1).

$$T = m_0 + m_2t + m_3 \ln t \quad (1)$$

Where:

m_0 is the ambient temperature during heating

m_2 is the rate of background temperature drift

m_3 is the slope of a line relating temperature rise to logarithm of temperature

Equation (2) represents the model during cooling.

$$T = m_1 + m_2t + m_3 \ln \frac{t}{t - t_h} \quad (2)$$

The thermal conductivity is computed from Equation (3).

$$k = \frac{q}{4m_3} \quad (3)$$

q is the heat flux applied to the needle probe for a set time. This heat dissipates along the sample in a different way so and as it can be seen in Equation (3), this value is used by the equipment KD2 Pro to calculate the thermal conductivity value of the sample in question. However, KD2 Pro does not provide the heat flux applied and it only supplies the final thermal conductivity value.

Since these equations are long-time approximations to the exponential integral equations, only the final 2/3 of the data collected are used (ignoring early-time data) during heating and cooling. This approach has several advantages; the effects of contact resistance appear mainly in these early time data, so by analyzing only the later time data the measurement represents better the thermal conductivity of the sample. Also, Equations (1) and (2) can be solved by linear least squares, giving a solid and more adjusted result (Kluitenberg et al., 1993; Shiozawa and Campbell, 1990).

In this study, the RK-1 probe (3.9 mm in diameter and 6 cm in length) has been used to measure the thermal conductivity of the different materials placed in the province of Ávila. This probe is capable of measuring the thermal conductivity between the range of 0.1 and 6 W/mK and $\pm 10\%$ of accuracy.

Additionally, KD2 Pro calculates the accuracy of each measurement by comparing the experimental temperature data to the modelled temperature predicted by the analytical solution of infinite line source theory (Carslaw and Jaeger, 1959). The difference between experimental and modelled temperature is displayed as the coefficient of correlation. It must be clarified that this error term is not a statistical indicator of the measuring quality, but it serves as a qualitative indicator.

The long read times for the RK-1 sensor help to prevent errors caused by effects from the large diameter needle and contact

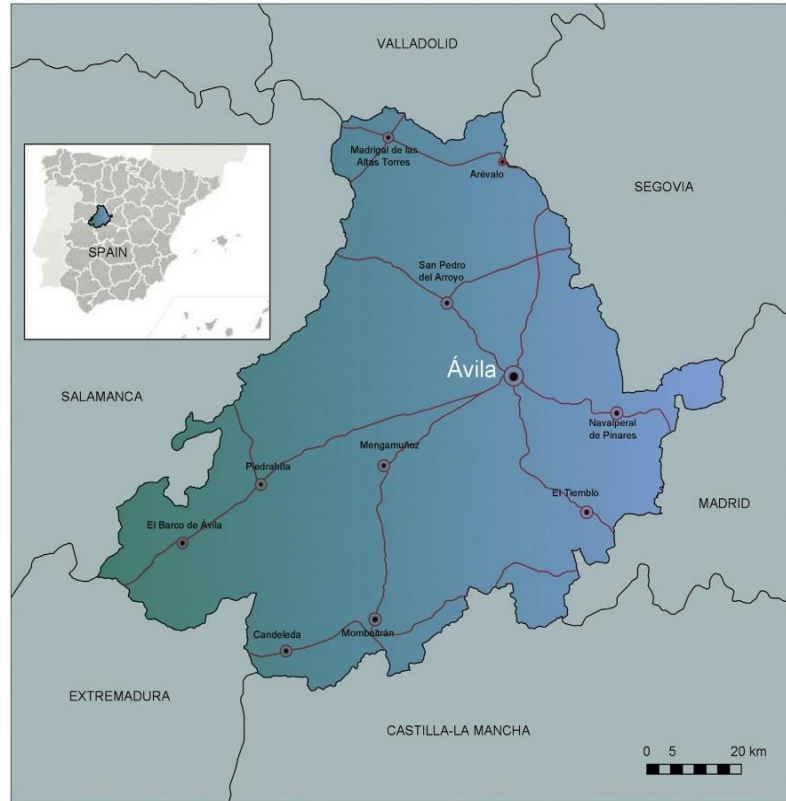


Fig. 1. Study location, province of Ávila.

Table 1
List of principal geologic materials by rock type and by geologic age of the province of Ávila and its area (m²).

	Geological Formation		Area (m ²)	Percentage (%)
ROCKS	1	Granitic Rocks	4727371144.80	58.73
	2	Granite	4141732.90	4.65
	3	Monzogranite	351222457.10	4.36
	4	Leucogranite	278550245.90	3.46
	5	Granitoid	519901676.90	6.46
	6	Granodiorite	2083912516.00	25.89
	7	Adamellite	1119642516.00	13.91
	8	Metamorphic Rocks	89364335.27	1.11
	9	Leuco gneiss	2787675.83	0.03
	10	Orto gneiss	59273484.05	0.74
	11	Gneiss	27303175.39	0.34
	12	Cambrian-low Pre-Cambrian	440678930.74	5.47
	13	Slate	80855662.67	1.00
SOILS	14	Quartzite	35654498.27	0.44
	15	Schist	324168769.80	4.03
	16	Pre-Arenigiense	99894327.99	1.24
	17	Meta-sediment	99894327.99	1.24
	18	Tertiary	2095838252.00	26.03
	19	Sand, arkoses, clay, mud and stone	2095838252.00	26.03
	20	Quaternary	597003009.50	7.42
	21	Terrace, alluvial, glaci	597003009.50	7.42
	22		8050150000.30	100

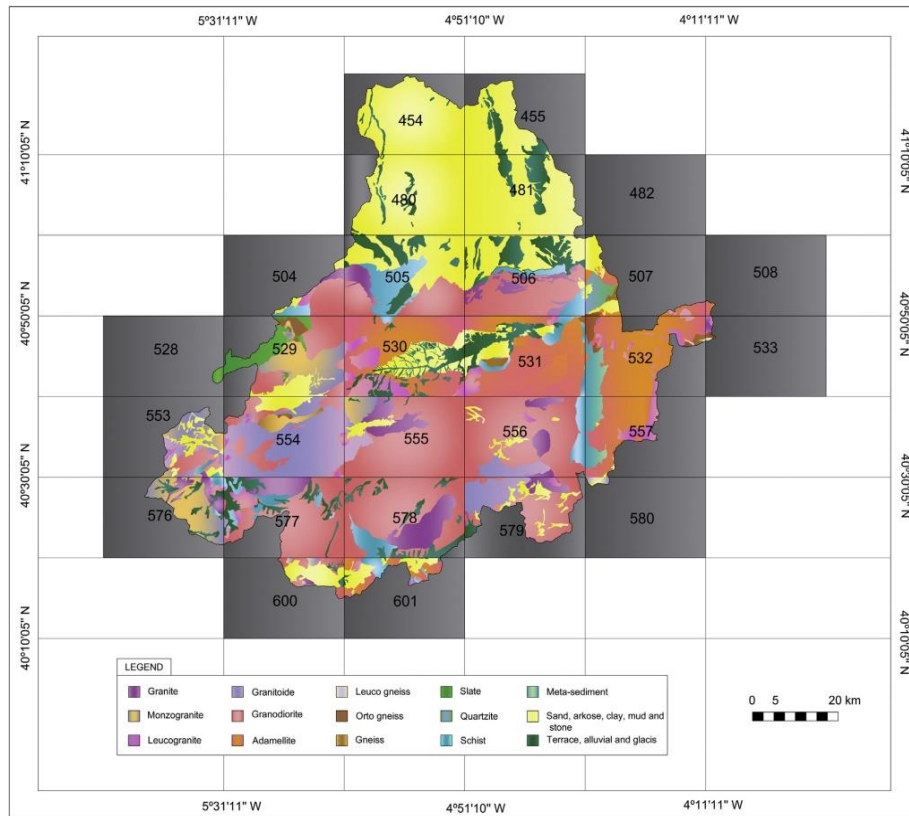


Fig. 2. Grids that divide the province of Ávila and its geology.

resistant between the sensor and the sample granular and solid materials. The contact between needle and tested material is guaranteed by putting thermal grease in the hole drilled for the emplacement of the needle.

It is convenient to mention that, RK-1 sensor was previously calibrated before its use by a test tube supplied by the manufacturer.

Despite the fact RK-1 sensor is specifically designed for its use in hard materials like rock or cured concrete, in this work; it was used in rocks but also in soils previously compacted. Before proceeding to use the equipment, the pertinent samples preparation was carried out. The sensor must be able to penetrate into the specimen to be measured (in drilled boreholes in case of solid rocks) or inserted into specially prepared (compacted) samples in case of unconsolidated material. In the case of rocks, samples were prepared in the lab, obtaining cylinder blocks of 5 cm of diameter and length superior to the sensor RK-1 length (6 cm), where a hole has been made with the purpose of containing the sensor. On the contrary, soils were compacted in *Proctor* essay conditions in order to reproduce the compaction state of these materials to greater depths, where, due to pressure and temperature effects, the compaction conditions differ from those in the surface where samples were taken. Once the soil was compacted in the appropriate mold, sensor RK-1 was

directly introduced in the sample obtained from the execution of the mentioned *Proctor* essay [UNE 103-500-94, 1994]. As this essay specifies, soil with defined water content was introduced in Proctor mold in three steps and 26 hits were made on each one of the three layers in the mold with the corresponding tenderizer. After carrying out this essay, the soil gets the compaction in Proctor conditions for certain water content.

The degree of consolidation of the sampled materials was the one resulting from the explained Proctor essay.

In respect to anisotropy factors, measurements with KD2 Pro have been carried out only in perpendicular direction to the layers, considering a horizontal position of them, similar to the one we would find in a hole given the tectonics of the region. In this way, anisotropy factors were not considered.

Fig. 4 shows the procedure followed from the data collection in the land to the measuring of the thermal conductivity parameter in the laboratory.

Location of materials (presented in Table 1) on the basis of geological information and collection of representative samples of each of them. Geographical coordinates were written down with the aim of verifying that the location of these samples coincides with the points marked in the map represented in Fig. 3.

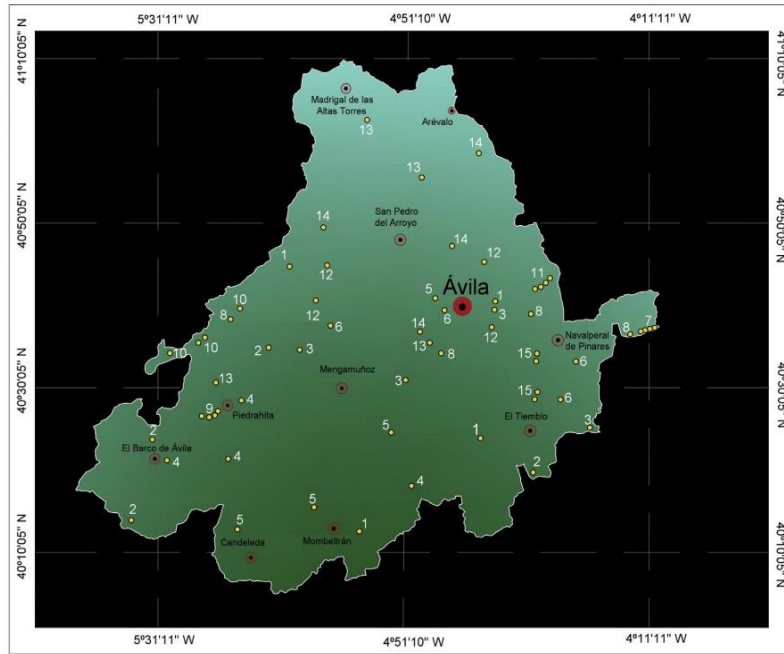


Fig. 3. Sampling point's position for the four samples of each material (rock types/formations 1–15, see Table 1).

- Rocks drilling and extraction of samples of 5 cm of diameter and variable length, depending on the rock block size.
- Carving of samples by using a cutting-machine supplied with diamond disk. The length of these samples was equal or longer than 6 cm so that the needle probe RK-1 (6 cm length) is totally inside them.
- Samples obtained and surplus rocky material.

Drilling of a hole in every rocky sample where the sensor RK-1 was introduced for the measuring of thermal conductivities. In all cases this hole was of 6 cm length and 3.9 mm of diameter, dimensions coinciding with the needle probe dimensions.

- Positioning of thermal grease in the samples holes to improve the contact and the thermal transfer between sensor and rock.
- Installation of the KD2 Pro and sensor RK-1 in the corresponding rock sample and measuring of the thermal conductivity parameter. The read time of this sensor is approximately 10 min.

KD2 Pro and sensor RK-1 measuring the thermal conductivity of a soil in the Proctor mold where the compaction of this material was previously made in the conditions established by the law of this essay.

Three measuring of the thermal conductivity parameter were made for each rocky sample and in the case of soils, three measuring for each sample and three different humidity states, modifying the water content of the sample. These three humidity states were established by determining in first place the optimal humidity of each soil and then selecting three humidity values next to this optimal humidity belonging to the ascending phase of Proctor essay,

where an increase of humidity also increases the density of the soil sample. Once known the optimal humidity of each soil, samples were dried in a laboratory heater to 105 °C during a week to then add a certain quantity of water (different for each humidity state and guaranteeing not to reach the optimal humidity). By differences of weight between dry and wet samples, densities were calculated. The accuracy of these measurements depends on the electronic scale used, which was able to provide five significant digits.

Given that samples were collected in surface from rocky outcrops, measurements with KD2 Pro provided thermal conductivity values from surface, that is to say, the thermal conductivity of the rocks along the entire borehole heat exchanger cannot be determined with the present methodology. Despite this fact, these measurements constitute a good basis in the calculation of a geothermal heat pump in special if there is not the possibility of carrying out a TRT. Moreover, according with the information of different holes provided by the Geological and Mining Institute of Spain "IGME", there is a high concordance between rocks in surface and in depth which means that data obtained in this research from surface samples offer extended information about the thermal conductivity of the entire borehole, although never as complete as the one supplied by a TRT.

2.3.2. ThermoMap

Given that the equipment KD2 Pro used in the measuring of thermal conductivities in this work is not specifically designed to be used in soils, the calculation of this thermal conductivity property in these materials was concurrently carried out utilizing ThermoMap software. In this way, it was possible to compare the thermal



Fig. 4. Sequence of the process of thermal conductivity measurement (a–h, see text).

conductivity values in soils obtained through two different procedures: KD2 Pro and ThermoMap.

ThermoMap is a project focused on the cartography of superficial geothermal resources areas that offers ground and ground water data to a certain depth (0–10 m), offering information about the geothermal potential of Europe. The project harmonizes a group of pre-existing data, related to the ground, climate, and geographical, hydrogeological and geological data with standardized methods. Also, by the data collection in fourteen European areas,

ThermoMap has designed a web GIS (Geographical Information System) where users can access to the geothermal potential of these countries. If the area is not considered by this GIS (like the area studied in the present study), ThermoMap additionally has a calculator that allows estimating the thermal conductivity of a certain soil. Therefore, a series of specific parameters of the material in question are required by the application, such as density (g/cm^3), humidity (%) and content of sands, clays and muds expressed in percentage (%).

Table 2
Values of thermal conductivity of the rock types of Ávila measured with KD2 Pro.

Geological Formation	Thermal Conductivity (W/mK)						
	K_1	K_2	K_3	$K_{1-3\text{medium}}$	σ	$K_{\text{Medium-Total}}$	
1. Granite							
M ₁	2.577	2.647	2.594	2.606	0.036	2.650	
M ₂	2.665	2.666	2.651	2.661	0.008		
M ₃	2.652	2.657	2.664	2.658	0.006		
M ₄	2.652	2.685	2.686	2.674	0.019		
2. Monzogranite	K_1	K_2	K_3	$K_{1-3\text{medium}}$	σ	$K_{\text{Medium-Total}}$	
M ₁	2.392	2.314	2.471	2.392	0.078	2.533	
M ₂	2.668	2.574	2.523	2.588	0.073		
M ₃	2.525	2.788	2.583	2.632	0.138		
M ₄	2.577	2.463	2.518	2.519	0.057		
3. Leucogranite	K_1	K_2	K_3	$K_{1-3\text{medium}}$	σ	$K_{\text{Medium-Total}}$	
M ₁	2.755	2.872	2.784	2.804	0.061	2.829	
M ₂	2.881	2.889	2.849	2.873	0.021		
M ₃	2.827	2.802	2.802	2.810	0.014		
M ₄	2.787	2.846	2.849	2.827	0.034		
4. Granitoid	K_1	K_2	K_3	$K_{1-3\text{medium}}$	σ	$K_{\text{Medium-Total}}$	
M ₁	2.668	2.751	3.086	2.835	0.221	2.633	
M ₂	2.381	2.430	2.435	2.415	0.029		
M ₃	2.643	2.649	2.641	2.644	0.004		
M ₄	2.656	2.556	2.698	2.637	0.073		
5. Granodiorite	K_1	K_2	K_3	$K_{1-3\text{medium}}$	σ	$K_{\text{Medium-Total}}$	
M ₁	2.112	2.198	2.187	2.166	0.047	2.207	
M ₂	2.206	2.285	2.296	2.262	0.049		
M ₃	2.147	2.158	2.215	2.173	0.036		
M ₄	2.242	2.178	2.256	2.225	0.041		
6. Adamellite	K_1	K_2	K_3	$K_{1-3\text{medium}}$	σ	$K_{\text{Medium-Total}}$	
M ₁	2.693	2.565	2.641	2.633	0.064	2.855	
M ₂	2.976	2.937	2.956	2.956	0.019		
M ₃	2.945	3.147	2.825	2.972	0.162		
M ₄	2.806	2.960	2.809	2.858	0.008		
7. Leuco gneiss	K_1	K_2	K_3	$K_{1-3\text{medium}}$	σ	$K_{\text{Medium-Total}}$	
M ₁	2.560	2.505	2.534	2.533	0.027	2.452	
M ₂	2.364	2.358	2.425	2.382	0.037		
M ₃	2.432	2.441	2.449	2.441	0.008		
M ₄	2.440	2.456	2.455	2.450	0.009		
8. Orthogneiss	K_1	K_2	K_3	$K_{1-3\text{medium}}$	σ	$K_{\text{Medium-Total}}$	
M ₁	2.152	2.599	2.359	2.370	0.050	2.590	
M ₂	2.632	2.596	2.655	2.628	0.030		
M ₃	2.668	2.653	2.675	2.665	0.011		
M ₄	2.669	2.666	2.751	2.695	0.048		
9. Gneiss	K_1	K_2	K_3	$K_{1-3\text{medium}}$	σ	$K_{\text{Medium-Total}}$	
M ₁	2.903	2.987	2.859	2.916	0.065	2.900	
M ₂	2.713	2.992	2.720	2.808	0.159		
M ₃	3.001	3.023	3.019	3.014	0.012		
M ₄	2.853	2.875	2.852	2.860	0.013		
10. Slate	K_1	K_2	K_3	$K_{1-3\text{medium}}$	σ	$K_{\text{Medium-Total}}$	
M ₁	2.851	2.952	2.911	2.905	0.051	3.102	
M ₂	3.178	3.118	3.210	3.169	0.002		
M ₃	3.179	3.258	3.165	3.201	0.050		
M ₄	3.227	3.060	3.112	3.133	0.085		
11. Quartzite	K_1	K_2	K_3	$K_{1-3\text{medium}}$	σ	$K_{\text{Medium-Total}}$	
M ₁	2.880	2.874	2.926	2.893	0.028	3.257	
M ₂	2.933	2.972	3.160	3.022	0.121		
M ₃	3.187	3.247	3.264	3.233	0.040		
M ₄	3.304	3.248	3.678	3.410	0.055		
12. Schist	K_1	K_2	K_3	$K_{1-3\text{medium}}$	σ	$K_{\text{Medium-Total}}$	
M ₁	3.024	3.026	3.036	3.029	0.006	3.019	
M ₂	3.009	3.011	3.009	3.010	0.001		
M ₃	3.005	3.031	3.007	3.014	0.014		
M ₄	3.020	3.025	3.026	3.024	0.003		
13. Meta-sediment	K_1	K_2	K_3	$K_{1-3\text{medium}}$	σ	$K_{\text{Medium-Total}}$	
M ₁	2.368	2.281	2.343	2.331	0.045	2.425	
M ₂	2.442	2.478	2.537	2.486	0.048		
M ₃	2.428	2.476	2.421	2.442	0.030		
M ₄	2.487	2.331	2.504	2.441	0.095		

Thermal conductivity depends largely on the pores size and its distribution as well as the saturation level. To calculate the thermal conductivity, ThermoMap considers these two assumptions:

- For percentages of sand >50%, thermal conductivity is computed as:

$$k = 0.1442 \left(0.7 \left(\lg \frac{PSD}{BD} \right) + 0.4 \right) 10^{(0.62438D)} \quad (4)$$

- For percentages of sand <50%, thermal conductivity is computed as:

$$k = 0.1442 \left(0.9 \left(\lg \frac{PSD}{BD} \right) - 0.2 \right) 10^{(0.6243BD)} \quad (5)$$

Where:

k = thermal conductivity (W/mK)

PSD = distribution of pores size (% per volume)

BD = bulk density (g/cm^3)

According to the texture class of the material, one or another equation is selected and applied in the corresponding calculation of the soil, using the PSD factor deduced from the hydrological state of the system and defining the bulk density values BD (usually $1.3 g/cm^3$ for the depth interval 0–3 m, $1.5 g/cm^3$ for the depth interval 3–6 m and $1.8 g/cm^3$ for the depth interval 6–10 m) (Bertermann et al., 2013).

This application incorporates automatically the climatic parameters of the area in question so it is only necessary to introduce the three data of density, humidity and soil grading, indicating this last parameter by a textural triangle.

ThermoMap calculator offers the possibility of selecting the depth where the material, whose thermal conductivity wants to be obtained, is, with values comprised between 0 m and 10 m. In this case, as it has already been mentioned, depth was not defined, because, although soil samples have been taken in surface, soils were compacted to simulate its state to greater depth. In this way, when introducing density values in this application, we are giving information about its depth, because, to higher compaction the density of the material is also greater, so the high compaction of soils increases its density and with that a position, to a depth typical of a very low enthalpy geothermal energy (< 100 m) submitted to internal temperatures and pressures, is being simulated (Abu-Hamdeh and Reeder, 2000).

In Section 3.2. Estimating thermal conductivities with ThermoMap, thermal conductivities of each soil sample were estimated by this procedure and for each of them three estimations were made, corresponding to three different humidity states and density.

3. Results and discussion

3.1. Measuring with KD2 Pro

Following, Table 2 shows the results of thermal conductivities measurements of the rocky samples taken to laboratory by the use of KD2 Pro. As it has been mentioned throughout this paper, four samples of each one of the rocks types of the province of Ávila were collected. As Table 2 shows, three measurements of each sample were made (K_1, K_2, K_3), the medium value of these three data was calculated ($K_{1-3medium}$) and finally the medium value of the group of values of all the samples of each formation ($K_{MediumTotal}$).

Additionally, standard deviation (σ), which represents the deviation of the measured values (K_1, K_2, K_3) with respect to the medium value ($K_{1-3medium}$), is also presented in Table 2 (Bevington and Robinson, 1992).

Table 3 presents the results of thermal conductivity of soils measured equally with the KD2 Pro. In this case, for each of the four samples of each soil, three different humidity conditions (H_1, H_2, H_3) were reproduced, making three measuring for each sample and humidity state and calculating as in the case of rocks, the medium values of the three values measures per sample and humidity ($K_{1-3medium}$) and the medium value of the group of samples and for each humidity ($K_{MediumTotal}$).

Analyzing both Tables 2 and 3, a series of observations can be deduced:

- The highest values of thermal conductivity belong to quartzite, slates and schist formations, that is to say, these materials would be the most appropriate ones to conduce the heat and, therefore, they would give the best results of efficiency in a geothermal installation. It would make possible to reduce the heat pump power and the total drilling length.
- The highest standard deviations have been obtained for samples of granites, adamellites, gneiss and terraces what indicates that, in these rocks types the measuring process with sensor RK-1 experimented higher variations possibly due to anomalies in the contact of this sensor with the rock because of changes at the thermal grease distribution.

Table 3
Values of thermal conductivity of the soils of Ávila measured with KD2 Pro.

Geological Formation		Thermal Conductivity (W/mK)					
		K_1	K_2	K_3	$K_{1-3medium}$	σ	$K_{MediumTotal}$
$H_1 = 6.32\%$	Sands, clays and muds						
	M ₁	1.444	1.405	1.456	1.435	0.027	1.502
	M ₂	1.421	1.498	1.499	1.473	0.045	
	M ₃	1.587	1.502	1.599	1.563	0.053	
M ₄	1.506	1.589	1.521	1.539	0.044		
$H_2 = 10.97\%$	M ₁	1.804	1.621	1.723	1.716	0.092	1.834
	M ₂	2.227	2.156	2.063	2.149	0.082	
	M ₃	1.900	1.897	1.841	1.879	0.033	
	M ₄	1.612	1.583	1.584	1.593	0.016	
$H_3 = 15.74\%$	M ₁	2.301	2.444	2.406	2.384	0.074	2.434
	M ₂	2.438	2.517	2.423	2.459	0.050	
	M ₃	2.389	2.352	2.439	2.393	0.044	
	M ₄	2.530	2.509	2.464	2.501	0.034	
$H_1 = 6.32\%$	Terraces, alluvial, glacies						
	M ₁	1.939	1.884	1.920	1.914	0.028	1.882
	M ₂	1.898	1.903	1.842	1.881	0.034	
	M ₃	1.849	1.850	1.903	1.867	0.031	
M ₄	1.838	1.877	1.882	1.866	0.024		
$H_2 = 10.97\%$	M ₁	1.793	1.653	1.857	1.768	0.104	2.041
	M ₂	2.430	2.251	2.217	2.299	0.114	
	M ₃	2.210	2.353	2.210	2.258	0.082	
	M ₄	2.071	1.736	1.711	1.839	0.201	
$H_3 = 15.74\%$	M ₁	2.052	2.102	2.156	2.103	0.052	2.125
	M ₂	1.996	1.998	2.115	2.036	0.068	
	M ₃	2.205	2.187	2.203	2.198	0.010	
	M ₄	2.158	2.146	2.187	2.164	0.021	

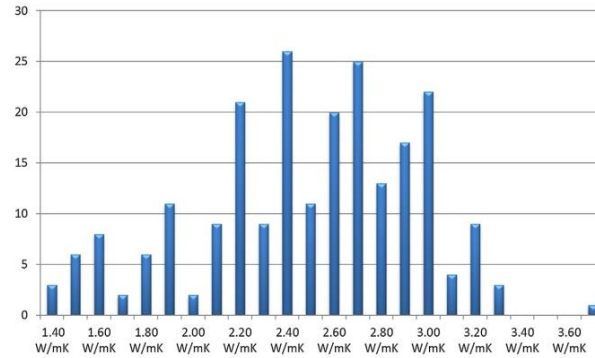


Fig. 5. Frequency distribution of measured conductivities.

- The highest differences among the four samples of each rock type were obtained at monzogranites, granites, adamellites, orthogneiss, quartzite and terraces. This fact means that, these rock types are more heterogeneous in composition or structural state and therefore, they exhibit thermal conductivity variations.
- In every case studied in Table 3, it can be concluded that, for a higher humidity content of the soil sample, thermal conductivity is also higher. This fact is derived from the pores filled with water; this substance has higher conductivity than the air, so the total soil conductivity also increases.
- Formations 14 and 15 (soils) do not exhibit significant differences in thermal conductivity.

Fig. 5 shows the distribution of the thermal conductivity measurements carried out on the solid rock samples by the use of the equipment KD2 Pro and the corresponding sensor RK-1. Analyzing this distribution, it can be observed that the most frequent value is 2.40 W/mK followed by 2.70 W/mK and 3.00 W/mK. These values represent quite high thermal conductivities that point out the suitable capacity of these materials to conduct the heat.

3.2. Estimating thermal conductivities with ThermoMap

By the thermal conductivity calculator of ThermoMap, thermal conductivities of the samples of each soil that occur in the province of Ávila were estimated. In this way, it is viable to make a comparative of the two methods considered for the calculation of this parameter in soils.

As it has already been mentioned, this application requires three parameters of the soils in question: humidity, density and soil grading. Firstly, both bulk density and water content of each sample were defined with the object of simulating the conditions to which soil would be to depths typical of very low enthalpy geothermal resources (<100 m). Thus, three humidity conditions (H_1 , H_2 , H_3) were reproduced on the samples of each soil studied in the present paper and densities of these samples were calculated [UNE 103-300-93, 1993].

The last factor to be determined is the percentage of sand, mud and clay of these soils. To this end, a gradation test was carried out on each one of them according to the procedure considered in the grading essay by sieve [UNE 103-101/95, 1995]. As a result of these essays, it was possible to know the soils grading to classify them according to Casagrande's Classification (Bjerrum et al., 1973). By way of example, Figs. 6 and 7 show the grading curves obtained

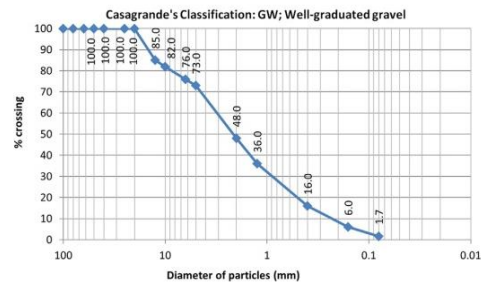


Fig. 6. Grading curve of sample 1 from formation 14: Sands, clays and muds.

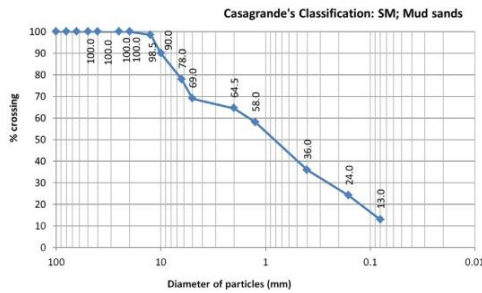


Fig. 7. Grading curve of sample 1 from formation 15: terraces, alluvial and glacia.

from the grading essays by sieve on the sample 1 (M_1) of both soils and its classification.

In this way, after carrying out the grading essay to each sample from formation 14, it was concluded that:

- M_1 = Well graduated stones, mixtures of stones and sands with few or none thin particles (GW)
- M_2 = Mud stones, mixtures of stones, sand and mud (GM)
- M_3 = Mud sands, mixtures of sand and mud (SM)
- M_4 = Well graduated stones, mixtures of stones and sands with few thin particles (GW)

3. Depth layer specific settings

Select depth layer definition

No depth information (like European Outline Map)

4. Depth layer specific parameters

Bulk density (g/cm ³)	Soil texture (USDA)			Water content Vol.-%				Saturation
	* Insert separates	o Select Soil texture group/class	Selection by triangle (optional)	minimum (arid/unsaturated)	maximum (humid/unsaturated)	saturated	measured (Vol.-%) (optional)	
1.59		sand (Class level)		4	11		6.32	unsaturated

5. Calculation

Heat capacity (MJ/m ³ K) DEHNER (2007)	Heat conductivity (W/mK) KERSTEN (1949)				vSGP (Test Area legend)
	Current vSGP value	minimum (arid/unsaturated)	maximum (humid/unsaturated)	saturated	
	1.16	0.96	1.40		medium conductivity

Fig. 8. Example of calculation of thermal conductivity of sample 1 from formation 14 by ThermoMap.

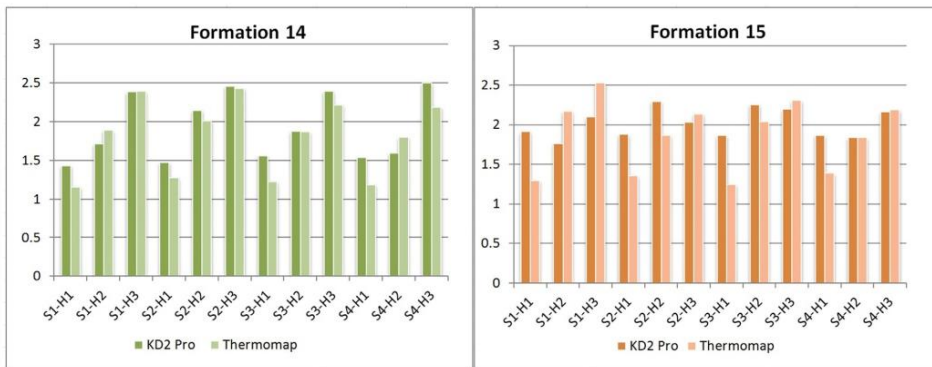


Fig. 9. Comparative thermal conductivities obtained by KD2 Pro-vs. ThermoMap.

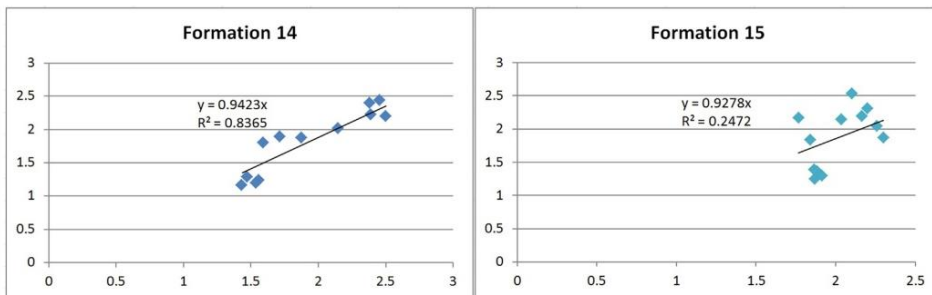


Fig. 10. ThermoMap results against KD2 Pro results with the regression coefficient R².

Table 4
Thermal conductivities of samples from formation 14 calculated by ThermoMap.

Formation 14: sands, clays and muds			
	Humidity	Density (gr/cm ³)	Thermal Conductivity (W/mK)
Sample 1	H ₁	1.59	1.16
	H ₂	1.83	1.89
	H ₃	1.90	2.31
Sample 2	H ₁	1.67	1.28
	H ₂	1.88	2.01
	H ₃	1.94	2.43
Sample 3	H ₁	1.64	1.23
	H ₂	1.82	1.87
	H ₃	1.87	2.22
Sample 4	H ₁	1.61	1.19
	H ₂	1.79	1.80
	H ₃	1.86	2.19

In this case, after completing the grading essay of formation 15 to each one of the samples, it was deduced that:

- M₁ = Mud sands, mixtures of sand and mud (SM)
- M₂ = Well graduated sands, sands with stones with few or none thin particles (SW)
- M₃ = Mud stones, mixtures of stone, sand and mud (GM)
- M₄ = Mud sands, mixtures of sand and mud (SM)

Once the grading compositions of each of the four samples of both materials are known, percentages of stones, sands and thin particles that these formations have, were also determined to be used in the calculator of ThermoMap to estimate thermal conductivities.

After obtaining the three parameters for each soil (density, humidity and soil grading), they have been introduced into ThermoMap calculator.

By way of example, Fig. 8 shows the variables inserted in the application (density, humidity and grading composition) and the result of thermal conductivity obtained for sample 1 from formation 14: *sands, clays and muds*.

Tables 4 and 5 outline this result of thermal conductivity presented in Fig. 9 and the values of thermal conductivity calculated for the rest of humidity states and samples of this same formation

Table 5
Thermal conductivities of samples from formation 15 calculated by ThermoMap.

Formation 15: terraces, alluvial and glacia			
	Humidity (%)	Density (gr/cm ³)	Thermal Conductivity (W/mK)
Sample 1	H ₁	1.68	1.30
	H ₂	1.94	2.17
	H ₃	1.97	2.53
Sample 2	H ₁	1.72	1.36
	H ₂	1.82	1.87
	H ₃	1.84	2.14
Sample 3	H ₁	1.65	1.25
	H ₂	1.89	2.04
	H ₃	1.90	2.31
Sample 4	H ₁	1.74	1.39
	H ₂	1.81	1.84
	H ₃	1.86	2.19

and those ones corresponding to the samples of the other soil (formation 15: *terraces, alluvial and glacia*). The term *glacia* is referred to colluvial and erosive sedimentary deposits.

3.3. Comparison of results, obtained by KD2 Pro and ThermoMap

Thermal conductivities of samples from the geological formations 14 and 15 of the Ávila region (soils) obtained with KD2 Pro were compared with ThermoMap estimations for same locations. As a rule, it can be said that there is a great concordance in the results obtained by both methods. The maximum difference among values resulting from both methods is 0.62 W/mK, being the rest of differences lowers, reaching as minimum difference as 0.001 W/mK. Fig. 9 offers a comparative graphic of the values obtained by each method for the two geological formations and Fig. 10 plots ThermoMap results against KD2 Pro results. In most cases, KD2 Pro presents higher lectures of conductivity than ThermoMap, although the opposite can also be the case. Finally, it can be affirmed that, in spite of the fact that sensor RK-1 of KD2 Pro is not designed to be used in soils, it has supplied acceptable values and similar to the ones obtained with ThermoMap, so it can be considered viable to its use in these conditions.

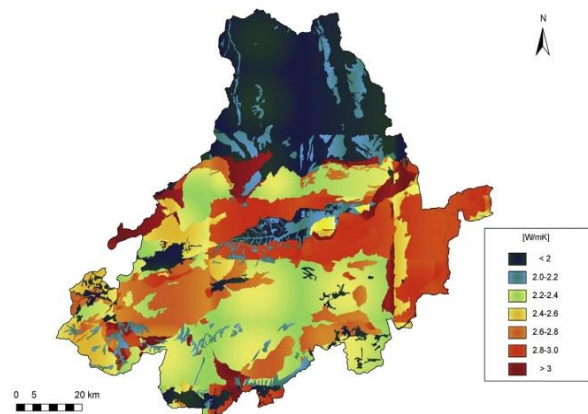


Fig. 11. Geothermal map of the Ávila region.

3.4. Thermal conductivity map of the province of Ávila

As a result of the analysis and calculation of thermal conductivities of the materials contained in the province of Ávila, a thermal conductivity map of Ávila was produced by grouping of materials according to their thermal conductivity. This map will constitute a valuable tool and help when making decisions about the location and calculation of a very low temperature geothermal installation. A good analysis and study of the area of placing the installation can mean an important economic saving and an improvement of its efficiency. Therefore, the importance of this map, that offers the possibility of locating the most appropriate areas (because of their thermal properties) to utilize this renewable energy, is emphasized. Fig. 11 shows the thermal conductivity map of Ávila. It must be mentioned that several other thermal conductivity maps have been already published in other different regions (Iosifina et al., 2016; Randi et al., 2015).

4. Conclusions

The measuring of the thermal conductivity parameter of a series of samples from each geological formation of the province of Ávila has made the production of a thermal conductivity map, possible. The two methods used in this paper were found to be suitable and concordant at the measuring of this thermal property. However, thermal conductivities obtained by ThermoMap are just estimations while measurements with equipment KD2 Pro represent real values of this parameter so this method means the best option to determine the thermal conductivity of rocks and soils.

Within each method, some variations of this parameter were registered in samples belonging to the same geological typology; although insignificant, calculating in each case a medium value to be used in the execution of the geothermal map.

Data collection covering the whole extension and lithology of this region has provided a great variety of thermal information that constitutes an important basis in the pre-design phase of a very low enthalpy geothermal installation. However and given that data were collected in the surface, the thermal conductivity map resulting from the present research has a limitation in its use, that is to say, results are completely reliable to be used in the calculation of the first meters. To greater depths, the most probable is to find the same rocky mass and therefore it would be acceptable the use of the proposed map but it cannot be guaranteed without drilling a hole to take rocky samples from it. For this reason, the use of data presented in this paper is thoroughly recommended and verified for the first meters of drilling but not completely reliable for the rest of the drilling depth. In this way, results should be cross-checked by Thermal Response Tests.

For big projects associated to other types of geothermal energy that require higher drilling lengths, the execution of a Thermal Response Test is highly advisable because it is even more difficult to assure the continuity of the materials from surface.

Acknowledgments

Authors would like to thank the Department of Cartographic and Land Engineering of the Higher Polytechnic School of Ávila,

University of Salamanca, for allowing us to use their facilities and their collaboration during the experimental phase of this research. Authors also want to thank the Ministry of Education, Culture and Sport for providing a FPU Grant (Training of University Teachers Grant) to the corresponding author of this paper what has made possible the realization of the present work.

References

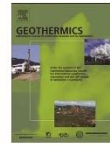
- Abu-Handeh, N.H., Reeder, R.C., 2000. Soil thermal conductivity: effects of density, moisture, salt concentration, and organic matter. *Soil Sci. Soc. Am. J.* 64, 1285–1290.
- Barry-Macaulay, D., Bouazza, A., Singh, R.M., Wang, B., Ranjith, P.G., 2013. Thermal conductivity of soils and rocks from the Melbourne (Australia) region. *Eng. Geol.* 164, 131–138.
- Bertermann, D., Bialas, C., Morper-Busch, L., Klug, H., Rohn, J., Stollhofen, H., Psyk, M., Jaudin, F., Maragna, C., Einarsson, G., Vikingsson, S., Orosz, L., Jordan, G., Vijdea, A.M., Lewis, M., Lawley, R.S., Latham, A., Declercq, P.Y., Peticlerc, E., Zacherl, A., Arvanitis, A.A., Stefuli, M., 2013. ThermoMap—an open-source web mapping application for illustrating the very shallow geothermal potential in Europe and selected case study areas. EGC2013_SG3-05. In: Proceedings European Geothermal Congress, Pisa, Italy, ISBN 978-2-8052-0226-1.
- Bevington, R. Philip, Robinson, Keith, 1992. *Data Reduction and Error Analysis for the Physical Sciences*, 2nd edition. WCB/McGraw-Hill.
- Bjerrum, L., Casagrande, A., Peck, R.B., Skempton, y.A.W., John Wiley and Sons, Terzaghi, K., 1973. *Mechanism of Landslides from theory to practice in soil mechanics*. V III.
- Blázquez, C.S., Martín, A.F., García, P.C., Sánchez Pérez, L.S., del Caso, S.J., 2016. Analysis of the process of design of a geothermal installation. *Renewable Energy* 89 (1), 188–199.
- César, R., Chamorro, José, L. García-Cuesta, María, E. Mondéjar, María, M. Linares, 2014. An estimation of the enhanced geothermal systems potential for the Iberian Peninsula. *Renewable Energy* 66, 1–14.
- Carslaw, H.S., Jaeger, J.C., 1959. *Conduction of heat in solid*, 2nd edition, Oxford, London.
- Clauser, C., Huenges, E., 1995. Thermal conductivity of rocks and minerals. In: Ahrens, T.J. (Ed.), *Rock Physics and Phase Relations, a Handbook of Physical Constants*. American Geophysical Union, Washington, pp. 105–126.
- Decagon Devices, 2016. *KD2 Pro Thermal Properties Analyzer Operator's Manual*. Decagon Devices, Inc.
- Galgara, Antonio, Di Sipiob, Eloisa, Teza, Giordano, Destro, Elisa, De Carli, Michele, Chiesa, Sergio, Zarella, Angelo, Emmi, Giuseppe, Manzella, Adele, 2015. Empirical modeling of maps of geo-exchange potential for shallow geothermal energy at regional scale. *Geothermics* 57, 173–184.
- Geological and Mining Institute of Spain (IGME), 1972–2003. *Geological National Mapping (MAGNA)*.
- Iosifina, Iosif Stylianou, Savvas, Tassou, Paul, Christodoulides, Ioannis, Panayides, Georgios, Florides, 2016. Measurement and analysis of thermal properties of rocks for the compilation of geothermal maps of Cyprus. *Renewable Energy* 88, 418–429.
- Jackson, R.D., Taylor, S.A., 1986. Thermal conductivity and diffusivity. *Methods of soil analysis*, part 1. *Phys. Mineral. Methods*, 945–956.
- Kluitenberg, G.J., Ham, J.M., Bristow, K.L., 1993. Error analysis of the heat pulse method for measuring soil volumetric heat capacity. *Soil Sci. Soc. Am. J.* 57, 1444–1451.
- Peláez, Pedro Casanova, Carnicero, José Manuel Palomar, García, Rafael López, Peragon, Fernando Cruz, 2014. Desarrollo de equipo para la realización de test de respuesta térmica del terreno (TRT) en instalaciones geotérmicas. *Dyna* 89, 316–324.
- Randi, K. Ramstad, Kirsti, Midttømme, Heiko, T. Liebel, Bjørn, S. Frengstad, Bjørn, Willemoes-Wissing, 2015. Thermal conductivity map of the Oslo region based on thermal diffusivity measurements of rock core samples. *Bull. Eng. Geol. Environ.* 74, 1275–1286.
- Shiozawa, S., Campbell, G.S., 1990. Soil thermal conductivity. *Remote Sens. Rev.* 5, 301–310.
- Thermo Map, 2013. ThermoMap MapViewer, web site, Available from <http://geoweb2.sbg.ac.at/thermomap/>.
- Vijdea, Anca-Marina, Weindl, Christopher, Cosac, Ana, Asimopolos, Natalia-Silvia, Bertermann, David, 2014. Estimating the thermal properties of soils and soft rocks for ground source heat pumps installation in Constanta county, Romania. *J. Therm. Anal. Calorim.* 118, 1135–1144.

PAPER 4



Contents lists available at ScienceDirect

Geothermics

journal homepage: www.elsevier.com/locate/geothermics

Thermal conductivity characterization of three geological formations by the implementation of geophysical methods



Cristina Sáez Blázquez*, Arturo Farfán Martín, Pedro Carrasco García, Diego González-Aguilera

Department of Cartographic and Land Engineering, University of Salamanca, Higher Polytechnic School of Avila, Hornos Caleros 50, 05003 Avila, Spain

ARTICLE INFO

Keywords:

Low enthalpy geothermal installations
Thermal conductivity
Multichannel analysis of surface waves
Seismic refraction
Wave's velocities

ABSTRACT

In very low enthalpy geothermal installations it is essential to know the thermal conductivity parameter of the surrounding ground. The present study uses seismic prospecting as a basis for the knowledge of the mentioned thermal property. Using the technique of Multichannel Analysis of Surface Waves (MASW) and seismic refraction, it has been possible to correlate the velocity of the *P* and *S* waves with the thermal conductivity of three study areas. Continuous measurements of the thermal conductivity parameter were performed on samples from the areas where the seismic prospecting was made. The maximum and minimum thermal conductivity values were connected to the highest and lowest *P* and *S* wave's velocities. From this relation, an interpolation between the couple of values allows to obtain a linear equation used to predict the intermediate thermal conductivity values. As a result, graphs of thermal conductivity against *P* and *S* wave's velocities were created for each of the study areas. Additionally, 2D images of the spatial distribution of the thermal conductivity of the subsoil of each formation were performed. Thus, seismic prospecting allows, besides knowing the geology of the subsoil, the possibility of estimating the thermal conductivity of a certain ground. This parameter is indispensable for the subsequent process of calculation and dimensioning of a very low temperature borehole heat exchanger.

1. Introduction

The growing demand of very low enthalpy geothermal installations encourages paying special attention in the design of these systems. An incorrect dimensioning could cause important consequences in the short and long term operation. It is therefore fundamental to carry out an exhaustive analysis of the ground where the installation will be placed.

In this context, the thermal conductivity of the surrounding ground is especially important. This parameter influences the thermal exchange between the ground and the rest of components of the installation. Thus, the value of this property affects the drilling length required to cover some specific needs (Blázquez et al., 2016). The thermal conductivity is an important physical property for predicting heat flow and corresponding subsurface temperatures (Haenel et al., 1988; Riihaak et al., 2015; Riihaak, 2015). It describes how well the heat is conducted through a material.

Although it is still difficult to estimate the thermal conductivities of rocks at a large scale required for geothermal applications, different methods currently estimate it for full geological formations, sections or boreholes (Fuchs and Balling, 2016a; Fuchs and Balling, 2016b). In this context, tools as the optical scanning technique, allows providing

measurements on cores samples directly (Popov et al., 2016). At present, there is tabulated information that assigns a value of thermal conductivity to each geological formation. It associates an approximate thermal conductivity value to a certain material without cost. However, its precision is quite low given that the thermal conductivity can still vary considerably, even for the same rock type (Cermak and Rybach, 1982). The opposite case would be the execution of a Thermal Response Test (TRT) in the corresponding ground. It provides an accurate thermal conductivity value despite the additional cost that this test involves. There are also numerous devices that measure the thermal conductivity of a material from samples analyzed in the laboratory. The controversy of these methods is that the whole rocky formation is not considered and the thermal conductivity results do not represent all the ground (Blázquez et al., 2017; Barry-Macaulay et al., 2013; Liou and Tien, 2016; Kukkonen and Lindberg, 1995; Lira-Cortés et al., 2008; Jorand et al., 2013; Krishnaiah et al., 2004).

For these reasons, it is important to look for alternatives to estimate the thermal conductivity of the whole geological formation that surrounds the borehole heat exchanger. The implementation of these techniques should not constitute an impediment from the economic point of view.

The integration of secondary data, like seismic velocities

* Corresponding author.

E-mail address: u107596@usal.es (C. Sáez Blázquez).

<https://doi.org/10.1016/j.geothermics.2017.11.003>

Received 21 June 2017; Received in revised form 2 November 2017; Accepted 2 November 2017

0375-6505/ © 2017 Published by Elsevier Ltd.

measurements could constitute an excellent option to balance the accuracy and the representation of the thermal conductivity results with the cost that its execution entails (Esteban et al., 2015; Pimienta et al., 2014). Before drilling the geothermal borehole/s, it is necessary to know the subsoil materials to choose the most suitable drilling method. Generally, seismic prospecting is commonly used for such purposes. The present research suggests the use of this technique with an additional aim: estimating the thermal conductivity parameter of the ground where is used. Thus, seismic prospecting would allow knowing the geological composition of a certain ground and in turn, its thermal conductivity by the correlation of this property with different seismic parameters.

The occurrence of a similar trend between thermal conductivity and compressional wave velocity has sufficiently been demonstrated in numerous previous studies (Balling et al., 1981; Fuchs et al., 2015; Gegenhuber and Schoen, 2012; Hartmann et al., 2008; Özkahraman et al., 2004a; Özkahraman et al., 2004b; Popov et al., 2003). This is why the principal objective of this research is to combine thermal conductivities from laboratory measurements and seismic velocities from in situ seismic prospecting. Thermal conductivity measurements are carried out on samples analyzed in the laboratory (rocks) or directly in their original place (loose materials). Seismic profiles are made throughout the study area where samples are collected to measure the thermal conductivity parameter. The principal purpose of this study is correlating both parameters: by the use of real seismic and thermal conductivity measurements and without model predictions. Thus, results will be completely representative of the area in question given the basis on real data. The final results provide a 2D thermal conductivity image of each area where the present methodology was implemented.

2. Materials and method

2.1. Theoretical basis

Geophysics includes a large number of techniques whose aim is the study of the Earth's crust materials. Throughout this work these techniques and the resulting parameters from them were analyzed to find a logical relation between them and the thermal conductivity. After an exhaustive analysis and study of state of the art, the seismic prospecting methods were selected as potential candidates to achieve the objective of this work.

Seismic prospecting techniques are based on the measurement of the arrival times of the *P* and *S* waves generated on the ground by a particular mechanical energy source. These waves are transmitted from a point to another where sensors (geophones) are connected to a seismograph recorder.

The way in which the seismic waves are transmitted through the ground presents a great similarity to the way in which the heat is transmitted by the mechanism of conduction. The propagation velocity of seismic waves in the ground is different depending on each material, as in the case of the heat conduction. In most cases, both parameters have a directly proportional relation (Özkahraman et al., 2004a; Özkahraman et al., 2004b; Özkahraman et al., 2004a; Özkahraman et al., 2004b), although, for certain materials and conditions this positive trend is not always observed (Fuchs and Förster, 2014; Gegenhuber, 2011). In this research, the positive correlation between both parameters was previously verified by in situ measurements in the study areas subsequently defined.

Thus, for the same geological composition, the transmission velocity of the seismic waves is higher in hard and compact rocks and lower in the case of poorly consolidated rocks. In the same way, the thermal conductivity of a ground is higher if the compaction and consolidation of that material is also high.

For a given material, its state of maximum deterioration and decomposition corresponds to the minimum velocity at which *P* and *S* waves propagate through it. In contrast, the state of maximum

Table 1
Study areas selected in the present research.

Area	Location	Rock type
1	40°37'37.57"N 4°36'38.45"O	Schists
2	40°39'48.99"N 4°42'47.27"O	Medium grain adamellite
3	40°39'23.68"N 4°40'13.99"O	Coarse-grained adamellite

consolidation and compaction of a formation corresponds to the highest velocity at which these waves are capable of being transmitted through it. Also, the thermal conductivity for that material will have the lowest value for its state of maximum decomposition and its highest value for its state of maximum consolidation.

Based on this fact, (and given the directly proportional relation between *P* and *S* waves' velocity and thermal conductivity) it is possible to establish a correlation between the propagation velocity of these waves in a given material and its thermal conductivity.

By carrying out seismic prospecting on a particular area and on the basis of its geology, some relevant information can be deduced:

- Distribution of materials in the subsoil.
- Detection of the most altered areas (maximum state of alteration) and those ones that present the maximum state of compaction. Each of these areas has an assigned velocity value of the *P* and *S* waves.

By taking samples of these zones and measuring the thermal conductivity of each one, we obtain the initial and final points of a relation between the seismic velocities and the thermal conductivity. From this pattern, it is possible to know by thermal seismic tests the thermal conductivity at any place (constituted by any of the materials tested in this article) where the geothermal installation will be placed.

2.2. Materials (Techniques)

Seismic prospecting and thermal conductivities used in this work were the following:

2.2.1. Seismic measurements

The exploration techniques used to achieve the objective of the present research are included in the seismic field:

2.2.1.1. Multichannel analysis of surface waves (MASW). It is a non-destructive seismic method that evaluates the thickness of the pavement as well as the linear elastic modules of the materials placed under this pavement (Park et al., 1999). This method analyzes the dispersion properties of the surface seismic waves, which horizontally propagate along the surface from the impact point to the receivers.

A set of receivers distributed along short (1–2 m) and long (50–100 m) distances simultaneously record the emissions from an impulsive or vibratory source. Statistical redundancy is provided to measure phase velocities. Multichannel data show a variable frequency format over time. From the analysis of these data it is possible the identification and rejection of non-fundamental Rayleigh waveforms and incoherent noise (Louie, 2001).

In the present work, MASW tests were carried out using a device of 10 (area 1) and 12 (area 2 and 3) geophones of 4.5 Hz placed every 5 m. The working methodology involved the execution of a series of shots by a 20 kg tenderiser. The equipment used in these tests was the commercially known as "Stratavisor Nx" belonging to "Geometrics". This device has 60 channels and an auto-calibration option.

After the execution of the in situ MASW tests, data were extracted and processed by the "Surface Wave Analysis Wizard" module of the software "Seisimager". This software allows obtaining the *S* wave by

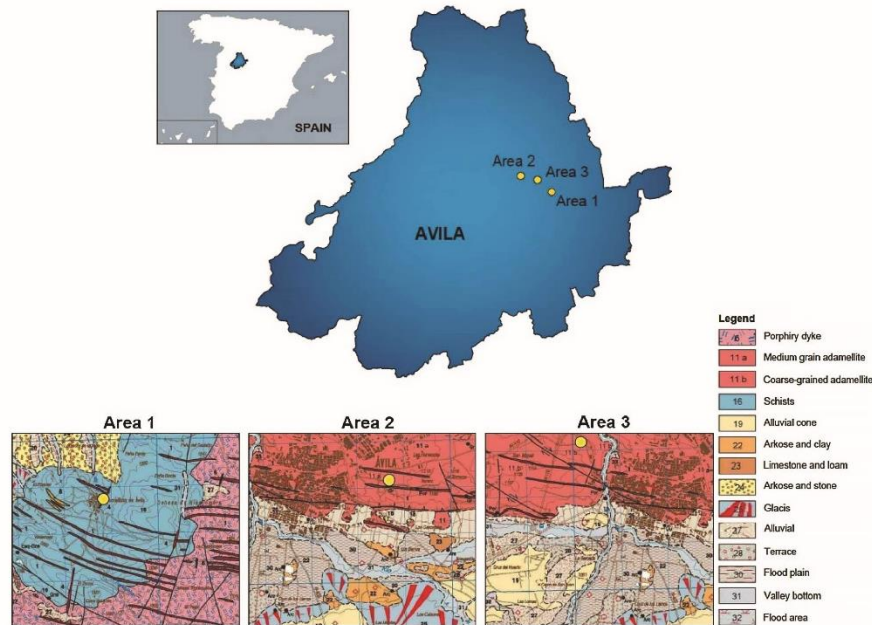


Fig. 1. Geological characterization of the three study areas.

the analysis of the frequencies and phase velocities of the surface seismic waves. Additionally, a series of secondary data (presented in Section 3. Results) are automatically calculated and provided by this equipment.

2.2.1.2. Seismic refraction. The other prospecting technique used in this study is based on seismic refraction. It consists of the generation of seismic waves by a hammer or an explosive, and the recording of those waves that suffer total refraction along the contacts of variable velocity layers. In this case, the recorded waves are the primary or longitudinal P waves, in which particles move in the propagation direction of the wave, by compressions and dilations.

This system records the arrival times of waves produced by impacts of a hammer on a steel sheet placed in the surface of the ground until its arrival to a set of geophones. These devices transform the ground vibrations produced by the waves into electrical signals.

Seismic refraction uses the times of the first arrivals in the seismograph. These arrival times correspond to the refracted waves in the different subsoil layers. Each of these layers is distinguished by its acoustic impedance called refractor.

As a result of the application of this method, a ground seismic image was obtained in the form of a velocity section ($V(x,z)$).

Each seismic refraction profile was 50 m in length (area 1) and 60 m in length (area 2 and 3) with geophones placed every 5 m, shooting at the ends and center of each profile.

2.2.2. Thermal conductivity measurements

Measurements of the thermal conductivity parameter were carried out using the KD2 Pro equipment developed by Decagon Devices (Decagon Devices, 2016). This device is constituted by a portable controller and a sensor (RK-1) that makes possible the measurement of

the thermal conductivity of rocks or previously compacted soils.

Its operation is based on the infinite line heat source theory and computes the thermal conductivity by monitoring the dissipation of heat from the needle probe. Heat is applied to the needle for a set heating time t_h , and temperature is measured in the monitoring needle during heating and for an additional time equal to t_h after heating. The temperature during heating is deduced from Eq. (1).

$$T = m_0 + m_2 t + m_3 \ln t \quad (1)$$

Where:

m_0 is the ambient temperature during heating

m_2 is the rate of background temperature drift

m_3 is the slope of a line relating temperature rise to logarithm of temperature

Eq. (2) represents the model during cooling.

$$T = m_1 + m_2 t + m_3 \ln \frac{t}{t - t_h} \quad (2)$$

Both Eqs. (1) and (2) are used by the equipment to provide the temperatures during the period of heating and after it when heating stops and needle starts cooling.

Thermal conductivity is calculated from Eq. (3) that also considers the heat flux (q).

$$k = \frac{q}{4m_3} \quad (3)$$

Only 2/3 of the data collected are used during heating and cooling (it ignores early-time data) since these equations are long-time approximations to the exponential integral equations. It helps to prevent errors derived from the placement of the needle. Eqs. (1) and (2) can be solved by linear least squares, giving a solid and more adjusted result (Kluitenberg et al., 1993; Shiozawa and Campbell, 1990).

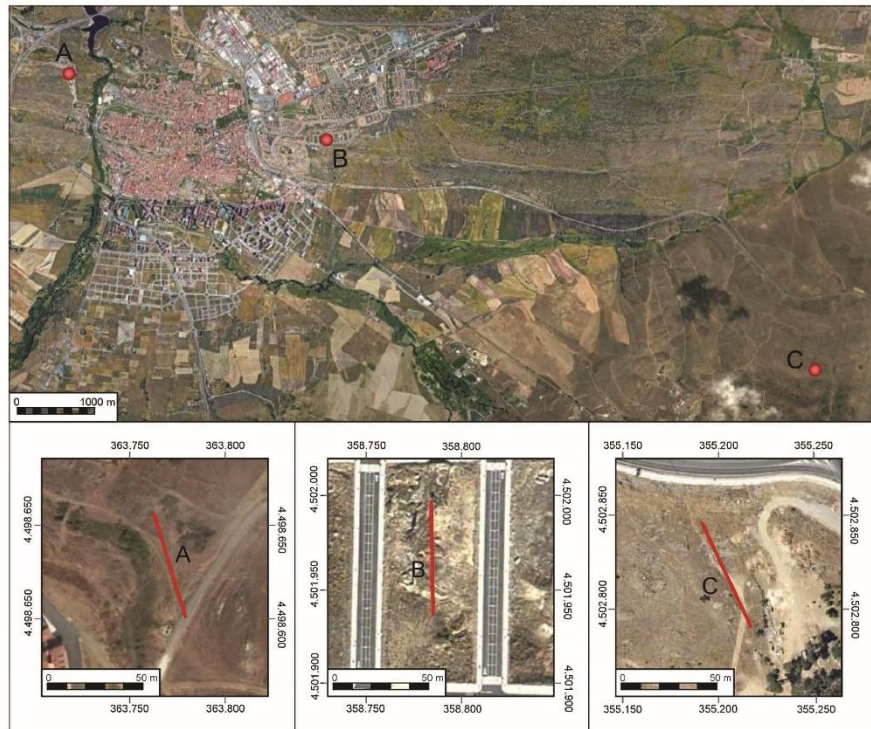


Fig. 2. Position of the seismic profiles (Geodetic Datum: WGS84, Cartographic projection: UTM, Time zone: 30). A) area 1, B) area 2, C) area 3.

Sensor RK-1 (3.9 mm in diameter and 6 cm in length) was used in the present research to measure the thermal conductivity of each sample collected from the ground. This sensor is capable of measuring the thermal conductivity in a range between 0.1 and 6 W/mK with $\pm 10\%$ of accuracy and three digits of precision. Before use, it was previously calibrated with samples supplied by the manufacturer.

The relatively long read times of sensor RK-1 (around 10 min) contribute to prevent errors derived from the large diameter needle and the contact resistance between the sensor and the granular sample and solid materials. The contact between needle and tested material is guaranteed by placing thermal grease in the hole where the needle is situated. Drilling could increase the uncertainty on results. Three measurements were made in each case to evaluate the possible uncertainties.

Measurements with KD2 Pro can be strongly affected by wrong practices. To obtain the most accurate data possible, ambient temperature was kept as constant as possible during the measurement. If sample temperature changes during the measurement period, it degrades the data and makes it difficult for the inverse calculation to find the correct values for the thermal properties. To minimize these sources of error, about 15 min for samples and needle to equilibrate with the ambient temperature before taking measurements and around 15 min between readings for temperatures to equilibrate.

2.3. Methodology

2.3.1. Selection of the study areas

Three areas of known geology were chosen for the analysis of the correlation between the seismic and thermal parameters. Table 1 shows the location of these three zones, placed in the province of Avila (Spain) and the predominant geology formations in each of them. Additionally, in Fig. 1, it is possible to observe in a more exhaustive way the geological information of the mentioned areas.

2.3.2. Seismic prospecting

After selecting the study areas, the following actions were carried out:

- Tracing of profiles (50 m long in area 1 and 60 m long in areas 2 and 3) for the subsequent execution of the seismic prospecting tests (MASW and seismic refraction). Fig. 2 shows the location of these profiles.
- Execution of the seismic prospecting tests. MASW and seismic refraction tests were carried out on the profiles presented in Fig. 2.

2.3.3. Thermal conductivity tests

Thermal conductivity tests were made as follows:

- Visual exploration of each area to detect the samples with the highest degree of alteration and those samples completely compact

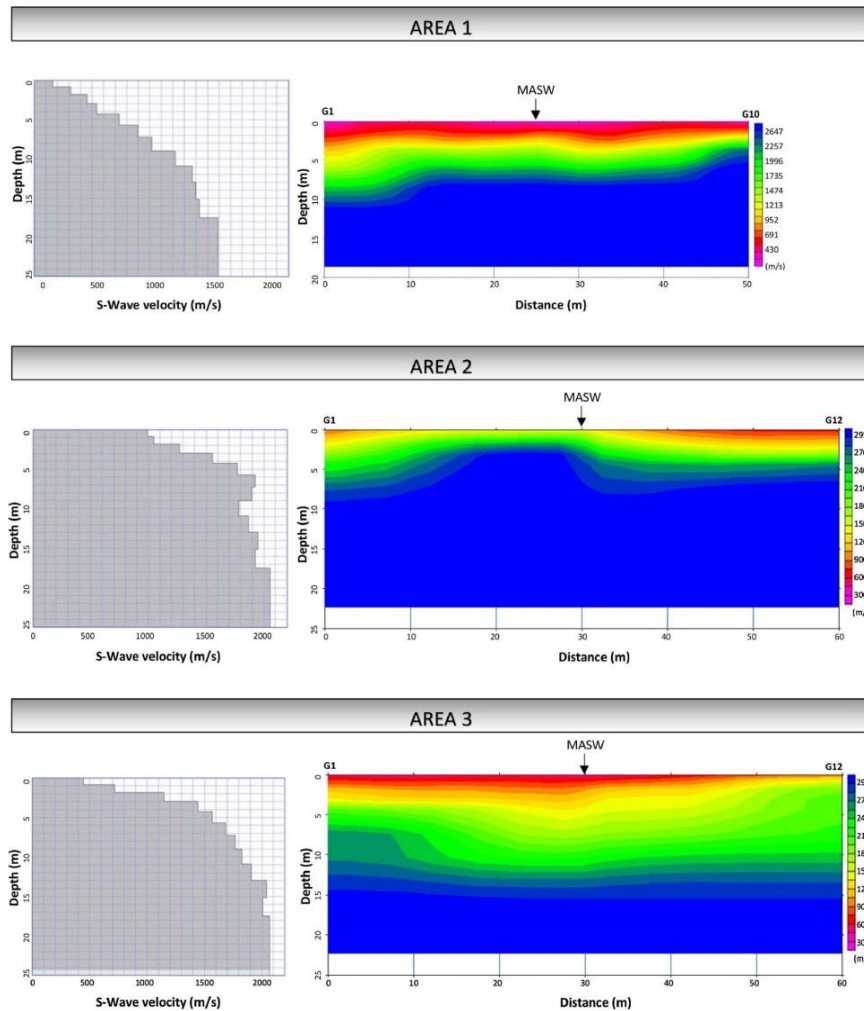


Fig. 3. Variation of the S-wave velocity with depth from MASW tests (on the left) and P-wave velocity distribution from seismic refraction (on the right) for each of the areas (area 1, area 2 and area 3).

- and with the least degradation. Both samples belonging to the same geological formation. A set of thermal conductivity measurements were made on the most and least decomposed samples to find the lowest and highest thermal conductivity values, respectively.
- When the most and least thermal conductive samples were identified, three thermal conductivity tests were made on each of them waiting about 15 min between readings for temperatures to equilibrate.
 - A specific methodology was established to carry out these tests. Loose material samples were measured in situ to reproduce its original conditions. Thirty measurements were carried out in the

upper ground layer to find the most decomposed samples. Appreciable differences in the thermal conductivity parameter would be obtained in deeper layers. However, it does not constitute an inconvenience since in this research only the lowest values are required, and these values are placed in the least compact layer (the upper one). The water-saturation would also be different in deeper layers, this fact would not either affect the present work due to the reasons previously explained. Regarding compact rocky samples were taken to the laboratory to facilitate the drilling of the hole where the needle of RK-1 sensor is placed. Thirty rocky samples were collected and from these ones, the four with the highest

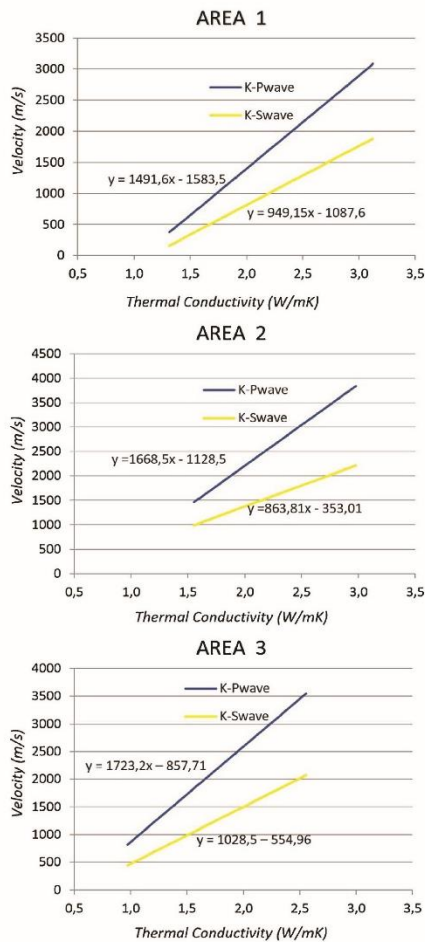


Fig. 4. Thermal conductivity versus *P* and *S* wave's velocities for each area. A) Area 1, B) Area 2, C) Area 3.

characterise each geological formation.

S-wave velocity values presented in Tables A1–A3 were used in the corresponding correlation with the thermal conductivity measurements presented in Section 3.2. *Thermal conductivity results*.

3.1.2. Seismic refraction

Seismic refraction prospecting provided the evolution of *P*-waves velocity from surface to a depth of 20 m and along 50 m for area 1 (length of profile 1) and 60 m for the rest of areas 2 and 3. These results (also presented in Fig. 3), are shown as sections with different tonalities depending on the *P*-wave velocity.

Graphs shown on the right side of Fig. 3 allow obtaining the *P*-wave velocity values for any point in depth and length. Values corresponding to MASW position (in different depths) have been correlated with the thermal conductivity measurements.

3.2. Thermal conductivity results

Thermal conductivity results are shown in Tables 2 and 3. Table 2 presents the maximum thermal conductivity values corresponding to the state of lowest degradation of each formation. On the contrary, Table 3 collects the minimum thermal conductivity values corresponding to the state of highest degradation. The methodology consisted of the realization of several thermal conductivity tests on different samples. As already mentioned, thirty measurements were carried out in the field on the most decomposed materials as well as thirty rocky specimens were measured in the laboratory. This work methodology allowed identifying the most and least decomposed materials of each area, selecting the final samples to be considered in the present research. From each of these samples (Samples 1, 2, 3 and 4) three measurements were made to verify the results (V_1 , V_2 and V_3). For each case, the lowest and highest values are shown in Tables 2 and 3, the mean of them, and finally the maximum/minimum value.

Maximum and minimum thermal conductivity values presented in Tables 2 and 3 were subsequently related with *P* and *S* wave's velocities as shown in the next section.

3.3. Correlation of *S* and *P* waves velocities with thermal conductivities

The correlation between the *P* and *S* wave's velocities and the values of thermal conductivities are shown below for each of the study areas. *P*-waves velocities were taken from the seismic refraction results and calculated in the position of the MASW test in each profile. *S*-waves velocities were directly taken from MASW tests.

The minimum thermal conductivity values (of the whole area) presented in Table 3 have associated the lowest *P* and *S* waves' velocity of the same global area. On the contrary, the maximum thermal conductivity values from Table 2 are associated to the highest *P* and *S* waves' velocity. Specific combinations of thermal conductivities and velocities data corresponding to the same point were not carried out. A straight line connects both correlations, so the equation of this line is used to calculate the intermediate values. The following sections show numerically and graphically the connection among the mentioned parameters for each area.

The correlations between *P* and *S* wave's velocities and the thermal conductivities values are shown in Table 4 (area 1), Table 5 (area 2) and Table 6 (area 3). Fig. 4 graphically presents the mentioned correlations for the three study areas. The lowest and highest thermal conductivity values measured in each of the areas were associated to the lowest and highest *P* and *S* wave velocities. Based on these initial and final points, the rest of wave's velocities values from the seismic prospecting were given a thermal conductivity value following the equation obtained in each case (Fig. 4).

4. Discussion

4.1. Data collection and processing

The most laborious task when carrying out this work was the data collection to measure the maximum and minimum thermal conductivity values. The study of any formation requires the collection of sufficient representative samples. In this case, the thermal conductivity of samples from continuous profiles was measured in situ (loose

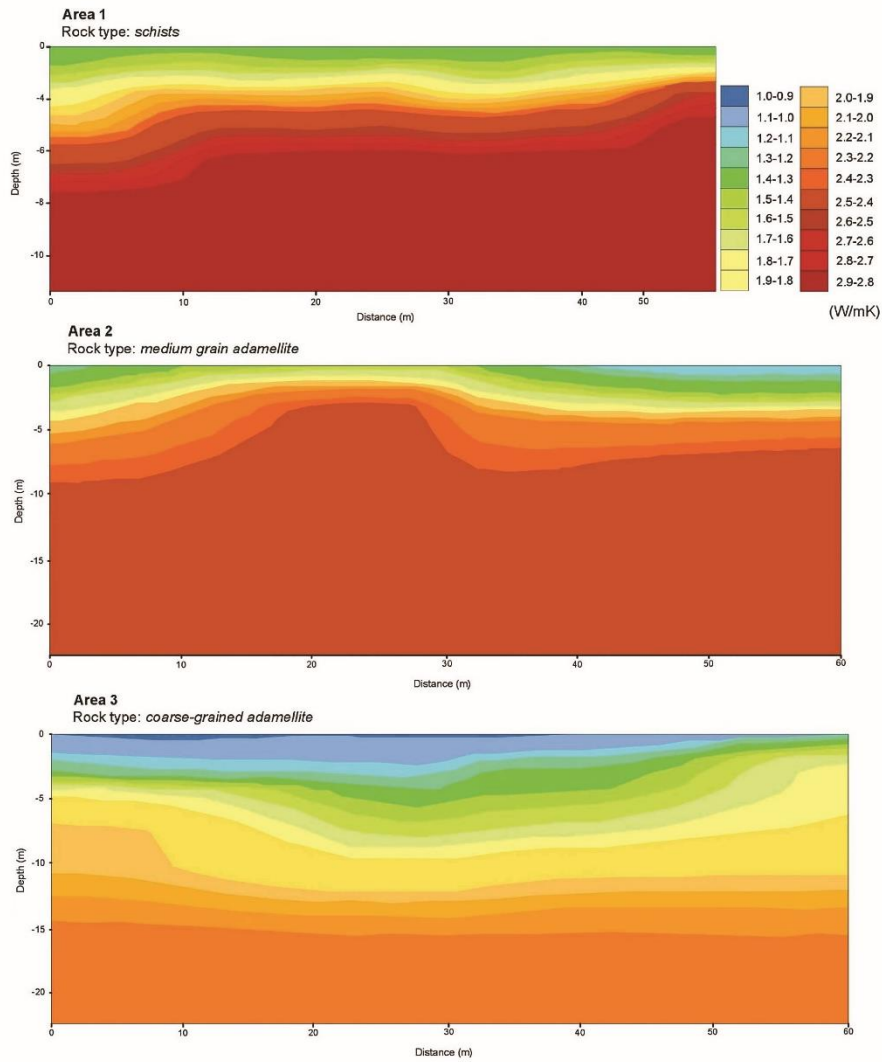


Fig. 5. 2D thermal conductivity image of the ground. A) area 1, B) area 2 and C) area 3.

material) or in the laboratory (rocky samples). An arduous methodology was followed to detect the most/least decomposed material, that is to say, the samples with the highest/lowest thermal conductivity in each area. Once detected the mentioned samples, the thermal conductivity measuring was properly verified due to the large number of

measurements made in each case. Additionally, the validity of these measurements was confirmed by comparing the results with the ones commonly accepted at the “*Technical Code of Building*” (CTE) for each geological formation (Constructive Solutions Compendium, 2007).

Relating the seismic prospecting, there were not significant

difficulties in the process of field measuring. P and S wave's velocities are representative of an area in question and it is difficult to compare those values with the ones of similar formations. This fact is due to the different conditions (pressure, compaction, humidity...) experienced in each case.

4.2. Method

Seismic velocities known from MASW and seismic refraction measurements have been used as secondary variables for estimating the thermal conductivity of the surrounding ground at a very low enthalpy borehole heat exchanger. P and S waves velocities are typically easier to obtain and more readily than sparse thermal conductivity values. Considering the similar trends between seismic waves and heat conduction, thermal conductivity values can be estimated from an interpolation of seismic profiles. It is important to highlight that seismic velocity qualitatively encompasses information of the ground, such as rock fracturing or possible heterogeneities in the rock lithology that can be identified from the different seismic velocities they cause. This information can be also used to interpolate the thermal conductivities of rocks in space. The quality of this interpolation will depend mainly on the closeness of the general trend between both variables. As shown in Fig. 4, from P or S wave's velocities, the corresponding thermal conductivity value can be known in each of the study areas.

The presented research shows valid and reasonable results for three different geological formations. These results can be used for future measurements of geothermal installations placed in these lithologies. For this reason, the method is limited to similar areas to the ones considered in this study. Studies about other formations will be performed in future.

The correlation P wave velocity-thermal conductivity is supported by a large number of researches (Zamora et al., 1993; Boulanouar et al., 2012; Gu et al., 2017). In this study, MASW prospecting provided S wave velocities which allowed having an additional source of correlation. It is also important to highlight the lack of previous works focused on the same rock types. Thus, the present research constitutes a useful tool when dimensioning a geothermal installation in similar geological formations.

Appendix A

Additional information is presented in Tables A1–A3, and .

Table A1
Parameters obtained from MASW tests in area 1.

Depth (m)	S-wave velocity (m/s)	Density (g/cm ³)	N – SPT (n° of hits)	Poisson coefficient "μ"	Young's modulus "E" (GPa)	Cutting modulus "G" (GPa)	Compressibility modulus "K" (GPa)
0.0	157.6	1.777	4.695	0.395	0.123	0.044	0.196
0.8	314.0	1.832	42.120	0.218	0.440	0.180	0.260
1.8	454.5	1.880	136.866	0.260	0.978	0.388	0.679
2.96	536.9	1.908	232.633	0.292	1.421	0.550	1.140
4.2	732.9	1.972	626.772	0.326	2.808	1.059	2.682
5.7	895.6	2.024	1186.543	0.435	4.658	1.622	12.022
7.3	1017.5	2.061	1781.919	0.418	6.050	2.133	12.299
9.0	1218.9	2.121	3166.991	0.379	8.687	3.150	11.939
10.9	1367.6	2.163	4568.773	0.345	10.877	4.045	11.660
13.0	1397.3	2.172	4892.658	0.340	11.364	4.239	11.871
15.2	1428.4	2.180	5247.748	0.333	11.859	4.447	11.862
17.5	1589.2	2.224	7371.032	0.314	14.761	5.615	13.250
25.0	1877.5	2.298	12534.741	0.207	19.558	8.099	11.139

5. Conclusions

Thanks to the development of these types of methodologies, it is possible to predict the thermal behaviour of geological formations. From MASW and seismic refraction tests together with thermal conductivity measurements, graphs of thermal conductivity against P and S wave's velocities have been presented (Fig. 4). From these graphs a 2D thermal conductivity image of the subsoil was obtained for each study area. These images, shown in Fig. 5, allow knowing the thermal conductivity of the different layers of the ground.

Knowing the real thermal conductivity of a certain geological formation is really useful when making the preliminary measuring of a very low enthalpy geothermal system. An appropriate estimation of the thermal conductivity parameter of the surrounding ground can avoid important over-measurements with the consequent economic saving. A slight variation of this parameter has a huge influence in the total drilling length of the borehole.

From a general perspective the results confirm that geophysical methods (MASW and seismic refraction) are of great value to evaluate the thermal conductivities of rocks in geothermal reservoirs. Apart from the general geological information provided by these methods, they also constitute a helpful practice in geothermal reservoir modelling in the depth of the present research.

Future researches in areas of different geology will complete the present work making it available to be used in a wider range of geothermal systems.

Acknowledgments

Authors would like to thank the Department of Cartographic and Land Engineering of the Higher Polytechnic School of Avila, University of Salamanca, for allowing us to use their facilities and their collaboration during the experimental phase of this research. Authors also want to thank the Ministry of Education, Culture and Sport for providing a FPU Grant (Training of University Teachers Grant) to the corresponding author of this paper what has made possible the realization of the present work.

Table A2
Parameters obtained from MASW tests in area 2.

Depth (m)	S-wave velocity (m/s)	Density (g/cm ³)	N – SPT (n° of hits)	Poisson coefficient “ μ ”	Young’s modulus “E” (GPa)	Cutting modulus “G” (GPa)	Compressibility modulus “K” (GPa)
0.0	989.3	2.053	1629.395	0.081	4.341	2.008	1.726
0.8	1046.1	2.070	1946.402	0.265	5.729	2.264	4.062
1.8	1269.2	2.136	3602.445	0.229	8.454	3.439	5.200
3.0	1554.2	2.215	6866.726	0.247	13.334	5.348	8.771
4.2	1770.1	2.271	10390.786	0.290	18.355	7.114	14.569
5.7	1925.6	2.310	13587.210	0.269	21.742	8.564	15.712
7.3	1894.9	2.303	12908.598	0.273	21.051	8.266	15.486
9.0	1784.8	2.275	10667.931	0.288	18.664	7.245	14.676
10.9	1866.2	2.296	12296.397	0.277	20.416	7.992	15.274
13.0	1947.0	2.316	14073.677	0.267	22.228	8.775	15.870
15.2	1925.5	2.310	13582.999	0.269	21.737	8.562	15.711
17.5	2055.2	2.342	16719.029	0.252	24.766	9.887	16.671
25.0	2216.7	2.396	21273.474	0.249	29.404	11.770	19.533

Table A3
Parameters obtained from MASW tests in area 3.

Depth (m)	S-wave velocity (m/s)	Density (g/cm ³)	N – SPT (n° of hits)	Poisson coefficient “ μ ”	Young’s modulus “E” (GPa)	Cutting modulus “G” (GPa)	Compressibility modulus “K” (GPa)
0.0	445.8	1.890	128.674	0.289	0.969	0.376	0.767
0.8	717.0	1.972	584.310	0.362	2.762	1.014	3.343
1.8	1144.1	2.091	2588.448	0.072	5.867	2.736	2.286
3.0	1443.6	2.171	5427.848	0.771	2.069	4.522	0.271
4.2	1566.4	2.199	7040.047	1.046	0.497	5.393	0.054
5.7	1685.0	2.230	8881.790	0.055	11.958	6.328	3.590
7.3	1768.6	2.255	10363.110	0.028	13.709	7.051	4.329
9.0	1827.7	2.273	11506.272	0.036	14.637	7.592	4.551
10.9	1905.7	2.294	13143.163	0.032	16.119	8.327	5.048
13.0	2040.9	2.325	16351.707	0.056	18.286	9.683	5.484
15.1	2007.4	2.314	15510.472	0.147	21.380	9.321	10.090
17.5	2069.2	2.325	17084.694	0.190	23.690	9.953	12.739
25.0	2075.0	2.325	17237.326	0.240	24.826	10.009	15.927

References

- Özkahraman, H.T., Selver, R., Isik, E.C., 2004a. Determination of the thermal conductivity of rock from P-wave velocity. *Int. J. Rock Mech. Min. Sci.* 41, 703–708.
- Özkahraman, H.T., Selver, R., Isik, E.C., 2004b. Determination of the thermal conductivity of rock from P-wave velocity. *Int. J. Rock Mech. Min. Sci.* 41, 703–708.
- Balling, N., Kristiansen, J.J., Breiner, N., Poulsen, K.D., Rasmussen, R., Saxov, S., 1981. Geothermal measurements and subsurface temperature modelling in Denmark. *Geol. Skt.* 16 (1), 172.
- Barry-Macaulay, D., Bouazza, A., Singh, R.M., Wang, B., Ranjith, P.G., 2013. Thermal conductivity of soils and rocks from the Melbourne (Australia) region. *Eng. Geol.* 164, 131–138.
- Blázquez, C.S., Martín, A.F., García, P.C., Sánchez Pérez, L.S., del Caso, S.J., 2016. Analysis of the process of design of a geothermal installation. *Renew. Energ.* 89 (1), 188–199.
- Blázquez, Cristina Sáez, Martín, Arturo Farfán, Nieto, Ignacio Martín, García, Pedro Carrasco, Sánchez Pérez, Luis Santiago, Aguilera, Diego González, 2017. Thermal conductivity map of the Avila region (Spain) based on thermal conductivity measurements of different rock and soil samples. *Geothermics* 65, 60–71.
- Boulanouar, A., Rahmouni, A., Boukalouch, M., Géraud, Y., El Amrani El Hassani, I., Hammami, M., Sebbaoui, M.J., 2012. A Correlation between P-wave velocity and thermal conductivity of heterogeneous porous materials. *MATEC Web Conf.* 2. <http://dx.doi.org/10.1051/mateconf/20120205004>.
- Cermak, V., Rybach, L., 1982. Thermal conductivity and specific heat of minerals and rocks. In: Beblo, M. (Ed.), *Geophysics – Physical Properties of Rocks*, 1. Springer, pp. 305–343.
- Constructive Solutions Compendium, 2007. Código Técnico de la Edificación. Instituto de Ciencias de la Construcción Eduardo Torroja e Instituto de Ciencias de la Construcción de Castilla y León. Castilla y León, Spain.
- Decagon Devices, 2016. KD2 Pro Thermal Properties Analyzer Operator’s Manual. Decagon Devices, Inc.
- Esteban, L., Pimentel, L., Sarout, J., Piane, C.D., Haffen, S., Gerard, Y., Timms, N.E., 2015. Study cases of thermal conductivity prediction from P-wave velocity and porosity. *Geothermics* 53, 255–269.
- Fuchs, S., Balling, N., 2016a. Improving the temperature predictions of subsurface thermal models by using high-quality input data. Part 1: Uncertainty analysis of the thermal-conductivity parameterization. *Geothermics* 64, 42–54.
- Fuchs, S., Balling, N., 2016b. Improving the temperature predictions of subsurface thermal models by using high-quality input data. Part 2: A case study from the Danish-German border region. *Geothermics* 64, 1–14.
- Fuchs, S., Förster, A., 2014. Well-log based prediction of thermal conductivity of sedimentary successions: examples from the North German Basin. *Geophys. J. Int.* 196, 291–311.
- Fuchs, S., Balling, N., Förster, A., 2015. Calculation of thermal conductivity, thermal diffusivity and specific heat capacity of sedimentary rocks using petro physical well logs. *Geophys. J. Int.* 203 (3), 1977–2000.
- Gegenhuber, N., Schoen, J., 2012. New approaches for the relationship between compressional wave velocity and thermal conductivity. *J. Appl. Geophys.* 76, 50–55.
- Gegenhuber, N., 2011. Compressional wave velocity-thermal conductivity correlation – From the laboratory to logs. Society of Petroleum Engineers – 73rd European Association of Geoscientists and Engineers Conference and Exhibition 2011 – Incorporating SPE EUROPEC.
- Gu, Yixi, Rühaak, Wolfram, Bär, Kristian, Sass, Ingo, 2017. Using seismic data to estimate the spatial distribution of rock thermal conductivity at reservoir scale. *Geothermics* 66, 61–72.
- Haenel, R., Rybach, L., Stegona, L., 1988. Thermal exploration methods. In: Haenel, R., Stegona, L., Rybach, L. (Eds.), *Handbook of Terrestrial Heat-Flow Density Determination*, Chapter 2. Kluwer Academic Publishers, Dordrecht.
- Hartmann, A., Pechinig, R., Clauser, C., 2008. Petro physical analysis of regional scale thermal properties for improved simulations of geothermal installations and basin scale heat and fluid flow. *Int. J. Earth Sci.* 97 (2), 421–433.
- Jorand, R., Vogt, C., Marquart, G., Clauser, C., 2013. Effective thermal conductivity of heterogeneous rocks from laboratory experiments and numerical modeling. *J. Geophys. Res.: Solid Earth* 118, 5225–5235.
- Kluitenberg, G.J., Ham, J.M., Bristow, K.L., 1993. Error analysis of the heat pulse method for measuring soil volumetric heat capacity. *Soil Sci. Soc. Am. J.* 57, 1444–1451.
- Krishnaiah, S., Singh, D.N., Jadhav, G.N., 2004. A methodology for determining thermal properties of rocks. *Min. Sci.* 1 (5), 877–882.
- Kukkonen, Lindberg, 1995. Thermal Conductivity of Rocks at the TVO Investigation Sites Olkiluoto, Romuvaara and Kivetty. Nuclear Waste Commission of Finnish Power Companies, Report YJT-95-08, pp. 29.
- Liou, Jyh-Chau, Tien, Neng-Chuan, 2016. Estimation of the thermal conductivity of granite using a combination of experiments and numerical simulation. *Int. J. Rock Mech. Min. Sci.* 81, 39–46.
- Lira-Cortés, L., González-Rodríguez, O.J., Méndez-Lango, E., 2008. Sistema de Medición de la Conductividad Térmica de Materiales Sólidos Conductores, Diseño y Construcción. In: Simposio de Metrología Santiago de Querétaro. México.
- Louie, John N., 2001. Shear-Wave velocity to 100 meters depth from refraction

- microtremor arrays. *Bull. Seismol. Soc. Am.* 91, 347–364.
- Park, Choon B., Miller, Richard D., Xia, Jianghai, 1999. Multichannel analysis of surface waves. *Geophysics* 64 (3), 800–808.
- Pimienta, L., Sarout, J., Esteban, L., Plane, C.D., 2014. Prediction of rocks thermal conductivity from elastic wave velocities, mineralogy and microstructure. *Geophys. J. Int.* 197 (2).
- Popov, Y., Terychnyi, Y., Romushkevich, R., Korobkov, D., Pohl, J., 2003. Interrelations between thermal conductivity and other physical properties of rocks: experimental data. *Pure Appl. Geophys.* 160, 1137–1161.
- Popov, Yu., Beardmore, G., Clauser, C., Roy, S., 2016. ISRM suggested methods for determining thermal properties of rocks from laboratory tests at atmospheric pressure. *Rock Mech. Rock Eng.* 49 (10), 4179–4207.
- Rühaak, W., Guadagnini, A., Geiger, S., Bär, K., Gu, Y., Aretz, A., Homuth, S., Sass, I., 2015. Upscaling thermal conductivities of sedimentary formations for geothermal exploration. *Geothermics* 58, 49–61.
- Rühaak, W., 2015. 3-D interpolation of subsurface temperature data with known measurement error using Kriging. *Environ. Earth Sci.* 73 (4), 1893–1900.
- Shiozawa, S., Campbell, G.S., 1990. Soil thermal conductivity. *Remote Sens. Rev.* 5, 301–310.
- Zamora, Maria, Vo-Thanh, Dung, Bienfait, Gérard, Poirier, Jean Paul, 1993. An empirical relationship between thermal conductivity and elastic wave velocities in sandstone. *Geophys. Res. Lett.* 20, 1679–1682.

PAPER 5

Article

Comparative Analysis of Different Methodologies Used to Estimate the Ground Thermal Conductivity in Low Enthalpy Geothermal Systems

Cristina Sáez Blázquez * , Ignacio Martín Nieto, Arturo Farfán Martín, Diego González-Aguilera  and Pedro Carrasco García

Department of Cartographic and Land Engineering, University of Salamanca, Higher Polytechnic School of Avila, Hornos Caleros 50, 05003 Avila, Spain; nachomartin@usal.es (I.M.N.); afarfan@usal.es (A.F.M.); daguilera@usal.es (D.G.-A.); retep81@usal.es (P.C.G.)

* Correspondence: u107596@usal.es; Tel.: +34-675-536-991

Received: 3 April 2019; Accepted: 29 April 2019; Published: 2 May 2019



Abstract: In ground source heat pump systems, the thermal properties of the ground, where the well field is planned to be located, are essential for proper geothermal design. In this regard, estimation of ground thermal conductivity has been carried out by the implementation of different techniques and laboratory tests. In this study, several methods to obtain the thermal properties of the ground are applied in order to compare them with the reference thermal response test (TRT). These methods (included in previous research works) are carried out in the same geological environment and on the same borehole, in order to make an accurate comparison. All of them provide a certain value for the thermal conductivity of the borehole. These results are compared to the one obtained from the TRT carried out in the same borehole. The conclusions of this research allow the validation of alternative solutions based on the use of a thermal conductive equipment and the application of geophysics techniques. Seismic prospecting has been proven as a highly recommendable indicator of the thermal conductivity of a borehole column, obtaining rate errors of below 1.5%.

Keywords: ground source heat pump; thermal conductivity; thermal response test; thermal conductive equipment; geophysics

1. Introduction

The global growing energy needs have sparked renewed interest in ground source heat pump systems. These systems are traditionally used for space heating and cooling by the extraction of the ground's energy through a borehole heat exchanger (BHE) [1]. High initial investments are commonly associated with these installations so that an optimal ground loop dimensioning is advisable to avoid unnecessary costs. In this regard, the design process requires knowing rather accurately the thermal conductivity of geological formation where the ground source heat pump (GSHP) system will be located [2,3]. Ground thermal conductivity is usually determined by the implementation of a Thermal Response Test (TRT), the main purpose of which is the measuring of the equivalent thermal conductivity of the ground volume tested and the thermal resistance of the BHE [4–7]. The conventional TRT is based on circulating heated water in a closed loop, which simulates heat transfer occurring in a ground heat exchanger. Inlet and outlet water temperatures and flow rate are measured during the test. These data are then analyzed by the implementation of analytical or numerical models that allow determining the ground thermal conductivity and the borehole thermal resistance [8,9]. The most used interpretation technique relies on the first-order approximation of the infinite line-source model. Assuming a constant heating power, a linear regression model is fitted to the late temperature measurements to calculate the

mean time derivative of the temperature and deduct the desired parameters. This first approach to linearize the infinite line source model requires rejecting the early measurements for the subsequent test interpretation. TRT duration is usually established between 36–72 h, but this duration has been thoroughly discussed in the past [10] and at the moment is an area of active research [11–15]. Despite the errors these test could involve [4], the high accuracy of ground thermal conductivity results represent essential information in the corresponding geothermal loop sizing. The main inconvenience associated with the realization of a TRT is its relatively high cost (around 3000 Euros), remaining an issue that prevents its widespread use. This problem is especially significant in small installations, where the test increases the initial investment without clear compensation.

Focusing on alternative solutions, some variations of a TRT are available in the existing literature. For example, Henke et al. [16] proposed an experimental apparatus that, as a TRT, measures the temperature response of a borehole. Freifeld et al. [17] developed a borehole methodology to estimate the formation thermal conductivity in situ with spatial resolution of one meter. However, the alternative techniques found in other authors' researches have similar economic issues [18] and their validity is still unclear.

In this research, a series of methodologies (already published and available in the current literature), aimed at the estimation of the ground thermal conductivity, are applied on a real area. These techniques are then evaluated by their comparison with the results of a thermal response test carried out on a borehole placed in the same location. In a nutshell, the thermal conductivity of a certain geological environment is determined by the implementation of affordable methods whose validity is thoroughly assessed. Thus, the main problematic addressed in this work is characterization of ground thermal from different methods to generally improve the design of a low enthalpy geothermal system.

2. Materials and Methods

2.1. Global Description of the Area under Study

The comparison of the methodologies considered in this research is derived from the thermal characterization of a 43 m length and 220 mm diameter borehole placed in the province of Ávila (Spain). The exact location of this well is detailed in Table 1.

Table 1. Location of the borehole where this research is focused.

Borehole Position	
Latitude	40°39'2,45 N
Longitude	4°40'44,84 O

The area contemplated in the present research is located in the center of Ávila (Spain). This region is geologically constituted by two main blocks. One of them is defined by igneous and metamorphic rocks from the Upper Carboniferous–Low Permian and Pre–Cambrian–Low Cambrian periods, respectively. The second block is characterized by the presence of sedimentary materials from the Mesozoic, Tertiary and Quaternary (oriental area of the Amble's valley) periods [19,20]. In the case of the volume of ground considered here, it belongs to granite formations and more specifically, adamellite rocks. This information can be deduced from the geological map of the region presented in Figure 1.

For a more precise geological characterization, geophysical tests were applied on the experimental borehole. A well logging system was used to obtain the specific earth information. It consists of the measuring of continuous and simultaneous record of different physical parameters throughout the borehole column. The equipment used for the mentioned purpose utilizes a series of interchangeable multi-parameter sensors that allowed to register the following parameters: spontaneous potential, resistivity, and natural gamma radiation. Figure 2 includes the register of the well logging test applied on the study borehole and the stratigraphic column derived from its interpretation.

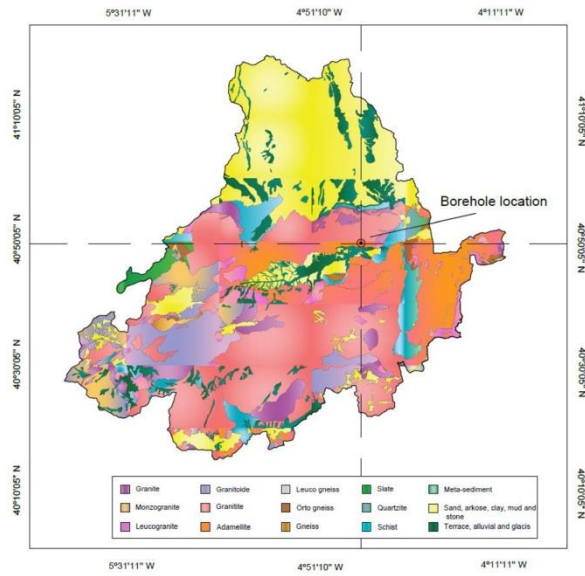


Figure 1. Principal geological formations integrating the region of Ávila [21].

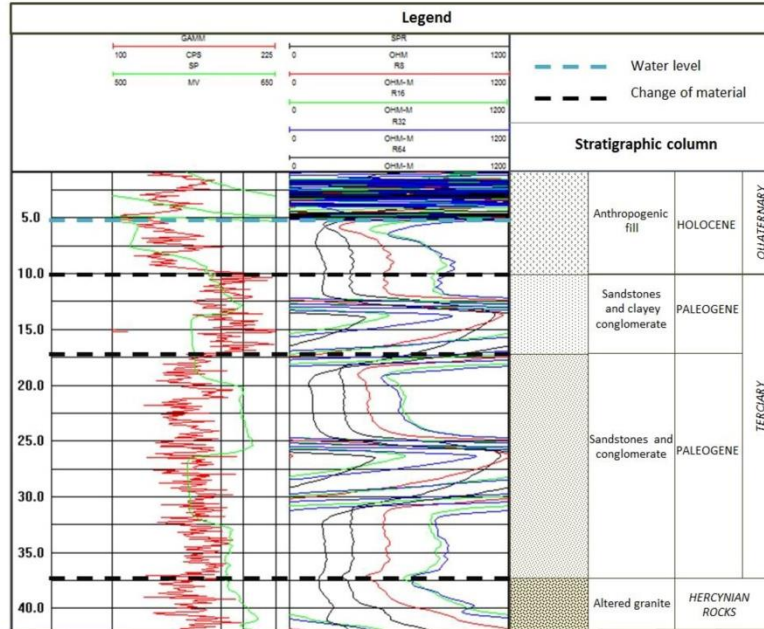


Figure 2. Well logging data and stratigraphic column of the borehole under study.

Once the geological levels that constitute the ground in the area of the borehole were accurately defined, different tests were conducted in the area with the objective of determining the thermal conductivity of the materials previously detected. The implemented methodologies are described in the following subsections.

2.2. Thermal Conductivity Characterization

The principal purpose of this section is the estimation of the thermal conductivity of the borehole column described above. To that end, different methods and procedures implemented in previous author's researches are considered here to finally compare them with the results of a TRT. The following subsections contain the description of each of the mentioned thermal conductivity estimator techniques.

2.2.1. KD2 Pro Measurements

In a previous research work, the thermal conductivity map of the province of Ávila (study area of this research) was created from experimental measurements on the principal geological formations of the region. Representative rocky samples were collected and taken to the laboratory, where the thermal conductivity parameter was measured.

After systematic sample processing—drilling and carving obtaining samples with a specific size, removal of excess material—KD2 Pro equipment was used to measure the thermal conductivity of each geological formation. Before its use, a hole of 6 cm length and 3.9 mm in diameter was made on each rocky sample in order to introduce the RK-1 sensor of KD2 Pro device. More information about the specific measuring methodology is provided in the full published version of the manuscript [21].

As a result of the KD2 Pro measurement, the mentioned research provides the thermal conductivity of the rocky and soil formations. According to the borehole column in Figure 2, the volume of ground under study is constituted by different layers of materials. In order to obtain a representative thermal conductivity value of the whole column well, the thermal conductivity of each layer and its thickness must be considered. Based on the results offered in the research, thermal conductivities of the borehole materials were deduced. All this information is included in Table 2. Thermal conductivity values presented in Table 2 correspond to the average values registered for each geological formation in the manuscript considered here. However, for the last layer of altered adamellites, the lowest values of the mentioned study were selected due to the presence of loose materials and the altered state of granite rocks in that level.

Table 2. Borehole column, geological layers, thicknesses and thermal conductivity values.

	Geological Composition	Thickness (m)	Thermal Conductivity (W/mK) *
Layer 1	Anthropogenic fills	10	1.502
Layer 2	Sandstones and clayey conglomerate	7.5	1.882
Layer 3	Sandstones and conglomerate	20	2.041
Layer 4	Altered adamellite	5.5	2.565

* According to the consulted research [21].

Finally, the thermal conductivity representative of the whole studied borehole can be obtained from the application of Equation (1) and the information previously attached in Table 2.

$$k_T(\text{W/mK}) = k_1 \cdot T_1 + k_2 \cdot T_2 + k_3 \cdot T_3 + k_4 \cdot T_4 \quad (1)$$

where:

k_T = Global thermal conductivity of the whole borehole column.

k_1 = Thermal conductivity of the geological formation of layer 1.

k_2 = Thermal conductivity of the geological formation of layer 2.

k_3 = Thermal conductivity of the geological formation of layer 3.

k_4 = Thermal conductivity of the geological formation of layer 4.

T_1 = Thickness of layer 1 expressed as a percentage of the total well thickness.

T_2 = Thickness of layer 2 expressed as a percentage of the total well thickness.

T_3 = Thickness of layer 3 expressed as a percentage of the total well thickness.

T_4 = Thickness of layer 4 expressed as a percentage of the total well thickness.

2.2.2. Geophysics

Geophysical prospecting has been used in previous works as a ground thermal conductivity estimator. The principal basis of these studies is the correlation of a geophysical parameter and thermal conductivity measurements (using KD2 Pro device) to finally predict the thermal behavior of the ground in depth. A more detailed description of these methods and their implementation in the area of the present research is included in the following subsections.

(1) Seismic data:

The first geophysical method makes reference to the implementation of seismic prospecting tests. In a previous research work, the mentioned tests were implemented on three different geological formations (schists, medium grain and coarse-grained adamellites) using MASW and seismic refraction techniques in order to register P and S waves velocities. At the same time, thermal conductivity of each formation was measured by the use of KD2 Pro equipment. These tests were made on the most and least decomposed samples of each geological environment to find the lowest and highest conductivity values. Finally, this published research correlates the propagation velocities of P and S waves and the thermal conductivity of samples from the same material [22].

The ultimate result of this work is to predict the thermal behavior of the geological formations included in the study. By identifying the propagation velocities of the seismic waves in a certain area, the evolution of the thermal conductivity of the ground in that area can be evaluated. Thus, 2D thermal conductivity sections provided in the mentioned research allow estimation of the evolution of ground thermal conductivity in depth for each specific formation.

In order to ensure application of this methodology, seismic refraction tests were conducted on the area where the borehole of study is located. The results of these tests are provided in Figure 3.

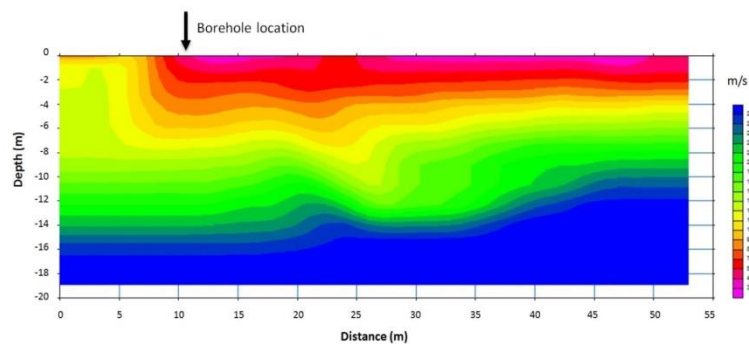


Figure 3. P-wave velocity distribution in the study area from seismic refraction tests.

After the distribution of the P wave velocity was identified in depth, different thermal conductivity measurements were taken in order to identify the most and least thermal conductive samples, meaning those with the highest and lowest compaction levels. These values correspond to the minimum thermal conductivity of anthropogenic fills and the maximum thermal conductivity for the altered adamellite;

they are presented in Table 3. It should be noted that altered adamellites were extracted from the drilling process at depths where they were identified. These samples were then used in thermal conductivity characterization.

Table 3. Highest and lowest thermal conductivity values detected for the formations constituting the borehole under study.

	Geological Formation	Thermal Conductivity * (W/mK)
Minimum value	Anthropogenic fills	1.105
Maximum value	Altered adamellite	2.672

* Thermal conductivity measuring was made by the use of KD2 Pro equipment.

By measuring P wave velocity and thermal conductivities in the study area, the correlation between both parameters was obtained (graphically presented in Figure 4). This is based on pairing the lowest thermal conductivity value with the lowest p wave velocity (in the same area) and the highest thermal conductivity with the highest p wave velocity. More information on this method is provided in the mentioned published research.

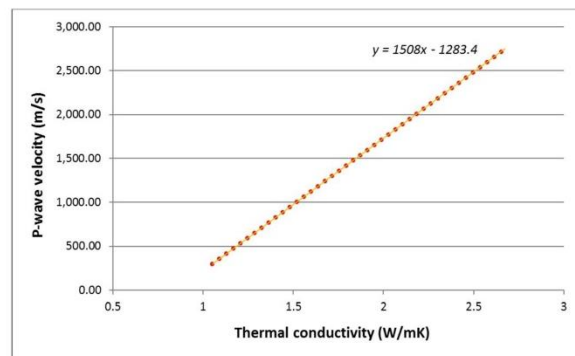


Figure 4. Thermal conductivity versus P-wave velocity in the study area.

From the above correlation and by following the instructions of the mentioned research, the distribution of the thermal conductivity parameter in the area considered here is displayed in the 2D section of Figure 5.

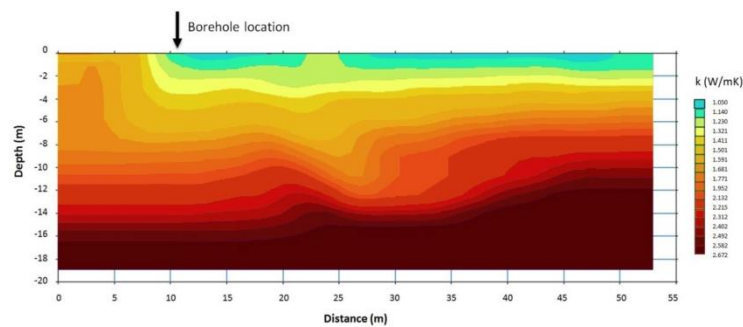


Figure 5. 2D thermal conductivity section in the area where the borehole of this research is located.

According to Figure 5, the volume of ground included under the borehole is constituted by a set of layers with different thermal conductivity values. This information can be observed in Table 4.

Table 4. Different thermal conductive layers identified in the volume of ground located under the borehole identified for this research.

	Thickness (m)	Thermal Conductivity (W/mK)
Layer 1	1.2	1.140
Layer 2	1.1	1.230
Layer 3	1.3	1.321
Layer 4	1.35	1.411
Layer 5	2	1.501
Layer 6	0.8	1.591
Layer 7	0.9	1.681
Layer 8	0.9	1.771
Layer 9	1	1.952
Layer 10	0.9	2.132
Layer 11	1.4	2.215
Layer 12	0.9	2.312
Layer 13	0.7	2.402
Layer 14	0.8	2.492
Layer 15	0.9	2.582
Layer 16 *	26.85	2.672

* From layer 16, the same thermal conductivity value is assumed until the end point of the drilling (43 m).

Finally, the global thermal conductivity of the borehole column is deduced from the application of the above data (Table 4) in Equation (1).

(2) Electrical resistivity:

In this case, electrical resistivity data were collected to finally create a 3D thermal conductivity map of the area of interest. The fundamentals of this method are similar to the one explained before; electrical resistivity results are correlated with thermal conductivity measurements and a relation between both parameters is obtained for a certain geological formation. The research work, including this methodology, was focused on granite rocks (adamellites), and the electrical resistivity was obtained using the Electrical Resistivity Tomography (ERT) technique. Thermal conductivity measurements were, in turn, taken using KD2 Pro equipment following the same operational procedure (tests were made on the most and least decomposed rocky samples) [23].

The results of this research disclose a certain relation between thermal conductivity and electrical resistivity. This relation can be observed in Equation (2).

$$k = 2 \cdot 10^{-7} x^2 + 0.0001x + 1.4881 \quad (2)$$

where:

k = thermal conductivity (W/mK)

x = electrical resistivity ($\Omega \cdot m$)

To apply Equation (2), the electrical resistivity of the materials in the study area must be known. To this end, an ERT test was conducted around the mentioned area, obtaining a 2D electrical resistivity section (presented in Figure 6).

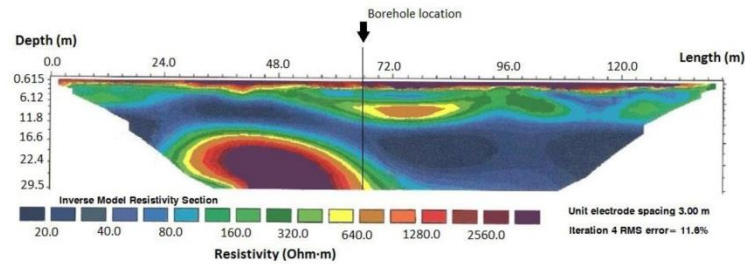


Figure 6. 2D electrical resistivity tomography in the area under study.

On interpretation of the above 2D electrical resistivity section, the borehole considered in this study is constituted by a series of layers with different thickness and characterized by variable electrical resistivity values. All these data are included in Table 5; the thermal conductivity of each layer is obtained by application of Equation (2).

Table 5. Layers detected in the borehole under study, according to the interpretation of ERT results.

	Thickness (m)	Electrical Resistivity (Ohm-m)	Thermal Conductivity (W/mK)
Layer 1	1	1280	1.943
Layer 2	4.12	100	1.498
Layer 3	6.88	450	1.574
Layer 4	10	55	1.494
Layer 5	7.5	360	1.550
Layer 6 *	13.5	2500	2.988

* Layer 6 is estimated based on the well logging of Figure 2.

As in the previous cases, Equation (1), must be used to finally define the global thermal conductivity of the borehole column from partial thermal conductivity values and thickness of each layer.

2.2.3. Thermal Response Test

The last procedure implemented in this research is the realization of a Thermal Response Test in the borehole. These tests are routinely used to estimate borehole thermal properties with regard to the mentioned thermal conductivity. The conventional TRT consists of circulating heated fluid (usually water) in a closed loop. During the test, fluid temperatures are measured at the ground heat exchanger inlet and outlet, along with the flow rate. These measured values are then analyzed by analytical or numerical models with the aim of calculating thermal conductivity and borehole thermal resistance [3,24].

(1) Test implementation

First, the borehole was geothermally prepared for the test by installing a polyethylene single-U tube heat exchanger of 32 mm with spacers located one meter apart. Taking advantage of the high groundwater level in the area, grouting material was not used [25,26]. The working fluid was water (during the test, low ambient temperatures were not expected) and the connection of the inlet and outlet heat exchangers and the TRT device was made with polyethylene tubes that were externally insulated. In order to set the initial condition of this test, a temperature register (PCE-T recorder) was used to measure the base temperature of the ground, obtaining a constant value of 14.6 °C at a depth of 40 m.

In this research, TRT was done according to UNE-EN ISO 17628:2017 regulations [27]. The TRT device implemented here constituted of a heat injection system, a circulating pump, and electrical

resistance as heat source. The resistance allows three different heating levels, corresponding to the injection of 3 kW (stage 1), 6 kW (stage 2), and 9 kW (stage 3). The TRT equipment also included a Kamstrup energy meter (to register a large number of parameters), commercially known as MULTICAL 801.

Once the borehole was properly equipped, the sequence of events was as follows:

- Circuit filling and establishment of the appropriate working pressure.
- Activation of the circulating TRT pump and starting of the first heating stage (3 kW).
- General system operation during a certain period of time.
- Downloading and data management from the Kamstrup register.
- Calculation of the global thermal conductivity parameter.

The TRT duration is a controversial subject—while reducing TRT duration could help reduce costs, the accuracy of results could be affected. Following the regulation mentioned before [27], the minimum duration of the TRT can be estimated by Equation (3).

$$t \text{ (s)} = \frac{5 \cdot r^2}{\alpha} \quad (3)$$

where:

r = borehole radius (m)

$$\alpha = \frac{k_e}{c_v}$$

k_e = estimated thermal conductivity (W/mK)

c_v = volumetric thermal capacity (J/m³/K)

By applying Equation (3) and estimating thermal conductivity of 1.80 W/mK and volumetric thermal capacity of 2.16×10^6 J/m³/K [28], the minimum duration required for the thermal response test in the studied borehole would be:

$$t \text{ (s)} = \frac{5 \cdot 0.11^2}{8.3 \cdot 10^{-7}} = 72891.56 \text{ s} \rightarrow 20.25 \text{ h}$$

Despite this value, the real duration of the test was 43 h, which sought to guarantee total stabilization of the system. Additionally, Figure 7 shows the TRT device and some sequences of the test.

(2) Thermal conductivity calculation

In a borehole heat exchanger of sufficient length in comparison with its radius, the analytical solution of Kelvin's Line Source can be applied to solve the heat equation and analyze TRT data. According to the infinite line-source model (use as a laboratory method since 1905), the thermal conductivity parameter can be obtained from the constant power rate and the slope of the temperature variation in time [29,30]. The interpretation of TRT results relies on a first-order approximation to linearize the mentioned infinite line-source model, neglecting the early measurements.

$$k = \frac{Q}{b \cdot 4 \cdot \pi \cdot H} \quad (4)$$

where:

Q = heat flux (kW/min)

b = slope (min)

H = borehole length (m)

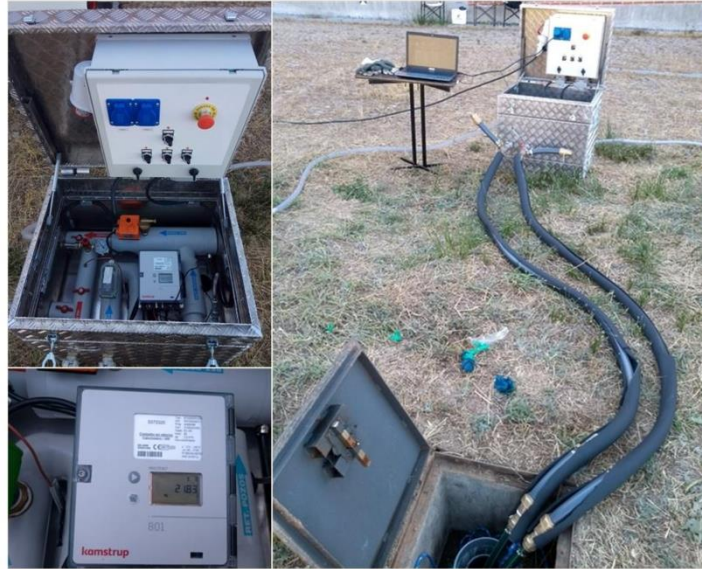


Figure 7. Thermal response test in the studied borehole. Left: TRT device and Kamstrup register; right: TRT connected to the borehole heat exchanger.

3. Results and Discussion

3.1. Previous Methods Results

Thermal conductivity results of each method considered in this research are shown in Table 6. These results are obtained by the application of the stages described for each individual procedure. The methodologies belong to validated and already published researches. Consequently, the validity of the mentioned results is guaranteed.

Table 6. Thermal conductivity results of each method considered in this research.

Methodology	Thermal Conductivity (W/mK)
KD2 Pro	1.955
Seismic prospecting	2.337
Electrical resistivity	1.997

3.2. TRT Results

In addition to the thermal conductivity results deduced from the alternative methodologies, the TRT also provided a thermal conductivity value that will be compared with the ones in Table 6. After the corresponding operation of the TRT during the established period of time (43 h), inlet (T1) and outlet (T2) temperatures were registered (shown in Figure 8). It should be mentioned that the low temperature difference between T1 and T2 (displayed in Figure 8) is derived from the fact that the borehole length is only 43 m.

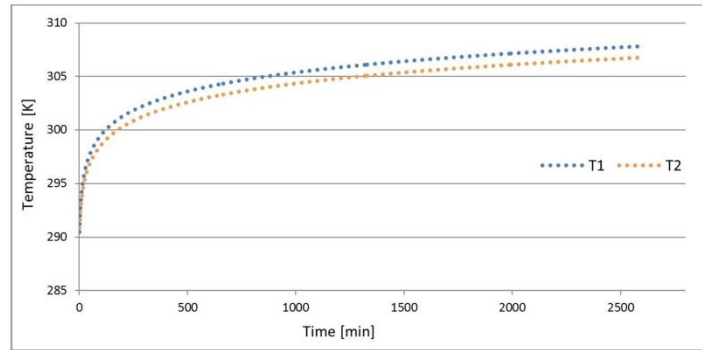


Figure 8. Evolution of inlet and outlet temperatures registered during the TRT.

From these results, the linear approximation required for the calculation of the thermal conductivity parameter was made for the period of time up to 1000 min (discarding the early measurements) in each temperature register. Figure 9 presents the equation of each linear approximation, consequently using the slope of these lines in corresponding thermal conductivity calculations. As shown in Figure 9, the interpretation of the TRT and the subsequent calculation of the thermal conductivity parameter is made by measuring the inlet and outlet fluid temperatures for time up to 1000 min.

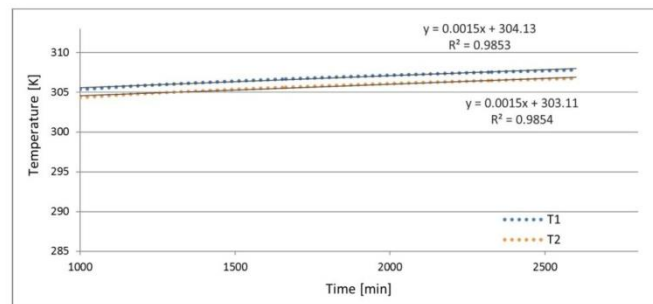


Figure 9. Equation of the linear approximation to temperature registers from time = 1000 min.

On observing Figure 9, we note that the slope of the linear approximation is the same for T1 and T2, such that the calculation of the thermal conductivity parameter is identical for both cases. When applying Equation (4), the following values were considered: $b = 0.0015$ min, $H = 43$ m and $Q = 1.875$ kW/min (resistance first stage (3000 kW)/time of the linear approximation (1600 min)). Thus, the global thermal conductivity of the borehole from TRT results takes a value of 2.313 W/mK.

3.3. General Comparison

Figure 10 graphically displays the results of each methodology considered in this research. It shows strong agreement in results between the different methods.

It is thus convenient to include the accuracy error of each of the methodologies shown in Figure 10: 10% for KD2 Pro, 14.2% for seismic prospecting, 16.7% for electrical resistivity, and 5% for TRT [4,31–33].

Considering TRT thermal conductivity value as the most accurate one and taking into account Figure 10, the following statements can be made:

- Thermal conductivities obtained by the alternative techniques are in strong agreement with the TRT result. The seismic prospecting method provides the most similar value, with a difference of only 0.024 W/mK with respect to the TRT value.
- The use of electrical resistivity tomography also allows to obtain thermal conductivity values close to the TRT result. In this case, the difference between both methods is 0.316 W/mK.
- The least accurate method is the use of the thermal conductivity map obtained by in situ KD2 Pro measurements. Despite having the least accuracy of all the procedures considered here, the difference with respect to the TRT is 0.358 W/mK.
- By evaluating the mentioned differences in terms of percentage, the errors of each alternative methodology in comparison with the TRT are 15.48% for the thermal conductivity map, 1.04% for seismic prospecting, and 13.66% when applying electrical resistivity tomography.

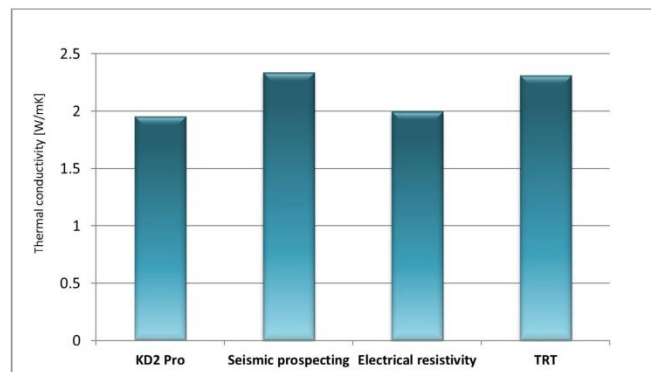


Figure 10. Thermal conductivity results of the implementation of the methodology used in this study.

4. Conclusions

TRT has been traditionally considered an appropriate technique to provide accurate thermal conductivity values of a borehole column. However, the high costs of these tests usually prompt researchers to look for alternative solutions that help characterize ground thermal behavior. This research integrates different existing methodologies to evaluate their validity through the results of a TRT made on the same study area. Provided that TRT is not always viable and based on the final results of this work, the most recommendable technique to be applied is seismic prospecting. It has been proved that this procedure is capable of providing highly accurate thermal conductivity values with errors below 1.5%. The high ground water level of the area may be a cause of deviation from the electrical and KD2 Pro methods, due to their sensitivity to this factor.

The remaining methodologies evaluated in this research could also be appropriate solutions to obtain approximate ground thermal conductivity. In the absence of a TRT or seismic profiles, the thermal conductivity map or electrical resistivity tomography could be of great help in ground thermal conductivity characterization. Despite the obvious advantages of TRT, the deep local nature of this test could be mitigated by using geophysical methods, as the ones presented in this study. The estimation of this parameter will be incredibly useful for the corresponding geothermal design, adjusting the number of boreholes and the total drilling length required in the shallow geothermal system. In view of the importance of identifying ground thermal conductivity in a GSHP system, the conclusions of this work are highly significant in the geothermal field.

Author Contributions: All authors performed the experimental and theoretical basis of the research. C.S.B., A.F.M. and I.M.N. implemented the methodology and calculations and analyzed the results. D.G.-A. provided

technical and theoretical support. P.C.G. carried out the geophysics tests. C.S.B. wrote the manuscript and all authors read and approved the final version.

Funding: This research received no external funding.

Acknowledgments: The authors would like to thank the Department of Cartographic and Land Engineering of the Higher Polytechnic School of Avila, University of Salamanca, for allowing us to use their facilities and their collaboration during the experimental phase of this research. The authors also want to thank the Ministry of Education, Culture and Sport for providing a FPU Grant (Training of University Teachers Grant) to the corresponding author of this paper, making possible the realization of this work.

Conflicts of Interest: The authors declare no conflict of interest.

References

1. Ally, M.R.; Munk, J.D.; Baxter, V.D.; Gehl, A.C. Exergy analysis of a two-stage ground source heat pump with a vertical bore for residential space conditioning under simulated occupancy. *Appl. Energy* **2015**, *155*, 502–514. [[CrossRef](#)]
2. Han, C.; Yu, X.B. Performance of a residential ground source heat pump system in sedimentary rock formation. *Appl. Energy* **2016**, *164*, 89–98. [[CrossRef](#)]
3. Pasquier, P. Interpretation of the first hours of a thermal response test using the time derivative of the temperature. *Appl. Energy* **2018**, *213*, 56–75. [[CrossRef](#)]
4. Henk, J.L. Witte, Error analysis of thermal response tests. *Appl. Energy* **2013**, *109*, 302–311.
5. Pasquier, P.; Zarrella, A.; Marcotte, D. A multi-objective optimization strategy to reduce correlation and uncertainty for thermal response test analysis. *Geothermics* **2019**, *79*, 176–187. [[CrossRef](#)]
6. Bandos, T.V.; Montero, A.; Fernández de Córdoba, P.; Urchueguía, J.F. Improving parameter estimates obtained from thermal response tests: Effect of ambient air temperature variations. *Geothermics* **2011**, *40*, 136–143. [[CrossRef](#)]
7. Choi, W.; Ooka, R. Interpretation of disturbed data in thermal response tests using the infinite line source model and numerical parameter estimation method. *Appl. Energy* **2015**, *148*, 476–488. [[CrossRef](#)]
8. ASHRAE. Geothermal energy. In *ASHRAE Handbook Heating, Ventilating, and Air-Conditioning Applications*; American Society of Heating, Refrigerating and Air-Conditioning Engineers: Atlanta, GA, USA, 2007; pp. 32.1–32.30.
9. Gehlin, S.; Hellström, G. Comparison of four models for thermal response test evaluation. *ASHRAE Trans.* **2003**, *109*, 131–142.
10. Spitler, J.D.; Gehlin, S.E. Thermal response testing for ground source heat pump systems: An historical review. *Renew. Sustain. Energy Rev.* **2015**, *50*, 1125–1137. [[CrossRef](#)]
11. Beier, R.A.; Smith, M.D. Minimum duration of in-situ tests on vertical boreholes. *ASHRAE Trans.* **2003**, *109*, 475–486.
12. Bozzoli, F.; Pagliarini, G.; Rainieri, S.; Schiavi, L. Short-time thermal response test based on a 3-D numerical model. *J. Phys. Conf. Ser.* **2012**, *395*, 012–056. [[CrossRef](#)]
13. Bujok, P.; Grycz, D.; Klempa, M.; Kunz, A.; Porzer, M.; Pytlík, A.; Rozehnal, Z.; Vojčínák, P. Assessment of the influence of shortening the duration of TRT (thermal response test) on the precision of measured values. *Energy* **2014**, *64*, 120–129. [[CrossRef](#)]
14. Poulsen, S.; Alberdi-Pagola, M. Interpretation of ongoing thermal response tests of vertical (BHE) borehole heat exchangers with predictive uncertainty based stopping criterion. *Energy* **2015**, *88*, 157–167. [[CrossRef](#)]
15. Choi, W.; Kikumoto, H.; Choudhary, R.; Ooka, R. Bayesian inference for thermal response test parameter estimation and uncertainty assessment. *Appl. Energy* **2018**, *209*, 306–321. [[CrossRef](#)]
16. Witte, H.J.L.; van Gelder, G.J.; Spitler, J.D. In Situ Measurement of Ground Thermal Conductivity: The Dutch Perspective. *ASHRAE Trans.* **2002**, *108*, 859–867.
17. Freifeld, B.M.; Finsterle, S.; Onstott, T.C.; Toole, P.; Pratt, L.M. Ground surface temperature reconstructions: Using in situ estimates for thermal conductivity acquired with a fiber optic distributed thermal perturbation sensor. *Geophys. Res. Lett.* **2008**, *35*, L14309. [[CrossRef](#)]
18. Sharqawy, M.H.; Said, S.A.; Mokheimer, E.M.; Habib, M.A.; Badr, H.M.; Al-Shayea, N.A. First in situ determination of the ground thermal conductivity for borehole heat exchanger applications in Saudi Arabia. *Renew. Energy* **2009**, *34*, 2218–2223. [[CrossRef](#)]

19. Geological and Mining Institute of Spain (IGME). *Geological National Mapping (MAGNA)*; IGME: Madrid, Spain, 2018.
20. Chamorro, C.R.; García-Cuesta, J.L.; Mondéjar, M.E.; Linares, M.M. An estimation of the enhanced geothermal systems potential for the Iberian Peninsula. *Renew. Energy* **2014**, *66*, 1–14. [[CrossRef](#)]
21. Blázquez, C.S.; Martín, A.F.; Nieto, I.M.; García, P.C.; Pérez, L.S.S.; Aguilera, D.G. Thermal conductivity map of the Avila region (Spain) based on thermal conductivity measurements of different rock and soil samples. *Geothermics* **2017**, *65*, 60–71. [[CrossRef](#)]
22. Blázquez, C.S.; Martín, A.F.; García, P.C.; González-Aguilera, D. Thermal conductivity characterization of three geological formations by the implementation of geophysical methods. *Geothermics* **2018**, *72*, 101–111. [[CrossRef](#)]
23. Nieto, I.M.; Martín, A.F.; Blázquez, C.S.; Aguilera, D.G.; García, P.C.; Vasco, E.F.; García, J.C. Use of 3D electrical resistivity tomography to improve the design of low enthalpy geothermal systems. *Geothermics* **2019**, *79*, 1–13. [[CrossRef](#)]
24. Raymond, J.; Therrien, R.; Gosselin, L. Borehole temperature evolution during thermal response tests. *Geothermics* **2011**, *40*, 69–78. [[CrossRef](#)]
25. Andersson, O.; Gehlin, S. State of the Art: Sweden, Quality Management in Design, Construction and Operation of Borehole Systems. Available online: http://media.geoenergicentrum.se/2018/06/Andersson_Gehlin_2018_State-of-the-Art-report-Sweden-for-IEA-ECES-Annex-27.pdf (accessed on 20 April 2019).
26. Gustafsson, A.-M.; Westerlund, L.; Hellström, G. CFD-modelling of natural convection in a groundwater-filled borehole heat exchanger. *Appl. Therm. Eng.* **2010**, *30*, 683–691. [[CrossRef](#)]
27. UNE-EN ISO 172628:2017. *Geotechnical Investigation and Testing. Geothermal Testing. Determination of Thermal Conductivity of Soil and Rock Using a Borehole Heat Exchanger*; International Organization for Standardization: Geneva, Switzerland, 2017.
28. Bates, D.R.; Estermann, I. *Advances in Atomic and Molecular Physics*; Elsevier: Amsterdam, The Netherlands, 1996.
29. Ingersoll, L.R.; Plass, H.J. Theory of the ground pipe heat source for the heat pump. *Heat. Pip. Air Cond.* **1948**, 119–122.
30. Carslaw, H.S.; Jaeger, J.C. *Conduction of Heat in Solids*, 2nd ed.; Clarendon Press: Oxford, UK, 1959.
31. *Decagon Devices*; KD2 Pro; Decagon Devices: Pullman, WA, USA, 2016.
32. *W-GeoSoft*; Geophysical Software; W-GeoSoft: Bioley-Orjulaz, Switzerland, 1988.
33. *Geotomo Software*; Geotomo Software: Penang, Malaysia, 2019.



© 2019 by the authors. Licensee MDPI, Basel, Switzerland. This article is an open access article distributed under the terms and conditions of the Creative Commons Attribution (CC BY) license (<http://creativecommons.org/licenses/by/4.0/>).

Chapter III
TECHNICAL EVALUATION OF
THE GEOTHERMAL DESIGN

III. Technical evaluation of the geothermal design

The present Chapter firstly addresses the influence of different geothermal components on the final performance of the system. Lastly, this section contains the Papers published in high impact journals concerning the analysis of some of the mentioned components; grouting material, heat exchangers and geothermal heat pumps.

III.I. Configuration of the geothermal system

Within the context of very low enthalpy geothermal installations, a series of elements that are part of these systems have an enormous influence on the global efficiency. The purpose of the Papers included in this Chapter is the analysis of three of the main actors in the thermal exchange with the ground. In this way, Paper 6 addresses the evaluation of traditional grouting materials and their improvement by the addition of new substances, Paper 7 is focused on the comparison of the most frequent heat exchanger configuration and finally, Paper 8 is responsible for analyzing the unavoidable geothermal heat pumps.

Grouting materials are one of the key components of ground source heat pump systems. This fact is especially evident in vertical closed-loop configurations, where the stability of the borehole walls is ensured by the injection of the mentioned materials. In addition to their stability function, grouting materials must present convenient thermal properties (above all high thermal conductivity) to transmit the heat from the pipes to the ground and vice versa. Given the important role of these materials, various researches have been directed to the analysis of different mixtures evaluating technical and thermal properties. Grouting materials using cement or bentonite as a base material have been tested in several occasions (Smith and Perry, 1999; Allan and Philippacopoulos, 2000). In addition to the common mixtures of bentonite, sand or cement, alternative materials have been used to enhance the grouts. In this context, graphite (natural flake or compressed expanded natural graphite), electric arc furnace slag or construction and demolition waste have been added and evaluated as constituents of grouting materials (Lee et al, 2010; Delaleux et al, 2012; Erol and François, 2014; Borinaga-Treviño et al, 2014). The contribution of the present Doctoral Thesis in this field is presented as Paper 6 and is based on the analysis of new grouting materials that help to improve the general heat exchange between ground and pipes.

Following up on the topic of Chapter III, heat exchangers are considered another key pillar of the GHSP performance. Traditional geothermal systems consist of the installation of closed loop tubes in the ground, within which a heat carrier fluid circulates. In this context, numerous studies have been focused on evaluating the differences in the thermal performance of vertical and horizontal ground-coupled heat exchangers (Petit and Meyer, 1997, 1998; Esen et al, 2006, 2007; Tarnawski et al, 2009; Zhai and Yang, 2011; Michopoulos et al, 2013). Within the framework of vertical heat exchangers, usually considered the most recommended configuration, there is a continuous effort to find the most efficient design. Computing and in situ simulations are frequently made on entire GSHP systems in order to evaluate the influence of using one or another heat exchanger design (Focaccia and Tinti, 2013; Zarrella et al, 2013; Lee et al, 2015). As part of the present Doctoral Thesis, Paper 7 studies, through laboratory tests, the influence (on the global system performance and initial investment) of using one or another heat exchanger configuration. To this effect, simple-U and double-U vertical pipes as well as the helical-shaped ones are tested in an experimental laboratory setup.

Another essential pillar in the shallow geothermal exchange of a GSHP system makes reference to the use of heat pumps. Geothermal heat pumps offer an attractive option for heating and cooling residential and commercial building thanks to their higher energy efficiency compared with conventional systems. The important role these devices play in the operation of low enthalpy geothermal installations forced to focus, a part of this Doctoral Thesis, on the analysis of geothermal heat pumps. In a world with limited natural resources and large energy demands, it becomes increasingly important to develop systematic approaches for improving systems and thus, reducing the environmental impact. In the heat pump context, improvements are focused on increasing the efficiency of its components to optimize the thermodynamic cycle. For that purpose, a large number of research studies have dealt with this issue by means of exergy and energy analysis applied to various types of heat pumps (Tsaros et al, 1987; Crawford, 1988; Salah El-Din, 1999; Hepbasli and Akdemir, 2004). Furthermore, one of the major issues regarding the use of traditional heat pumps is their associated electricity consumption. As a way of avoiding the use of electrical energy coming from fuel power plants, recent experimental studies have also considered the use of gas engine heat pumps (using natural gas propane of LPG) as a part of a geothermal system (Hepbasli et al, 2009; Liu et al, 2017; Hu et al, 2017). Within this last context, Paper 8 of the present

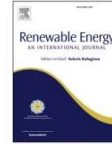
Doctoral Thesis addresses a wide technical comparison of three heat pumps variants: the common electrical heat pump and the gas engine heat pump aided by natural gas and biogas. Such arrangement provides the advantage of evaluating the most appropriate heat pump model based on the specific conditions of the location.

PAPER 6



Contents lists available at ScienceDirect

Renewable Energy

journal homepage: www.elsevier.com/locate/renene

Analysis and study of different grouting materials in vertical geothermal closed-loop systems



Cristina Sáez Blázquez*, Arturo Farfán Martín, Ignacio Martín Nieto, Pedro Carrasco García, Luis Santiago Sánchez Pérez, Diego González-Aguilera

Department of Cartographic and Land Engineering, University of Salamanca, Higher Polytechnic School of Avila, Hornos Caleros 50, 05003 Avila, Spain

ARTICLE INFO

Article history:

Received 6 March 2017
Received in revised form
27 July 2017
Accepted 5 August 2017
Available online 6 August 2017

Keywords:

Geothermal energy
Vertical closed-loop geothermal systems
Grouting material
Total drilling length

ABSTRACT

In vertical closed-loop geothermal systems, the material used to fill the boreholes is an essential element since it facilitates the exchange of heat between holes and pipes which contain the heat transfer fluid. Therefore, the thermal conductivity of this grouting material plays a vital role in conducting heat to the installation; not only does it increase its efficiency with higher thermal conductivity values, but it also makes the reduction of the total drilling length required to cover some particular energetic needs, possible. In view of the importance of this grouting material, a series of mixtures were produced and both thermal and mechanical properties were analysed in the laboratory. The use of aluminium shavings and sulpho-aluminate cement improved the thermal conductivity of these mixtures and offered excellent mechanical properties. However, non-satisfactory results were obtained for the bentonite due to the contractile effects caused in samples of this nature.

© 2017 Elsevier Ltd. All rights reserved.

1. Introduction and background

As a renewable, efficient and environmentally-friendly source, geothermal energy is, at the moment, in an expansion process, which places it at a very important position in the energy sector. With respect to very low temperature geothermal energy, commonly used to produce SHW (Sanitary Hot Water) or to heat/cool a certain place [6], heat exchangers can be divided into two main groups: open and closed geothermal systems. Open systems use groundwater coming from an adjacent aquifer to exchange heat with the ground, while closed systems use a fluid flowing inside a pipe to carry out the thermal exchange. The latter system is not conditioned to the existence of a nearby aquifer to provide the water exchange. Closed systems can be classified as: horizontal closed-loop systems, in which pipes are buried up to 5 m, and vertical closed-loop systems, constituted by deeper vertical drillings [16]. The grouting material injected inside these holes must fulfil a series of functions. It must guarantee the stability of holes and pipes. It must constitute a hydraulic barrier, avoiding the pollution of close aquifers due to a possible leak. Finally, grouts must allow the heat exchange between ground and pipes fluid. This

last function will determine the right working and efficiency of the installation; hence one of the most important properties of grouting materials is the thermal conductivity or the capacity to conduct heat. Fig. 1 shows the schematic of a geothermal borehole [19].

Numerous authors have analysed the thermal conductivity of a wide variety of grouting materials to discard those materials whose thermal properties make them unsuitable for use as grout in these installations. As a rule, it is considered important that the grouting material has a thermal conductivity value equal to or higher than that of the surrounding ground, so as to avoid reducing the efficiency of the system. It should also be noted that the possible gaps (pores of different geometry filled with air or water) in the grout negatively affect the installation reducing the heat flux to the pipes [2,21,24,26,37]. Grouting materials are typically grouped into grouts whose primary components are either bentonite or cement. Bentonite is flexible, with low permeability and easy placement, although it has a relatively low thermal conductivity: a range of between 0.65 W/(m K) and 0.90 W/(m K) in saturated conditions [11]. It is, however, commonly used in geothermal boreholes in spite of its limited capacity to conduct heat. In order to improve this thermal property, the addition of other materials to bentonite has been analysed. Remund and Lund [20], demonstrated that the thermal conductivity of bentonite is substantially improved by the addition of sand and can vary by modifying the water content of the mixture. Allan and Philippopoulos [27], elaborated a mixture

* Corresponding author.
E-mail address: u107596@usal.es (C.S. Blázquez).

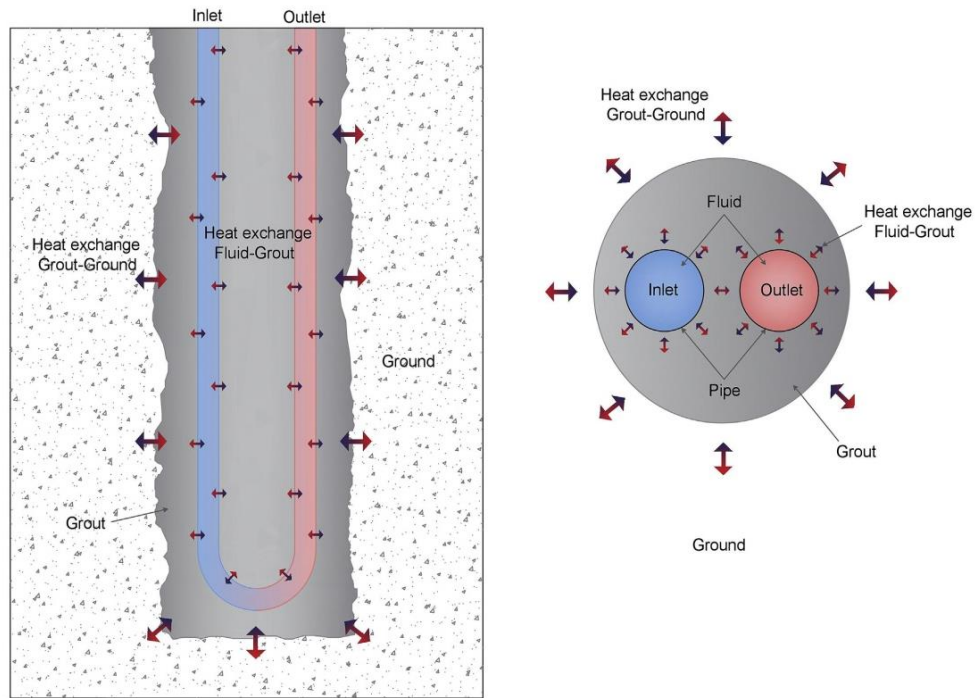


Fig. 1. Two different views of a geothermal borehole.

enhanced with silica sand which tripled the thermal conductivity of a bentonite mixture. Jobmann et al. [25], studied the influence of adding graphite to the grouting material and recorded a thermal conductivity of 3 W/(m K) for a mixture with a basis of bentonite constituting 14% water and 15% graphite. Lee et al. [8,9], noted that by increasing the quantity of silica sand and graphite, the thermal conductivity of the sample increased; although so did its viscosity. In this way, by adding 30% graphite; they attained a thermal conductivity of 3.5 W/(m K) . They also obtained 2.6 W/(m K) of thermal conductivity for a mixture of cement, silica sand and graphite. Delaleux et al. [14], have recently pointed out that by adding less than 15% of graphite powder, thermal conductivities of around 5 W/(m K) can be achieved. Engelhardt [18], added ballast to bentonite, acquiring thermal conductivities up to 2.6 W/(m K) . The shrinkage potential of bentonite is another important factor to be considered. In this field, Olson and Mesri [35] focused on the impact of pore fluid on the volume change of bentonites under various stress states.

With respect to cement based mixtures, the addition of silica sand was studied in depth by Allan et al., [28–32]. They demonstrated that the total drilling length could be reduced by around 22–37% with the use of this grout, depending on the type of ground and the diameter of the drilling in question. Xu and Chung [44] proved that by adding silica sand to cement, the thermal conductivity of the mixture increased by 22%. Altimiri et al. [1], made mixtures with different amounts of sand, cement, fluorite, glass and PFA (Pulverized Fuel Ash) obtaining thermal conductivities of up to

2.88 W/(m K) for a PFA of 20%. Recent studies based on energy piles deal with the use of cement as concrete in deep foundations [7,23,34].

The main objective of the present research is to suggest new alternatives, suitable to be used as grouting materials in a geothermal installation. On the basis of the information mentioned before, experiments with grouts that incorporate aluminium as a new element were carried out. Thus, a series of test tubes of different materials (including aluminium) were produced and analysed to check its suitability as geothermal grouting materials. Aluminium was added to the grouts in two ways: from a batch of cement or added to the mixture separately. Parameters like thermal and hydraulic conductivity, workability, compression strength and the possible contractions or reductions of volume over time have been considered in this work.

The innovative element in these mixtures is aluminium, which, due to its extraordinary capacity to conduce heat, was incorporated in the shape of cement and shavings or small filings. Thus, its cohesion with the rest of components of the mixture was significantly easier.

2. Experimental methodology

2.1. Materials

Specimens produced in laboratory are composed by: water (w), sodium bentonite (b), silica fine-grain sand (s), detritus from a hole

of granitic origin (*d*), cement portland CEM II-B (c_c), superplasticizer (*sp*), sulpho-aluminate cement ALI CEM (c_a) and aluminium shavings (*a*). Bentonite, silica sand and CEM II-B are commonly used for this purpose. Superplasticizer was tested in some mixtures to analyse its influence. It allows the improvement of the pump-ability of the mixture avoiding at the same time its segregation. Detritus (*d*) were taken from a drilling placed in the province of Ávila (Spain) in a granitic ground. Its grain distribution can be seen in Fig. 2.

Sulpho-aluminate cement supplied by FYM (*Heidelberg Cement Group*) is a conglomerate constituted by a sulpho-aluminate clinker of calcium and high quality anhydrite [15]. It provides a rapid development of the initial resistances for the medium and long term, exceeding the values given by high output portland cement.

"Aluminosis" is the term given to a series of chemical and physical transformations that reduce the hardness, strength and compactness of the concrete constituted by aluminium cement. This cement provoked structural problems, especially during the third quarter of the twenty century [3]. However, its use is thoroughly regulated by normative *UNE-EN-80310:96* [43]. This fact does not result in an inconvenience in the possible utilization of this material as grout in geothermal drillings because its function differs from that required for the support of large structures. Its use, therefore, would be totally feasible in these renewable installations. Both aluminium cement and cement portland used in this research fulfil the specifications considered in the normative *EN 197-1* and *EN 197-4* [39,40].

Aluminium, used as metal in the form of shavings, was previously crushed in order to reduce its size and consequently guaranteeing the correct uniformity of the mixture. It is important to highlight there is not any risk of chemical reactions with other components from the ground given the chemical behaviour of this element and the poor proportion in the mixtures. Table 1 shows the main characteristics of the two kinds of cements that are part of this study.

2.2. Mixtures

Cylinder specimens of 5 cm in diameter and 11 cm in height were used to test the different mixtures studied as grouting materials. The amounts of each of the components of the mixtures were set according to the results observed by other authors cited in Section 1. This way, the advisable ratios in dry conditions among the different aggregates (*g*) and cement (g/c_c and g/c_a) are around 1,

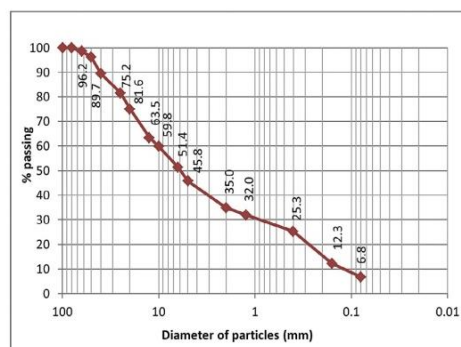


Fig. 2. Grain distribution of the detritus used in mixtures 10, 11 and 12.

Table 1
Main characteristics of sulpho-aluminate cement (ALI CEM) and cement portland (CEM II-B).

	ALI CEM	CEM II-B
Principal chemical components	CO: 37–41% Si ₂ O: ≤ 9% Al ₂ O ₃ : 27–33% Fe ₂ O ₃ : ≤ 1.5% SO ₃ : 10–14% MgO: ≤ 5%	Clinker: > 65% ashes + limestones: < 30% SO ₃ : < 2.4% Chlorides: < 0.003% Chromium VI soluble in water: < 0.0002%
Setting time	Initial- 25 min Final- 50 min	Initial- 200 min Final- 300 min
Compression resistance	7 days- 42.5 MPa 28 days- 47.5 MPa	7 days- 28.0 MPa 28 days- 40.0 MPa
Main applications	<ul style="list-style-type: none"> ■ Refractory concrete - Base and temporal bench - Constructions and prefabricated elements of bulk concrete or non-structural concrete - Certain cases of foundations of bulk concrete - Sprayed concrete 	<ul style="list-style-type: none"> - Concrete slab for roads - Bulk and reinforced concrete - Mortars and bricklaying's - Concrete with reactive arid - Concreting in hot weather - Compacted concrete dam - Soils stabilization - Non-structural prefabricated

2 and 3. In the present research the relation was set in g/c_c and $g/c_a = 2$. For those samples that incorporate superplasticizer (*sp*), the defined ratio was sp/c_c and $sp/c_a = 0.02$ [36]. With regard to sand and bentonite mixtures, a percentage of bentonite equal to 10–12% was selected because it provides a notable value of thermal conductivity [17]. With respect to aluminium shavings, several sand-shavings mixtures saturated to 80% with water were tested, modifying the percentages by weight of aluminium in relation to the total dry weight of the sample. The aim was to establish the most appropriate amount of aluminium in relation to the thermal conductivity results. Table 2 shows the thermal conductivity results of each mixture of sand-shavings tested.

As can be seen in Table 2, it gets to the point where increasing the amount of aluminium shavings actually reduces the thermal conductivity. An excessive amount of shavings causes the appearance of an increasing number of holes that alters the thermal conductivity of the sample. In the manufacture of the rest of the grouts, the quantity of aluminium was set at 1.0% of total weight of the dry sample, given that it has a thermal conductivity value very close to higher percentages of shavings but using a lower amount of aluminium.

The quantity of water added to each mixture depends in each case on the absorption capacity of the integrated materials. In any case, the aim was that every resultant specimen has the suitable consistency to be easily injected into a hole, making their use as

Table 2
Thermal conductivities for the different percentages of shavings in sand-shavings mixtures.

Percentage by weight of aluminum shavings (%)	Thermal conductivity (W/mK)
0.5	3.270
1.0	3.651
1.5	3.692
2.0	3.752
2.5	3.860
3.0	3.798
3.5	3.620

grouting material, possible. Abrams cone method defined by the Spanish Law UNE 83313:1990 (annulled by UNE-EN 12350-2:2006) [42] was used to define the consistency of the samples. According to this method, the consistency of all samples was fluid (category S4 in Abrams cone method), with variable ratios (w/c_c and w/c_a) in function of the different aggregates that constitute the mixtures. As an alternative to this method, the Marsh funnel [5], which is commonly used as an indicator of bentonite-based grouts viscosity, could also be used in this research. Table 3 contains the mixtures made in laboratory and the components of each of them.

2.3. Laboratory samples characterization

With the purpose of suggesting the most suitable grout in geothermal installations, a series of laboratory tests were carried out for each of the samples presented in Table 3. These tests made it possible to determine the aptitude of these materials as geothermal grouts.

2.3.1. Density and workability

Every specimen analysed in this study containing cement (c_c or c_a) among other components as well as the remaining mixtures, behave like fluids and have the appropriate consistency to inject them into a borehole (to a particular depth and without any extra mechanical means). In order to carry out a complete characterization of cement mortars, densities of fresh mortar and after 28 days of hardening were calculated. For the rest of samples (without cement), only the initial density was calculated. In any case, the amount of water added to the samples was set according to Abrams cone method, so none of them generate difficulties during the injection into the hole.

2.3.2. Thermal conductivity

Thermal conductivity is an essential property to be considered in a grout. However, the effect of increasing the conductivity of the grout on the overall efficiency of the borehole heat exchanger (BHE) is highly limited by the ground conductivity.

Thermal conductivity of laboratory specimens was determined using KD2-PRO analyser with sensor RK-1 (Fig. 4) developed by Decagon Devices [12]. Its operation is based on the infinite line heat source theory and computes the thermal conductivity by monitoring the dissipation of heat from the needle probe. Heat is applied to the needle for a set heating time t_h , and temperature is measured in the monitoring needle during heating and for an additional time equal to t_h after heating. The temperature in the needle during heating is deduced from Equation (1) [10].

Table 3

Compositions of each of the tested mixtures, where: s-sand, b-bentonite, d-detritus, c_c - cement portland, c_a - aluminium cement, a-aluminium shavings, sp-superplasticizer, w-water.

Mixture	Percentage in relation to total weight (%)							
	s	b	d	c_c	c_a	a	sp	w
1	77.65					0.78		21.57
2	53.18			19.46		0.80		19.16
3	46.14	6.29				0.59		46.98
4	50.00				25.00			25.00
5	40.24	5.49			22.93			31.34
6		19.12			9.56			71.32
7	51.39				25.70	0.76		22.14
8	57.41			30.26		0.87	0.60	10.86
9	57.91				30.52		0.61	10.96
10			74.52					25.48
11			50.00		25.00			25.00
12			50.00	25.00				25.00

$$T = m_0 + m_2t + m_3 \ln t \quad (1)$$

Where:

- m_0 is the ambient temperature during heating
- m_2 is the rate of background temperature drift
- m_3 is the slope of a line relating temperature rise to logarithm of temperature

Equation (2) represents the model during cooling [7].

$$T = m_1 + m_2t + m_3 \ln \frac{t}{t - t_h} \quad (2)$$

Both equations (1) and (2) are used by the equipment to provide the temperatures during the period of heating and after it when heating stops and needle starts cooling. Fig. 3 shows the evolution of temperatures during a process of measuring of KD2-PRO.

Thermal conductivity can be calculated from Equation (3) that also considers the heat flux (q).

$$k = \frac{q}{4m_3} \quad (3)$$

Only 2/3 of the data collected are used during heating and cooling (it ignores early-time data) since these equations are long-time approximations to the exponential integral equations. This approach prevents errors derived from the placement of the needle. Equations (1) and (2) can be solved by linear least squares, giving a solid and more adjusted result [22,38].

In the current research, sensor RK-1 (3.9 mm in diameter and 6 cm in length) was used to determine the thermal conductivity of each sample (Fig. 4). This sensor is capable of measuring the thermal conductivity in a range between 0.1 and 6 W/(m K) with $\pm 10\%$ of accuracy. The relatively long read times of sensor RK-1 (around 10 min) contribute to prevent errors derived from the large diameter needle and the contact resistance between the sensor and the granular sample and solid materials. The contact between needle and tested material is guaranteed by placing thermal grease (a ceramic polysynthetic thermal compound) in the hole where the needle is situated. Drilling could increase the uncertainty on results. Three samples of each mixture were made and three measurements were carried out for each of these samples to evaluate the uncertainties. It is advisable to mention that the RK-1 sensor was previously calibrated with samples supplied by the manufacturer. Measurements with KD2 Pro can be strongly affected by wrong practices. To obtain the most accurate data possible, ambient

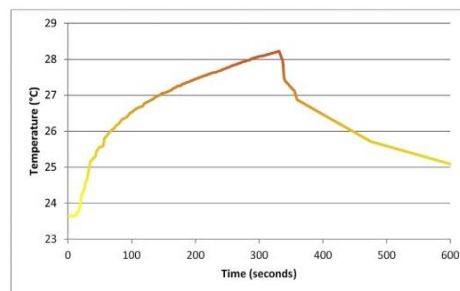


Fig. 3. Evolution of temperatures during a process of measuring with KD2-PRO.



Fig. 4. (a) Drilling of a hole to insert sensor RK-1. (b) Measuring of thermal conductivity with equipment KD2 Pro.

temperature was kept as constant as possible during the measurement. If sample temperature changes during the measurement period, it degrades the data and makes it difficult for the inverse calculation to find the correct values for the thermal properties. To minimize these sources of error, about 15 min for samples and needle to equilibrate with the ambient temperature before taking measurements and around 15 min between readings for temperatures to equilibrate.

Once the specimens were manufactured, they were left to dry and harden (in case of mixtures with cement, a period of 28 days, time required so that this material reaches its maximum resistance). After this time, a hole of 6 cm in length and 3.9 mm in diameter (needle size) was drilled to place the sensor RK-1 and carry out the thermal conductivity measurements (three for each sample) always using the thermal paste. Sand mixtures without cement or bentonite were previously compacted in a standard Proctor mould [41] to prepare the test tubes. Pushing of the needle into the prepared soil specimen was carefully made to avoid possible effects of soil densification.

2.3.3. Compression strength

Despite the fact that there is not any specific requirement about the minimum unconfined compressive strength of mortars used as grout in vertical closed-loop systems, it is recommended that these grouts, considered as non-structural concrete, have a compression strength of at least 15 MPa according to the Spanish regulation EHE08 [33]. Mechanical strength of the grout is important to

guarantee the stability of the borehole and to protect the heat exchangers. Continuing with the characterization of these grouts, compression strength of cementitious mixtures (2, 4, 5, 6, 7, 8, 9, 11 and 12) was determined after 28 days of hardening. After this time, compression tests provided the highest values of resistance that the sample can support before breaking. Simple compression tests were used in this work given that grouting materials mainly supports compression efforts. Freezing impacts in grouts are not considered in this work; otherwise traction strength test should be carried out [13]. In Fig. 5 it is possible to observe the state of one of the test tubes studied before and after the simple compression test.

2.3.4. Volumetric reduction

Another factor studied in the grouts is the reduction of volume and the presence of holes over time. These aspects result in negative effects for the thermal transfer function of a grouting material. The possible gaps created in the grouting material can be refilled with water (in the case of boreholes with the presence of groundwater) or air, deficient thermal conductor that could constitute a barrier in the thermal exchange between ground and pipes. Accordingly, a visual inspection and physical characterization of each test tube was carried out and initial and final dimensions (after 28 days) were measured. Volume reductions were controlled to discard those mixtures unsuitable for use as geothermal grout.

Boundary conditions were previously defined to analyse the contractions. Room temperature was set in 18 °C for all cases. Most tests were performed in unsaturated conditions exposed to air with

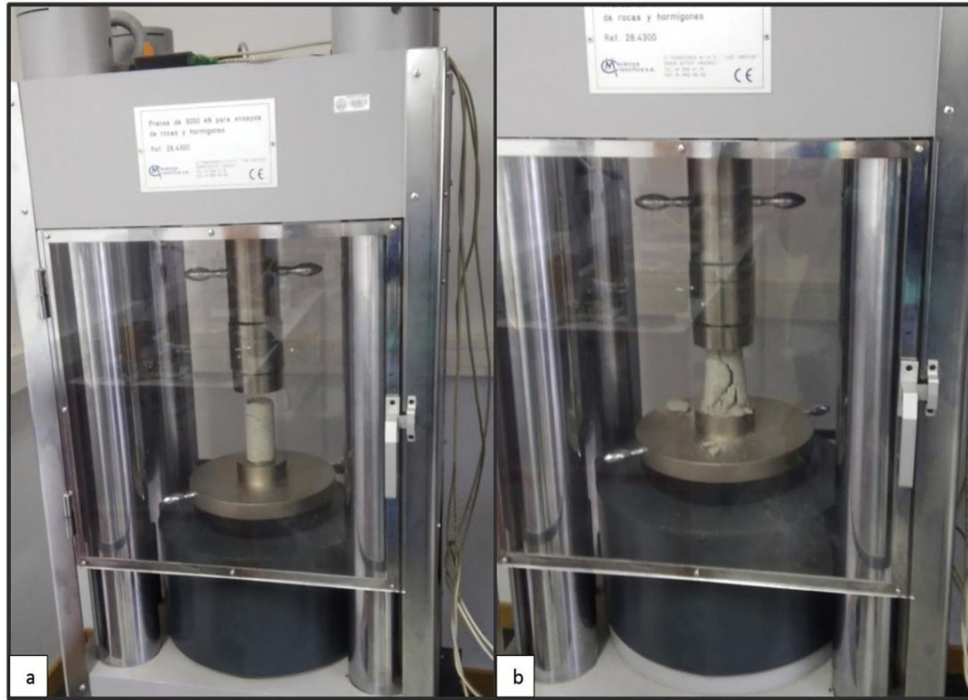


Fig. 5. Simple compression test. (a) Test tube ready to start the test. (b) Test tube after breaking.

the exception of saturated sand grout. Grouts were not subjected to any vertical effective stresses during the period of visual inspection. This research focuses on free shrinkage experiments that may not be representative of the constraints in a borehole. Tests represent the conditions expected near the ground surface that probably change deeper in a borehole.

2.3.5. Hydraulic conductivity

Hydraulic conductivity constitutes another essential parameter in a grout. However, it was verified that saturated sand, mixtures of bentonite or the rest of cementitious samples do not allow any flux of water through them. For this reason, and given that all mixtures used in this work have insignificant (even zero) hydraulic conductivity values, measurements of this parameter are not presented in this research.

3. Results and discussion

3.1. Laboratory test results

Results of the laboratory tests are presented in Table 4. Compression strength results (not presented in Table 4) were all greater than 15 MPa for all cementitious mixtures.

A series of important considerations regarding the grouts analysed in this research can be deduced from Table 4:

Table 4

Laboratory test results. *Values measured in fresh samples, **Values measured after a period of hardening of 28 days.

Mixture	Density [kg/m^3] $\times 10^3$	Thermal conductivity [W/mK]	Contractions [%]
1	2.44*/2.44**	3.651**	0**
2	1.92*/1.77**	2.199**	0**
3	1.58*/2.04**	1.566**	44.02**
4	2.10*/2.07**	2.453**	0**
5	1.86*/1.68**	1.270**	3.97**
6	1.24*/1.29**	1.096**	27.91**
7	2.15*/2.05**	2.789**	0**
8	1.94*/1.78**	1.016**	0**
9	2.39*/2.24**	1.317**	0**
10	2.39*/2.39**	1.949**	0**
11	2.01*/1.92**	2.036**	0**
12	1.96*/1.87**	1.829**	0**

- Density values measured after the period of hardening of 28 days are in every case equal to or lower than the values corresponding to initial densities, except for those mixtures that experienced a high reduction of volume (mixtures 3 and 6) due to the evaporation of a fraction of water they initially had. The highest densities correspond to sand and detritus mixtures with a degree of saturation of 80% of water (mixtures 1 and 10). The initial and final densities of these samples are identical given that the grout would always be under saturated conditions and therefore its density would not vary. In general, mixtures with

Table 5
Set of thermal conductivity measurements, average and maximum deviation.

Mixture	Thermal Conductivity [W/mK]									Maximum Deviation	
	Sample 1			Sample 2			Sample 3				Average
1	3.652	3.649	3.651	3.650	3.651	3.649	3.652	3.651	3.650	3.651	0.002
2	2.197	2.199	2.198	2.197	2.202	2.198	2.200	2.197	2.199	2.199	0.003
3	1.563	1.564	1.564	1.567	1.569	1.568	1.567	1.565	1.566	1.566	0.003
4	2.457	2.456	2.455	2.452	2.450	2.452	2.454	2.453	2.452	2.453	0.004
5	1.269	1.268	1.269	1.272	1.273	1.270	1.271	1.272	1.270	1.270	0.003
6	1.093	1.092	1.094	1.096	1.095	1.096	1.098	1.099	1.098	1.096	0.003
7	2.789	2.788	2.788	2.786	2.784	2.784	2.794	2.791	2.794	2.789	0.005
8	1.012	1.013	1.014	1.016	1.015	1.016	1.019	1.017	1.018	1.016	0.003
9	1.318	1.318	1.319	1.314	1.312	1.311	1.322	1.321	1.320	1.317	0.006
10	1.948	1.949	1.949	1.952	1.953	1.954	1.945	1.947	1.947	1.949	0.005
11	2.032	2.035	2.034	2.035	2.033	2.033	2.039	2.039	2.04	2.036	0.004
12	1.834	1.832	1.829	1.825	1.827	1.828	1.829	1.826	1.827	1.829	0.005

aluminium shavings (mixtures 1, 2, 3, 7 and 8) do not have the highest values of density. The low density of this element allows the formation of combinations with interesting properties but without increasing the density of these mixtures. Finally, there are no significant differences of density among samples with cement portland (c_c) and those ones constituted by aluminium cement (c_a). In conclusion, the use of aluminium does not generate higher density mixtures than the commonly used for these purposes.

- Thermal conductivity values presented in Table 4 represent the average of the measurements carried out for each mixture (three samples for each mixture and three measurements for sample). Table 5 shows the set of measurements, the average for each mixture and the maximum deviation in these values.

As a rule, all specimens provide quite notable thermal conductivity values. Mixture 1 of saturated sand (s) and aluminium shavings (a) stands out, constituting, from a thermal point of view, an excellent option for those boreholes with groundwater. Mixtures with aluminium cement (c_a) present higher thermal conductivity values than those samples with cement portland (c_c), reaching values of 2.453 W/(m K) as in the case of mixture 4 only constituted by sand and aluminium cement. Aluminium shavings improve, in

all cases examined, the thermal conductivity of the sample in question with an amount of only 1% in relation to the total weight of the dry sample. Thus, mixture 7, containing aluminium cement (c_a), sand (s) and aluminium shavings (a), achieves a thermal conductivity value of 2.789 W/(m K) as well as mixture 2 with a thermal conductivity of 2.199 W/(m K). Mixtures (10–11–12) formed by detritus (d) from a borehole offer quite acceptable thermal conductivity values, including both saturated detritus (mixture 10) and detritus with cement portland (c_c) (mixture 12) or with aluminium cement (c_a) (mixture 11) which reaches the most remarkable value. Mixtures with bentonite (b) also stand out but in a negative way providing comparatively low values as a result, among other factors, of the low thermal conductivity of this material.

Finally, specimens including superplasticizer (sp) (mixtures 8 and 9), offer lower thermal conductivity values than those ones with similar composition (mixtures 2 and 4) but without this substance. This may be due to the large number of holes observed in these mixtures caused by the use of superplasticizer. Both mixtures were reproduced with identical composition (without superplasticizer) and examined to verify that this element was the source of the increase of holes in these samples. Fig. 6 graphically presents the distribution of thermal conductivities of the group of mixtures.

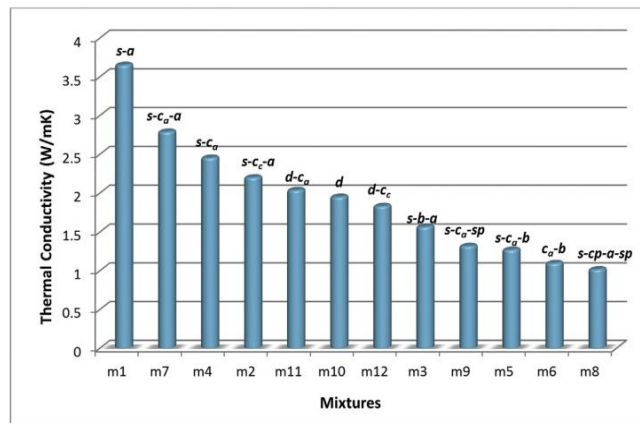


Fig. 6. Graphic of the distribution of thermal conductivities of the mixtures.

- Simple compression tests carried out on mixtures with cement (c_c or c_a) provided favourable results, superior to the recommended 15 MPa, except in mixtures with bentonite (b) which do not get such compression resistance since this material does not allow the complete solidification of the sample. However, the compressive strength is probably not the best indicator of performance in this application; more importance should be given to the shrinkage behaviour and the thermal conductivity of grouts.
- With regard to volume reductions or contractions after a period of 28 days, this phenomenon was observed in all mixtures with bentonite (b). The contractile nature of this material caused strong contractions in the samples, coming to generate volume reductions up to 44.02% in mixture 3 or 3.97% and 27.91% in mixtures 5 and 6 that counteracted this property of bentonite because of the cement they also contained. It is important to highlight these results are representative of a worst-case scenario (near the ground surface, without vertical effective stress and above the water table). The daily evolution of the volume

reductions experimented by mixtures 3, 5 and 6 can be observed in Fig. 7.

Because of the negative impact this grout may cause in vertical closed-loop systems, a more exhaustive study of this phenomenon was carried out. A series of additional specimens made of bentonite-water or bentonite-cement ($b-c_c$ or $b-c_a$) were manufactured, this time with lower percentages of cement (3%, 6%, 9% and 15% of cement in relation to the total weight of the dry sample). The volume reductions experimented in each case were analysed. In all assumptions studied, high volume decreases were registered, always exceeding the percentages previously expounded in Table 4. Fig. 8 shows the final appearance of the bentonite test tubes after 28 days in comparison with the initial size represented in the central test tube that did not experienced contractions due to the absence of bentonite.

Although all specimens experienced a high degree of contractions, the most extreme case was found in one of the bentonite-aluminium cement samples with an amount of cement of 6% in

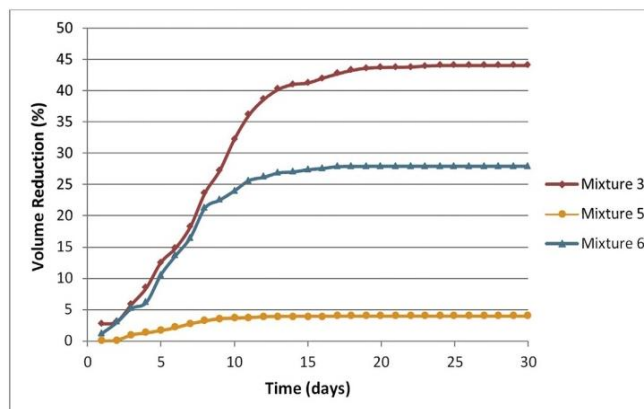


Fig. 7. Daily evolution of the volume reductions experimented by mixtures 3, 5 and 6. *Test were made with an ambient temperature of 18 °C, in unsaturated conditions and not subjected to any vertical effective stresses.

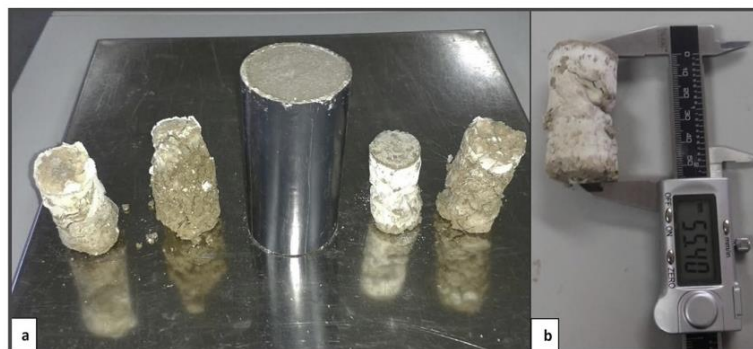


Fig. 8. (a) Comparison of the final appearance of bentonite samples in relation to the central sample exempt of bentonite, (b) Measuring of bentonite sample with a digital calibre.

respect to the total weight of the dry sample. The volume reduction for this sample was of 89.79%. Fig. 9 schematizes the reductions of size this sample experienced.

All experiments were made at constant temperature and humidity. Results denote this grout is not suitable in boreholes without groundwater where almost the totality of water is evaporated. An exhaustive analysis of the borehole conditions should be carried out before choosing bentonite as grout.

3.2. Proposed solutions

Considering the tests made in laboratory, Table 6 indicates those suitable mixtures to be used as geothermal grout in boreholes with groundwater and without it. This Table 6 also establishes the non-recommendable mixtures to this end, because of the size reductions, porosity and hence deficient capacity to conduce the heat these samples have.

The selected solutions for each of the assumptions are

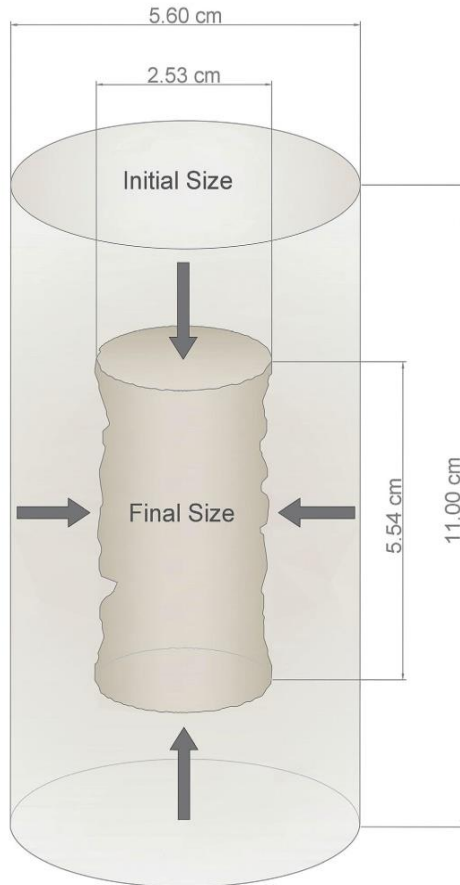


Fig. 9. Schema of the size reduction of the sample b-c₀ to 6%.

Table 6

Suitability of the proposed mixtures for the two considered assumptions. *Suitable but non-recommendable mixture.

Mixture	Boreholes without groundwater	Boreholes with groundwater
1	x	✓
2	✓	✓
3	✓*	✓*
4	✓	✓
5	✓*	✓*
6	✓*	✓*
7	✓	✓
8	✓*	✓*
9	✓*	✓*
10	x	✓
11	✓	✓
12	✓	✓

expanded below.

> Boreholes without groundwater

In this kind of boreholes, mixtures that require a continuous saturation (mixtures 1 and 10) are totally discarded. The following solutions are highly recommended:

- Mixture 7 (aluminium cement-sand-shavings): apparently, it is the best solution for these types of holes considering that it is the mortar with the most notable thermal conductivity value. It also presents excellent resistance capacities and being simultaneously exempt of contractions.
- Mixture 4 (aluminium cement-sand): this grout, which has an excellent thermal conductivity, means an ideal solution in holes without groundwater because of the same reasons described in the above mixture.
- Mixture 2 (cement portland-sand-shavings): equally recommendable in holes without groundwater due to its proper thermal conductivity and resistance properties with a minimum amount of aluminium.
- Mixture 11 (aluminium cement-detritus): this mortar, that contains the detritus from a borehole, has a moderate thermal conductivity (around 2 W/(m K)), sufficient compression strength and does not present size decreases. However, its aptitude depends on the characteristics of the detritus in question that change thoroughly from a hole to another.
- Mixture 12 (cement portland-detritus): as in the previous case, its ability to be used as grout depends on the particular detritus. In this instance, the mixture means a proper alternative with lower thermal conductivity than the previous solutions but it is equally acceptable because of its resistance capacities and constant volume.

> Boreholes with groundwater

It can be assumed that grouts are water-saturated in the case that the phreatic level is near the ground surface. The grouts suggested in these conditions are:

- Mixture 1 (saturated sand-shavings): this grout constitutes an appropriate solution, it reaches an excellent thermal conductivity value (>3 W/(m K)), without size reductions and it does not mean an inconvenient from an economical point of view. It would only be applicable to these boreholes since if it was not saturated, its capacity to conduce the heat would sharply descend.
- Mixture 10 (saturated detritus): as in the last mixture, this grout means a proper solution for these cases although it has a lower

thermal conductivity. It does not experience volume reductions and does not imply an additional expense since it derives from a borehole.

In addition to these two solutions, for those holes where the presence of water is not completely guaranteed, the circulation is sporadic or the intention is to seal the hole, samples suggested in the previous section (mixtures 4, 2, 7, 11 and 12) are equally suitable and recommendable in these conditions.

Table 7 presents a multi-criteria analysis for mixtures 7 (Option A), 4 (Option B), 2 (Option C) and 1 (Option D). Mixtures 10, 11 and 12 were not considered given that the particular conditions of these samples will depend on the detritus in question. Three criteria were used; criterion 1 (density, workability), criterion 2 (thermal conductivity) and criterion 3 (cost per test tube). The optimal ranking is *DABC* and *DACB*; Option D followed by Option A, followed by Option B, followed by Option C or Option D followed by Option A followed by Option C followed by Option B. In any case, the most optimal option is D, mixture 1. When mixture 1 cannot be used, the optimal ranking is ABC and ACB, mixture 7 will be the most recommendable.

3.3. Environmental and economic impact

It is important to consider the environmental and economic impacts of the different mixtures considered in this research:

- In relation to the environmental issue, most of the mixtures of this research provide a total sealing of the hole, preventing leakages of circulating fluid. Mixtures with bentonite in boreholes without groundwater experience volume reductions, however, this fact should not affect the borehole sealing. Special attention should be paid to mixtures 1 and 10 (sand or detritus saturated and shavings) which could not seal the hole if they are not completely saturated. Another environmental issue is the chemical interaction between compounds of the grouting and the ground. Nature of the components used in the mixtures does not suppose chemical reactions with the surrounding materials of the ground.

- Regarding the economic aspect, the use of aluminium (as shavings or cement) does not mean a significant increase with respect to the rest of grouts commonly used. Also, these grouts contribute to increase the efficiency of the installation generating economic savings in the process of energetic extraction. Table 8 shows an estimation of the cost per test tube of 270.93 cm³ produced in laboratory.

Although the difference by test tube is quite low, if the hole is considerably deep, the cost of the grout could define its choice. Thus, whenever possible, saturated sand could provide proper results with a relatively low cost.

Table 7
Multi-criteria analysis for mixture 7 (Option A), mixture 4 (Option B), mixture 2 (Option C) and mixture 1 (Option D).

Criteria	Weight	Direction	Option A		Option B		Option C		Option D		
			Performance	Weighted performance	Performance	Weighted performance	Performance	Weighted performance	Performance	Weighted performance	
1	0.15	-1	2.15	-0.32	2.10	-0.31	1.92	-0.29	2.44	-0.37	
2	0.6	1	2.79	1.67	2.45	1.47	2.2	1.32	3.65	2.19	
3	0.25	-1	0.13	-0.032	0.11	-0.027	0.024	-0.006	0.014	-0.003	
Outranking Matrix			A		B		C		D		
A			0		0.6		0.6		0.15		
B			0.4		0		0.4		0.15		
C			0.4		0.4		0		0.15		
D			0.85		0.85		0.85		0		
Policy Ranking Permutation			Policy Parings				Final Score				
ABCD			AB + AC + AD + BC + BD + CD				2.05				
ABDC			AB + AD + AC + BD + BC + DC				2.75				
ACBD			AC + AB + AD + CB + CD + BD				2.05				
ACDB			AC + AD + AB + CD + CB + DB				2.75				
ADBC			AD + AB + AC + DB + DC + BC				3.45				
ADCB			AD + AC + AB + DC + DB + CB				3.45				
BACD			BA + BC + BD + AC + AD + CD				1.85				
BADC			BA + BD + BC + AD + AC + DC				2.55				
BCAD			BC + BA + BD + CA + CD + AD				1.65				
BCDA			BC + BD + BA + CD + CA + DA				2.35				
BDAC			BD + BA + BC + DA + DC + AC				2.85				
BDCA			BD + BC + BA + DC + DA + CA				3.05				
CABD			CA + CB + CD + AB + AD + BD				1.85				
CADB			CA + CD + CB + AD + AB + DB				2.55				
CBAD			CB + CA + CD + BA + BD + AD				1.65				
CBDA			CB + CD + CA + BD + BA + DA				2.35				
CDAB			CD + CA + CB + DA + DB + AB				3.25				
CDBA			CD + CB + CA + DB + DA + BA				3.05				
DABC			DA + DB + DC + AB + AC + BC				4.15				
DACB			DA + DC + DB + AC + AB + CB				4.15				
DBAC			DB + DA + DC + BA + BC + AC				3.95				
DBCA			DB + DC + DA + BC + BA + CA				3.75				
DCAB			DC + DA + DB + CA + CB + AB				3.95				
DCBA			DC + DB + DA + CB + CA + BA				3.75				

Bold letters shows the best options

Table 8
Cost per test tube made in laboratory.

Mixture	Cost per test tube (€)
1	0.023
2	0.027
3	0.035
4	0.090
5	0.098
6	0.079
7	0.101
8	0.038
9	0.127
10	0
11	0.077
12	0.014

4. Conclusions

Grouting material used in vertical closed-loop systems must guarantee a series of thermal, physical and mechanical requirements. In the present research, a set of mixtures were made and analysed by laboratory tests, examining different properties. Specimens were manufactured with a certain consistence (according to flow cone method) to allow their injection in a borehole. Tests allowed deducing the following conclusions:

- Thermal conductivity values of the tested samples are in general considerably notable. The combination of saturated sand-shavings, the mixtures of aluminium cement-sand-shavings and aluminium cement-sand stand out with a thermal conductivity value of around 3 W/(m K). Aluminium shavings contribute to increase the thermal conductivity of a sample with only 1% of the total dry weight. Aluminium cement also improves the thermal conductivity in comparison with cement portland. Mixtures with bentonite or superplasticizer present the lowest values of this thermal property.
- Compression strength tests show that all mortars considered have a resistance superior to 15 MPa (value recommended for non-structural materials) with the exception of those cements that incorporate bentonite to the composition.
- Contractions studies reveal the negative effect that bentonite causes on samples that incorporate it. Thus, the higher amount of bentonite in the mixture, the higher size reductions will experience the test tube over time. These effects reject bentonite as grouting material in this type of installations.
- Finally, a multi-criteria analysis was used to select the most suitable grouts. The first option would be mixture 1 (saturated sand-aluminium shavings) followed by mixture 7 (aluminium cement-sand). In function of the borehole conditions, these mixtures are the most appropriate solutions to be used as grouting materials.

Acknowledgments

Authors would like to thank the Department of Cartographic and Land Engineering of the Higher Polytechnic School of Avila, University of Salamanca, for allowing us to use their facilities and their collaboration during the experimental phase of this research. Authors also want to thank the Ministry of Education, Culture and Sport for providing a FPU Grant FPU014/0218 (Training of University Teachers Grant) to the corresponding author of this paper what has made possible the realization of the present work.

References

- [1] A.A. Altimi, M. Rouainia, D.A.C. Manning, Thermal enhancement of PFA-based grout for geothermal heat exchangers, *Appl. Therm. Eng.* 54 (2) (2013) 559–564.
- [2] A.J. Philippopoulos, M.L. Berndt, Influence of debonding in ground heat exchangers used with geothermal heat pumps, *Geothermics* 30 (2001) 527–545.
- [3] A. Argandoña, Ethical aspects of an urban catastrophe, *J. Bus. Ethics* 14 (1995) 511–530.
- [5] ASTM D6910/D6910M-09, Standard Test Method for Marsh Funnel Viscosity of Clay Construction Slurries.
- [6] C.S. Blázquez, A.F. Martín, P.C. García, L.S. Sánchez Pérez, S.J. del Caso, Analysis of the process of design of a geothermal installation, *Renew. Energy* 89 (1) (2016) 188–199.
- [7] H. Brandl, Energy foundations and other thermo-active ground structures, *Geotechnique* 56 (2) (2006) 81–122.
- [8] C. Lee, K. Lee, H. Choi, H.P. Choi, Characteristics of thermally-enhanced bentonite grouts for geothermal heat exchanger in South Korea, *Sci. China Technol. Sci.* 53 (1) (2010) 123–128.
- [9] C. Lee, M. Park, T. Nguyen, B. Sohn, J.M. Choi, H. Choi, Performance evaluation of closed-loop vertical ground heat exchangers by conducting in-situ thermal response tests, *Renew. Energy* 42 (2011) 77–83.
- [10] H.S. Carslaw, J.C. Jaeger, *Conduction of Heat in Solids*, second ed., Oxford, London, 1959.
- [11] Daehoon Kim, Gyoungman Kim, Hwanjo Baek, Relationship between thermal conductivity and soil–water characteristic curve of pure bentonite-based grout, *Int. J. Heat Mass Transf.* 84 (2015) 1049–1055.
- [12] Decagon Devices, KD2 Pro Thermal Properties Analyzer Operator's Manual, Decagon Devices, Inc., 2016.
- [13] S. Erol, B. François, Freeze damage of grouting materials for borehole heat exchanger: experimental and analytical evaluations, *Geomech. Energy Environ.* 5 (2016) 29–41.
- [14] F. Delaleux, X. Py, R. Olives, A. Dominguez, Enhancement of geothermal borehole heat exchangers performances by improvement of bentonite grouts conductivity, *Appl. Therm. Eng.* 33–34 (2012) 92–99.
- [15] FYM, Heidelberg Cement Group, <http://www.fym.es/ES>.
- [16] G. Florides, S. Kalogirou, Ground heat exchangers—a review of systems, models and applications, *Renew. Energy* 32 (2007) 2461–2478.
- [17] Huajun Wang, Junchao Lu, Chengying Qi, Thermal conductivity of sand-bentonite mixtures as a backfill material of geothermal boreholes, *GRC Trans.* 35 (2011).
- [18] I. Engelhardt, S. Finsterle, Thermal-hydraulic experiments with bentonite/crushed rock mixtures and estimation of effective parameters by inverse modeling, *Appl. Clay Sci.* 23 (2003) 111–120.
- [19] I. Indacochea-Vega, P. Pascual-Muñoz, D. Castro-Fresno, M.A. Calzada-Pérez, Experimental characterization and performance evaluation of geothermal grouting materials subjected to heating-cooling cycles, *Constr. Build. Mater.* 98 (2015) 583–592.
- [20] J.P. Remund, J.T. Lund, Thermal enhancement of bentonite grouts for vertical ground source heat pump systems, in: *AES 29: Heat Pump and Refrigeration Systems, Design, Analysis and Applications*, The American Society of Mechanical Engineers (ASME), 1993.
- [21] Johan Desmedt, Johan Van Bael, Hans Hoes, Nico Robeyn, Experimental performance of borehole heat exchangers and grouting materials for ground source heat pumps, *Int. J. Energy Res.* 36 (2012) 1238–1246.
- [22] G.J. Kluitenberg, J.M. Ham, K.L. Bristow, Error analysis of the heat pulse method for measuring soil volumetric heat capacity, *Soil Sci. Soc. Am. J.* 57 (1993) 1444–1451.
- [23] L. Laloui, C.G. Olgun, M. Sutman, J.S. McCartney, C.J.R. Coccia, H.M. Abuel-Naga, G.A. Bowers, Issues involved with thermo-active geotechnical systems: characterization of thermo-mechanical soil behavior and soil-structure interface behaviour, *J. Deep Found. Inst.* 8 (2) (2014) 107–119.
- [24] M.D. Smith, R.L. Perry, Borehole grouting: field studies and thermal performance testing, *ASHRAE Trans.* 105 (1999).
- [25] M. Jobmann, G. Buntebarth, Influence of graphite and quartz addition on the thermal-physical properties of bentonite for sealing heat-generating radioactive waste, *Appl. Clay Sci.* 44 (2009) 206–210.
- [26] M.L. Allan, A.J. Philippopoulos, Performance characteristics and modelling of cementitious grouts for geothermal heat pumps, in: *Proceedings world geothermal congress, Japan, 2000*.
- [27] M.L. Allan, A.J. Philippopoulos, Properties and Performance of Thermally Conductive Cement-based Grouts for Geothermal Heat Pumps Applications, 1999, Upton, US-NY: FY 99 Final Report, BNL 67006.
- [28] M.L. Allan, Thermal conductivity of Cementitious Grouts for Geothermal Heat Pumps, Progress Report FY 1997, Department of Applied Science, Brookhaven National Laboratory, New York, 1997.
- [29] M.L. Allan, A.J. Philippopoulos, Thermally Conductive Cementitious Grouts for Geothermal Heat Pumps, Progress Report FY, Department of Applied Science, Brookhaven National Laboratory, New York, 1998.
- [30] M.L. Allan, S.P. Kavanaugh, Thermal conductivity of cementitious grouts and impact on heat exchanger length design for ground source heat pumps, *HVAC&R Res.* 5 (2) (1999) 87–98.
- [31] M.L. Allan, A.J. Philippopoulos, Ground water protection issues with

- geothermal heat pumps, *Geothermal Resource, Counc. Trans.* 23 (1999) 101–105.
- [32] M.L. Allan, Materials characterization of superplasticized cement-sand grout, *Cem. Concr. Res.* 30 (6) (2000) 937–942.
- [33] Ministerio de fomento, *Instrucción De Hormigón Estructural*, EHE08, Centro de Publicaciones, Madrid, 2008.
- [34] C.G. Olgun, J.S. McCartney, Outcomes from the international workshop on thermoactive geotechnical systems for near-surface geothermal energy: from research to practice, *J. Deep Found. Inst.* 8 (2) (2014) 58–72.
- [35] R. Olson, C. Mesri, Mechanisms controlling compressibility of clays, *J. Soil Mech. Found. Div. ASCE SM6* (1970) 1863–1878.
- [36] Roque Borinaga-Treviño, Pablo Pascual-Muñoz, Daniel Castro-Fresno, Juan José Del Coz-Díaz, Study of different grouting materials used in vertical geothermal closed-loop heat exchangers, *Appl. Therm. Eng.* 50 (1) (2013) 159–167.
- [37] Selçuk Erol, Bertrand François, Efficiency of various grouting materials for borehole heat exchangers, *Appl. Therm. Eng.* 70 (1) (2014) 788–799.
- [38] S. Shiozawa, G.S. Campbell, Soil thermal conductivity, *Remote Sens. Rev.* 5 (1990) 301–310.
- [39] UNE-EN 197-1, *Cement - Part 1: Composition, Specifications and Conformity Criteria for Common Cements*, Asociación Española de Normalización y Certificación (AENOR), 2000.
- [40] UNE-EN 197-4, *Cement - Part 4: Composition, Specifications and Conformity Criteria for Low Early Strength Blastfurnace Cements*, Asociación Española de Normalización y Certificación (AENOR), 2004.
- [41] UNE-103-500-94, *Ensayo Proctor de Compactación*, 1994.
- [42] UNE-EN-83313:1990, *Ensayos de hormigón. Medida de la consistencia del hormigón fresco. Método del cono de Abrams*, annulled by UNE-EN 12350-2: 2006.
- [43] UNE-EN-80310:96, *Cementos de aluminato de calcio*.
- [44] Y. Xu, D.D.L. Chung, Effect of sand addition on the specific heat and thermal conductivity of cement, *Cem. Concr. Res.* 30 (1) (2000) 59–61.

PAPER 7

Article

Efficiency Analysis of the Main Components of a Vertical Closed-Loop System in a Borehole Heat Exchanger

Cristina Sáez Blázquez *, Arturo Farfán Martín, Ignacio Martín Nieto, Pedro Carrasco García, Luis Santiago Sánchez Pérez and Diego González-Aguilera

Department of Cartographic and Land Engineering, University of Salamanca, Higher Polytechnic School of Avila, Hornos Caleros 50, 05003 Avila, Spain; afarfan@usal.es (A.F.M.); nachomartin@usal.es (I.M.N.); retep81@usal.es (P.C.G.); Issanchez@usal.es (L.S.S.P.); daguilera@usal.es (D.G.-A.)

* Correspondence: u107596@usal.es; Tel.: +34-67-553-6991

Academic Editor: Rajandrea Sethi

Received: 22 November 2016; Accepted: 3 February 2017; Published: 10 February 2017

Abstract: In vertical closed-loop systems, it is common to use single or double U-tube heat exchangers separated by longitudinal spacers. In addition, the helical-shaped pipe is another configuration that requires lower drilling lengths but it is less used. The aim of the present research is to study the influence of these components on the total efficiency of a borehole heat exchanger (BHE). Thus, the differences between using single/double U-tubes (with or without spacers) and helical pipes are analysed in terms of efficiency. Through different laboratory tests, a small vertical closed-loop system was simulated in order to analyse all these possible configurations. The grouting materials and the temperatures of the ground were modified at the same time in these tests. Regarding the heat exchange process between the ground and the heat carrier fluid, it must be highlighted that the best results were obtained for the helical-shaped pipe configuration. Some of the improvements offered by this heat exchanger typology with respect to the vertical configuration is that a lower drilling depth is required even it requires a larger diameter. This leads to significant economic savings in the performing drilling process. Finally, it is also worth noting the importance of using spacers in vertical U-tubes and that no improvements have been found regarding the use of single or double configuration of U-tubes. Thanks to the laboratory results derived from this study it is possible to establish the optimum behaviour pattern for the entire vertical closed-loop systems.

Keywords: vertical closed-loop systems; U-tube heat exchangers; helical-shape pipe; grouting materials; heat carrier fluid; borehole heat exchanger (BHE)

1. Introduction

Renewable energies are getting more and more important to address the increasing demand of energy. With respect to the geothermal energy, the number of installations has increased over the past decade and continues growing [1]. A conventional closed-loop system of very low temperature is commonly used to heat/cool a certain space or to produce Domestic Hot Water (DHW) [2]. Focusing on the geothermal systems that use closed-loop heat exchangers [3] and in particular on those vertical borehole heat exchangers; they are usually constituted by vertical pipes, generally made of polyethylene PE 100 PN16. A heat carrier fluid (usually a mixture of water and glycol) flows inside these pipes behaving as thermal transmitter between the ground and the rest of components of the installation [4–6]. The length of these drillings typically varies from 60 to 300 m (when using vertical pipes), according to the energetic needs to cover in each certain case. For these vertical installations, the most common configurations in relation to the drilling diameter and the design of heat exchangers are presented in Table 1 [7].

Table 1. Usual configurations used in vertical closed-loop systems, ✓ = Pipes with spacers, 7 = Pipes without spacers.

Borehole Diameter (mm)	Type of Tube	Tube Diameter (mm)	Spacers
127	Single U	32 or 40	✓ / 7
127	Double U	32	7
152	Double U	32	✓
200	Double U	40	✓

Another less known design is the helical heat exchanger. This type of pipe with diameters of around 400 mm requires much smaller drilling lengths and they are equally made of high quality polyethylene. These helical pipes can be installed in boreholes of only 3–5 m although drilling lengths can vary and be higher depending on the installation in question [8–10].

In both types of configurations (vertical or helical), the space between the hole wall and the heat exchangers is filled by a thermal conductive material to ensure the thermal exchange between ground and fluid inside the pipe. This material, known as geothermal grout, must have a series of mechanical and thermal characteristics [11,12].

Particular attention is needed for the following factors:

- Compactness, to guarantee the borehole stability and its easy injection to the hole.
- Sealing ability, providing a hydraulic barrier that avoids the pollution of aquifers.
- Low hydraulic conductivity.
- High thermal conductivity for an efficient heat transfer between the pipe and the ground. As a rule, it is recommended that the grouting material has a higher thermal conductivity value than the thermal conductivity of the ground to guarantee an efficient working of the borehole heat exchanger. In any cases, both thermal conductivities should be the highest possible. Some relations between the ground and the grout should be implemented. When the thermal conductivity of the ground is < 2 W/mK, the thermal conductivity of the grout should be \geq than the thermal conductivity of the ground and when the thermal conductivity of the ground is ≥ 2 W/mK, the thermal conductivity of the grout should be ≥ 2 W/mK [13].

The main objective of this research is to study the efficiency of different designs depending on the heat exchangers and the grouting material used. Through the representation in laboratory of a series of configurations commonly used and other more innovative systems, it was possible to select the design that provides the most favourable results in the thermal exchange with the ground constituting at the same time the best solution to achieve the greatest possible effectiveness for this kind of installations. A good decision in the design of the geothermal heat exchangers and the grouting material could mean important economic savings since the total drilling length could be reduced [14].

Several studies have been found about the comparison of the different heat exchangers considered in this manuscript and the main decisive parameters in a borehole heat exchanger. Zarrella et al. [15] concluded that the thermal performance of the helical-shaped pipe was better than the double U-tube heat exchanger. When the helical heat exchanger was 33% shorter than the double U-tube, each heat exchanger provided the same thermal performance; it denotes that this non-conventional type of heat exchanger could be used to reduce installation costs. Han and Yu [16] emphasized the importance of optimizing the thermal conductivity and specific heat capacity of backfill materials. Congedo et al. [17] resolved that the most important parameter for the heat transfer performance of the system is the thermal conductivity of the ground around the heat exchanger. They also established that the optimal ground type is that with the highest thermal conductivity.

However, most of these studies only offer a theoretical simulation not based on the practical experience as this study does [18–20]. On top of that, this study combines different heat exchangers with different grouting materials and different ground temperatures which allow making a complete comparison and description of a borehole heat exchanger.

2. Materials and Methods

The experimental methodology consisted of the representation in laboratory of a vertical borehole heat exchanger with a drilling length of only one meter. From this installation, a set of configurations were tested for selecting the one that, contributes to increase the total efficiency of the geothermal system. The comparison among the different cases of study has been made based on the difference of temperatures of the heat carrier fluid in the entry and exit of the borehole. When this difference is high, the efficiency of the thermal exchange between the ground and fluid is also considerably high. The heat extraction from the ground by the heat carrier fluid is determined by the grouting material (responsible for the heat transmission) and the heat exchanger. Thus, the higher the difference of temperature between the hot and the cold tube of the heat exchanger, the greater the amount of heat collected by the circulating fluid. This fact constitutes an indicator of the heat exchanger and grouting material quality [21,22].

Components used to create the borehole heat exchanger and the configurations tested in the laboratory are presented in Section 2.1.

2.1. Components Used in the Laboratory Tests

A vertical borehole heat exchanger was reproduced in the laboratory to use it as a basis for the analysis of the effectiveness of this kind of systems according to the heat exchangers, the grouting materials and the temperatures of the ground. The components of this prototype of installation were the following:

- Heat exchangers
Heat exchangers considered in the present research were the commonly used single or double U-tube heat exchangers and the helical-shaped pipe, both made of polyethylene and diameter of 32 mm.
- Spacers
In some tests, spacers were placed in single and double U-tube heat exchangers to avoid the contact between cold and hot pipes. These elements were of polyethylene.
- Boost pump
A boost pump, of 3 W of power, allowed the circulation of the heat carrier fluid through the heat exchangers. The constant volume of flow supplied by this pump was of 6.91 L/h.
- Bucket
The system includes a bucket containing water that simulates the ground at a certain temperature. This bucket has a diameter of 0.45 m and a length of 1 m and is made of polyethylene. The rest of components of the geothermal drilling: pipes, heat carrier fluid and grouting material are housed inside this bucket.
- Resistant heater
Water contained in the bucket simulating the surrounding ground (considering the ground temperature as constant during the heat extraction) was set at a temperature thanks to the use of a resistant heater that keeps the whole water at a constant temperature.
- Heat carrier fluid
The function of the heat carrier fluid is to absorb the heat from the ground by its circulation through the geothermal heat exchangers. The heat carrier fluid used in the present study was a mixture of water-propylene glycol to 30%. It was chosen for being one of the least toxic antifreeze. It does not present any risks for the environment and it can be handled without special security measures.

- Grouting material

Several materials are usually used as grout in borehole heat exchangers such as bentonite, sand, cement and detritus coming from the drilling. These materials allow the heat exchange between ground and pipes and must comply with a series of factors explained in Section 1 [23–27]. After testing a series of mixtures, the materials selected as grout were the sand in saturated conditions, in boreholes with presence of water and a mixture constituted by aluminium cement-sand, for the case of boreholes without water. Both mixtures have the suitable thermal and mechanical characteristics to be used as grouting material, with significant values of thermal conductivity, 2.83 W/mK in the case of saturated sand and 2.45 W/mK in the mixture of aluminium cement-sand. Table 2 shows the main characteristics of both materials selected as grouts in the present work.

- Water

Water contained in the bucket simulates the surrounding ground. The temperature of this fluid was controlled to study the heat exchange with the rest of components of the installation. Heating this water was possible thanks to a resistant heater which allows setting the temperature at a known value. Additionally, temperature of the water was controlled by an external thermometer to verify the correct working of the resistant heater.

- Thermocouples

Inlet and outlet temperatures of the heat carrier fluid were controlled at the end of the heat exchangers by thermocouples connected to a measuring device. These values were essential in the research to compare the different configurations.

Thermocouples (with an accuracy of ± 0.1 °C) were constituted by chrome and aluminium alloys and were connected to a digital thermometer to measure simultaneous temperature in different horizons or areas. Before its use, these sounding lines were duly calibrated according to the International Law ASTM E220 (Test Method for Calibration of Thermocouples by Comparison Techniques) [28].

- Heat carrier fluid cooling

Once the heat carrier fluid (mixture of water-propylene glycol) has absorbed the heat from the ground through the drilling, it gets in a cooling tank where its temperature gradually drops back to start a new cycle of heat exchange with the ground.

Table 2. Main characteristic of the materials chosen to be used as grout.

Parameter	Saturated Sand	Aluminium Cement-Sand
Composition	Silica fine-grain sand completely saturated by water	Sulpho-aluminate cements ALI CEM (25%), silica fine-grain sand (50%) and water (25%)
Thermal Conductivity (W/mK)	2.83	2.45
Density ($\text{Kg/m}^3 \cdot 10^{-3}$)	2.44	2.10
Hydraulic Conductivity	Very low (When sand is totally saturated, the hydraulic conductivity is very low making this material suitable for its use as grout)	Very low
Compression strength (MPa)	-	>15 MPa (minimum value recommended for cement mixtures)
Retractions	It does not experiment retractions of volume	It does not experiment retractions of volume

Figure 1 shows the schema of the borehole heat exchanger represented in laboratory with the single U-tube heat exchanger (Figure 1a) and the helical-shaped pipe (Figure 1b).

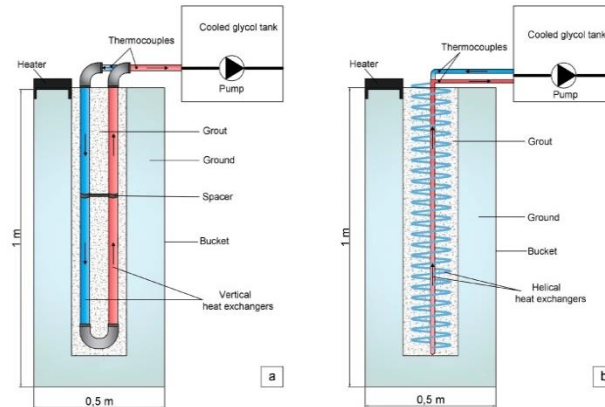


Figure 1. Schema of the vertical borehole heat exchanger reproduced in laboratory. (a) Vertical heat exchangers; (b) helical heat exchangers.

The bucket contains water that simulates the ground close to the geothermal drilling. This fluid is set at a specific temperature by a heater placed in the upper area of the bucket that recirculates the whole fluid facilitating a constant temperature at any part of it. A series of thermometers placed in different areas of this bucket allowed to verify that the temperature of the water was in effect constant.

Heat exchangers (vertical or helical) were also inside this bucket and the space between these pipes and the ground (water) was filled by the grouting material.

Finally, a pump placed in the cooled tank of propylene-glycol circulates the heat carrier fluid inside the pipes allowing the absorption of heat on its way through the ground. Thermocouples were placed in the upper part of the pipes to control inlet and outlet temperatures.

2.2. Tested Configurations

Based on the above installation, different configurations were tested modifying three fundamental parameters: heat exchangers, grouting material and ground temperature (water).

2.2.1. Heat Exchangers

Pipes used were the single or double U-tube heat exchangers and the helical-shaped pipe. Different configurations were used in the laboratory tests:

- Single U-tube with spacers: single vertical pipe with spacer placed in the middle of both tubes to avoid any contact between cold and hot pipes.
- Single U-tube without spacers: single vertical pipe without spacers and thus, both tubes (cold and hot) are in contact.
- Double U-tube with spacers: double vertical pipes with spacers to avoid any contact between the four pipes (two cold and two hot).
- Double U-tube without spacers: double vertical pipes without spacers, that is to say, cold and hot tubes are in contact.
- Helical-shaped pipe: helical pipe with a central tube where the heat carrier fluid rises up once has taken the heat from the ground.

Figure 2 shows the influence of the use of spacers relative to the position of the single and double U-tubes heat exchangers.

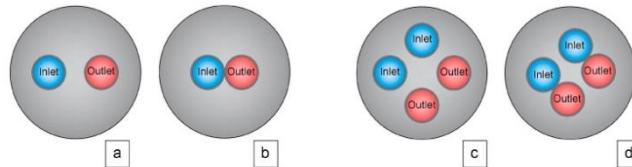


Figure 2. Position of single and double U-tube heat exchangers when using or not spacers. (a) Single U-tubes with spacers; (b) Single U-tubes without spacers; (c) Double U-tubes with spacers; (d) Double U-tubes without spacers.

2.2.2. Grouting Material

As previously cited in Section 2.1, two types of grouts were selected to carry out the present research. These grouts comply with a series of general characteristics making them suitable for this use. Additionally, they have a high thermal conductivity value, that is, they have an excellent capacity to conduce the heat. After preparing mixtures constituted by materials commonly used as grouts, some particular thermal and mechanical tests were carried out [29]. One of these tests, that stands out because of its importance is the measuring “in situ” of the thermal conductivity parameter [30,31]. This property was determined by the thermal properties analyser commercially known as KD2 Pro developed by Decagon Devices [32].

KD2 Pro equipment is constituted by a portable controller and a certain sensor (RK-1) that make possible the measuring of two thermal properties: the thermal resistivity and the thermal conductivity. Its operation is based on the infinite line heat source theory and calculates the thermal conductivity by monitoring the dissipation of heat from the needle probe. Heat is applied to the needle for a set heating time, t_h and temperature is measured in the monitoring needle during heating and for an additional time equal to t_h after heating. The temperature during heating is computed from Equation (1).

$$T = m_0 + m_2t + m_3 \ln t \quad (1)$$

where, m_0 is the ambient temperature during heating; m_2 is the rate of background temperature drift; m_3 is the slope of a line relating temperature rise to logarithm of temperature.

Equation (2) represents the model during cooling.

$$T = m_1 + m_2t + m_3 \ln \frac{t}{t - t_h} \quad (2)$$

The thermal conductivity is computed from Equation (3).

$$k = \frac{q}{4m_3} \quad (3)$$

The RK-1 probe (3.9 mm in diameter and 6 cm in length), used in the present work, is capable of measuring the thermal conductivity between the range of 0.1 and 6 W/mK and $\pm 10\%$ of accuracy.

The use of this equipment in samples previously prepared (cylinder blocks of 5 cm of diameter and length superior to the sensor RK-1 length) led to select for the present work the following grouts:

- Saturated sand: for those cases of boreholes where water is present, an appropriate solution is to use sand as geothermal grout. When this element is saturated of water (in this case from the borehole) has excellent thermal transmission capacities. It has a thermal conductivity value of 2.83 W/mK.

- Mixture of aluminium cement-sand: this mixture consisting of sand and aluminium cement in proportion 2:1 is suitable for both boreholes with water and without it. Aluminium cement comprised of calcium sulpho-aluminate provides the mixture with a higher thermal conductivity value in comparison with the conventional cement. In addition, the mechanical properties of the mixture make it appropriate to be used as geothermal grout. It has a thermal conductivity value of 2.45 W/mK.

2.2.3. Temperatures

Temperatures of the water that simulates the ground were set in several values to cover a range of possibilities. It allows analysing the behaviour of the installation with different values of this parameter. Thus, temperature values were set in 30, 40 and 50 °C. Temperature of the ground is often under these values (although it depends on the borehole depth), especially in these installations of very low enthalpy geothermal energy. However, and given that it is a small installation with a length of only one meter, temperature increases between hot and cold sources are required to appreciate significant differences among the different assumptions considered.

Cold source was kept constant to the temperature of 6 °C. Due to the presence of this source, the heat carrier fluid coming from the drilling, transfers the heat taken from the ground. Once this fluid has transferred the heat to the cold source, it cools down to start a new cycle.

Table 3 shows each of the configurations tested in laboratory according to the parameters previously described. It should be noted that in the case of helical-shaped pipe, the original design of this pipe was used. In this design there is not contact among the different sections of the pipes, therefore, spacers were not used.

Table 3. Different tests experimented in laboratory and temperature and time results.

Test	Heat Exchanger	Spacer	Grout	Ground T (°C)	Inlet T (°C)	Outlet T (°C)	Increment (°C)	Time for Stabilization (s)
T ₁	Single U-Tube	✓	Saturated Sand	30	18.0	18.9	0.9	1320
T ₂				40	19.7	20.7	1.2	1860
T ₃				50	19.9	21.5	1.6	1980
T ₄	Single U-Tube	-	Saturated Sand	30	18.0	18.6	0.6	1119
T ₅				40	19.8	20.7	0.9	1589
T ₆				50	20.0	21.2	1.2	1960
T ₇	Single U-Tube	✓	A. Cement Sand	30	18.8	19.5	0.7	2160
T ₈				40	19.1	20.0	0.9	2560
T ₉				50	20.3	21.7	1.4	2721
T ₁₀	Single U-Tube	-	A. Cement Sand	30	18.6	19.1	0.5	2058
T ₁₁				40	19.3	20.0	0.7	2422
T ₁₂				50	20.4	21.5	1.1	2712
T ₁₃	Double U-tube	✓	Saturated Sand	30	18.5	19.4	0.9	1436
T ₁₄				40	18.9	20.1	1.2	1887
T ₁₅				50	19.7	21.2	1.5	2025
T ₁₆	Double U-tube	-	Saturated Sand	30	18.2	18.8	0.6	1421
T ₁₇				40	19.1	20.1	1.0	1798
T ₁₈				50	20.1	21.3	1.2	1996
T ₁₉	Double U-tube	✓	A. Cement Sand	30	18.3	19.0	0.7	2153
T ₂₀				40	18.9	19.8	0.9	2421
T ₂₁				50	19.8	21.1	1.3	2816
T ₂₂	Double U-tube	-	A. Cement Sand	30	18.5	19.1	0.6	2120
T ₂₃				40	19.1	19.8	0.7	2315
T ₂₄				50	20.6	21.7	1.1	2798
T ₂₅	Helical-shaped pipe		Saturated Sand	30	25.2	27.0	1.8	2940
T ₂₆				40	26.0	27.9	1.9	3254
T ₂₇				50	26.2	28.4	2.2	3621
T ₂₈	Helical-shaped pipe		A. Cement Sand	30	25.4	26.9	1.5	3456
T ₂₉				40	26.2	27.9	1.7	3987
T ₃₀				50	26.6	28.7	2.1	4258

Figure 3 shows several images illustrating the testing process in laboratory. Figure 3a–c represent the three types of heat exchangers used in the present research and the rest of Figure 3d–f show different views of the installation reproduced in laboratory.

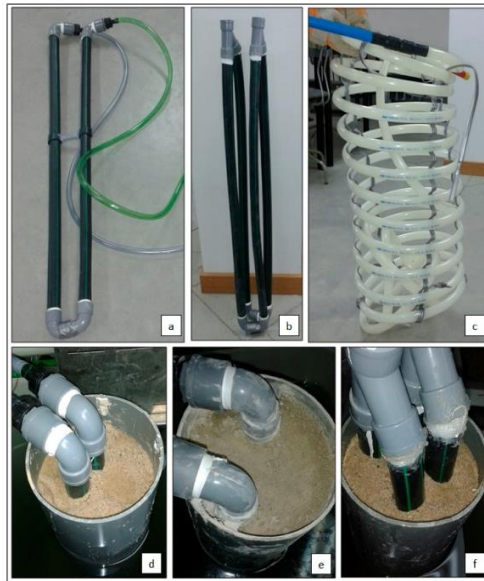


Figure 3. Images of the different configurations tested in laboratory. (a) Single U-tube heat exchanger with spacer; (b) Double U-tube heat exchanger without spacers; (c) Helical-shaped pipe; (d) Single U-tube heat exchanger without spacers and grout of saturated sand; (e) Single U-tube heat exchanger with spacers and grout of the mixture aluminium cement-sand; (f) Double U-tube heat exchanger with spacers and grout of saturated sand.

3. Results and Discussion

During the test of each of the configurations presented in Table 3, temperatures of the heat carrier fluid were continuously controlled by thermocouples placed at the top of the pipes (in both cold and hot tubes). Once these temperatures were stable (time for stabilization was also measured), they were registered. In this way, the increments of temperatures reached by this fluid (when temperatures were stable) constitute an indication of efficiency of the system tested in each particular case. This fact allows for establishing a comparison among the set of systems represented in laboratory.

Table 3 includes the tests carried out in laboratory and the results of the thermocouples measurements for each of the configurations analysed and the increment reached in each of them. Times for stabilization of inlet and outlet temperatures were also measured and are equally presented in Table 3. Thermocouples were previously calibrated before use and each of the tests were repeated three times to avoid any kind of measurement error. Temperature increments presented in Table 3 are the average of the three tests made for each assumption with identical conditions.

Data recorded by the thermocouples allows showing in Figure 4 a plot of temperatures before stabilization for test T_3 (see Table 3). The trend of temperatures for the rest of tests was very similar, so only this test will be shown as an example.

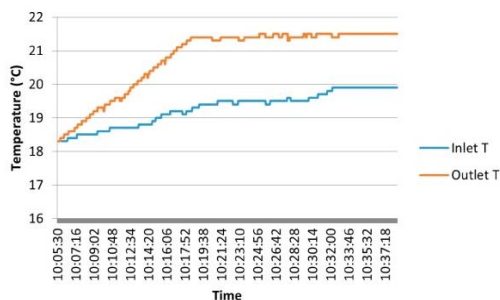


Figure 4. Plot of temperatures before stabilization for test T₃.

3.1. Comparison of Results

A series of considerations about the parameters studied can be derived from the analysis of Table 4.

Table 4. Comparison helical-shaped pipe and single U-tube heat exchanger.

Parameter	Helical-Shaped Pipe	Single U-Tube
Drilling length (m)	1.00	1.00
Total pipe length (m)	6.91	6.91
Flow rate (L/h)	1.92×10^{-6}	1.92×10^{-6}
Drilling diameter (m)	0.35	0.11
ΔT between cold and hot pipes (°C)	1.8 *	0.9 *
Time to stabilize (s)	1320	3456

* Values corresponding to the ground temperature of 30 °C and the grout of saturated sand.

3.1.1. Ground Temperatures

In all tests, when the temperature of the ground increases, the increment of temperature reached by the heat carrier fluid also grows, as expected given the higher difference between the cold and hot source (ground). As a result, the highest increments were obtained for the ground temperature of 50 °C.

3.1.2. Heat Exchangers

Three types of heat exchangers (single U-tube, double U-tube and helical-shaped pipe) were used. In the cases of vertical pipes, spacers were used in some of the tests.

U-Tube Heat Exchangers

Single and double U-tube heat exchangers (with and without spacers), were used in some of the laboratory tests.

In the first place, the influence of using spacers in U-tube heat exchangers is analysed. As shown in Table 4, the highest temperature increments (in the case of U-tube heat exchangers) correspond to those tests in which spacers were used. In either case, single or double U-tube heat exchangers, the use of spacers allows to increase the temperature increment by an average of 0.3 °C (a fairly high value considering the limited length of the installation). When both tubes (cold and hot) are in contact, the thermal exchange is affected, and hence, the efficiency of the geothermal installation is also affected.

Another important issue to tackle in this research is the difference between using single or double U-tube heat exchangers. Reanalysing Table 4, it is possible to observe that, for the same conditions

of grout and ground temperature, the increments of temperature (in the heat carrier fluid) obtained with the use of single U-tube heat exchangers were, in all instances, identical or very similar to the ones reached with double U-tube heat exchangers. This information allows concluding that the use of double U-tube heat exchangers does not produce any improvement in terms of efficiency compared to the use of single U-tube heat exchangers.

Helical-Shaped Pipes

The other type of heat exchanger analysed in the present research is the helical-shaped pipe. All tests made with this pipe showed that the heat exchange between the ground and the heat carrier fluid is more efficient regarding single and double U-tube heat exchangers and considering the same drilling length. Thus, the increments of temperature presented in Table 3, are in all cases higher (more than double in some cases) than the ones reached with vertical pipes (either single or double U-tubes).

3.1.3. Grouting Material

The last variable to analyse is the material used as grout filling the space between ground and heat exchangers. All configurations represented in laboratory were tested with two types of grouts. With the first of them, saturated sand, the increments of temperature registered were higher than the ones obtained with the mixture of aluminium cement-sand and keeping the same conditions. It was highly expected because, as mentioned above, the thermal conductivity of the saturated sand is higher than the cement-based grout thermal conductivity. In all cases, differences of around 0.2 °C were registered between both grouts. A significant value for the high similarity between thermal conductivities (2.83 W/mK saturated sand and 2.45 W/mK the mixture of aluminium cement-sand).

3.1.4. Time for Stabilization

Times for stabilization of inlet and outlet temperatures were measured to complete the comparison among the different systems.

In the first place, the highest times presented in Table 4 correspond in each system to the highest difference of temperature between hot and cold source (for the ground temperature of 50 °C).

With respect to the grouting material, saturated sand always involves lower times than the grout of aluminium cement-sand. This happens because heat is transmitted in an easier and faster way throughout saturated sand given its higher thermal conductivity.

Finally, the most important comparison of this parameter is related to the heat exchanger used. The lowest times for stabilization belong to single U-tube heat exchangers. The shorter length of this system facilitates the stabilization of temperatures between cold and hot sources. On the contrary, the helical-shape pipes present the highest times for stabilization given the total length of these pipes.

Although this parameter is not decisive when selecting the most suitable heat exchanger, it is convenient to consider the different behaviour of each system with respect to the stabilization time.

The most relevant results agree with the conclusions of other similar researches cited in Section 1. The efficiency of a vertical closed-loop system is highly conditioned by the thermal conductivity of ground and grouting material.

In addition, helical heat exchanger constitutes the best option to reach the highest thermal exchange in the installation. In these previous works, these systems are supposed to be the most economical solution. This aspect will be address in Section 3.3.

3.2. Proposed Systems

Following the above considerations, the most appropriate configurations to be used in vertical close-loop systems are listed below:

- Helical-shaped pipe using saturated sand or mixture of aluminium cement-sand as grout based on the conditions of the borehole. The presence of water in the borehole limits the use of saturated sand as geothermal grout; however, it will be selected wherever possible.
- Single U-tube heat exchanger with spacers to avoid the contact between inlet and outlet pipes. The suggested grouts are also the saturated sand (when conditions allow) and the mixture of aluminium cement-sand.

Although the drilling length tested for each of these configurations was identical, the design of these two heat exchangers is not the same. Therefore, it is appropriate to make a more detail comparison between both pipes regarding the system tested in the laboratory. Table 4 includes the comparison between both heat exchangers concerning a series of parameters.

The most remarkable parameters of Table 4 are the total length of pipes and the drilling diameter.

While the length of the drilling of the laboratory tests was the same for both heat exchangers, the total length of these pipes differs substantially between them. The helical-shaped pipe, given its helical design, requires a longer pipe (more than double) than the one used by the single U-tube heat exchanger. It causes an increase in the total cost of the borehole heat exchanger for the helical-shaped pipes. However, and as was verified before, the system efficiency (on equal terms) is higher for these helical heat exchangers. Thus, to achieve the same efficiency, single U-tube heat exchangers require a longer drilling length.

Single U-tube heat exchanger would need the total pipe length of the helical-shaped pipe (8.06 m) to reach the same increments of temperature obtained by this heat exchanger in the laboratory tests. Considering the design of the single U-tube heat exchanger constituted by an inlet and an outlet pipe, the drilling length required would be of at least 4.12 m.

The other parameter that differentiates these heat exchangers is the drilling diameter they require. To achieve the same efficiency, the diameter needed to install the helical-shaped pipe would be of at least 0.35 m in contrast to the diameter of 0.11 m that would be enough in the case of single U-tube heat exchanger.

Thus, under equal conditions in the borehole heat exchanger, single U-tube heat exchangers require more drilling length but fewer diameters than helical-shaped pipes need (double or even more than vertical heat exchangers).

3.3. Practical Example

As an example, the drilling length required to cover some specific energy needs was calculated by the software "Earth Energy Designer" (EED). This software, developed by "Blocon Software" [26], allows determining the most important parameters of a vertical closed-loop system: the number of holes and the drilling depth. Given that the software only refers to U-tube heat exchangers, simulation was carried out considering the use of a single U-tube heat exchanger with spacers. Based on this calculation, the drilling length that the use of a helical-shaped pipe would involve (for the same assumption) was estimated according to laboratory results. The economic difference between both configurations was also calculated.

The process of calculation of EED is based on a series of initial data (provided by the user) of the ground where the installation is going to be placed and the heat exchanger and heat carrier fluid selected.

Table 5 shows the input data of the supposed vertical geothermal system.

Using the parameters presented in Table 5, software EED calculated the drilling length required to cover the energy demand in question. Over the calculation, this software offers several options regarding the drilling length and number of holes. The first of them is always the most suitable option (with the lowest length and number of holes).

Additionally, Table 6 provides an estimation of the cost corresponding to the process of drilling by the rotary-percussive technique given that the system is considered to be placed in a granitic ground.

Based on the information supplied by a Spanish Company specialized in drillings “Sondeos Seymar”, the cost per meter of drilling for a borehole of 0.11 m of diameter placed in a granitic ground is about 50 €/m. Table 6 shows output data from the calculation of the borehole heat exchanger by EED.

Table 5. Input data used in the calculation with the software “Earth Energy Designer”.

Ground (Granitic Origin)	
Thermal conductivity W/(m·K)	2.5
Volumetric heat capacity MJ/(m ³ ·K)	2.16
Average annual temperature of the surface °C	8
Heat flow W/m ²	0.06
Heat Carrier Fluid	
Thermal conductivity W/(m·K)	0.47
Mass heat capacity J/(Kg·K)	3930
Density Kg/m ³	1033
Viscosity Kg/(m·s)	0.0079
Freezing point °C	−10
Flow rate per hole L/s	2
Grouting Material	
Thermal conductivity W/(m·K)	2.83
Heat Exchanger	
Configuration	Vertical Simple-U
Pipe diameter (m)	0.032
Basic Demand	
Annual demand of SHW MWh	5
Heat annual demand MWh	16.2
Cooling annual demand MWh	0
Seasonal operation coefficient (ACS)	3
Seasonal COP (heating)	3
Seasonal COP (cooling)	3

Table 6. Calculation of the geothermal drilling by the software “Earth Energy Designer” using single U-tube heat exchangers. Value provided by the Spanish company “Sondeos Seymar”.

Single U-Tube Heat Exchangers	
Number of holes	1
Drilling depth (m)	110
Total drilling length (m)	110
Cost per meter of drilling (€/m)	50
Total drilling cost (€)	5,500

From values presented in Table 6 (corresponding to a single U-tube heat exchanger), it was possible to estimate the parameters for a helical-shaped pipe considering the same thermal efficiency and identical input data. Using the relation deduced in this research (4.12 m of drilling with single U-tube heat exchanger per each meter of drilling with the helical-shaped pipe), output data were calculated for the helical heat exchanger. These output data are included in Table 7. In this case, the drilling unit cost for this pipe is considered as higher given the higher drilling diameter (0.35 m) these exchangers need. This cost, provided by “Sondeos Seymar” for a granitic ground is of around 90 €/m of drilling.

Table 7. Calculation of the geothermal drilling using helical-shaped pipes. Value provided by the Spanish company “Sondeos Seymar”.

Helical-Shaped Pipes	
Number of holes	1
Drilling depth (m)	27
Total drilling length (m)	27
Cost per meter of drilling (€/m)	90
Total drilling cost (€)	2.430

4. Conclusions

The present work analyses and tests the most common configurations used in vertical closed-loop systems of very low enthalpy. The behaviour of these installations is studied based on the heat exchangers, grouting material and temperatures of the ground.

It is important to mention that this work made some simplifications:

- The subsoil temperature was kept constant underground;
- The long-term depletion of underground was not considered.

As a result of the laboratory tests described throughout this work, some conclusions are deduced:

- Helical-shaped pipes are the best solution to provide the highest efficiency in the thermal exchange between ground and heat carrier fluid. For the same drilling length, these heat exchangers improve the performance of the borehole heat exchanger regarding single/double U-tube heat exchangers (with or without spacers).
- Helical-shaped pipes allow reducing the total drilling length required to cover some particular energy needs. Under the same thermal efficiency conditions, vertical heat exchangers require a drilling length four times greater than that required by the helical pipes. The use of these helical heat exchangers involves important economic savings in spite of the higher drilling diameter they need.
- Double U-tube heat exchangers do not provide significant improvements in the process of thermal exchange in relation to single U-tube heat exchangers. Laboratory tests results reveal that the use of single U-tube heat exchangers supply the same efficiency than the double ones. The use of these double vertical pipes would only be an interesting solution if one of the U-tubes failed or became blocked so the other U-tube could go on working.
- The use of spacers in vertical U-tube heat exchangers offer better results than in those cases where inlet and outlet pipes are in contact. Laboratory tests have shown improvements of around 30% when using tubes with these separating elements.
- As expected, the higher thermal conductivity of the grouting material, the greater efficiency of the process of heat gaining by the heat carrier fluid. This fact was verified by testing two grouts with different thermal conductivity values. Thus, the most thermally conductive grout (saturated sand) provided the best result of thermal exchange.

In future researches, a calibration of the results presented in this manuscript will be carried out through a thermal resistance capacity model “TRCM” with the aim of making a comparison with the theoretical value. Finally, studying the behaviour of the systems considered by modifying the flow inserted to the pipes would be interesting to enrich the present study.

Acknowledgments: Authors would like to thank the Department of Cartographic and Land Engineering of the Higher Polytechnic School of Avila, University of Salamanca, for allowing us to use their facilities and their collaboration during the experimental phase of this research. Authors also want to thank the Ministry of Education, Culture and Sport for providing a FPU Grant (Training of University Teachers Grant) to the corresponding author of this paper what has made possible the realization of the present work.

Author Contributions: All authors conceived, designed and performed the experimental campaign. Cristina Sáez Blázquez, Arturo Farfán Martín and Ignacio Martín Nieto implemented the methodology and analyzed the results. Pedro Carrasco García, Luis Santiago Sánchez Pérez and Diego González-Aguilera provided technical and theoretical support. Cristina Sáez Blázquez wrote the manuscript and all authors read and approved the final version.

Conflicts of Interest: The authors declare no conflicts of interest.

References

- Antics, M.; Bertani, R.; Sanner, B. Summary of EGC 2016 country update reports on geothermal energy in Europe. In Proceedings of the European Geothermal Congress, Strasbourg, France, 19–23 September 2016.
- Stober, I.; Bucher, K. *Geothermal Energy: From Theoretical Models to Exploration and Development*; Springer: Berlin/Heidelberg, Germany, 2013.
- Florides, G.; Kalogirou, S. Ground heat exchangers—A review of systems, models and applications. *Renew. Energy* **2007**, *32*, 2461–2478. [[CrossRef](#)]
- Florides, G.A.; Christodoulides, P.; Pouloupatis, P. Single and double U-tube ground heat exchangers in multiple-layer substrates. *Appl. Energy* **2013**, *102*, 364–373. [[CrossRef](#)]
- Jalaluddin, J.; Miyara, A. Thermal performance investigation of several types of vertical ground heat exchangers with different operation mode. *Appl. Therm. Eng.* **2012**, *33–34*, 167–174. [[CrossRef](#)]
- Yang, H.; Cui, P.; Fang, Z. Vertical-borehole ground coupled heat pumps: A review of models and systems. *Appl. Energy* **2010**, *87*, 16–27. [[CrossRef](#)]
- Focaccia, S.; Tinti, F. An innovative Borehole Heat Exchanger configuration with improved heat transfer. *Geothermics* **2013**, *48*, 93–100. [[CrossRef](#)]
- Zarrella, A.; Emmi, G.; De Carli, M. Analysis of operating modes of a ground source heat pump with short helical heat exchangers. *Energy Convers. Manag.* **2015**, *97*, 351–361. [[CrossRef](#)]
- Park, H.; Lee, S.-R.; Yoon, S.; Shin, H.; Lee, D.-S. Case study of heat transfer behavior of helical ground heat exchanger. *Energy Build.* **2012**, *53*, 137–144. [[CrossRef](#)]
- Yanga, W.; Lua, P.; Chena, Y. Laboratory investigations of the thermal performance of an energy pile with spiral coil ground heat exchanger. *Energy Build.* **2016**, *128*, 491–502. [[CrossRef](#)]
- Sáez Blázquez, C.; Farfán Martín, A.; Carrasco García, P.; Sánchez Pérez, L.S.; del Caso, S.J. Analysis of the process of design of a geothermal installation. *Renew. Energy* **2016**, *89*, 188–199. [[CrossRef](#)]
- Sáez Blázquez, C.; Farfán Martín, A.; Martín Nieto, I.; Carrasco García, P.; Sánchez Pérez, L.S.; González Aguilera, D. Thermal conductivity map of the Avila region (Spain) based on thermal conductivity measurements of different rock and soil samples. *Geothermics* **2017**, *65*, 60–71. [[CrossRef](#)]
- UNE-EN 100715-1. *Diseño, Jecución y Seguimiento de una Instalación Geotérmica Somera, Parte 1: Sistemas de Circuito Cerrado Vertical*; Asociación Española de Normalización y Certificación (AENOR): Madrid, Spain, 2014. (In Spanish)
- Park, S.; Sung, C.; Jung, K.; Sohn, B.; Chauchois, A.; Choi, H. Constructability and heat exchange efficiency of large diameter cast-in-place energy piles with various configurations of heat exchange pipe. *Appl. Therm. Eng.* **2015**, *90*, 1061–1071. [[CrossRef](#)]
- Zarrella, A.; Capozza, A.; De Carli, M. Analysis of short helical and double U-tube borehole heat exchangers: A simulation-based comparison. *Appl. Energy* **2013**, *112*, 358–370. [[CrossRef](#)]
- Han, C.; Yu, X. Sensitivity analysis of a vertical geothermal heat pump system. *Appl. Energy* **2016**, *170*, 148–160. [[CrossRef](#)]
- Congedo, P.M.; Colangelo, G.; Starace, G. CFD simulations of horizontal ground heat exchangers: A comparison among different configurations. *Appl. Therm. Eng.* **2012**, *33–34*, 24–32. [[CrossRef](#)]
- Soldoa, V.; Borović, S.; Lepoša, L.; Boban, L. Comparison of different methods for ground thermal properties determination in a clastic sedimentary environment. *Geothermics* **2016**, *61*, 1–11. [[CrossRef](#)]
- Lee, J.-U.; Kim, T.; Leigh, S.-B. Applications of building-integrated coil-type ground-coupled heat exchangers—Comparison of performances of vertical and horizontal installations. *Energy Build.* **2015**, *93*, 99–109. [[CrossRef](#)]
- Zarrella, A.; Capozza, A.; De Carli, M. Performance analysis of short helical borehole heat exchangers via integrated modelling of a borefield and a heat pump: A case study. *Appl. Therm. Eng.* **2013**, *61*, 36–47. [[CrossRef](#)]

21. Yoon, S.; Lee, S.-R.; Go, G.-H. Evaluation of thermal efficiency in different types of horizontal ground heat exchangers. *Energy Build.* **2015**, *105*, 100–105. [CrossRef]
22. Sledz, D.; Sakaki, T.; Nakagawa, M. Efficiency of vertical U-Tube under varied soil moisture content conditions: Laboratory experiments. In *GRC Transactions*; Geothermal Resources Council: Davis, CA, USA, 2010; Volume 34.
23. Lee, C.; Lee, K.; Choi, H.; Choi, H.P. Characteristics of thermally-enhanced bentonite grouts for geothermal heat exchanger in South Korea. *Sci. China Technol. Sci.* **2010**, *53*, 123–128. [CrossRef]
24. Wang, H.; Lu, J.; Qi, C. Thermal conductivity of sand-bentonite mixtures as a backfill material of geothermal boreholes. In *GRC Transactions*; Geothermal Resources Council: Davis, CA, USA, 2011; Volume 35.
25. Desmedt, J.; Van Bael, J.; Hoes, H.; Robeyn, N. Experimental performance of borehole heat exchangers and grouting materials for ground source heat pumps. *Int. J. Energy Res.* **2012**, *36*, 1238–1246. [CrossRef]
26. Borinaga-Treviño, R.; Pascual-Muñoz, P.; Castro-Fresno, D.; del Coz-Díaz, J.J. Study of different grouting materials used in vertical geothermal closed-loop heat exchangers. *Appl. Therm. Eng.* **2013**, *50*, 159–167. [CrossRef]
27. Xu, Y.; Chung, D.D.L. Effect of sand addition on the specific heat and thermal conductivity of cement. *Cem. Concr. Res.* **2000**, *30*, 59–61. [CrossRef]
28. ASTM E220, *Test Method for Calibration of Thermocouples by Comparison Techniques*; ASTM International: West Conshohocken, PA, USA, 2013.
29. Sáez Blázquez, C.; Farfán Martín, A.; Martín Nieto, I.; Carrasco García, P.; Sánchez Pérez, L.S.; González Aguilera, D. Analysis and study of different grouting materials in vertical geothermal closed-loop systems. *Renew. Energy* (under review).
30. Allan, M.L.; Philippacopoulos, A.J. Performance characteristics and modelling of cementitious grouts for geothermal heat pumps. In *Proceedings of the World Geothermal Congress, Beppu-Morioka, Japan, 28 May–10 June 2000*.
31. Allan, M.L. *Thermal Conductivity of Cementitious Grouts for Geothermal Heat Pumps*; Progress Report FY 1997; Department of Applied Science, Brookhaven National Laboratory: New York, NY, USA, 1997.
32. Decagon Devices. *KD2 Pro Thermal Properties Analyzer Operator's Manual*; Decagon Devices, Inc.: Pullman, WA, USA, 2016.

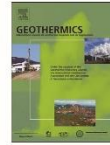


PAPER 8



Contents lists available at ScienceDirect

Geothermics

journal homepage: www.elsevier.com/locate/geothermics

Technical optimization of the energy supply in geothermal heat pumps

Cristina Sáez Blázquez^{a,*}, David Borge-Diez^b, Ignacio Martín Nieto^a, Arturo Farfán Martín^a, Diego González-Aguilera^a

^a Department of Cartographic and Land Engineering, University of Salamanca, Higher Polytechnic School of Avila, Hornos Caleros 50, 05003 Avila, Spain

^b Department of Electric, System and Automatic Engineering, Universidad de León, León, Spain



ARTICLE INFO

Keywords:

Very low enthalpy geothermal systems
Electric heat pumps
Gas engine heat pumps
Natural gas
Biogas

ABSTRACT

Very low enthalpy geothermal systems have been traditionally associated to the use of electricity as primary energy heat pumps supply. Gas engine heat pumps (GEHP) have been recently introduced in the current market. In this research, the electric heat pumps (EHP) as well as the GEHPs (considering natural gas and biogas as combustibles) have been analysed. The calculation of the ground source heat pump (GSHP) system has been made for a building placed in three different areas. Results reveal the influence of the heat pump configuration on the whole geothermal design. This research finally considers the European policies whose aim is a sustainable low-carbon economy by 2020. According to the existing Energy Efficiency Directive, energy requirements are defined for new and existing residential and non-residential buildings in the Member States. Based on these standards, the research compares the geothermal heat pump scenarios and a traditional one to determine if they would meet the regulation. Final results show that the Directive is a highly-demanding regulation that can only be respected by using EHP in one of the areas. The rest of geothermal heat pumps scenarios are much closer to meeting the energy standards than the traditional fossil heating sources.

1. Introduction and background

Ground source heat pump systems use the geothermal energy for heating and cooling purposes (including the production of domestic hot water). The utilization of these systems is increasing in the recent years, especially in China, Europe, USA and Canada (Zhou et al., 2015; Liang et al., 2011; Gao et al., 2012; Verda et al., 2012; Sommer et al., 2015; Sanner et al., 2003; Kranz and Frick, 2013; Freedman et al., 2012, 2013). Heat pumps constitute the key technology of the mentioned installations. In heating mode, heat is extracted from the ground by the set of boreholes. The energy taken from the ground is then lifted by a geothermal heat pump. For cooling applications, this device can be reversed, injecting the excess of heat into the ground. Heat pumps systems commonly use vapor-compression cycle which includes two low (evaporator) and high (condenser) temperature levels. Thus, the indoor heat exchanger is operated as evaporator in cooling mode and condenser in heating mode (Renedo et al., 2007).

One of the main issues concerning the use of heat pumps (HPs) is associated to their primary energy consumption. The performance of a HP is commonly quantified by the COP and SPF_{hp} coefficients, both define the ratio between the heat produced by the HP and the primary energy consumed by it. COP refers to instantaneous values whereas

SPF_{hp} considers annual values (Fraga et al., 2018; Hernández-Magallanes et al., 2018; Borge-Diez et al., 2015; Kontu et al., 2019).

The above mentioned primary energy that a heat pump uses depends on the way of powering the compressor shaft. In this regard, heat pumps are usually categorized as electric heat pumps (EHPs) or gas engine heat pumps (GEHPs) (Lian et al., 2005). Most of the current heat pumps models are driven by electric motors that use electricity as motive power. Regarding gas engine heat pumps, these equipment's are recently used as an alternative of the conventional electric heat pumps. They use clean energy such as natural gas, liquefied petrol gas (LPG) or biogas and are able to recover the waste heat released by the engine to enhance the total heating capacity.

Efficiency of electric engines is reasonably high (around 90%), while the energy efficiency of a gas engine is about 30–40%. However, these devices allow recovering the waste heat of the fuel combustion in a range of 60–80% thanks to the engine cylinder jacket. The efficiency difference between both models also affects the performance coefficient (COP) of each one. Thus, given that this coefficient plays a fundamental role in the design of the geothermal loop, the selection of one or the other model (EHP or GEHP) will determine the global drilling dimensioning. Table 1 presents the main characteristics of the mentioned geothermal heat pumps.

* Corresponding author.

E-mail address: u107596@usal.es (C. Sáez Blázquez).

<https://doi.org/10.1016/j.geothermics.2019.04.008>

Received 11 March 2019; Received in revised form 11 April 2019; Accepted 25 April 2019

0375-6505/ © 2019 Elsevier Ltd. All rights reserved.

Nomenclature			
Acronyms		<i>HP</i>	Heat pump
		<i>COP_{Co}</i>	efficient of performance
		<i>SPF_{hp}</i>	Heat pump seasonal performance factor
		<i>LPG</i>	Liquefied petrol gas
		<i>EPBD</i>	Energy Performance of Buildings Directive
		<i>EED</i>	Earth energy designer
		<i>IDEA</i>	Institute for the Diversification and Energy Saving
		<i>HCV</i>	Higher calorific value
<i>GSHP</i>	Ground source heat pump		
<i>GEHP</i>	Gas engine heat pump		
<i>EHP</i>	Electric heat pump		
<i>nZEB</i>	Nearly zero energy building		

This research focuses on presenting a technical analysis of the main differences in a very low geothermal system depending on the heat pump contemplated. This analysis is based on the calculation of a ground source heat pump system in three different areas. For each of these study areas, three heat pump alternatives will be considered: (i) electric heat pump, (ii) gas engine heat pump using natural gas and (iii) gas engine heat pump using biogas.

1.1. Nearly zero energy buildings

The European Union is committed to developing a sustainable, competitive, secure and decarbonised energy system. In this regard, the Energy Union and the Energy and Climate Policy Framework for 2030 pretend to reduce greenhouse gas emissions further by at least 40% by 2030 as compared with 1990, increasing the use of renewable energies. The building stock plays an important role in this field since it is responsible for approximately 36% of the total of CO₂ emissions in the Union. In order to achieve an increase of the energy efficiency in this sector, the transformation of existing buildings into nearly zero-energy buildings is of extreme importance. The principal instrument to achieve that aim is the Energy Efficiency Directive that is focused on increasing the energy efficiency at EU level (DIRECTIVE (EU), 2018).

A nearly zero-energy building (nZEB) is defined as a building having a very high energy performance, requiring nearly zero or low amount of energy for covering the energy demand associated with a certain use. That low amount of energy should be covered to a large extent by renewable sources (D'Agostino and Parker, 2018; Deng et al., 2014; Zhang et al., 2016). The ratio of renewable energy production depends on the country and widely varies from one to another Member State. The 2010 Energy Performance of Buildings Directive (EPBD), (DIRECTIVE, 2010) established for all new building in the European Union to accomplish the nearly zero-energy buildings norm from 1 January 2021.

Definitions of nZEB were set in 15 Member States with different terms of what they consider and the values they prescribe. Thus, some countries establish the maximum primary energy consumption, others the maximum carbon emissions and there are others that measure

Table 1
Principal characteristics of the heat pumps considered in this research, EHP and GEHP.

	EHP	GEHP
<i>Engine performance</i>	about 90%	about 30%
<i>COP</i>	4–4.5	1.5–1.6
<i>Fluid temperature</i>	High sensitivity of the evaporator inlet temperature	Low sensitivity of the evaporator inlet temperature
<i>Energy consumption</i>	Reduced electric consumption	High gas consumption
<i>Refrigeration</i>	–	Required
<i>Heat recovery</i>	–	Around 80%
<i>Equipment cost</i>	High	Very high
<i>Operation costs</i>	Dependent on the electric price of the area	Dependent on the gas price of the area
<i>CO₂ emissions</i>	Dependent on the electricity mix	Dependent on the gas fuel mix

primary energy use of a reference building or the minimum energy efficiency that the building should reach. Regarding the maximum primary energy of a new nZEB, the annual range for the Member States usually reaches values from 20 kW h/m² to 220 kW h/m² in the case of residential buildings, being the range of 45–50 kW h/m² the most common one for a large number of areas. These limits are mainly established for new buildings (residential and non-residential) and are rarely introduced for the existing ones.

From the technical calculations of all the assumptions considered in this research (electric heat pumps and gas engine heat pumps in three different areas), these scenarios will be evaluated in relation to the Energy Efficiency Directive previously described. In this way, it will be possible to determine which options respect the energy requirements defined for a nZEB or how close they are of them.

2. Workflow description

As already mentioned in Section 1, the aim of the present research is to compare the conventional electric heat pumps and those pumps which use a gas engine, contemplating natural gas and biogas as fuel compounds. Hence, the dimensioning of a low enthalpy geothermal system has been made in three study areas for each of the heat pumps models considered. For an easier reader comprehension, the following Fig. 1 shows the general workflow followed in this study.

2.1. Selection and characterization of the study areas

As shown in Fig. 2, the European Directive 2009/28/CE (Directiva, 2009) differentiates the areas representatives of the typical European climates (warm, medium and cold climates).

According to the above classification, three study areas belonging to each of the mentioned climates were selected as part of the present research. These areas, graphically situated in the European map of Fig. 3, are described in Table 2.

In the consecutive thermal and geothermal calculations of each scenario, it is indispensable to know a series of characteristics of the areas previously expounded. Such characterization involves the description of the main geology formations that constitute the study areas

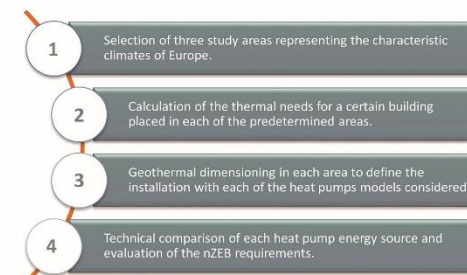


Fig. 1. Description of the workflow followed in the present research.



Fig. 2. Representative climates in Europe according to the European Directive 2009/28/CE (Directiva, 2009).

and their meteorological conditions. This information can be found in Appendix A.

2.2. Definition of the building basis of the study

With the aim of achieving the purpose of the study, a specific building was defined as the basis of the subsequent calculations in each of the set areas. This building, identical for all the study areas, is a two-storey building whose main dimensions are presented in Table 3.

3. Principal calculations

Although the procedure followed for the calculations in each study area is identical, results widely differ. Thus, the following subsections contemplate the three scenarios in a separated way.

Table 2
Description of the areas selected to address the present research.

Area	Locality	Country	Climate
1	Ancona	Italy	Warm
2	Edimburgh	Scotland	Medium
3	Karlstad	Sweden	Cold

Table 3
Description of the building selected to carry out the present study.

Building main dimensions	
Total Surface (m ²)	173.38
Height (m)	6.25
Windows Surface (m ²)	31.00
Roof Surface (m ²)	86.69
Floor Surface (m ²)	86.69

3.1. Determination of the energy demand

Once known the geological and climatological conditions of the study areas, the next step is the estimation of the energy demand for the building previously defined in each area. With that aim, a tool based on the Standard Law UNE-EN ISO 13790:2011 was implemented (AENOR, 2011). This tool calculates the annual energy demand of a building in a certain area by the previous introduction of the building dimensions and the monthly mean temperatures of the place. The following Table 4 presents the results obtained for each study area. It must be mentioned that for the places considered in this research, only heating demand was required. It is also believed that calculations would be identical in cooling mode and they would lead to draw the same final conclusions.

Additionally, the tool monthly itemises the thermal gains and losses corresponding to the thermal transfer, ventilation and solar and internal gains. As an example, Fig. 4 shows the simulation for area 1.

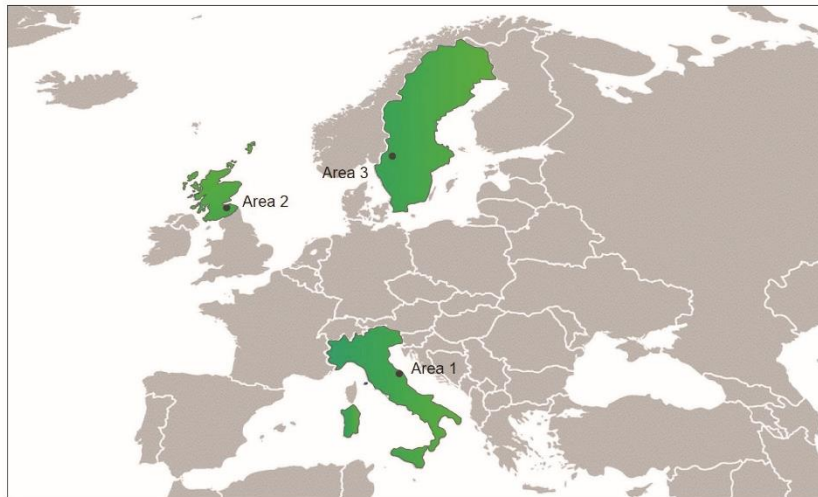


Fig. 3. Location of the study areas considered in this research.

Table 4
Annual energy demand of the building placed in each of the study areas.

	Heating Demand (kWh/year)
Area 1	39,088
Area 2	71,742
Area 3	88,882

3.2. Geothermal evaluation

The final purpose of this section is determining the geothermal schema (number of borehole and total drilling length) required in each of the assumptions previously described (electric and gas engine heat pumps in each study area). The specific geothermal software “Earth Energy Designer” (EED), developed by Blocon Software, was implemented for the geothermal dimensioning of each solution. Since the geothermal heat pump design determines the remaining parameters, an individual geothermal calculation was required for each heat pump in each study area.

3.2.1. Electric heat pump

In the first place, EED software requires the introduction of a series of parameters concerning each area (thermal demand and climate and geological conditions) and the main installation characteristics (heat exchanger design, working fluid...). One of the requested data is the “Seasonal performance factor” (SPF) which makes reference to the heat pump used in the installation. In the present case, using an electric heat pump, this factor usually takes a value of around 4–4.5. Thus, in this first scenario, a SPF of 4.5 was introduced in EED software for the three areas contemplated in this research. Fig. 5 presents the stage of EED calculation process where the annual demand and SPF are required. Information presented in the mentioned Fig. 5 belongs to area 1.

Applying this software in each area by the introduction of the specific parameters of each case (keeping the SPF of 4.5), the geothermal characterization of each area with the use of electric heat pump is presented in Table 5.

Once known the drilling schema required in each of the study areas, the electric heat pump of each case was defined. First of all, peak power was obtained from the initial demand and the operating hours of each assumption. This power is then oversized since the ground contribution

is not exactly known and it could be possible to find additional thermal losses in the building or unexpected energy demands. A habitual practice is to increase the heat pump power on the basis of 35–50 W per m² of building area for new constructions (as the building considered in this research). Given that the building is identical for all the cases, a value belonging to the range 35–50 W/m² was taken in function of the climatic conditions of each area. In this way, the characteristics of the electric heat pump system related to each area can be found in the following Table 6.

After obtaining the nominal power of each system, a commercial heat pump model was chosen for each area from one of the main producers of electric geothermal heat pumps (Integral systems of heating/cooling with renewable energies, 2018). The electric heat pumps selected in each case are defined by a certain COP for some specific conditions (inlet temperature of 0 °C and outlet temperature of 35 °C). With the aim of estimating the real COP for the conditions given in each area, the temperatures of the working fluid during the installation service life must be known. This information is obtained from the simulations provided by EED software. From these simulations, a medium temperature value (for service life of 30 years) was calculated for each study area. Fig. 6 shows the fluid temperature simulation for area 1. For the rest of areas the simulation methodology was identical.

UE 813/2013 regulation (REGLAMENTO (UE), 2013) establishes a certain relation between the COP and the heat pump fluid inlet temperature. According to this law and the fluid temperatures of each location (deduced from EED simulations), real COPs for each heat pump selected were estimated. Finally, the electricity consumption required to cover the annual thermal needs of each assumption was calculated. All this information is shown in Table 7.

3.2.2. Gas engine heat pump: natural gas

The dimensioning process followed in this second assumption is also based on the use of EED software. Operational conditions are the same than in the last case (electric heat pump) and only the SPF must be modified. For gas engine heat pumps, this factor is significantly reduced to values around 1.5 since the amount of fuel consumed relative to the supplied power is higher than in the electric heat pumps. A SPF of 1.5 means a lower ground contribution and a higher heat pump supplying. In the case of electric heat pumps the relation between the ground and the heat pump contribution is 3.5/1. On the contrary, in a gas engine heat pump, the previous ratio is reduced to 1/0.5, meaning that the

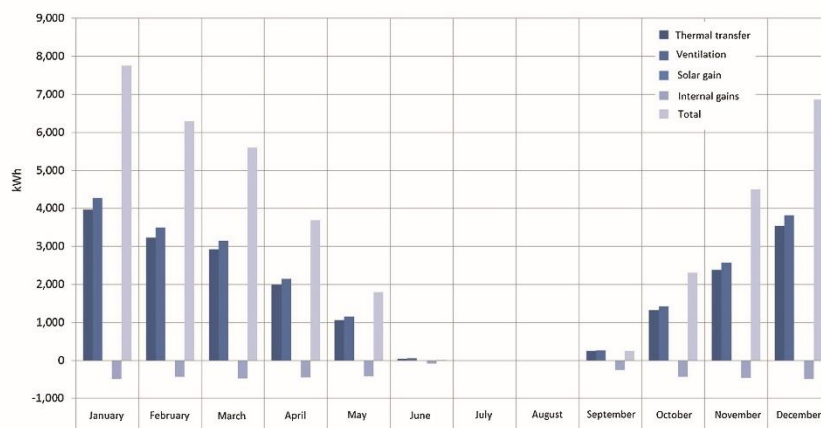


Fig. 4. Thermal balance simulated for the building placed in area 1.

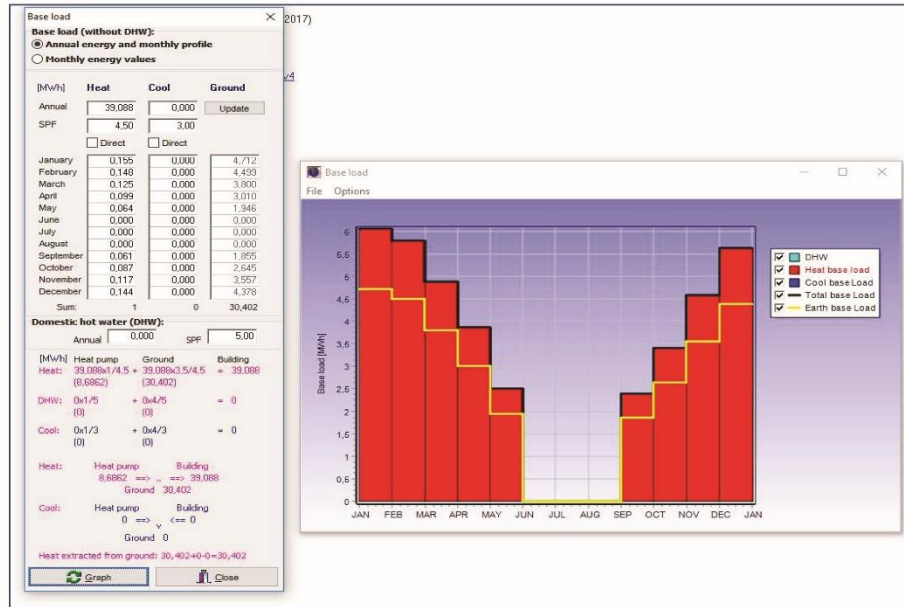


Fig. 5. EED calculation process requiring the thermal demand and SPF of area 1.

Table 5
Design of the geothermal system using electric heat pump in each location.

	Area 1	Area 2	Area 3
Number of boreholes	2	3	2
Borehole spacing (m)	30	20	30
Total drilling length (m)	227	446	376

Table 6
Characteristics of the electric heat pump system in each location.

	Area 1	Area 2	Area 3
Base load (kWh)	39,088	71,742	88,882
Annual operational period (h)	2,040	2,310	2,700
Power (kW)	19.16	31.06	32.92
Oversizing (kW)	6.07	7.28	8.67
System nominal power (kW)	25.23	38.34	41.59

ground must contribute with 1 part and the heat pump must provide 0.5 parts. Table 8 presents the results derived from the EED calculation using natural gas heat pumps.

The next step is, as in the previous alternative, the dimensioning of the natural gas heat pump from the initial energy needs and the expected operational hours. Since the ground contribution is lower in these systems (33% compared to 77% of contribution in electric heat pumps), the oversizing range of 35–50 W/m² previously applied is now reduced to 15–22 W/m² given that such additional power is not required in this case. Thus, depending on the climatic conditions of each area, a different value from the range 15–22 W/m² was applied. The description of the natural gas heat pump system of each area is presented in the following Table 9.

Once known the nominal power of the system, a gas engine heat pump was selected for each study area. Producers of these devices do not provide the fluid temperature for which the characteristic COP of them is achieved. The residual heat generated in a gas engine could be used to increase the inlet temperature of the working fluid. Additionally, the fluid temperature does not decrease as much as in the electric heat pumps since the ground contribution is not the same, so fluid temperature is commonly higher. For these reasons, the COP of these heat pumps is not so affected by the working fluid temperature. In this way, the COP provided for each heat pump model was directly taken for the corresponding calculations of the natural gas consumption according to the energy needs of each scenario. It is important to highlight that this consumption was increased by 10% with the aim of compensating the additional energy these devices require during the starting mechanism. Table 10 presents the mentioned information for this second assumption.

3.2.3. Gas engine heat pump: biogas

The last assumption is based on the use of gas engine heat pumps aided by biogas. The principal difference regarding the above equipment's is that the internal combustion engine is not supplied by natural gas but biogas. As of today, it is not possible to find commercial gas engine heat pumps specifically designed to work with biogas. Therefore, the dimensioning process expected in this section must be addressed from the natural gas heat pumps previously described, considering that the natural gas and biogas consumptions will not be the same. In a natural gas heat pump, the natural gas consumption is lower than the one needed of biogas to achieve the same amount of energy. Since the biogas higher calorific value (HCV) is lower than the natural gas HCV, the volumetric consumption of biogas will be higher than the natural gas use to reach the same effective power.

According to the Institute for the Diversification and Energy Saving

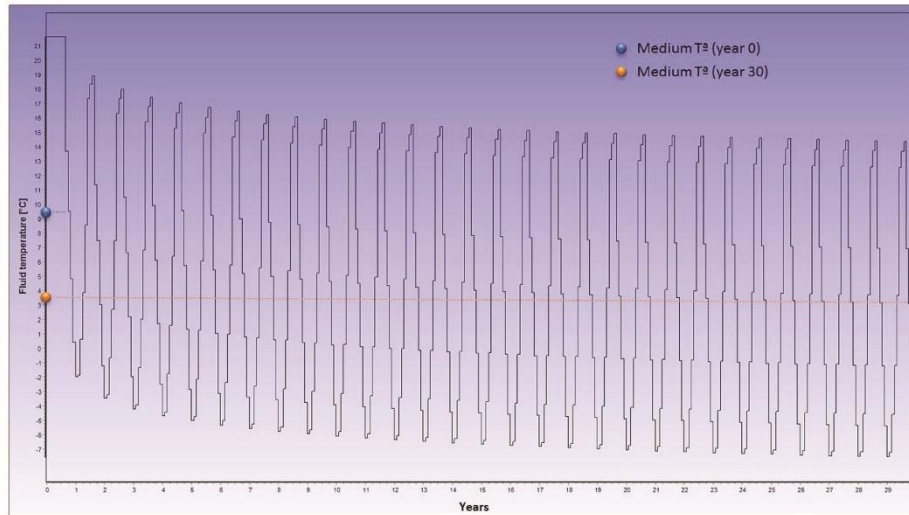


Fig. 6. EED fluid temperature simulations for area 1 using electric heat pump.

Table 7

Working fluid temperature, heat pump COP and annual electricity consumption in each study area.

	Area 1	Area 2	Area 3
Medium fluid temperature (°C)	6.62	6.00	4.25
Heat pump real COP	5.17	5.05	4.98
Annual electricity consumption (kWh)	7,560.54	14,206.34	17,847.79

Table 8

Design of the geothermal system using natural gas heat pump in each location.

	Area 1	Area 2	Area 3
Number of boreholes	1	1	1
Total drilling length (m)	114	199	173

Table 9

Characteristics of the natural gas heat pump system in each location.

	Area 1	Area 2	Area 3
Base load (kWh)	39,088	71,742	88,882
Annual operational period (h)	2,040	2,310	2,700
Power (kW)	19.16	31.06	32.92
Oversizing (kW)	2.60	3.12	3.81
System nominal power (kW)	21.76	34.18	36.73

Table 10

Gas engine heat pump COP and annual natural gas consumption in each study area.

	Area 1	Area 2	Area 3
Heat pump real COP	1.57	1.48	1.48
Annual natural gas consumption (kWh)	27,386.50	53,321.75	66,060.95

Table 11

Characteristics of the biogas heat pump system in each location.

	Area 1	Area 2	Area 3
Number of boreholes	1	1	1
Total drilling length (m)	114	199	164
Base load (kWh)	39,088	71,742	88,882
Annual operational period (h)	2,040	2,310	2,700
Power (kW)	19.16	31.06	32.92
System nominal power (kW)	21.76	34.18	36.73
Annual biogas consumption (kWh)	27,386.50	53,321.75	66,060.95

"IDAE" (Instituto para la Diversificación y Ahorro de la Energía, 2014), the biogas HCV is of around 46.21% lower than the natural gas HCV. In this way, the volumetric biogas consumption will be 46.21% higher than the natural gas one. In spite of this fact, the heat pump COP will stay constant given that it just depends on the thermodynamic aspect of the cycle. It means that the energy consumption to produce a heat unity is the same, although the volumetric gas consumption is higher. Thus, the dimensioning of these devices and the whole geothermal system will be identical to the process described in the previous section for the natural gas. The design of the geothermal installation for each area is then summarized in Table 11.

4. Discussion

This paper presents an evaluation of several energy sources to supply a geothermal heat pump in a series of places. In the first place, a global discussion of the technical parameters obtained from the set of calculations (Section 3) is required. Regardless of the study area, the technical differences between the electric heat pumps and the gas engine heat pumps are significant.

The use of an electric heat pump in the geothermal system results in a series of important facts:

- The characteristic high COPs of these devices mean a high ground contribution. Therefore, the temperature of the working fluid must

be thoroughly controlled during the whole operational period to avoid too low temperatures that could affect the right heat pump operation. Additionally, the notable ground contribution produces high drilling lengths.

- As a result of the mentioned above (high COPs and ground contribution) the electricity contribution is significantly reduced.
- The economy of the process will depend on the electricity price of the area where the system is planned to be placed. In the same way, the environmental field will be also determined by the origin of the electricity used to supply the heat pump and this fact equally depends on the specific area. Both aspects, the economic and the environmental dimensions, will be evaluated in a future research considering the particular characteristics of the three study areas considered here.

Regarding the gas engine heat pumps implemented in a geothermal system, some remarks can be extracted from this work:

- COPs of these heat pumps are lower and thus, the ground contribution is also lower. In this way, the temperature of the working fluid does not require such a comprehensive control because too low temperature levels are not expected in these systems. As a consequence of the above, the drilling lengths are generally lower than the ones required in the traditional electric heat pump systems.
- Since the ground contribution is not high, the gas engine heat pump must cover a large proportion of the total energy demand. Therefore, the gas consumption is considerably high.
- As in the case of the electric heat pumps commented before, the economy of the system will be conditioned by the prices of the gas used as heat pump fuel (natural gas and biogas in this research) that will be specific to each area. In relation to the environmental dimension, it will also depend on the gas selected. Since the natural gas composition is similar in most places, its environmental impact will be equally the same (independent of the place). With respect to

the biogas, the emissions associated to this gas are usually considered as zero because of the neutral cycle contemplated during its production.

Focusing on this specific work, Fig. 7 shows the differences among the three heat pumps (electric heat pump, gas engine heat pumps aided by natural and biogas) in each study area from the points of view of the number of boreholes, drilling length, annual energy consumption and real COP.

Analyzing the above Fig. 7 that represents the main results obtained from this work, it is possible to deduce the following statements:

- Gas engine heat pumps present the same technical results for both assumptions, using natural gas or biogas. This is because the devices are the identical, and the only difference makes reference to the fuel used in each case. Thus, as explained in section 3, the energy use will be the same but the volumetric consumption will be much higher for the biogas since it has a lower higher calorific value. The rest of differences between both scenarios will depend on the economic and environmental characteristics of the area where these systems were planned to be installed.
- In regards to the first parameter represented in Fig. 7, the number of boreholes required the geothermal scenario that uses EHP is 50% higher in areas 1 and 3 and 66.7% in area 2 compared to the GEHPs.
- From the drilling length point of view, EHP also requires a higher total drilling length in comparison to the GEHPs. For area 1, this length is 49.78% higher using EHP, 55.38% for area 2 and 53.99% for area 3.
- Comparing now the annual energy consumption, as seen in Fig. 7, this factor is considerably higher when using GEHPs. In area 1, the consumption of gas is 72.40% higher than the electricity use, 73.36% in the case of area 2 and 72.98% in area 3.
- Finally, the real COPs of each system are evaluated. For each scenario (EHP and GEHPs), COPs are quite similar in the three study

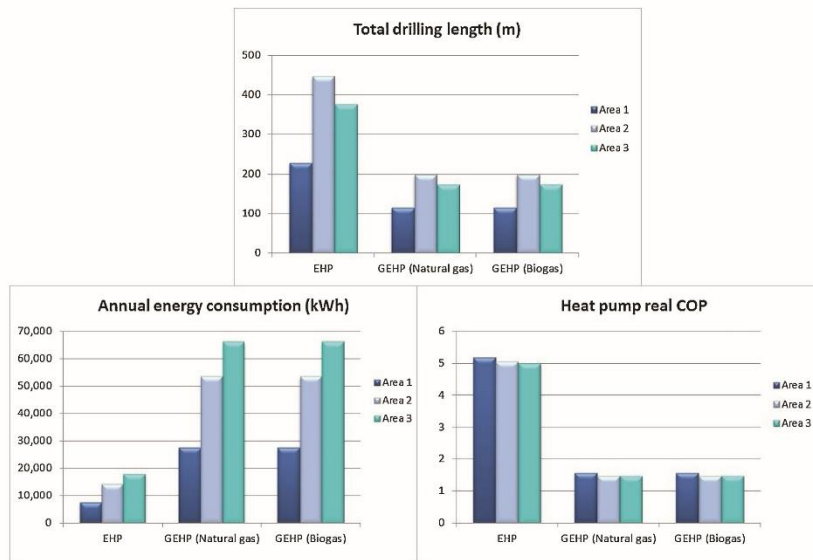


Fig. 7. Comparison of the heat pumps models considered in this research based on the main results obtained before.

Table 12
Maximum primary energy ranges according to the national nZEB definitions.
*Still to be approved, **National nZEB Plan (DIRECTIVE, 2010).

	Area 1	Area 2	Area 3
Maximum primary energy [kWh/m ² y] recommended range	45–50*	44**	30–75**
Oversized maximum primary energy value [kWh/m ² y] considered for the study	65	57.2	97.5

Table 13
Maximum annual primary energy for the building of the present research in each area.

	Area 1	Area 2	Area 3
Maximum annual primary energy [kWh/y]	11,269.70	9,917.34	16,904.55

Table 14
Annual primary energy consumption of the geothermal heat pump for each energy source in each study area.

	Area 1	Area 2	Area 3
Annual electricity consumption (kWh)	7,560.54	14,206.34	17,847.79
Annual natural gas consumption (kWh)	27,386.50	53,321.75	66,060.95
Annual biogas consumption (kWh)	27,386.50	53,321.75	66,060.95

Table 15
Differences between the maximum primary energy according to nZEB regulation and the consumption of each energy source in each study area.

	Area 1	Area 2	Area 3
Geothermal electric heat pump	✓ -3,709.16	✗ +4,289.00	✗ +943.24
Geothermal gas engine heat pump	✗ +16,116.80	✗ +43,404.41	✗ +49,156.40
Natural gas boiler	✗ +31,727.10	✗ +68,998.86	✗ +80,865.65

areas. However, differences between the heat pumps models are considerable. COP of the system using EHP in area 1 is 69.63% higher than using GEHPs, 70.69% in area 2 and 70.28% in area 3.

For all the parameters evaluated before, differences between heat pumps are almost stable regardless of which study area is taken into account.

4.1. NZEB regulation

As mentioned in the introductory section, some energy requirements are defined for new and existing residential and non-residential nZEB. Since the basis of the present research is a single family house, the energy indicators that must be taken into account are those referring to new residential nZEB. This numeral indicator is expressed in terms of maximum primary energy in kWh/m²y and as already said, usually reaches a value included in the range of 45–50 kWh/m²y. However, each Member State has own energy requirements. Focusing on the countries selected for the present research, the maximum primary energy for a new residential building in each of the study areas is contemplated in Table 12.

It is convenient to mention that the indicators presented in the above Table 12 make reference to general residential buildings. The building considered in this study is a single family house without surrounding buildings. This fact means a high initial energy demand as presented in Section 3 since the thermal losses are higher in this kind of buildings that have not external protections (surrounding structures). For this reason, the numerical indicators of Table 12 have been oversized to consider the negative aspect of a single house. Thus, numerical

indicators (maximum value of the range) of Table 12 were increased in a 30%.

Additionally, in the case of Italy (study area 1), the numerical indicator regarding the maximum annual primary energy is still to be approved. For this reason, the most common indicator (45–50 kWh/m²y) was implanted in this area.

The aim of this section is to compare the maximum primary energy annually required in each of the assumptions contemplated in this study (energy source and area). Based on the calculations of Section 3, the consumption of the primary energy (electricity, natural gas or biogas) for each study area is known. Thus, these data will be compared with the ones defined by the National nZEB Plan (Table 12). According to the oversized parameters of Table 12, for the building included in this study (with an area of 173.38 m²), the maximum annual primary energy for each area would be limited to the values presented in the following Table 13.

These values would be the limit of primary energy consumption for the building placed in each of the study areas. Remembering the previous section 3.2. *Geothermal evaluation*, the consumptions of primary energy in function of the energy source used in the geothermal heat pump were for each area (Table 14):

Observing both Tables 13 and 14, it is easily observable that only using the electric heat pump in area 1, the maximum annual primary energy indicator could be respected.

However, if instead of considering one of the geothermal solutions contemplated before, a traditional energy source was used, the annual consumption would be completely different. If the building of the study was supplied by a common gas natural boiler, the annual energy consumption would correspond with the energy demand already calculated incremented in a 10% because of the efficiency these equipment's have (around 0.9). In this way, the natural gas consumption for a common boiler would be; 42,996.80 kWh for area 1; 78,916.20 kWh for area 2 and 97,770.20 kWh for area 3. Considering the assumption of this research and a traditional natural gas boiler, the following Table 15 shows the differences of consumptions of each scenario in each area regarding the limits of maximum primary energy consumption of Table 13.

In the previous Table 15, there is a unique negative difference meaning that only in the area 1 using a geothermal heat pump system, requirements of a nZEB would be respected. For the rest of scenarios (presenting positive differences) the limits of the mentioned regulation are far from being achieved, especially using a common natural gas boiler.

5. Final conclusions

The present research is mainly constituted by a technical comparison of three different geothermal heat pumps. From a set of calculations in three study areas, some general and more specific differences between the mentioned systems could be deduced. In general terms, the EHP system allows for all the study areas the reduction of the annual heat pump energy consumption thanks to the high COPs these devices have. However, since the ground contribution is higher, using an EHP the temperature of the working fluid must be exhaustively controlled. On the contrary, the use of GEHPs reduce (in all the scenarios) the number of boreholes and hence the global drilling length of the geothermal system. COPs of these last equipment's are considerably lower as well as the ground contribution so that a thorough control of the working fluid temperature is not required. Regarding the fuel considered to supply the GEHPs, the only difference between them makes reference to the gas volumetric consumption which is much higher in the case of the biogas.

Besides the technical evaluation of the three heat pump models, the Energy Efficiency Directive about nZEB is discussed in this research. On this matter, the scenarios considered here (EHP and GEHP systems) and an additional one (traditional natural gas boiler) are analysed to determine if they respect the requirements of the nZEB regulation in each of the study area. Results show that only the electric heat pump system

implemented in area 1 would meet the primary energy limits of the mentioned regulation. For the rest areas with EHP (area 2 and 3), the electricity consumption is close to the established limitations. In the case of GEHPs, the differences regarding the energy requirements of the law are notable (specifically for area 2 and 3) but these differences are especially high when the traditional natural gas is implemented.

It follows from all of the preceding that the compliance with the nZEB requirements that the Energy Efficiency Directive establishes could be feasible for some specific renewable systems (as the geothermal EHP). However, as this research proves, the regulatory compliance would be difficult for other systems of the same nature like the geothermal GEHPs, but it would be especially difficult using a non-re-

newable energy source, as the natural gas boiler.

Finally, it is also worth mentioning that, for the geothermal systems considered here, the energy requirements of a nZEB would be easily achieved by the implementation of different solutions; improved building isolations, heat recovery systems, active construction procedures such as the Trombe mur (BenYedder and Bilgen, 1991) or the increase of the heat pumps COPs, especially for the GEHPs.

It is also necessary to mention that the environmental and economic dimensions considered as fundamental for a complete comparison of the heat pump models will be included in a second part as a new scientific research.

Appendix A

See Tables A1 and A2.

Table A1

Characterization of the main geological formations that constitute the study areas.

Area	Geological Age	Geological formation	Thermal Conductivity (W/mK)
1	Tertiary	Non-consolidated rocks (gravel, mud and sand)	1.0
2	Cambrian Carboniferous	Basalts	1.7
3	Pre-cambrian and Paleozoic	Granites and gneisses	3.1

Table A2

Mean monthly temperatures in each of the study areas.

Month	Temperatures (°C)		
	Area 1	Area 2	Area 3
January	5.4	2.9	-3.8
February	6.9	3.0	-4.1
March	9.5	5.0	-0.4
April	12.9	7.5	4.2
May	16.8	10.2	10.2
June	20.8	13.1	14.7
July	23.3	14.8	16.2
August	23.1	14.4	15.3
September	20.0	12.3	11
October	15.8	9.5	6.7
November	11.3	5.7	1.5
December	7.1	4.0	-2.5

References

- AENOR, 2011. UNE-EN ISO 13790:2011. Eficiencia energética de los edificios. Cálculo del consumo de energía para calefacción y refrigeración de espacios. (ISO 13790:2008).
- BenYedder, R., Bilgen, E., 1991. Natural convection and conduction in Trombe wall systems. *Convection naturelle et conduction dans les systemes a mur Trombe*. Int. J. Heat Mass Transf. 34 (4-5), 1237–1248.
- Borge-Diez, David, Colmenar-Santos, Antonio, Pérez-Molina, Clara, López-Rey, África, 2015. Geothermal source heat pumps under energy services companies finance scheme to increase energy efficiency and production in stockbreeding facilities. *Energy* 88, 821–836.
- D'Agostino, Delia, Parker, Danny, 2018. A framework for the cost-optimal design of nearly zero energy buildings (nZEBs) in representative climates across Europe. *Energy* 149, 814–829.
- Deng, S., Wang, R.Z., Dai, Y.J., 2014. How to evaluate performance of net zero energy building – a literature research. *Energy* 71, 1–16.
- Directiva, 2009. 2009/28/CE del Parlamento Europeo y del Consejo, de 23 de abril de 2009, relativa al fomento del uso de energía procedente de fuentes renovables y por la que se modifican y se derogan las Directivas 2001/77/CE y 2003/30/CE (Texto pertinente a efectos del EEE).
- DIRECTIVE, 2010. 2010/31/EU OF THE EUROPEAN PARLIAMENT AND OF THE COUNCIL, on the energy performance of buildings. Off. J. Eur. Union.
- DIRECTIVE (EU), 2018. 2018/844 OF THE EUROPEAN PARLIAMENT AND OF THE COUNCIL, amending Directive 2010/31/EU on the energy performance of buildings and Directive 2012/27/EU on energy efficiency. Off. J. Eur. Union.
- Fraga, Carolina, Holmüller, Pierre, Schneider, Stefan, Lachal, Bernard, 2018. Heat pump systems for multifamily buildings: potential and constraints of several heat sources for diverse building demands. *Appl. Energy* 225, 1033–1053.
- Freedman, V.L., Waichler, S.R., Mackley, R.D., Horner, J.A., 2012. Assessing the thermal environmental impacts of a groundwater heat pump in southeastern Washington State. *Geothermics* 42, 65–77.
- Freedman, V.L., Mackley, R., Waichler, S.R., Horner, J., 2013. Evaluation of analytical numerical techniques for defining the radius of influence for an open-loop ground source heat pump system. *J. Hydrol. Eng.* 18, 1170–1179.
- Gao, Q., Zhou, X., Zhao, X., Ma, C., Yan, Y., 2012. Development and challenges of groundwater heat pump in China. *Appl. Mech. Mater.* 193–194, 115–120.
- Hernández-Magallanes, J.A., Heard, C.L., Best, R., Rivera, W., 2018. Modeling of a new absorption heat pump-transformer used to produce heat and power simultaneously. *Energy* 165 (Part A), 112–133.
- Instituto para la Diversificación y Ahorro de la Energía, 2014. "IDAE". Factores de emisión de CO2 y coeficientes de paso a energía primaria de diferentes fuentes de energía final consumidas en el sector edificios en España.
- Integral systems of heating/cooling with renewable energies, 2018. *Geothermal Heat Pumps Catalogue*. ENERTRES.
- Konttu, K., Rinne, S., Junnila, S., 2019. Introducing modern heat pumps to existing district heating systems – global lessons from viable decarbonizing of district heating in Finland. *Energy* 166, 862–870.
- Kranz, S., Frick, S., 2013. Efficient cooling energy supply with aquifer thermal energy storages. *Appl. Energy* 109, 321–327.
- Lian, Z., Park, S.R., Huang, W., et al., 2005. Conception of combination of gas-engine driven heat pump and water-loop heat pump system. *Int. J. Refrigeration* 28 (6), 810–819.
- Liang, J., Yang, Q., Liu, L., Li, X., 2011. Modelling and performance evaluation of shallow ground water heat pumps in Beijing plain, China. *Energy Build.* 43, 3131–3138.

- REGLAMENTO (UE), 2013. Nº 813/2013 DE LA COMISIÓN de 2 de agosto de 2013 por el que se desarrolla la Directiva 2009/125/CE del Parlamento Europeo y del Consejo respecto de los requisitos de diseño ecológico aplicables a los aparatos de calefacción y a los calefactores combinados.
- Renedo, C.J., Ortiz, A., Mañana, M., et al., 2007. A more efficient design for reversible air-air heat pumps. *Energy Build.* 39, 1244–1249.
- Sanner, B., Karytsas, C., Mendrinós, D., Rybach, L., 2003. Current status of ground source heat pumps and underground thermal energy storage in Europe. *Geothermics* 32, 579–588.
- Sommer, W., Valstar, J., Leuschrock, I., Grotenhuis, T., Rijnaarts, H., 2015. Optimization and spatial pattern of large-scale aquifer thermal energy storage. *Appl. Energy* 137, 322–337.
- Verda, V., Baccino, G., Sciacovelli, A., Russo, S.L., 2012. Impact of district heating and groundwater heat pump systems on the primary energy needs in urban areas. *Appl. Therm. Eng.* 40, 18–26.
- Zhang, Sheng, Huang, Fci, Sun, Yongjun, 2016. A multi-criterion renewable energy system design optimization for net zero energy buildings under uncertainties. *Energy* 94, 654–665.
- Zhou, X., Gao, Q., Chen, X., Yan, Y., Spittler, J.D., 2015. Development status and challenges of GWHP and ATEs in China. *Renew. Sustain. Energy Rev.* 42, 973–985.

Chapter IV
DISTRICT HEATING SYSTEMS
AIDED BY GEOTHERMAL
ENERGY

IV. District Heating Systems Aided by Geothermal Energy

Chapter IV deals with the integration of very low enthalpy geothermal energy in district heating systems. To this end, a Paper published in a high impact journal evaluates the principal characteristics of the mentioned systems from an economic and environmental point of view.

IV.I. Renewable district heating review

District heating networks have an important role to play in the task of improving energy efficiency based on centralized plants or distributed heat producing units. In the frame of promoting renewable energy resources, district heating means an additional opportunity of using these systems. District heating systems have been extensively reviewed in the past years from different angles; waste heat recovery (BCS, 2008), thermal energy storage (Harris, 2011), technology and potential enhancements (Rezaie and Rosen, 2012) or 4th generation (Lund et al, 2014) among others.


In the geothermal field, the development of geothermal district heating has been one of the fastest growing segments of the geothermal space heating industry. Thus, in countries like Turkey, the majority of geothermal applications have been made thanks to district heating systems (Hepbasli and Ozgener, 2004). Given the importance of these systems in the geothermal growth, numerous scientific researches have been focused on analyzing the implementation of geothermal district heating applications (Ozgener et al, 2007; Coskun et al, 2009; Hepbasli, 2010; Østergaard and Lund, 2011; Kyriakis and Younger, 2016; Yürüsoy and Keçebas, 2017; Halit and Arslan, 2017).

In the context of this topic, the purpose of Paper 9, included in the present Doctoral Thesis, is to highlight the versatility and potential of very low enthalpy geothermal energy as the principal energy source in district heating systems. The research work is based on the implementation and comparison of different alternative energies applied on the same real study case. Geothermal district heating thoroughly stands out on the rest of options considered in the Paper, emphasizing the economic and environmental strengths on the basis of the results coming from actual technical calculations.

PAPER 9

Article

Economic and Environmental Analysis of Different District Heating Systems Aided by Geothermal Energy

Cristina Sáez Blázquez * , Arturo Farfán Martín, Ignacio Martín Nieto and Diego González-Aguilera 

Department of Cartographic and Land Engineering, University of Salamanca, Higher Polytechnic School of Avila, Hornos Caleros 50, 05003 Avila, Spain; afarfan@usal.es (A.F.M.); nachomartin@usal.es (I.M.N.); daguilera@usal.es (D.G.-A.)

* Correspondence: u107596@usal.es; Tel.: +34-675-536-991

Received: 16 March 2018; Accepted: 10 May 2018; Published: 15 May 2018



Abstract: As a renewable energy source, geothermal energy can provide base-load power supply both for electricity and direct uses, such as space heating. Regarding this last use, in the present study, district heating systems aided by geothermal energy, the so-called geothermal district heating systems, are studied. Thus, three different options of a geothermal district heating system are evaluated and compared in terms of environmental and economic aspects with a traditional fossil installation. Calculations were carried out from a particular study case, a set of buildings located Province of León in the north of Spain. From real data of each of the assumptions considered, an exhaustive comparison among the different scenarios studied, was thoroughly made. Results revealed the most suitable option from an economic point of view but always considering the environmental impacts of each one. In this regard, the assumption of a district heating system totally supplied by geothermal energy clearly stands out from the rest of options. Thus, the manuscript main objective is to emphasise the advantages of these systems as they constitute the ideal solution from both the economic and environmental parameters analysed.

Keywords: geothermal energy; district heating systems; renewable energy; economic and environmental comparison

1. Introduction

Sustainable development has become an issue of crucial importance for the present society. In this context, district heating systems aided by renewable energies play a fundamental role. In regards to geothermal energy, it appears to have the potential of a suitable alternative for this kind of installations [1–3]. The use of this energy has recently been the focus of increasing attention because of its minimum negative environmental impact, low operating costs and the simplicity of the required technologies [4–8]. For these reasons, numerous district heating plants supplied by the mentioned energy were implemented in many countries during the last decade [9]. Most of them were installed in Europe, being France and Iceland in the lead [10–14].

In the particular case of Spain, in 2016, the number of district heating installations was of 306, or 59 more than in 2015, with a total installed capacity of 1219 MW. In most of the autonomous communities there has been a clear increase in the number of these systems [15,16]. Cataluña stands out with 19 new installations and represents the 35.8% of the total capacity installed in Spain. It is followed by Madrid, whose 316 MW represent 25.9% of the 1219 MW total.

A remarkable fact is that 74% of the Spanish district heating uses a renewable energy source. A total of 225 installations are aided by these energies, of which 218 use biomass [17]. In relation to the

geothermal energy, only two of the total 225 installations use this energy, that is to say, the number of geothermal district heating installations is less than 1.0% for this country representing 0.51 MW. The high initial investment this energy requires is often the reason why this option is commonly rejected. This fact together with the lack of knowledge in the field of this energy does not allow its expansion. For this reason, it is highly advisable and necessary to clarify the economic and environmental advantages these systems present in the medium and long term [18–20].

The objective of this work is to emphasize the benefits of a geothermal district heating from an economic and environmental point of view [21–23]. For this purpose, different district heating scenarios using exclusively geothermal energy or combined with gas boilers were contemplated. The group of assumptions was applied to a certain case of study implementing real data and making the corresponding dimensioning. Results derived from the set of calculations allowed to know how the use of geothermal technology positively affects the economy of the whole process being at the same time largely environmentally friendly.

2. Materials and Methods

2.1. Initial Description of the Study Area

The different heating options contemplated in this work were designed to cover the thermal needs of three buildings placed at the University Campus of Vegazana in the province of León (Spain):

- The university school of education (A)
- The higher and technical school of mining engineers (B)
- The higher and technical school of industrial and aerospace engineering (C)

Figure 1 shows the regional situation and location of the buildings in question.

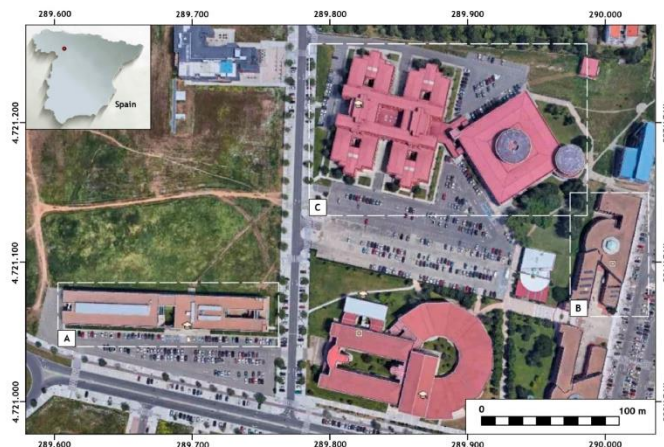


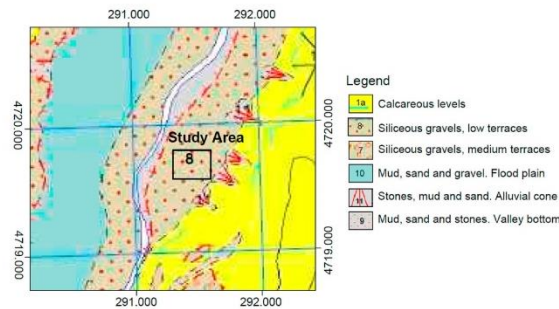
Figure 1. Position of the buildings considered in the present research (Geodetic Datum: WGS84, Cartographic projection: UTM, Time zone: 30).

The present heat source that covers the thermal demand of these universities is a common installation of natural gas where each building is supplied by an individual boiler. The annual use of fuel of each construction can be found in Table 1. Additional information is provided in Table A1 of Appendix A.

Table 1. Annual use of natural gas of each building.

Building	Annual Use of Natural Gas (kWh)
University school of education (A)	455,541.00
Higher and technical school of mining engineers (B)	264,666.00
Higher and technical school of industrial and aerospace engineering (C)	1,429,101.00

Figure 2 shows the geological characterization of the area where the research is set. The geological formations play a fundamental role in the process of thermal exchange between ground and the heat carrier fluid. For this reason, geology is subsequently required during the process of calculation of the future geothermal district heating system. Parameters such as the total drilling length or the heat pump power are closely related to the capacity of the ground to conduct the heat (thermal conductivity of the ground). Table 2 presents the parameter of thermal conductivity for each of the geological formations described in Figure 2.

**Figure 2.** Geological description of the study area [24].**Table 2.** Thermal conductivity of the materials presented in the study area.

Geological Formation	Thermal Conductivity (W/mK) *
Calcareous levels	1.40
Siliceous gravels	0.80
Mud, sand and stones	1.10
Mud, sand and gravel	1.30

* Values based on laboratory measurements in materials with similar geological composition [25].

Additionally, the meteorological information of the study area is presented in Table A2 belonging to Appendix A.

2.2. Description of the Proposed Solutions

● Case 1

The first alternative was designed to cover the thermal needs of the set of buildings by a district heating system exclusively aided by geothermal energy. The integrated installation was defined to supply the thermal demand of each of the buildings connected to the network. The generator plant was constituted by a vertical closed-loop geothermal system of very low enthalpy since the drilling depths (as Section 3.1 shows) are moderate. Additionally, the geological characteristics of the area in question did not allow implementing any other version of geothermal energy, given that high temperature points are not found in that kind of materials.

The central installation was planned to follow a branched pattern (fishbone schema) where each building was connected to the same generator plant by a single supplying network. The structure of the fishbone schema can be found in Figure 3. This figure presents an initial schema of the primary and secondary nets that constitutes the projected district heating plant.

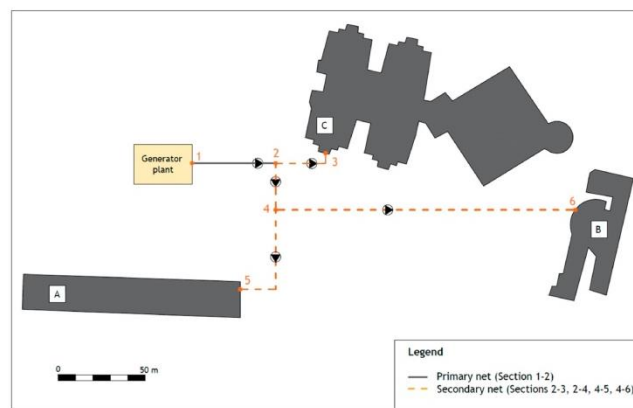


Figure 3. Network distribution.

Since it was designed to just cover the heating needs, the circuit consisted of a double pipe pattern. In this system, one of the pipes is responsible for transporting the fluid to each building which returns through a second pipe to the main plant. Both pipes were properly insulated and protected, as Figure 4 shows.

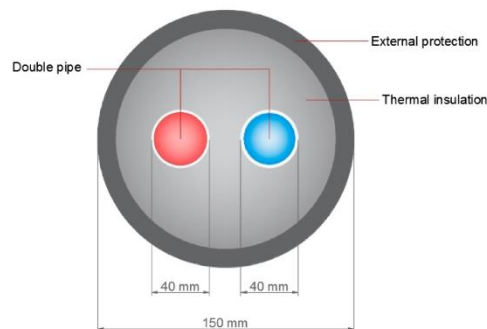


Figure 4. Schema of the double pipe system of 40 mm in diameter.

- Case 2

The second solution to supply the demand of the buildings in question was projected to combine the geothermal district heating considered above and the existing natural gas installation. Thus, it was possible to reduce the total drilling length as well as the heat pump power of the geothermal plant. In this case the thermal demand was fundamentally covered by the geothermal district heating while the individual natural gas system (already existing) provided the remaining needs. The design of the

geothermal district heating was identical to the one presented for case 1. However, the calculation of this option must be carried out independently.

- Case 3

The third assumption is quite similar to the above presented. However, this case proposes a district heating system where the generator plant is constituted by a single natural gas boiler in addition to the geothermal plant. Thus, the distribution system is common for both thermal sources. The geothermal system covers most of the total thermal demand (as in the previous case 2) while the natural gas boiler supplies the remaining demand. As it will be described in subsequent sections, the initial investment will be higher than in the previous case where the fossil installation is already set. Nevertheless, the higher efficiency of this natural gas boiler (in comparison with the individual heaters) will contribute to decrease the global operational costs.

Although cases 2 and 3 use as auxiliary energy source the natural gas, both cases present important differences. While case 2 need an individual natural gas boiler for each building, case 3 only implements a natural gas heater that will be common for the set of buildings.

2.3. Test Procedure

Initially, the proposed solutions previously described were technically calculated. The dimensioning of the district heating system derived from the thermal and geological description presented in the above section. Afterwards, an economic analysis of each option was also established. Once known this information, the proposed solutions (case 1, 2 and 3) and the existing installation were properly compared and evaluated. By way of clarification, the following Figure 5 describes the workflow followed throughout this research.

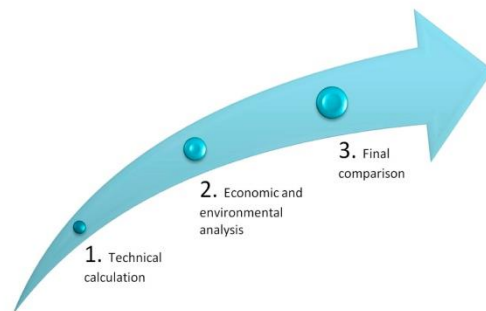


Figure 5. Workflow established in the present research.

3. Results

3.1. Dimensioning

- Case 1 calculation

The dimensioning process of a district heating system involves the calculation of three main sections: the generator plant, the distribution system and the substations. Geothermal energy was in this case selected as the energy source to constitute the generator plant. By using the energy demand of the set of buildings integrating the district heating, the geothermal installation was calculated by the software “Earth Energy Designer” (EED). This software, developed by Blocon Software (Lund, Sweden), allows knowing the total drilling depth of the vertical closed-loop system and the heat pump power required in the plant. The calculation process of EED is based on a series of initial data (provided

by the user) about the installation and the ground where it will be placed [26–28]. These initial data include the selection of the heat exchangers design. For this research, double-U polyethylene pipes of 32 mm in diameter, will allow the thermal exchange with the ground.

Once introduced the particular data of the system in question, EED evaluates the main parameters of the geothermal installation. In this way, the heat pump power and the number and length of boreholes required to cover the specific demand were calculated. During the process of calculation, the software suggests a series of alternatives. For the present assumption, the most optimal option (the first one) was selected so the installation requires a heat pump power of at least 330.62 kW and 49 boreholes of 178 m depth spaced every 20 m. The general distribution of each of the components of the geothermal district heating is presented in Figure 6.

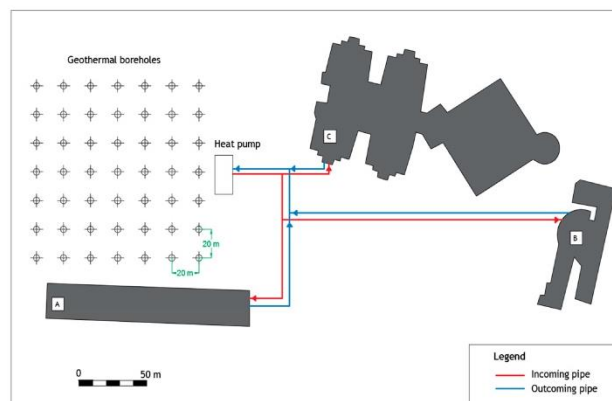


Figure 6. Schema of the main components of the whole geothermal district heating system.

By the above calculations, the part of the system corresponding to the geothermal installation (generator plant) was completely defined.

In relation to the distribution system, it was designed as a double-pipe system connecting the generator plant with each building. As made in the generator plant, this section was also thoroughly established. The diameters of the pipes were defined according to the mass flow rate. The required mass flow rate was calculated using Equation (1):

$$qm = \frac{\varnothing}{\Delta t \cdot cp} \quad (1)$$

where: qm = mass flow rate (kg/s), \varnothing = Capacity (kW), Δt = temperature difference (K) and cp = specific heat capacity (kJ/kgK).

Considering PEX-a pipes, it was possible to observe at the nomogram of Figure 7 the recommended pressure loss area (in darker colour) for this kind of pipes. This nomogram allows knowing the diameter of piping required in function of the power installed and the expected thermal increase. On the basis of these data, the pipe diameter (mm), pipe friction resistance (kPa/m) and velocity (m/s) are directly deduced.

Entering in the nomogram the power installed in each section, the diameters of each pipe were directly obtained. The pipe friction resistances and velocities corresponding to those pipes were also established. Table 3 lists the descriptions of each section of pipe.

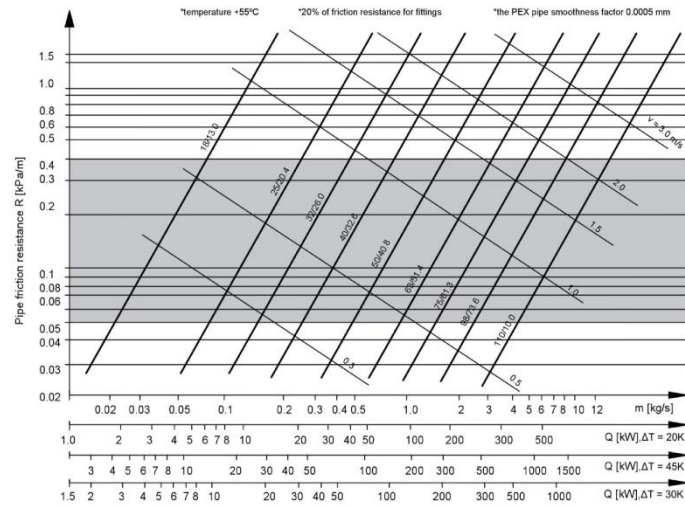


Figure 7. Nomogram of pipe friction resistance-flow-velocity for PEX-a pipes [29].

Table 3. Main parameters of the pipes used in the geothermal district heating.

Section *	Power Installed (kW)	Thermal Increase (K)	Flow Rate (L/h)	Velocity (m/s)	Pipe Friction Resistance (kPa/m)	Pipe Diameter (mm)
1–2	360	20	15,480	1.59	0.34	75
2–3	239.40	20	10,292	1.25	0.22	63
2–4	120.60	20	5186	1.00	0.26	50
4–5	76.28	20	3280	1.10	0.37	40
4–6	44.32	20	1906	0.65	0.17	40

* Sections can be found in Figure 3.

It must be clarified that the total power installed (section 1–2) should be 330.62 kW according to the calculations presented above. However, it is not possible to find commercial heat pumps with that exact power. Thus, the most similar commercial power was the 360 kW listed in Table 3.

Another important aspect to be considered is the heat loss through the pipes previously selected. They were accordingly calculated from the thermal transmittance provided by the manufacturer for each pipe diameter (considering pipes mounted in the air). These calculations can be found in Table A3 of Appendix A. Heat losses results are obtained for each section by the product of the thermal transmittance, the piping length and the thermal increase. The thermal increase considered in this Table A3 (80 K) represents the maximum increase that could be achieved in the system conditions for which the maximum heat losses would be found. Since the total losses are fewer than 3%, they have not been considered for subsequent calculations.

Substations were the last modules to be defined. They must be integrated by a set of heat exchangers, a buffer tank and different regulation and control devices. The buffer tank is responsible for adjusting the temperature and pressure conditions of the fluid coming from the generator plant. Its capacity was defined according to the “Regulation of thermal installations in buildings” (RITE) [30], which recommends a volume of 15–30 litres per kW of usable nominal power generated. Additionally, heat exchangers connect the generator plant with the primary circuit as well as the primary circuit with the rest of secondary nets. These systems were selected in function of the power installed in the section where they are placed. All of them were designed to work with the following conditions (Table 4):

Table 4. Heat exchangers working conditions.

Condition	Primary Circuit	Secondary Circuit (User)
Inlet temperature (°C)	Minimum 80	Maximum 25
Outlet temperature (°C)	Maximum 60	Maximum 50

- Case 2 calculation

The process of calculation of the geothermal district heating in this second case was equally performed by using the EED software. In the present option, the 70% of the whole demand (demands of buildings presented in Table 1) is covered by the renewable part of the mixed system (geothermal district heating). Therefore, entering in the software with the pertinent demand and the rest of specific values of the ground and installation, new working conditions were obtained. Thus, a heat pump power of 229.38 kW was needed and 36 boreholes of 193 m depth spaced every 24 m were required.

The same methodology than in the previous assumption was also applied to define the distribution system and substations in case 2. Given that the system of piping is identical, Equation (1) and nomogram presented in Figure 7 were also used to define the main parameters of each section of piping. These parameters can be found in Table 5.

Table 5. Main parameters of the pipes used in the case 2.

Section	Power Installed (kW)	Thermal Increase (K)	Flow Rate (L/h)	Velocity (m/s)	Pipe Friction Resistance (kPa/m)	Pipe Diameter (mm)
1-2	230	20	9890	1.20	0.24	63
2-3	152.95	20	6577	1.18	0.30	50
2-4	77.05	20	3313	1.10	0.39	40
4-5	48.74	20	2096	0.77	0.21	40
4-6	28.31	20	1217	0.60	0.20	32

Substations are constituted by the same elements described in case one. A buffer tank was also selected in this second option with a lower capacity since the total power was also lower. Relative to heat exchangers, they were designed to operate with the conditions previously collected in Table 4. The selection of these devices was also made depending on the power installed in each section.

Lastly, the remaining 30% of the global demand was covered by the set of individual natural gas boilers placed in each of the buildings. Thus, additional calculations were not needed given that the mentioned heaters were already installed and operating.

- Case 3 calculation

The generator plant was in this case planned to be constituted by a geothermal system and a sole natural gas heater. The geothermal plant was identical to the one calculated above for case 2 (since it covers the 70% of the demand too). Regarding the natural gas boiler, considering an efficiency of 0.9 (higher than the existing devices), to cover the 30% of the current demand (obtained from the consumptions of Table 1), a heater device of at least 218.9 kW would be needed. Thus, three commercial natural gas heaters of 80 kW (each one) were chosen providing enough power to supply the requested demand.

In relation to the distribution system and substations, they were designed to transport the whole power produced in the generator plant. Since the total distributed power was the same than in case one, the dimensioning process was identical and therefore parameters were those presented in Tables 3 and 4. Therefore, piping, buffer tank and heat exchangers were the same than in case one.

3.2. Economic Analysis

Along this subsection an economic calculation is presented for each of the assumption considered in this research. This analysis includes the initial investment and operational costs as can be seen below.

3.2.1. Initial Investment

● Case 1

Once the first case was designed, it was possible to calculate the initial investment required. Table 6 presents the unitary and the total price of each of the components of the generator plant, distribution system and substations that are part of the geothermal district heating. Additionally, the total investment for this assumption is also collected in Table 6.

Table 6. Summary of the initial investment for case 1.

Initial Investment Case 1				
	Element	Quantity	Unitary Price (€)	Total Price (€)
Generator plant	Drilling	8722 *	44.00	383,768.00
	Heat pumps	2 **	115,010.00	230,020.00
	Heat exchangers	49 **	880.00	43,120.00
	Control device	1 **	120.00	120.00
	Accessory elements	-	-	11,573.20
Distribution system	Double piping	395.69 *	-	35,048.19
	Circulating pumps	5 **	-	8664.00
	Leak detection system	1 **	948.00	948.00
	Accessory elements	-	-	4712.58
Substation	Buffer tank	1 **	10,700.00	10,700.00
	Heat exchangers	3 **	-	2782.00
Total investment (€)				731,455.97

* (meters), ** (units).

● Case 2

As in the first option, the initial investment was calculated as follows: regarding the natural gas installation, and given that it already exists, the initial costs of this part of the mixed system are zero. For this reason, the initial investment corresponding to the second case only includes the elements required in the geothermal district heating. Thus, the same elements of the previous option were also considered in this second assumption. Table 7 presents the initial investment of the mentioned elements belonging to the geothermal district heating of the second option.

Table 7. Summary of the initial investment for case 2.

Initial Investment Case 2				
	Element	Quantity	Unit Price (€)	Total Price (€)
Generator plant	Drilling	6948 *	44.00	305,712.00
	Heat pumps	2 **	69,379.00	138,758.00
	Heat exchangers	36 **	880.00	31,680.00
	Control device	1 **	120.00	120.00
	Accessory elements	-	-	9196.80
Distribution system	Double piping	395.69 *	-	30,734.97
	Circulating pumps	5 **	1678.80	8394.00
	Leak detection system	1 **	948.00	948.00
	Accessory elements	-	-	4712.59
Substation	Buffer tank	1 **	6588.00	6588.00
	Heat exchangers	3 **	-	2316.00
Total investment (€)				539,160.36

* (meters), ** (units).

- Case 3

The initial investment for case three includes the costs associated to the general district heating system. On this matter, the investment of the generator plant must consider the implementation of the geothermal module and the natural gas boiler. The costs connected to the distribution system and substations were identical to those calculated in case one. Table 8 collects the initial investment that case three involves.

Table 8. Summary of the initial investment for case 3.

Initial Investment Case 3				
	Element	Quantity	Unitary Price (€)	Total Price (€)
Generator plant	Drilling	6948 *	44.00	305,712.00
	Heat pumps	2 **	69,379.00	138,758.00
	Heat exchangers	36 **	880.00	31,680.00
	Control device	1 **	120.00	120.00
	Natural gas boiler	3 **	4600.00	13,800.00
	Accessory elements	-	-	-
Distribution system	Double piping	395.69 *	-	35,048.19
	Circulating pumps	5 **	1678.80	8664.00
	Leak detection system	1 **	948.00	948.00
	Accessory elements	-	-	4712.58
Substation	Buffer tank	1 **	10,700.00	10,700.00
	Heat exchangers	3 **	-	2782.00
Total investment (€)				565,246.57

* (meters), ** (units).

3.2.2. Operational Costs

- Case 1

Despite being a completely renewable installation, in addition to the initial investment, several additional costs have to be considered. Such costs mainly correspond to the heat and circulating pump operation and the periodic installation maintenance.

Most of the energy consumption derives from the heat pumps working. The excellent coefficient of operation (COP) of these devices allows them to provide a notable quantity of thermal energy consuming a minor amount of electricity. For the present case, two heat pumps of 180 kW (produced by ENERTRES, Galicia, Spain) connected in series provide a total of 360 kW that thoroughly cover the demand of 330.62 kW previously calculated. According to the manufacturer's data, the power consumption of each of these devices is 40.92 kW, given the high COP (4.27) they have. This COP was calculated from the mean temperature of the fluid simulated with EED software for a thirty years operational period. From this simulation presented in Figure 8, the mean temperature of the fluid (3 °C) was estimated in order to obtain the mentioned COP for that period and according to the European Normative UE 813/2013 [31].

Heat pumps will be operational during 9 months a year for an average of 10 h a day (considering the climatic conditions of the area and the use of the buildings). It means an electrical use of 220.968 kWh/year for the set of geothermal heat pumps. It is important to clarify that the high seasonal COP is possible thanks to a combination of different factors. The heat pumps connection (in series) increases the COP of the second heat pump, this fact joined to the favourable geological and hydrogeological ground conditions result in an improvement of the global COP. Additionally, the ground/heat pump contribution ratio shoots up the COP with a small ground contribution increase. This fact can be observed in Figure 9.

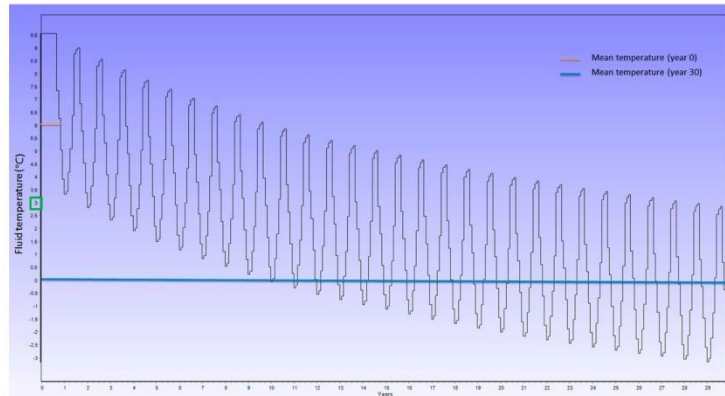


Figure 8. Fluid temperature evolution for the period of thirty years.

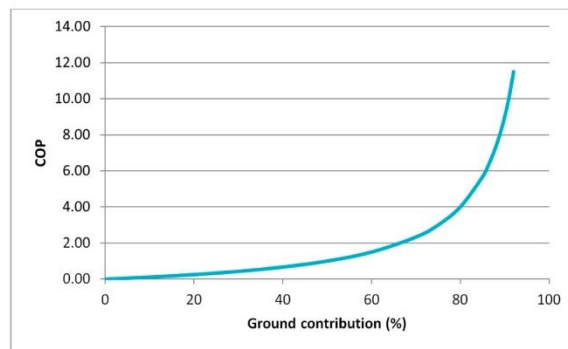


Figure 9. Relation COP-Ground contribution.

Since the electrical use of the rest of components that integrate the geothermal district heating was comparatively lower, in this section, only the heat pumps consumption and the maintenance of the whole installation were considered. Table 9 provides the costs associated to the mentioned items.

Table 9. Operational costs for case 1.

Operational Costs Case 1	
Item	Cost (€/year)
Heat pumps working	28,725.84 *
District heating system maintenance	3733.00
Total operational costs	32,498.84

* total cost per year for the two heat pumps required to cover the demand in question and considering a local rate of 0.13 €/kWh.

- Case 2

The operational costs in this case derive from the heat pumps operation and maintenance of the whole district heating system as well as the fossil installation working. Regarding the geothermal plant, two heat pumps (of 90 kW and 140 kW) connected in series provide 230 kW to supply the previously calculated power of 229.38 kW. The COP of these pumps is also extraordinary (of 4.27 and 4.33 respectively) and hence, the power consumptions of these devices are 20.46 kW and 32.76 kW. These COP values were equally calculated as in the previous case 1. Likewise, heat pumps will be operational during 9 months a year to an average of 10 h a day. Thus, the electricity use of both heat pumps will be of 143.694 kWh/year. As in the previous case, the electricity use of the rest of components of the geothermal district heating was not considered (since it is comparatively lower).

Thanks to the geothermal system, the 70% of the total demand is covered. The remaining demand is provided by the existing fossil installation. For this reason, the operational costs must also include the pertinent natural gas use. Table 10 collects the operational costs including all the mentioned items.

Table 10. Operational costs for case 2.

Operational Costs Case 2	
Item	Cost (€/Year)
Heat pumps working	18,680.22 *
District heating system and fossil plant maintenance	4120.00
Natural gas use	36,147.72 **
Total operational costs	58,947.94

* total cost per year for the two heat pumps required to cover the 70% of the demand and considering a local rate of 0.13 €/kWh. ** Natural gas rate of 0.056 €/kWh + 4.54 €/month.

- Case 3

In this last case, operational costs include the district heating working which, in turn, involves the heat pumps and natural gas heater operation besides the maintenance of the whole general system.

Since the geothermal plant was designed to cover the same demand than in case two (70% of the total demand), heat pumps described in that case are also used here. Thus, a power consumption of 143.694 kWh/year is required to supply two heat pumps of 90 kW and 140 kW. Natural gas use of the heater that integrates the generator plant must be also considered in this section. As in the previous case, operational costs for the natural gas are calculated considering the natural gas use (kW/h) and a local rate of 0.056 €/kWh + 4.54 €/month.

Table 11 shows the operational cost corresponding to case three.

Table 11. Operational costs for case 3.

Operational Costs Case 3	
Item	Cost (€/Year)
Heat pumps working	18,680.22 *
District heating system maintenance	3980.00
Natural gas use	33,138.82 **
Total operational costs	55,799.04

* total cost per year for the two heat pumps required to cover the 70% of the demand and considering a local rate of 0.13 €/kWh. ** Natural gas rate of 0.056 €/kWh + 4.54 €/month.

3.3. Environmental Analysis

The environmental analysis is performed according to the CO₂ emissions associated with each scenario. The estimation of the greenhouse gases is based on a series of emission factors commonly accepted for each of the energy sources used [32]. Thus, Table 12 presents the quantity of CO₂ emitted

by the installations implemented in each of the cases described in the manuscript. It is important to clarify that for case 1, CO₂ emissions are the corresponding to the heat pumps operation. For case 2, emissions are associated to the heat pumps working as well as the fossil installation. For case 3, these emissions derive from the operation of the heat pumps and the unique natural gas boiler. Therefore, for cases 2 and 3, two conversion factors are considered. Finally, CO₂ emissions of the system currently installed (designated here as case 4) correspond to the fossil plant constituted by three individual natural gas devices.

Table 12. Conversion factor and emissions of CO₂ for each assumption.

	Conversion Factor (kg CO ₂ /kWh of Final Energy)	CO ₂ Emission (kg/Year)
CASE 1	0.331	73,140.41
CASE 2	0.331/0.252	210,374.59
CASE 3	0.331/0.252	196,503.52
CASE 4	0.252	541,602.94

4. Discussion

Three different scenarios have been described in the present manuscript. These options together with the existing fossil installation (case 4) are now evaluated and compared from an economic and environmental point of view.

Table 13 presents the economic balance based on the calculations made in the above section. The comparison considers the initial investment and operational costs per year of each assumption until a period of thirty years (lifespan of these plants). With the aim of updating the costs of each year to the real value in that moment, data are expressed in terms of the “Net Present Value” (NPV). Equation (2) shows the expression for NPV:

$$NPV = -I_0 - \frac{C_1}{(1-k)} - \frac{C_2}{(1-k)^2} - \dots - \frac{C_T}{(1-k)^T} \quad (2)$$

where: I_0 = Initial investment, C_1 = Operational costs for year 1, C_2 = Operational costs for year 2, C_T = Operational costs for year T and k = Discount rate.

Every term of Equation (2) is negative given that initial investment and operational costs are both outlays and there are no positive cash flows. Additionally, it must be mentioned that a discount rate of 1.8% has been used in all the calculations. The operational costs for case 4 presented in this Table 13, are exclusively those corresponding to the use of natural gas.

Table 13. Economic balance of each case for a period of 30 years.

	CASE 1	CASE 2	CASE 3	CASE 4
Initial Investment (€)	731,345.38	539,055.45	565,135.98	0
Year 1	33,094.54	60,028.45	56,821.83	122,687.16
Year 5	177,942.80	322,761.12	305,519.74	659,664.56
Year 10	389,720.26	706,893.15	669,132.04	1,444,760.01
Year 15	640,157.45	1,161,148.04	1,099,121.36	2,373,173.73
Year 20	934,691.08	1,695,387.16	1,604,822.28	3,465,060.56
Year 25	1,279,442.21	2,320,713.16	2,196,744.36	4,743,112.26
Year 30	1,681,297.17	3,049,616.80	2,886,711.13	6,232,857.69
NPV (€)	-2,412,752.56	-3,588,777.15	-3,451,957.70	-6,232,857.69

Figure 10 graphically shows the final economic results presented in the above Table 13 at the end of the period considered.

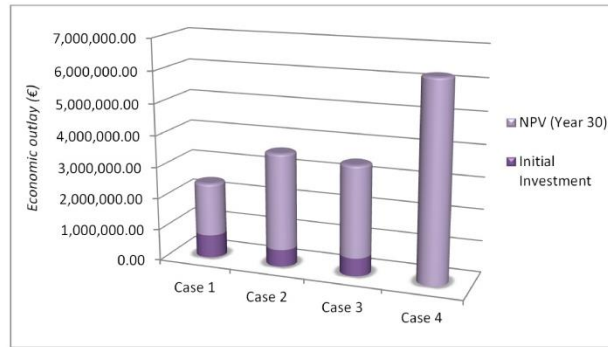


Figure 10. Economic position at the end of the period studied (thirty years).

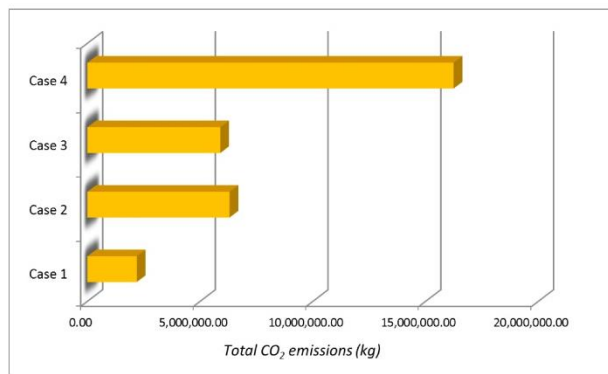


Figure 11. CO₂ emissions associated to each scenario at the end of year 30.

At same time, from the annual environmental analysis previously presented in Section 3.3, it was possible to estimate the total CO₂ emissions accumulated at the end of the period considered (year 30). In this way, Figure 11 schematically shows the mentioned parameter for each of the cases described in this study. From the economic and environmental comparisons expounded above, a series of statements can be made:

- The first option (case 1) requires the highest initial investment in contrast with the existing system (case 4) where this item is null. Regarding the initial investment of cases 2 and 3 (quite similar), it is significantly lower (around 25%) than in case 1.
- Analysing the operational costs, it is easily observable that case 4 has the highest costs due to the plant working in each one of the years considered. On the contrary, the lowest operational costs belong to case 1, with case 2 and 3 in the middle of both scenarios.
- Differences of operational costs between cases 1 and 4 progressively increase until year 30 where the maximum deviation is found. Thus, the high initial investment of case 1 would be more than amortized in the eighth year in comparison with the present installation (case 4). Case 2 and 3 would also be amortized in year 8. However, the total savings in the last year (year 30) are much more favourable for case 1.

- In economic terms, and considering the global balance of Table 13 named “NPV”, the most favourable option is case 1, followed by case 3 and case 2. From an economic point of view these assumptions (case 2 and 3) are quite similar and significant differences are not detected. On the other hand, case 4 is clearly distanced from the rest of scenarios constituting the worst option regarding the economic issue.
- In respect of the environmental point of view, case 1 involves the lowest quantity of annual CO₂ emissions. In case 2 and 3 these emissions are of around three times larger than in the first assumption. Regarding case 4, CO₂ emissions are seven times larger than in case 1. Therefore, with reference to the environmental aspect, case 1 represents the most respectful and appropriate solution for the area studied in this research. At the other extreme, case 4 constitutes the least favourable option given the high level of CO₂ emissions its operation involves.

5. Conclusions

An exhaustive calculation of three options specifically designed to cover the thermal needs of a set of buildings has been carried out in this study. From these calculations, an economic and environmental analysis has been presented in order to compare the different scenarios and select the most suitable one. Based on this comparison, case 1, where a geothermal district heating is proposed, means the ideal solution from both the economic and environmental point of view. Although it requires the highest initial investment, the operational costs are significantly lower than in the current fossil system and in the rest of cases studied. Thus, the investment would be easily amortized in a short period of time and important savings could be achieved in the remaining lifetime of the system in question. Additionally, this case 1 is also supported by the environmental side since it presents the lowest CO₂ emission rate. Even the mixed systems (case 2 and 3) constituted by geothermal energy and natural gas heaters are substantially better than the existing fossil installation thanks to the introduction of the mentioned renewable source. In any case, it has been demonstrated how the use of the geothermal energy offer a large number of interesting advantages. The initial investment of this kind of geothermal plants is always amortized in the first years of operation. In addition, the scarce electricity demand of the geothermal heat pumps causes the low operational costs as well as a limited greenhouse gases emission.

Author Contributions: All authors conceived, designed and performed the experimental and theoretical basis of the research. C.S.B., A.F.M. and I.M.N. implemented the methodology and calculations and analysed the results. D.G.-A. provided technical and theoretical support. C.S.B. wrote the manuscript and all authors read and approved the final version.

Acknowledgments: Authors would like to thank the Department of Cartographic and Land Engineering of the Higher Polytechnic School of Avila, University of Salamanca, for allowing us to use their facilities and their collaboration during the experimental phase of this research. The gratitude is extensible to the University of León for providing the real data used in this work. Authors also want to thank the Ministry of Education, Culture and Sport for providing a *FPU Grant* (Training of University Teachers Grant) to the corresponding author of this paper what has made possible the realization of the present work.

Conflicts of Interest: The authors declare no conflict of interest.

Appendix

Table A1. Additional characterization of the buildings studied.

Building	Total heated Surface (m ²)	Usual Number of Occupants	Operational Schedule
A	4914.09	148	9 months/year Mean value of 10 hours/day
B	3402.39	102	
C	13,096.88	393	

Table A2. Meteorological information of the place where the study is focused.

Month.	Mean Temperature (°C)	Minimum Temperature (°C)	Maximum Temperature (°C)
January	3.2	−0.7	7.1
February	4.6	0	9.3
March	7.6	2.6	12.7
April	9.7	3.8	15.6
May	12.6	6.5	18.8
June	17.1	10.1	24.2
July	19.7	11.8	27.7
August	19.5	12	27
September	16.7	10	23.4
October	11.9	6.3	17.6
November	7.3	2.7	12
December	4.2	0.6	7.9

Table A3. Power losses of each section of pipes and total loss for the set of piping.

Section	Length (m)	ΔT (K)	Thermal Transmittance (W/mk)	Power Loss * (kW)	Power Flow (kW)	Loss (%)
1–2	36.72	80	0.40	1.17	360.00	0.33
2–3	41.29	80	0.38	1.25	239.40	0.52
2–4	32.11	80	0.34	0.69	120.60	0.57
4–5	79.04	80	0.32	2.02	76.28	2.65
4–6	206.53	80	0.32	5.29	44.32	11.93
Total loss				10.42	360.00	2.89

* Calculated from the product of Length, temperature increment and thermal transmittance.

References

- Carotenuto, A.; Figaj, R.D.; Vanoli, L. A novel solar-geothermal district heating, cooling and domestic hot water system: Dynamic simulation and energy-economic analysis. *Energy* **2017**, *141*, 2652–2669. [CrossRef]
- Mink, L.L. The Nation's Oldest and Largest Geothermal District Heating System. *Geotherm. Resour. Coun. Trans.* **2017**, *41*, 205–212.
- Oktay, Z.; Coskun, C.; Dincer, I. Energetic and exergetic performance investigation of the Bigadic Geothermal District Heating System in Turkey. *Energy Build.* **2008**, *40*, 702–709. [CrossRef]
- Pinto, J.F.; da Graça, G.C. Comparison between geothermal district heating and deep energy refurbishment of residential building districts. *Appl. Therm. Eng.* **2007**, *27*, 1303–1310.
- Arat, H.; Arslan, O. Exergoeconomic analysis of district heating system boosted by the geothermal heat pump. *Energy* **2017**, *119*, 1159–1170. [CrossRef]
- Unternährer, J.; Moret, S.; Joost, S.; Maréchal, F. Spatial clustering for district heating integration in urban energy systems: Application to geothermal energy. *Appl. Energy* **2017**, *190*, 749–763. [CrossRef]
- Keçebaş, A.; Hepbasli, A. Conventional and advanced exergoeconomic analyses of geothermal district heating systems. *Energy Build.* **2014**, *69*, 434–441. [CrossRef]
- Kyriakis, S.A.; Younger, P.L. Towards the increased utilisation of geothermal energy in a district heating network through the use of a heat storage. *Appl. Therm. Eng.* **2016**, *94*, 99–110. [CrossRef]
- Lund, J.W.; Boyd, T.L. Direct utilization of geothermal energy 2015 worldwide review. *Geothermics* **2016**, *60*, 66–93. [CrossRef]
- Hepbasli, A.; Canakci, C. Geothermal district heating applications in Turkey: A case study of Izmir–Balcova. *Energy Convers. Manag.* **2003**, *44*, 1285–1301. [CrossRef]
- Abdurafikov, R.; Grahm, E.; Ypyä, L.K.J.; Kaukonen, S.; Heimonen, I.; Paiho, S. An analysis of heating energy scenarios of a Finnish case district. *Sustain. Cities Soc.* **2017**, *32*, 56–66. [CrossRef]
- Carotenuto, A.; De Luca, G.; Fabozzi, S.; Figaj, R.D.; Iorio, M.; Massarotti, N.; Vanoli, L. Energy analysis of a small geothermal district heating system in Southern Italy. *Int. J. Heat Technol.* **2016**, *34*, S519–S527. [CrossRef]

13. Sander, M. Geothermal district heating systems: Country case studies from China, Germany, Iceland, and United States of America, and schemes to overcome the gaps. *Trans. Geotherm. Resour. Counc.* **2016**, *40*, 769–775.
14. Muñoz, M.; Garat, P.; Flores-Aqueveque, V.; Vargas, G.; Rebolledo, S.; Sepúlveda, S.; Daniele, L.; Morata, D.; Parada, M.Á. Estimating low-enthalpy geothermal energy potential for district heating in Santiago basin-Chile (33.5 °S). *Renew. Energy* **2015**, *76*, 186–195. [[CrossRef](#)]
15. Soltero, V.M.; Chacartegui, R.; Ortiz, C.; Velázquez, R. Evaluation of the potential of natural gas district heating cogeneration in Spain as a tool for decarbonisation of the economy. *Energy* **2016**, *115*, 1513–1532. [[CrossRef](#)]
16. Rodríguez-Aumente, P.A.; del Carmen Rodríguez-Hidalgo, M.; Nogueira, J.I.; del Carmen Venegas, M. District heating and cooling for business buildings in Madrid. *Appl. Therm. Eng.* **2013**, *50*, 1496–1503. [[CrossRef](#)]
17. Ioakimidis, C.S.; Gutiérrez, I.A.; Genikomsakis, K.N.; Stroe, E.R.; Savuto, E. The use of district heating on a small Spanish village. In Proceedings of the 26th International Conference on Efficiency, Cost, Optimization, Simulation and Environmental Impact of Energy Systems, ECOS, Guilin, China, 19 July 2013.
18. Ozgener, L.; Hepbasli, A.; Dincer, I.; Rosen, M.A. Exergoeconomic analysis of geothermal district heating systems: A case study. *Appl. Therm. Eng.* **2007**, *27*, 1303–1310. [[CrossRef](#)]
19. Möller, B.; Lund, H. Conversion of individual natural gas to district heating: Geographical studies of supply costs and consequences for the Danish energy system. *Appl. Energy* **2010**, *87*, 1846–1857. [[CrossRef](#)]
20. Keçebaş, A. Performance and thermo-economic assessments of geothermal district heating system: A case study in Afyon, Turkey. *Renew. Energy* **2011**, *36*, 77–83. [[CrossRef](#)]
21. Keçebaş, P.; Gökgedik, H.; Alkan, M.A.; Keçebaş, A. An economic comparison and evaluation of two geothermal district heating systems for advanced exergoeconomic analysis. *Energy Convers. Manag.* **2014**, *84*, 471–480. [[CrossRef](#)]
22. Hepbasli, A.; Keçebaş, A. A comparative study on conventional and advanced exergetic analyses of geothermal district heating systems based on actual operational data. *Energy Build.* **2013**, *61*, 193–201. [[CrossRef](#)]
23. Aslan, A.; Yüksel, B.; Akyol, T. Energy analysis of different types of buildings in Gonen geothermal district heating system. *Appl. Therm. Eng.* **2011**, *31*, 2726–2734. [[CrossRef](#)]
24. Ministerio de Economía. *Industria y Competitividad*; Instituto Geológico y Minero de España (IGME): Madrid, Spain, 2003.
25. Blázquez, C.S.; Martín, A.F.; Nieto, I.M.; García, P.C.; Pérez, L.S.S.; Aguilera, D.G. Thermal conductivity map of the Avila region (Spain) based on thermal conductivity measurements of different rock and soil samples. *Geothermics* **2017**, *65*, 60–71. [[CrossRef](#)]
26. Sliwa, T.; Nowosiad, T.; Vytiaz, O.; Sapinska-Sliwa, A. Study on the efficiency of deep borehole heat exchangers. *SOCAR Proc.* **2016**, *2*, 29–42. [[CrossRef](#)]
27. Blázquez, C.S.; Martín, A.F.; Nieto, I.M.; González-Aguilera, D. Measuring of Thermal Conductivities of Soils and Rocks to Be Used in the Calculation of A Geothermal Installation. *Energies* **2017**, *10*, 795–813. [[CrossRef](#)]
28. Blázquez, C.S.; Martín, A.F.; García, P.C.; Pérez, L.S.S.; del Caso, S.J. Analysis of the process of design of a geothermal installation. *Renew. Energy* **2016**, *89*, 1–12. [[CrossRef](#)]
29. Uponor. *Guía de Microrredes de Distrito de Calor y Frío*, 1st ed.; Uponor: Pfungen, Switzerland, 2011.
30. Ministerio de Industria. *Energía y Turismo, Dirección General de Política Energética y Minas, Reglamento de Instalaciones Térmicas en los Edificios (RITE)*; Ministerio de Industria: Madrid, Spain, 2013.
31. European Commission. *Reglamento (UE) 813/2013 de la Comisión de 2 de Agosto de 2013 por el que se Desarrolla la Directiva 2009/125/CE del Parlamento Europeo y del Consejo Respecto de Los Requisitos de Diseño Ecológico Aplicables a Los Aparatos de Calefacción y a los Calefactores Combinados*; European Commission: Brussels, Belgium, 2013.
32. Ministerio de Industria. *Energía y Turismo, IDEA (Instituto Para la Diversificación y Ahorro de la Energía), Factores de Emisión de CO₂ y Coeficientes de Paso a Energía Primaria de Diferentes Fuentes de Energía Final Consumidas en el Sector de Edificios en España*; Ministerio de Industria: Madrid, Spain, 2014.



Chapter V
CONCLUSIONS AND FUTURE
WORK

V. Conclusions and future work

Finally, Chapter V collects the principal conclusions deduced from the research works presented in the above sections and the future research lines that will provide a continuation of the existing work.

V.I. Conclusions

The present Doctoral Thesis deals with an extensive analysis and evaluation of different components and parts involved in the thermal exchange of very low enthalpy geothermal systems. The methodological procedure and the results have been published in several impact journals as research Scientific Papers.

Chapter V summarizes the main contributions of all the scientific works and highlights the most relevant results of them. This Chapter also includes a discussion of possible directions for future works. In the first place, general conclusions are mentioned below in order to make reference then to some specific topics of the field.

V.I.I. In general terms

- After the development of this research work, a general improvement of the global geothermal knowledge has been achieved. The deep study carried out on geothermal systems has allowed increasing their characterization and optimization.
- It is possible to improve the efficiency of very low geothermal systems through an appropriate assessment and design of the principal components; ground thermal characterization, geothermal exchangers, grouting materials and heat pump operation.
- The implementation of geothermal district heating means an important solution from the environmental, operational and economic dimensions.
- All the results obtained from this Thesis allowed the development of Software GES – Cal to assist and automate the design of a ground source heat pump system located in the province of Ávila (Spain).

V.I.II. Ground thermal conductivity

- The importance of accurately defining the thermal conductivity of the ground in very low enthalpy geothermal systems has been confirmed throughout Chapter II.
- The present Doctoral Thesis applies a series of alternative techniques to determine the ground thermal conductivity contributing to improve the efficiency of the general ground source heat pump system. The results of these methodologies are then compared to the ones obtained by the implementation of a Thermal Response Test. Despite TRT is the most accurate method, the suggested techniques are proven to be suitable for the estimation of the ground thermal conductivity.
- The measuring of the ground temperature has been confirmed as an useful tool for the subsequent estimation of its thermal conductivity parameter.
- Geothermal map of the location of Ávila allows selecting the most suitable areas to implement a geothermal installation as well as acting as the basis for the corresponding geothermal design in the mentioned province.
- Geophysical methods can be used for geothermal purposes to efficiently improve the thermal knowledge of the ground.

V.I.III. Geothermal design

- It is essential to analyze in each specific case the material used as grout in the geothermal borehole. The thermal conductivity of grouting materials highly influences the global heat exchange process between ground and working fluid. Results from the tests of this Thesis include new material mixtures with improved thermal conductivity values and suitable properties to be used as grouting materials.
- Helical-shaped heat exchangers constitute the most appropriate option for vertical closed-loop systems in those areas where the geological conditions allow the drilling of large diameter boreholes. The use of double U-tube heat exchangers (regarding single U-tube) does not mean significant improvements in the global geothermal operation.
- The selection of the geothermal heat pump must be made taking into account the particular energy supply conditions of the area. A geothermal system using electric heat pumps is characterized by high COPs and deeper drillings in comparison to those systems using gas engine heat pumps where COPs and

drilling lengths are considerably reduced. Biogas means a viable solution for supplying gas engine heat pumps in order to reduce the greenhouse gases emission.

- nZEB regulation can be only satisfied in certain cases where the selection of the geothermal heat pump energy supply is based on the characteristics of the energy mix of the particular area.

V.I.IV. Geothermal district heating

- District heating systems aided by geothermal energy mean an ideal solution to reduce the greenhouse gases emission and the operational costs of a set of buildings.
- Despite the elevated high initial investment required by a geothermal district heating, it would be amortized in a short period of time in comparison with a traditional fossil installation.
- Mixed systems constituted by geothermal energy and fossil heaters are also a better solution in relation to the individual and unique use of fossil sources.

V.II. Future works

Once developed the present Doctoral Thesis, a series of research lines and implementations are open to improve, complement and optimize the use of very low enthalpy geothermal systems. The continuous study in the field will allow a continuous improvement of all the parameters that take part in the ground thermal exchange. In this context, the following issues are expected to be addressed in the near future:

- Considering the substantial level of knowledge reached in the thermal characterization of the ground in very low temperature geothermal systems, it would be desirable to extend it on medium and high enthalpy geothermal resources with the aim of contributing to make them more accessible.
- Within the framework of deep geothermal resources, the most frequent technologies currently used in the electricity generation (such as the Kalina cycle) could be taken into account for a possible utilization in low enthalpy geothermal systems.
- Broaden the range of possibilities offered by GES – Cal software so that it enables the geothermal design for an extensive number of locations. To this

effect, the thermal and geological conditions of these areas would have to be evaluated.

- Continuing with the improvement of the geothermal design, additional components of low temperature systems could be also analyzed. Thus, different heat carrier fluids could be experimentally tested to define the most appropriate mixtures depending on the particular conditions of the area and installation.
- Finally, the possibility of monitoring a real geothermal borehole could be considered. It would mean an excellent tool in the constant search of improving and optimizing the geothermal design.

REFERENCES

References

- [1] Younger, P.L. *Energy: All That Matters*; Hodder and Stoughton/John Murray: London, UK, (2014).
- [2] Dickson, M., Fanelli, M. *Geothermal Energy*. London: Routledge, (2003). <https://doi.org/10.4324/9781315065786>.
- [3] Armstead, H.C.H., *Geothermal Energy. Its Past, Present and Future Contribution to the Energy Needs of Man*. 2nd Edition. E. & F.N. Spon, London (1983), 404.
- [4] Enrico Barbier, *Geothermal energy technology and current status: an overview*. *Renewable and Sustainable Energy Reviews*, 6 (1–2), 2002, 3-65.
- [5] M.P. Hochstein, *Classification and assessment of geothermal resources*. M.H. Dickson, M. Fanelli (Eds.), *Small geothermal resources*, UNITAR/UNDP Centre for Small Energy Resources, Rome Italy (1990), 31-59.
- [6] White, D.E. and D.L. Williams, Eds., 1975, *Assessment of Geothermal Resources of the United States: U.S. Geological Survey Circular 727*, U.S., Government Printing Office, (1975) 155.
- [7] Lund, J.W., *Chena Hot Springs: Geo-Heat Center Quarterly Bulletin*, Klamath Falls, OR, (2006) 27 (3). 2–4.
- [8] IDAE, Instituto para la Diversificación y Ahorro de la Energía. *Evaluación del potencial de energía geotérmica. Estudio Técnico per 2011-2020*. (2011).
- [9] Guillermo Llopis Trillo, Vicente Rodrigo Angulo, *Guía de la Energía Geotérmica*. Fundación de la Energía de la Comunidad de Madrid. (2008).
- [10] Stober, I.; Bucher, K., *History of geothermal energy use*. In *Geothermal Energy: From Theoretical Models to Exploration and Development*; Stober, I., Bucher, K., Eds.; Springer-Verlag:Berlin/Heidelberg, Germany, (2013).
- [11] Dickson, M.H.; Fanelli, M. *Geothermal Energy: Utilization and Technology*; Earthscan: London, UK, (2005).
- [12] Lund, J. W.; Freeston, D. *Worldwide direct uses of geothermal energy 2000*. *Geothermics*, (2000) 30, 29–68.

-
- [13] John W. Lund, Tonya L. Boyd, Direct utilization of geothermal energy 2015 worldwide review. *Geothermics* (2016) 60, 66–93.
- [14] Dickson, M. H.; Fanelli, M. Geothermal R. & D. in developing countries: Africa, Asia and the Americas. *Geothermics*, (1988) 17, 815–77.
- [15] Ruggero Bertani, Geothermal Power Generation in the World 2010-2014 Update Report. Proceedings World Geothermal Congress (2015).
- [16] Sanner, B., Shallow geothermal energy. *Bulletin Geo-Heat Center*, (2001) 22, No. 2, 19–25.
- [17] Cui P, Li X, Manc Y, Fang Z., Heat transfer analysis of pile geothermal heat exchangers with spiral coils. *Appl Energy* (2011) 88, 4113–9.
- [18] Yang W, Shi M, Liu G, Chen Z., A two-region simulation model of vertical U-tube ground heat exchanger and its experimental verification. *Appl Energy* (2009) 86, 2005–12.
- [19] Stuart J. Self, Bale V. Reddy, Marc A. Rosen, Geothermal heat pump systems: Status review and comparison with other heating options. *Applied Energy* (2013) 101, 341–348.
- [20] Omer AM. Ground-source heat pumps systems and applications. *Renew Sust Energy Rev* (2008) 12, 344–71.
- [21] Wu R. Energy efficiency technologies – air source heat pump vs. ground source heat pump. *J Sust Dev* (2009) 2, 14–23.
- [22] Bi Y, Wang X, Liu Y, Zhang H, Chen L. Comprehensive exergy analysis of a ground-source heat pump system for both building heating and cooling modes. *Appl Energy* (2009) 86, 2560–5.
- [23] Bloomquist RG. Geothermal space heating. *Geothermics* (2003) 32, 513–26.
- [24] Hamza, V.M., An appraisal of geothermal energy use in Brazil. *Transactions - Geothermal Resources Council* (2003) 27, 59-63.

-
- [25] Méndez, C.A.O., Armenta, M.F., Silva, G.R., Geothermal potential in Mexico. *Geothermia* (2011) 24 (1), 50-58.
- [26] Colmenar-Santos, A., Rosales-Asensio, Borge-Díez, D., Castro-Gil, M., An assessment of geothermal potential in Spain and its end-uses. *Energy Planning: Approaches and Assessment* (2017), 67-130.
- [27] A. Aragón-Aguilar, E. Santoyo-Castelazo and E. Santoyo, Evaluation of the productivity of geothermal wells by analyzing production measurements and the damage effect. *Int. J. Energy Res.* (2017) 41, 817–828.
- [28] P. Jalili, D. D. Ganji, S. S. Nourazar, Investigation of convective-conductive heat transfer in geothermal system. *Results in Physics* (2018) 10, 568-587.
- [29] Xianzhi Song, Yu Shi, Gensheng Li, Zhonghou Shen, Xiaodong Hu, Zehao Lyu, Rui Zheng, Gaosheng Wang, Numerical analysis of the heat production performance of a closed loop geothermal system. *Renewable Energy* (2018) 120, 365-378.
- [30] Di Sipio, E., Destro, E., Galgaro, A., Chiesa, S., Manzella, A., Shallow geothermal energy use: Mapping of geothermal potential and legal status in Italy. *Rendiconti Online Società Geologica Italiana*, (2012) 21, PART 2, 809-811.
- [31] Antonio Galgaro, Eloisa Di Sipio, Giordano Teza, Elisa Destro, Michele De Carli, Sergio Chiesa, Angelo Zarrella, Giuseppe Emmi, Adele Manzella, Empirical modeling of maps of geo-exchange potential for shallow geothermal energy at regional scale. *Geothermics*, (2015) 57, 173-184.
- [32] Alessandro Casasso, Rajandrea Sethi, G.POT: A quantitative method for the assessment and mapping of the shallow geothermal potential. *Energy* (2016) 106, 765-773.
- [33] Iosifina Iosif Stylianou, Savvas Tassou, Paul Christodoulides, Ioannis Panayides, Georgios Florides, Measurement and analysis of thermal properties of rocks for the compilation of geothermal maps of Cyprus. *Renewable Energy* (2016) 88, 418-429.

- [34] Alessandro Casasso, Rajandrea Sethi, Assessment and mapping of the shallow geothermal potential in the province of Cuneo (Piedmont, NW Italy). *Renewable Energy* (2017) 102, Part B, 306-315.
- [35] Drew L. Siler, James E. Faulds, Nicholas H. Hinz, Gregory M. Dering, Joel H. Edwards and Brett Mayhew, Three-dimensional geologic mapping to assess geothermal potential: examples from Nevada and Oregon. *Geothermal Energy Science – Society – Technology* (2019) 7:2.
- [36] S. A. Ghoreishi-Madiseh, F. Hassani, F. Abbasy, Numerical and experimental study of geothermal heat extraction from backfilled mine stopes. *Applied Thermal Engineering*, (2015) 90 (5), 1119-1130.
- [37] Zehao Lyu, Xianzhi Song, Gensheng Li, Xiaodong Hu, Yu Shi, Zhipeng Xu, Numerical analysis of characteristics of a single U-tube downhole heat exchanger in the borehole for geothermal wells. *Energy* (2017) 125, 186-196.
- [38] Yunus Emre Yuksel, Murat Ozturk, Thermodynamic and thermoeconomic analyses of a geothermal energy based integrated system for hydrogen production. *International Journal of Hydrogen Energy* (2017) 42 (4), 2530-2546.
- [39] Gaosheng Wang, Xianzhi Song, Yu Shi, Baojiang Sun, Rui Zheng, Jiacheng Li, Zhijun Pei, Hengyu Song, Numerical investigation on heat extraction performance of an open loop geothermal system in a single well. *Geothermics*, (2019) 80, 170-184.
- [40] Nurullah Kayaci, Hakan Demir, Barış Burak Kanbur, Şevket Ozgur Atayilmaz, Ozden Agra, Ruşen Can Acet, Zafer Gemici, Experimental and numerical investigation of ground heat exchangers in the building foundation. *Energy Conversion and Management*, (2019) 188, 162-176.
- [41] Zongliang Qiao, Youfei Tang, Lei Zhang, Chunjian Pan, Carlos E. Romero, Xingchao Wang, Joshua Charles, Fengqi Si, Carlos Rubio Maya, Performance analysis and optimization design of an axial-flow vane separator for supercritical CO₂ (sCO₂)-water mixtures from geothermal reservoirs. *International Journal of Energy Research* (2019) 43 (6), 2327-2342.

- [42] Simon Schüppler, Paul Fleuchaus and Philipp Blum, Techno-economic and environmental analysis of an Aquifer Thermal Energy Storage (ATES) in Germany. *Geothermal Energy Science – Society – Technology* (2019) 7:11.
- [43] J. D. Templeton, S. A. Ghoreishi-Madiseh, F. Hassani, M. J. Al-Khawaja, Abandoned petroleum wells as sustainable sources of geothermal energy. *Energy* (2014) 70, 366-373.
- [44] N. M. Wight, N. S. Bennett, Geothermal energy from abandoned oil and gas wells using water in combination with a closed wellbore. *Applied Thermal Engineering* (2015) 89, 908-915.
- [45] Loredo, C., Ordóñez, A., Garcia-Ordiales, E., Álvarez, R., Roqueñi, N., Cienfuegos, P., Peña, A., Burnside, N.M., Hydrochemical characterization of a mine water geothermal energy resource in NW Spain. *Science of the Total Environment* (2017) 576, 59-69.
- [46] Marius Røksland, Tommy A. Basmoen, Dan Sui, Geothermal Energy Extraction from Abandoned Wells. *Energy Procedia* (2017) 105, 244-249.
- [47] Javier Menéndez, Almudena Ordóñez, Rodrigo Álvarez, Jorge Loredo, Energy from closed mines: Underground energy storage and geothermal applications. *Renewable and Sustainable Energy Reviews* (2019) 108, 498-512.
- [48] D. Sui, E. Wiktorski, M. Røksland, T. A. Basmoen, Review and investigations on geothermal energy extraction from abandoned petroleum wells. *J Petrol Explor Prod Technol* (2019) 9: 1135.
- [49] Sayem Zafar, Ibrahim Dincer, Energy, exergy and exergoeconomic analyses of a combined renewable energy system for residential applications. *Energy and Buildings* (2014) 71, 68-79.
- [50] Reza Ghezelbash, Mahmood Farzaneh-Gord, Hamidreza Behi, Meisam Sadi, Heshmatollah Shams Khorramabady, Performance assessment of a natural gas expansion plant integrated with a vertical ground-coupled heat pump. *Energy* (2015) 93, Part 2, 2503-2517.

- [51] Nurdan Yildirim, Seda Genc, Thermodynamic analysis of a milk pasteurization process assisted by geothermal energy. *Energy* (2015) 90, Part 1, 987-996.
- [52] Martin J. Atkins, Michael R. W. Walmsley, Timothy G. Walmsley, James R. Neale, Integration of Biomass Conversion Technologies and Geothermal Heat into a Model Wood Processing Cluster. *Chemical Engineering Transactions*, (2015) 45.
- [53] Jradi, M., Veje, C., Jørgensen, B.N., Performance analysis of a soil-based thermal energy storage system using solar-driven air-source heat pump for Danish buildings sector. *Applied Thermal Engineering* (2017) 114, 360-373.
- [54] Mohamed E. Zayed, Jun Zhao, Ammar H. Elsheikh, Farid A. Hammad, Ling Ma, Yanping Du, A. E. Kabeel, S. M. Shalaby, Applications of cascaded phase change materials in solar water collector storage tanks: A review. *Solar Energy Materials and Solar Cells* (2019) 199, 24-49.
- [55] G. Yang, X. Q. Zhai, Optimal design and performance analysis of solar hybrid CCHP system considering influence of building type and climate condition. *Energy* (2019) 174, 647-663.
- [56] Wansheng Pei, Wenbing Yu, Shuangyang Li, Jiazuo Zhou, A new method to model the thermal conductivity of soil-rock media in cold regions: An example from permafrost regions tunnel. *Cold Regions Science and Technology* (2013) 95, 11-18.
- [57] L. Lira-Cortés, González Rodríguez, O. J., Méndez-Lango, E., Sistema de Medición de la Conductividad Térmica de Materiales Sólidos Conductores, Diseño y Construcción. *Simposio de Metrología* (2008).
- [58] Randi Kalskin Ramstad, Hans de Beer, Kirsti Midttømme, Janusz Koziel and Bjørn Wissing, Thermal diffusivity measurement at NGU - Status and method development 2005-2008. *Geological Survey of Norway* (2009).
- [59] D. Barry-Macaulay, A. Bouazza, R.M. Singh, B. Wang, P.G. Ranjith, Thermal conductivity of soils and rocks from the Melbourne (Australia) region. *Engineering Geology* (2013) 164, 131-138.

-
- [60] Anca-Marina Vijdea, Christopher Weindl, Ana Cosac, Natalia-Silvia Asimopolos, David Bertermann, Estimating the thermal properties of soils and soft rocks for ground source heat pumps installation in Constanta county, Romania. *J Therm Anal Calorim* (2014) 118:1135–1144.
- [61] Jorand, R., C. Vogt, G. Marquart, and C. Clauser, Effective thermal conductivity of heterogeneous rocks from laboratory experiments and numerical modeling, *J. Geophys. Res. Solid Earth*, (2013) 118, 5225–5235.
- [62] Mogensen, P. 1983. Fluid to duct wall heat transfer in duct system heat storages. *International Conference on Subsurface Heat Storage in Theory and Practice*, Stockholm, (1983) 652-657.
- [63] Jasmin Raymond, *Colloquium 2016: Assessment of the subsurface thermal conductivity for geothermal applications*. Natural Resources Canada (2018).
- [64] M.D. Smith, R.L. Perry, Borehole grouting: field studies and thermal performance testing, *ASHRAE Transactions* (1999) 105.
- [65] M.L. Allan, A.J. Philippacopoulos, *Performance Characteristics and Modelling of Cementitious Grouts for Geothermal Heat Pumps* (2000).
- [66] C. Lee, K. Lee, H. Choi, H.- Choi, Characteristics of thermally-enhanced bentonite grouts for geothermal heat exchanger in South Korea, *Science China Technological Sciences* (2010) 53, 123-128.
- [67] F. Delaleux, X. Py, R. Olives, A. Dominguez, Enhancement of geothermal borehole heat exchangers performances by improvement of bentonite grouts conductivity, *Applied Thermal Engineering* (2012) 33-34, 92-99.
- [68] Selçuk Erol, Bertrand François, Efficiency of various grouting materials for borehole heat exchangers. *Applied Thermal Engineering* (2014) 70, 788-799.
- [69] Roque Borinaga-Treviño, Pablo Pascual-Muñoz, Miguel Ángel Calzada-Pérez, Daniel Castro-Fresno, Freeze–thaw durability of cement-based geothermal grouting materials. *Construction and Building Materials* (2014) 55, 390–397.

- [70] P.J. Petit, J.P. Meyer, A technoeconomic analytical comparison of the performance of air source and horizontal-ground-source air conditioners in South Africa, *Int. J. Energy Res.* (1997) 21, 1011–1021.
- [71] P.J. Petit, J.P. Meyer, Economic potential of vertical ground source heat pumps compared to air source air conditioners in South Africa, *Energy* (1998) 23, 137–143.
- [72] H. Esen, M. Inalli, Esen M., Technoeconomic appraisal of a ground source heat pump system for a heating season in eastern Turkey, *Energy Convers. Manage* (2006) 47, 1281–1297.
- [73] H. Esen, M. Inalli, M: Esen, A technoeconomic comparison of the ground-coupled and air-coupled heat pump systems for space cooling, *Build. Environ.* (2007) 42, 1955–1965.
- [74] V.R. Tarnawski, W.H. Leong, T. Momose, Y: Hamada, Analysis of ground source heat pumps with horizontal ground heat exchangers for northern Japan, *Renewable Energy* (2009) 34, 127–134.
- [75] X.Q. Zhai, Y. Yang, Experience in the application of a ground source heat pump system in an archives building, *Energy Build.* (2011) 43, 3263–3270.
- [76] A. Michopoulos, T. Zachariadis, N: Kyriakis, Operation characteristics and experience of a ground source heat pump system with a vertical ground heat exchanger, *Energy* (2013) 51, 349–357.
- [77] S. Focaccia, F. Tinti, An innovative Borehole Heat Exchanger configuration with improved heat transfer. *Geothermics* (2013) 48, 93–100.
- [78] Angelo Zarrella, Antonio Capozza, Michele De Carli, Performance analysis of short helical borehole heat exchangers via integrated modelling of a bore field and a heat pump: A case study. *Applied Thermal Engineering* (2013) 61, 36-47.
- [79] Jin-Uk Lee, Taeyeon Kim, Seung-Bok Leigh, Applications of building-integrated coil-type ground-coupled heat exchangers—Comparison of performances of vertical and horizontal installations. *Energy and Buildings* (2015) 93, 99-109.
- [80] T.L. Tsaros, R.A. Gaggioli, P.A. Domanski, Exergy analysis of heat pumps. *ASHRAE Trans.*, (1987) 93 (2), 1781-1793.

- [81] R.R. Crawford, An experimental laboratory investigation of second law analysis of a vapor-compression heat pump. *ASHRAE Trans.*, (1988) 94 (2), 1491-1504.
- [82] M.M. Salah El-Din, Optimization of totally irreversible refrigerators and heat pumps. *Energy Convers. Manage.*, (1999) 40, 423-436.
- [83] A. Hepbasli, O. Akdemir, Energy and exergy analysis of a ground source (geothermal) heat pump system. *Energy Conversion and Management*, (2004) 45 (5), 737-753.
- [84] Arif Hepbasli, Zafer Erbay, Filiz Icier, Neslihan Colak, Ebru Hancioglu, A review of gas engine driven heat pumps (GEHPs) for residential and industrial applications. *Renewable and Sustainable Energy Reviews* (2009) 13, 85-99.
- [85] Feng-Guo Liu, Zhong-Yun Tian, Fu-Jiang Dong, Chao Yan, Rui Zhang, Ai-Bin Yan, Experimental study on the performance of a gas engine heat pump for heating and domestic hot water. *Energy and Buildings* (2017) 152, 273-278.
- [86] Bin Hu, Cuichao Li, Xiang Yin, Feng Cao, Pengcheng Shu, Thermal modeling and experimental research of a gas engine-driven heat pump in variable condition. *Applied Thermal Engineering* (2017) 123, 1504-1513.
- [87] BCS, 2008. Waste Heat Recovery: Technology Opportunities in the US Industry. *Waste Heat Recovery: Technology Opportunities in the US Industry*, 1-112.
- [88] M. Harris, Thermal energy storage in Sweden and Denmark, *Potentials Technol. Transfer* (2011), 42.
- [89] B. Rezaie, M.A. Rosen, District heating and cooling: review of technology and potential enhancements. *Appl. Energy*, (2012) 93, 2-10.
- [90] H. Lund, S. Werner, R. Wiltshire, S. Svendsen, J.E. Thorsen, F. Hvelplund, B.V. Mathiesen 4th Generation District Heating (4GDH). Integrating smart thermal grids into future sustainable energy systems. *Energy*, (2014) 68, 1-11.
- [91] A. Hepbasli, L. Ozgener, Development of geothermal energy utilization in Turkey: a review. *Renew Sustainable Energy Rev.*, (2004) 8, 433-460.

- [92] Leyla Ozgener, Arif Hepbasli, Ibrahim Dincer, A key review on performance improvement aspects of geothermal district heating systems and applications. *Renewable and Sustainable Energy Reviews* (2007) 11 (8), 1675-1697.
- [93] C. Coskun, Zuhul Oktay, I. Dincer, New energy and exergy parameters for geothermal district heating systems. *Applied Thermal Engineering* (2009) 29 (11-12), 2235-2242.
- [94] A. Hepbasli, A review on energetic, exergetic and exergoeconomic aspects of geothermal district heating systems (GDHSs). *Energy Convers. Manage.*, (2010), 51 (10), 2041-2061.
- [95] Poul Alberg Østergaard, Henrik Lund, A renewable energy system in Frederikshavn using low-temperature geothermal energy for district heating. *Applied Energy* (2011) 88 (2), 479-487.
- [96] Sotirios A. Kyriakis, Paul L. Younger, Towards the increased utilization of geothermal energy in a district heating network through the use of a heat storage. *Applied Thermal Engineering* (2016) 94, 99-110.
- [97] Muhammet Yürüsoy, Ali Keçebas, Advanced exergo-environmental analyses and assessments of a real district heating system with geothermal energy. *Applied Thermal Engineering* (2017) 113, 449-459.
- [98] Halit Arat, Oguz Arslan, Optimization of district heating system aided by geothermal heat pump: A novel multistage with multilevel ANN modelling. *Applied Thermal Engineering* (2017) 111, 608-623.

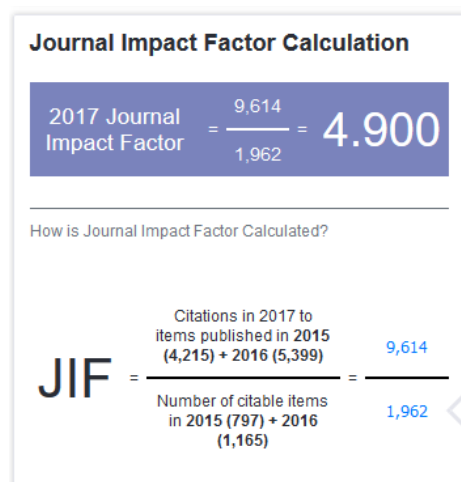
APPENDIX A
INDEXATION AND IMPACT
FACTOR OF THE JOURNALS

Indexation and impact factor of journals

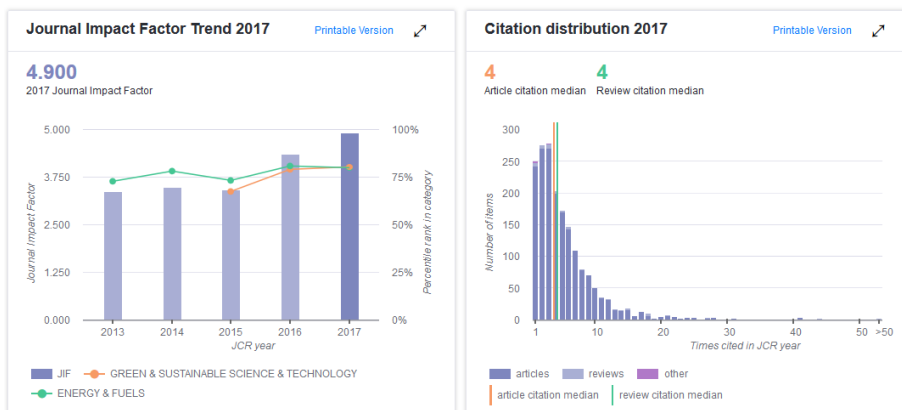
Paper 1: "Analysis of the process of design of a geothermal installation"

Paper 6: "Analysis and study of different grouting materials in vertical geothermal closed-loop systems"

Journal	Renewable Energy
Editorial	PERGAMON-ELSEVIER SCIENCIE LTD
ISSN	0960-1481
Impact Factor (2017)	4.900
Ranking	7/33
Quartile	Q1



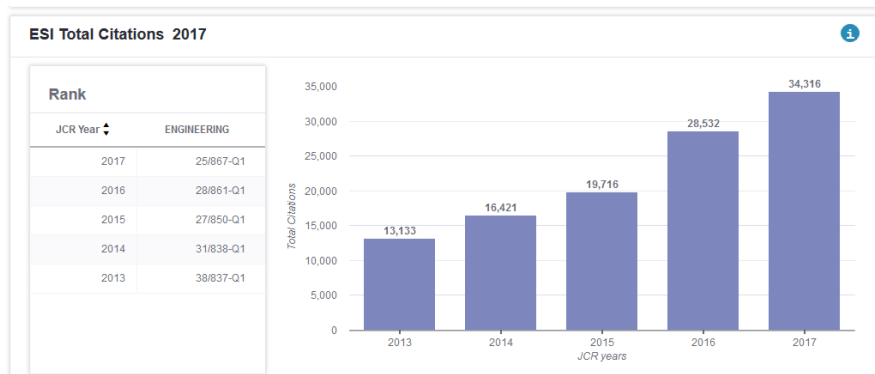
Appendix A. Indexation and impact factor of the journals



Rank 2017

JCR Impact Factor

JCR Year	GREEN & SUSTAINABLE SCIENCE & TECHNOLOGY			ENERGY & FUELS		
	Rank	Quartile	JIF Percentile	Rank	Quartile	JIF Percentile
2017	7/33	Q1	80.303	20/97	Q1	79.897
2016	7/31	Q1	79.032	18/92	Q1	80.978
2015	10/29	Q2	67.241	24/88	Q2	73.295
2014	N/A	N/A	N/A	20/89	Q1	78.090
2013	N/A	N/A	N/A	23/83	Q2	72.892



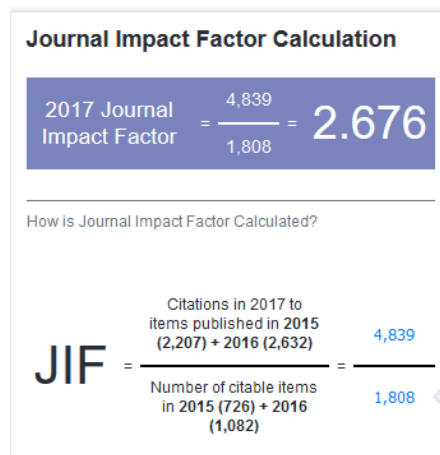
Paper 2: "Measuring of thermal conductivities of soils and rocks to be used in the calculation of a geothermal installation"

Paper 5: "Comparative analysis of different methodologies used to estimate the ground thermal conductivity in low enthalpy geothermal systems"

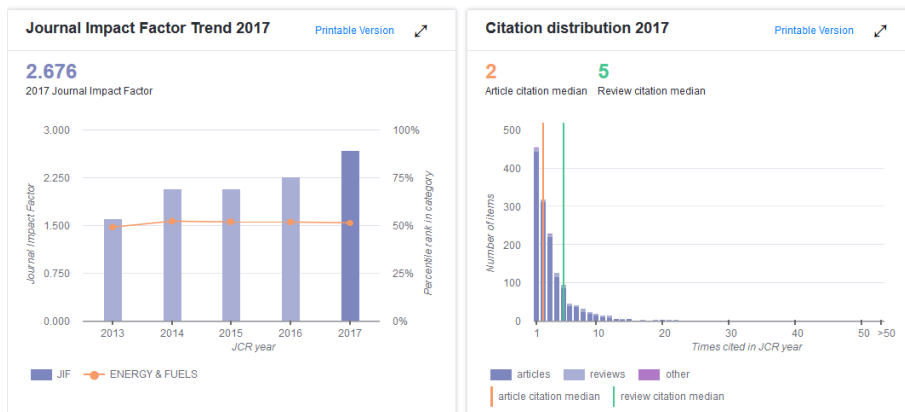
Paper 7: "Efficiency analysis of the main components of a vertical closed-loop system in a borehole heat exchanger"

Paper 9: "Economic and environmental analysis of different district heating systems aided by geothermal energy"

Journal	Energies
Editorial	MDPI
ISSN	1996-1073
Impact Factor (2017)	2.676
Ranking	48/97
Quartile	Q2



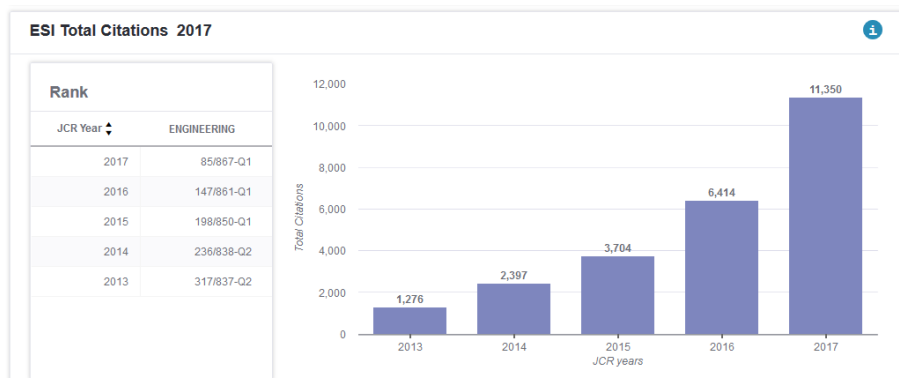
Appendix A. Indexation and impact factor of the journals



Rank 2017

JCR Impact Factor

JCR Year ↓	ENERGY & FUELS		
	Rank	Quartile	JIF Percentile
2017	48/97	Q2	51.031
2016	45/92	Q2	51.630
2015	43/88	Q2	51.705
2014	43/89	Q2	52.247
2013	43/83	Q3	48.795

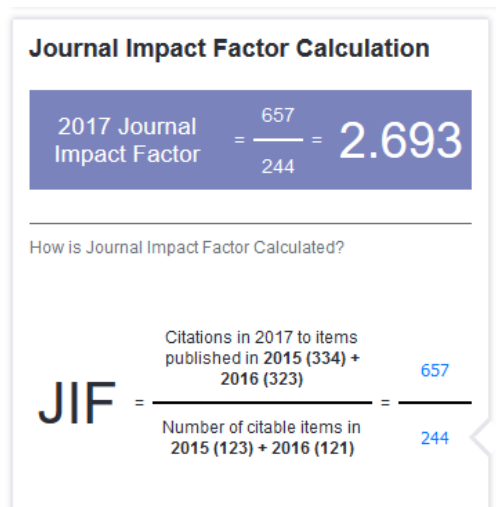


Paper 3: "Thermal conductivity map of the Avila region (Spain) based on thermal conductivity measurements of different rock and soil samples"

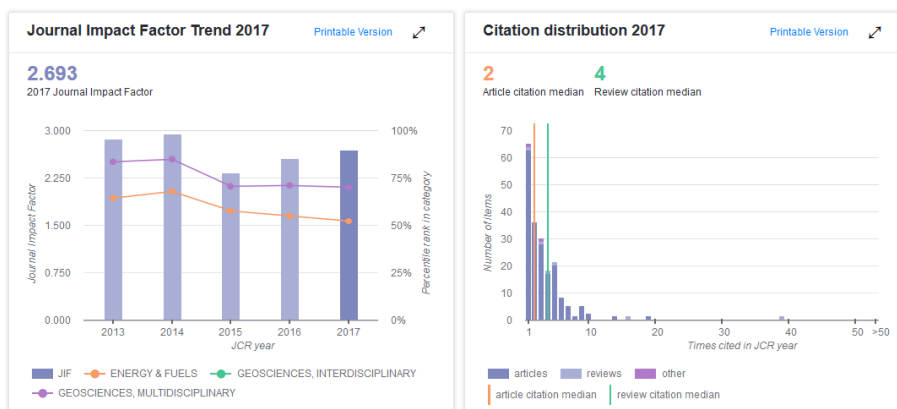
Paper 4: "Thermal conductivity characterization of three geological formations by the implementation of geophysical methods"

Paper 8: "Technical optimization of the energy supply in geothermal heat pumps"

Journal	Geothermics
Editorial	PERGAMON-ELSEVIER SCIENCIE LTD
ISSN	0375-6505
Impact Factor (2017)	2.693
Ranking	47/97
Quartile	Q2



Appendix A. Indexation and impact factor of the journals

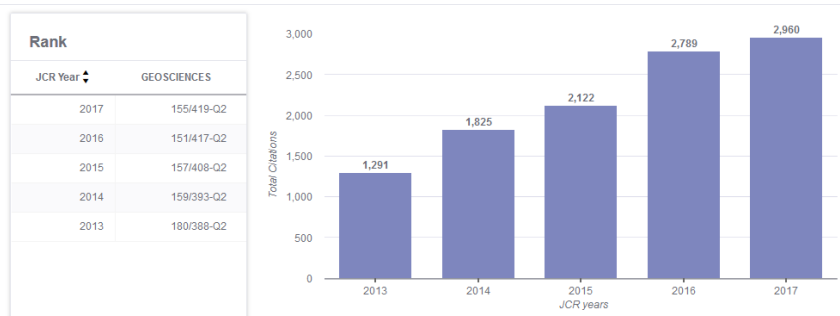


Rank 2017

JCR Impact Factor

JCR Year	ENERGY & FUELS			GEOSCIENCES, MULTIDISCIPLINARY			GEOSCIENCES, INTERDISCIPLINARY		
	Rank	Quartile	JIF Percentile	Rank	Quartile	JIF Percentile	Rank	Quartile	JIF Percentile
2017	47/97	Q2	52.062	57/190	Q2	70.263	N/A	N/A	N/A
2016	42/92	Q2	54.891	55/188	Q2	71.011	N/A	N/A	N/A
2015	38/88	Q2	57.386	55/184	Q2	70.380	N/A	N/A	N/A
2014	29/89	Q2	67.978	27/175	Q1	84.857	N/A	N/A	N/A
2013	30/83	Q2	64.458	29/174	Q1	83.621	N/A	N/A	N/A

ESI Total Citations 2017



APPENDIX B
GES – Cal SOFTWARE

GES – Cal SOFTWARE



Type: Registration of intellectual property

Reference: SA – 92- 19

University: University of Salamanca

Abstract:

GES – Cal Software, developed in Python, is software built-up for the design of ground source heat pump systems. All the calculations included in the software follow the principles and theoretical basis of the “*Institute for the Diversification and Energy Saving*” (IDEA) but also implementing the results from the experimental research period. The combination and inclusion of these results have allowed obtaining the most optimal geothermal design for each particular case. The first version of GES – Cal is only conceived for low enthalpy geothermal systems located in the province of Ávila since most of the tests and studies have been focused on this area.

Applications:

It is highly necessary to have an automatic tool for designing a ground source heat pump system as accurately as possible. With that purpose, GES – Cal is a response to the need of adapting the configuration of the geothermal system to the particular

conditions of the area and needs. In this way, this software solves the problems identified in existing geothermal applications that do not consider the specific properties of the ground in the area or the most optimal design of the particular case.

Authors:

- Cristina Sáez Blázquez
- Ignacio Martín Nieto
- Rocio Mora Fernández de Córdoba
- Arturo Farfán Martín
- Diego González Aguilera

Additional information:

By the introduction of a series of initial data corresponding to the energy demand, building characteristics, specific location and preferences in the geothermal configuration, GES – Cal automatically presents the most appropriate solutions for the case.

Once all the inputs have been selected and the design has been developed, the software offers the possibility of comparing the geothermal resource with other energy alternatives from an economic and environmental point of view. Thus, GES – Cal calculates the initial investment and operational costs of the suggested geothermal solution and makes an exhaustive comparison with other energy sources. Additionally, the mentioned software estimates the greenhouse gases emission of the geothermal solution and the rest of possible energy alternatives.

Inputs:

- Energy demands to be covered by the ground source heat pump system, building dimensions and characteristics and ground availability.
- Heat pump model and operation period.
- Heat exchanger design.
- Specific location of the system.

Outputs:

- Heat pump power.
- Principal design parameters.
- Drilling length, number of boreholes and most optimal loop configuration.
- Initial investment required.
- Economic comparison.
- Greenhouse gases emission and comparison with other energy solutions.



Figure B1. Main GES – Cal software interface.

The screenshot displays the 'Datos Iniciales' (Initial Data) section of the GES-Cal software. It is divided into four main input areas:

- 1. Demanda (Demand):** Includes 'Autoclavado Demanda' (Demand Autoclaving) set to 'Constante', 'Tipo de Demanda' (Demand Type) set to 'Calentamiento', and 'Superficie [m²]' (Area [m²]) set to 100.0.
- 2. Bomba de calor (Heat Pump):** Includes 'Tipo de bomba' (Pump Type) set to 'Electrica', 'Horas de funcionamiento' (Operating Hours) set to 2000, 'COP' set to 4.00, 'Caudal Potencia' (Power Flow) set to 5.00 [kW], 'Subdimensionamiento' (Undersizing) set to 2.00 [kW], and 'Potencia Final' (Final Power) set to 7.00 [kW].
- 3. Terreno (Terrain):** Includes 'Dimensiones de terreno disponibles' (Available terrain dimensions) with 'Ancho' (Width) set to 20 [m] and 'Largo' (Length) set to 20 [m], and 'Conductividad Terreno' (Soil Conductivity) set to 0.3 [W/mK].
- 4. Intercambiadores de calor (Heat Exchangers):** Includes 'Tipo' (Type) set to 'horizontal', 'Material' (Material) set to 'PE', and 'Diámetro' (Diameter) set to 'Estándar geotérmico horizontal'.

On the right side, there is a 3D topographic map of the site, a 'Zona Selección' (Selection Area) button, and a 'SIGUIENTE' (NEXT) button at the bottom right.

Figure B2. Input data introduction in GES – Cal software.

The screenshot displays the 'Proyecto' (Project) section of the GES-Cal software, showing calculated parameters and a final design table.

Parámetros de diseño (Design Parameters):

- Temperatura de salida (Outlet Temperature): 5.23 [°C]
- Temperatura mínima de entrada (Minimum inlet temperature): 5.61 [°C]
- Temperatura mínima del terreno (T_g) (Minimum ground temperature): 17.00 [°C]
- Resistencia de las sondas (R_g) (Well resistance): 0.2394
- Resistencia de la tierra (R_t) (Ground resistance): 0.3704
- Factor de utilización (F_u) (Utilization factor): 0.403

Longitud del intercambiador (Exchanger Length): 266.43 [m]

Diseño Final (Final Design):

	Opción 1	Opción 2	Opción 3
Número de sondas (Number of wells)	1	2	2
Longitud de cada sonda (Length of each well) [m]	133	74	76
Longitud total de perforación (Total drilling length) [m]	133	147	152
Distancia entre sondas (Distance between wells) [m]	0	28	28

An illustration of a house with a geothermal well is shown on the right. A 'SIGUIENTE' (NEXT) button is located at the bottom right.

Figure B3. Final geothermal design proposed by GES – Cal software.

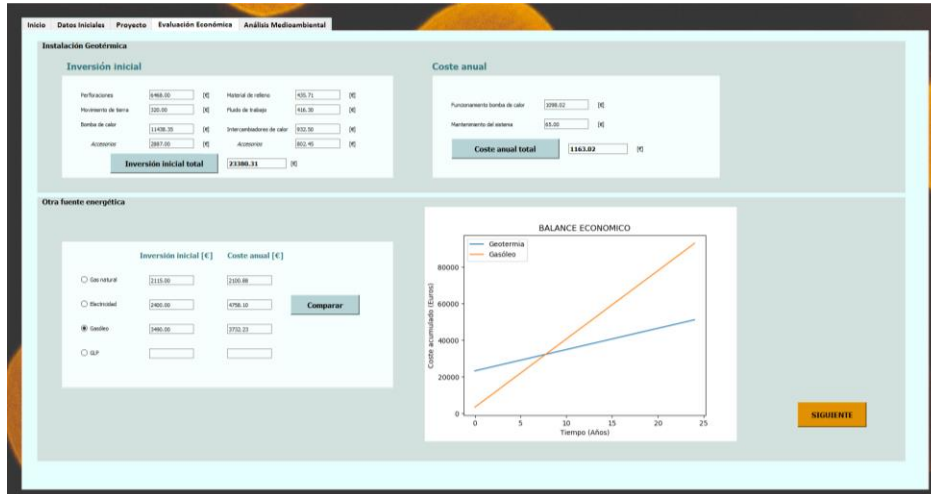


Figure B3. Economic analysis made by GES – Cal software.

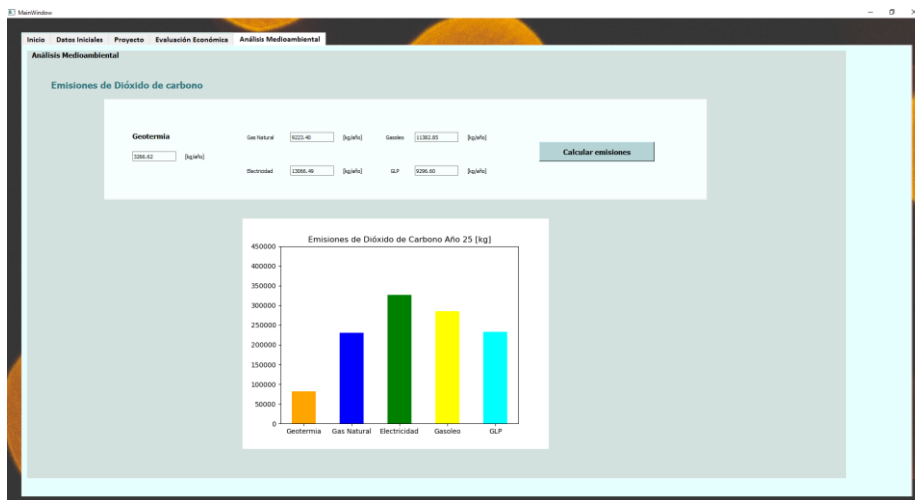


Figure B4. Environmental evaluation of the geothermal system made by GES – Cal software.

Curriculum Vitae

Cristina Sáez Blázquez

22/03/1990, Ávila (Spain)

Education

- **2015-2019**
PhD at the Department of Cartographic and Land Engineering, Higher Polytechnic School of Ávila University of Salamanca, Spain
- **2016-2018**
Master's Degree in Mining Engineering and Energy Resources, Higher and Technic School of Mining Engineers, University of León, Spain
- **2012-2014**
Engineering Degree in Mining and Energy Technology, Higher Polytechnic School of Ávila, University of Salamanca, Spain
- **2012-2013**
Master's Degree in Occupational Risk Prevention Camilo José Cela University, Spain
- **2008-2012**
Technical Engineering in Mining, area: drillings and mining prospecting, Higher Polytechnic School of Ávila, University of Salamanca, Spain

Work and Research Experience

- **2015-2019**
FPU researcher at TIDOP Research Group
- **2018**
Research stay at Padua University, Italy (2 months)
- **2017**
Research stay at Polytechnic School of Turin, Italy (3 months)
- **2016**
Research stay at Industrial Polytechnic School of Vigo, Spain (1 week)

Research grants

- **2013-2014**
Grant aimed at the collaboration with university departments
Ministry of Education, Culture and Sport
- **2015-2019**
FPU, University professor formation
Ministry of Education, Culture and Sport

Awards and mentions

- **2017**
Finalist at the EDP University Challenge
- **2015**
Winner at the TECUE call
- **2013**
Finalist at the Hueco Energy Starter
- **2012**
Winner at the EDP University Challenge
Extraordinary award for the Technical Engineering in Mining, area:
drillings and mining prospecting

Educational practice

- **2016-2019**
Subject: Drillings
Degree: Engineering Degree in Mining and Energy Technology
Higher Polytechnic School of Ávila, University of Salamanca

Subject: Working engineering
Degree: Engineering Degree in Mining and Energy Technology
Higher Polytechnic School of Ávila, University of Salamanca
- **2018-2019**
Subject: Market, logistics and petroleum products distribution
Degree: Engineering Degree in Mining and Energy Technology
Higher Polytechnic School of Ávila, University of Salamanca

Subject: Online course "Specialization in the advance design of low enthalpy geothermal systems"
Higher Polytechnic School of Ávila, University of Salamanca

Participation in educational innovation projects

- **2018-2019**
Project: "Design of the initial phase of a software for the calculation of renewable energy installations"
Project: "Analysis of the different possibilities of integration renewable energies"
- **2013**
Project: "Implementation of a drilling for the realization of different practices at the Higher Polytechnic School of Ávila."

Participation in research projects

- **2018-2019**
Project: "Development of an intelligent motor of wind predictor"
- **2014-2017**
Project: "Integrated system for energy optimization in buildings: BIM technologies, indoor mapping, UAV and energy simulation tools (ENERBIUS)"
- **2015-2016**
Project: "Energy modeling of building facades. EFECONS"

Scientific committee participation

Reviewer in indexed journals

- **2017-2019**
Editorial: MDPI
Editorial: ELSEVIER
Editorial: SCIENCE DOMAIN

Evaluating Committee

- **2018-2019**
ICSC-CTIES IBERIAN CONGRESS 2018

CYPA CONGRESS 2019

Publications*Journal Papers*

- Cristina Sáez Blázquez, Arturo Farfán Martín, Pedro Carrasco García, Luis Santiago Sánchez Pérez, Sara Jiménez del Caso. "Analysis of the process of design of a geothermal installation", *Renewable Energy* 89 (2016) 1-12.
- Cristina Sáez Blázquez, Arturo Farfán Martín, Ignacio Martín Nieto, Pedro Carrasco García, Luis Santiago Sánchez Pérez, Diego González Aguilera. "Thermal conductivity map of the Avila region (Spain) based on thermal conductivity measurements of different rock and soil samples", *Geothermics* 65 (2017) 60-71.
- Cristina Sáez Blázquez, Arturo Farfán Martín, Ignacio Martín Nieto, Pedro Carrasco García, Luis Santiago Sánchez Pérez and Diego González-Aguilera. "Efficiency Analysis of the Main Components of a Vertical Closed-Loop System in a Borehole Heat Exchanger", *Energies* (2017), 10, 201-216; Special Issue "Low Enthalpy Geothermal Energy".
- Cristina Sáez Blázquez, Arturo Farfán Martín, Ignacio Martín Nieto and Diego González-Aguilera. "Measuring of Thermal Conductivities of Soils and Rocks to Be Used in the Calculation of A Geothermal Installation", *Energies* (2017), 10, 795-813.
- Sara Jiménez Del Caso, Emilio López Cano, Arturo Farfán Martín, Cristina Sáez Blázquez, Javier Martínez Moguerza. "Interrelationship between variables relating to the day ahead market's electricity price". *DYNA Energía y Sostenibilidad* 6, no. 1 (2017).
- Sara Jiménez Del Caso, Emilio Lopez Cano, Arturo Farfan Martín, Cristina Sáez Blázquez, Javier Martínez Moguerza. "Analysis of relevant predictive variables within the day-ahead electricity market". *DYNA* 92, no. 6 (2017).
- Cristina Sáez Blázquez*, Arturo Farfán Martín, Ignacio Martín Nieto, Pedro Carrasco García, Luis Santiago Sánchez Pérez, Diego González-Aguilera. Analysis and study of different grouting materials in vertical geothermal closed-loop systems, *Renewable Energy* 114 (2017) 1189-1200.
- Cristina Sáez Blázquez, Arturo Farfán Martín, Pedro Carrasco García, Diego González-Aguilera. "Thermal conductivity characterization of three geological formations by the implementation of geophysical methods", *Geothermics* 72 (2018) 101-111.

- Cristina Sáez Blázquez, Arturo Farfán Martín, Ignacio Martín Nieto and Diego González-Aguilera. "Economic and Environmental Analysis of Different District Heating Systems Aided by Geothermal Energy", *Energies*, Special Issue, *Geothermal Energy: Utilization and Technology*, (2018), 11, 1265.
- Ignacio Martín Nieto, Arturo Farfán Martín, Cristina Sáez Blázquez, Diego González Aguilera, Pedro Carrasco García, Emilio Farfán Vasco, Javier Carrasco García, Use of 3D electrical resistivity tomography to improve the design of low enthalpy geothermal systems. *Geothermics* 79 (2019) 1–13.
- Cristina Saez Blazquez, David Borge-Diez, Ignacio Martin Nieto, Arturo Farfan Martin, Diego Gonzalez-Aguilera, Technical optimization of the energy supply in geothermal heat pumps. *Geothermics* 81 (2019) 133-142.
- Cristina Sáez Blázquez, Ignacio Martín Nieto, Arturo Farfán Martín, Diego González-Aguilera and Pedro Carrasco García, Comparative Analysis of Different Methodologies Used to Estimate the Ground Thermal Conductivity in Low Enthalpy Geothermal Systems. *Energies* (2019), 12(9), 1672.

Book Chapters

- Blázquez C.S., Nieto I.M., Martín A.F., González-Aguilera D. (2019) Optimization of the Dimensioning Process of a Very Low Enthalpy Geothermal Installation. In: Nesmachnow S., Hernández Callejo L. (eds) *Smart Cities. ICSC-CITIES 2018. Communications in Computer and Information Science*, vol 978, 179-191 Springer, Cham.

Conference Proceedings

- Cristina Sáez Blázquez, Arturo Farfán Martín, Pedro Carrasco García, Luis Santiago Sánchez Pérez and Sara Jiménez del Caso, Nuevas posibilidades de generación eléctrica mediante energía geotérmica. *SPAIN MINERGY CONGRESS* (2015) vol 1, 356-363.
- Sara Jiménez del Caso, Arturo Farfán Martín, Pedro Carrasco García, Luis Santiago Sánchez Pérez and Cristina Sáez Blázquez, Sistemas de Gestión de la Energía. *SPAIN MINERGY CONGRESS* (2015) vol 1, 451-458.

General indicators of the scientific production quality

- **2017-2019**
Total citations: Google Scholar – 56
h index: Google Scholar – 5